



UNIVERSITAT DE  
BARCELONA

## Characterization of mRNA expression and localization in synaptic plasticity

Mónica Mendoza Blanco

**ADVERTIMENT.** La consulta d'aquesta tesi queda condicionada a l'acceptació de les següents condicions d'ús: La difusió d'aquesta tesi per mitjà del servei TDX ([www.tdx.cat](http://www.tdx.cat)) i a través del Dipòsit Digital de la UB ([diposit.ub.edu](http://diposit.ub.edu)) ha estat autoritzada pels titulars dels drets de propietat intel·lectual únicament per a usos privats emmarcats en activitats d'investigació i docència. No s'autoritza la seva reproducció amb finalitats de lucre ni la seva difusió i posada a disposició des d'un lloc aliè al servei TDX ni al Dipòsit Digital de la UB. No s'autoritza la presentació del seu contingut en una finestra o marc aliè a TDX o al Dipòsit Digital de la UB (framing). Aquesta reserva de drets afecta tant al resum de presentació de la tesi com als seus continguts. En la utilització o cita de parts de la tesi és obligat indicar el nom de la persona autora.

**ADVERTENCIA.** La consulta de esta tesis queda condicionada a la aceptación de las siguientes condiciones de uso: La difusión de esta tesis por medio del servicio TDR ([www.tdx.cat](http://www.tdx.cat)) y a través del Repositorio Digital de la UB ([diposit.ub.edu](http://diposit.ub.edu)) ha sido autorizada por los titulares de los derechos de propiedad intelectual únicamente para usos privados enmarcados en actividades de investigación y docencia. No se autoriza su reproducción con finalidades de lucro ni su difusión y puesta a disposición desde un sitio ajeno al servicio TDR o al Repositorio Digital de la UB. No se autoriza la presentación de su contenido en una ventana o marco ajeno a TDR o al Repositorio Digital de la UB (framing). Esta reserva de derechos afecta tanto al resumen de presentación de la tesis como a sus contenidos. En la utilización o cita de partes de la tesis es obligado indicar el nombre de la persona autora.

**WARNING.** On having consulted this thesis you're accepting the following use conditions: Spreading this thesis by the TDX ([www.tdx.cat](http://www.tdx.cat)) service and by the UB Digital Repository ([diposit.ub.edu](http://diposit.ub.edu)) has been authorized by the titular of the intellectual property rights only for private uses placed in investigation and teaching activities. Reproduction with lucrative aims is not authorized nor its spreading and availability from a site foreign to the TDX service or to the UB Digital Repository. Introducing its content in a window or frame foreign to the TDX service or to the UB Digital Repository is not authorized (framing). Those rights affect to the presentation summary of the thesis as well as to its contents. In the using or citation of parts of the thesis it's obliged to indicate the name of the author.

# CHARACTERIZATION OF mRNA EXPRESSION AND LOCALIZATION IN SYNAPTIC PLASTICITY

---

Mònica Mendoza Blanco

2023







Programa de doctorat en Biomedicina  
Facultat de Biologia de la Universitat de Barcelona

## **Characterization of mRNA expression and localization in synaptic plasticity**

Dissertation submitted by:

**Mònica Mendoza Blanco**

to qualify for the Doctorate degree by the Universitat de Barcelona

This work was performed at the Institute of Molecular Biology of Barcelona (IBMB) of the Spanish Research Council (CSIC) under the supervision of Dr Carme Gallego González



Mònica Mendoza Blanco

Carme Gallego González

Fernando Aguado Tomás

(Director)

(Tutor)



*¿Qué haría yo sin lo absurdo y lo fugaz?*





*A mi padre,*



## **ACKNOWLEDGMENTS**



## ACKNOWLEDGMENTS

Han pasado algo más de cuatro años y medio desde que llegué al IBMB y aunque en algunos momentos esta aventura ha sido complicada y me he quejado hasta la saciedad, tengo que reconocer que ha valido la pena. Soy consciente de que he sido muy afortunada en esta etapa, donde he coincidido con gente que no sólo han sido compañeros de trabajo, sino que han pasado a ser grandes amigos. Las palabras de agradecimiento hacia ellos nunca serán suficientes y posiblemente no reflejen lo que en realidad pienso de cada uno de ellos, pero me gustaría que quedase constancia de, al menos, una pequeña parte.

En primer lloc, a la Carme, per obrir-me les portes del laboratori quan pràcticament l'únic que podia aportar eren ganexes. Però més enllà d'aquell dia, per sempre tenir les portes obertes del despatx, per comentar qualsevol qüestió científica o personal. A en Martí, per les discussions científiques que tot i que a vegades m'han desesperat, sé que m'han fet molt millor científica. Y a Sara y Raül, por acogerme cuando era una niña del verano. Intentaron avisarme de lo que sería la tesis y no les hice caso, pero los tres sabíamos que no lo haría. Gracias por todo.

Mi primera gran suerte fue llegar a un laboratorio donde las meriendas y los cafés eran sagrados. A Alexis, por ser tan diferentes pero compenetrarnos en muchas otras cosas. Por todos esos trenes que has estado dispuesto a perder por escuchar un drama más o por jugar al juego de la moneda. A Marta, por todo lo que me aportó cuando estuvo en el lab y por todo lo que vino después. Encontrarnos en cultivos siempre hacía que el experimento fuese mejor. Y qué decir de las innumerables horas en la sala amarilla. Gracias, de verdad, por estar siempre dispuesta a escucharme. A la Blanca, per formar part de la gran majoria de records del lab. Perquè ha arribat un punt en que no cal que ens diguem moltes coses, les mirades parlen per si soles. Espero que algun dia acabis de creure't que ets realment molt bona científica i que jo estigui a prop per veure-ho.

A Laura, por tantas cosas que no sé muy bien ni por dónde empezar. Está bien, porque sé que no te gustan mucho estas cosas, pero gracias por ser un apoyo fundamental a lo largo de esta tesis y por ser una amiga increíble. Ahora que acaba esta etapa para las dos, solo pido seguir manteniendo los desayunos y cenas de los reyes del cotilleo (aunque a uno de los integrantes haya que hacerle videollamada). No me puedo dejar lo bueno de que mi tesis haya llegado un poco antes que la tuya: el día de tu defensa podré hacer lo que no me dejaste en el puente de Brooklyn. Sé que lo disfrutarás.

A Pilar, porque aunque ella no lo sepa, sus ganas de saber me han recordado muchas veces las cosas buenas de la tesis y me ha hecho reconciliarme con la ciencia en muchas ocasiones. Y lógicamente por estar siempre dispuesta a escuchar, discutir sobre el mundo y cotillear, ya sea en la sala de microscopía o dando vueltas

## ACKNOWLEDGMENTS

en el pasillo de la segunda planta. Te prometo que miraré “The L world”. A la Mar, per ser simplement increïble. Per fer-ho tot sense mai esperar res a canvi i per sempre tenir un somriure i bones paraules per tothom. Ara comença una nova etapa i estic segura de que sortirà genial, perquè t’ho mereixes.

A Mónica, la auténtica PI en la sombra. Por todas esas horas en cultivos (y también en la sala amarilla). Y especialmente por todos esos afterworks, karaokes y noches en plataforma donde competíamos para ver quien la liaba más. Aunque en estos años ya te hayas convertido en mi PI favorita, sé que lo que queda por venir será aún mejor. A Núria, mi fiel compañera de afonía. Gracias por cada comida, quejándonos del mundo. Aunque seas la persona más dramática del mundo, sé que tu tesis acabará genial. Y si, por fin podremos celebrarlo con un poco de techno.

A las Cristinas, por ser dignas sucesoras de M&M. Menos mal que empezamos a vernos fuera del lab! A Cris C, por enseñarme las llaves de judo que han permitido que escriba esta tesis (yo sé que he sido la mejor alumna del IBMB). A Cris B, por quererme aunque mi carta de presentación en nuestra primera noche de fiesta no fuese la mejor. Bueno, la segunda tampoco lo fue. En definitiva, gracias a las dos (C&C también es un pack indivisible) por haber hecho que esta tesis haya sido muchísimo más fácil. Aunque a veces cueste verlo, sé que ambas conseguiréis todo lo que os propongáis.

A Mariajo, por preocuparse siempre de sus niños M&M. Es verdad que muchas veces no teníamos muy buena cara pero trabajar juntas hacía todo más ameno. Por si en unos años se me olvida, que quede constancia que tú eras la del pipí y el plátano antes de electroporar. A María Logroño, por tener siempre esa energía y ganas de comerte el mundo. Gracias por todo, de verdad. A Antonia, por alegrarme las mañanas. Ha sido un placer coincidir contigo en esta etapa y ojalá hubiese más gente como tú.

Als meus amics (però oficialment enemics) de Gatbio: la Iulia, la Judit, en Jaime i en David. Per haver-me fet molt més amenes totes les hores a la sala de pre-cultius i per omplir la meitat del mur de targetes de “Viejas glorias”. Especialment a la Iulia, per ser la millor càncer del món (després de mi), si és que hem arribat a aclarir què implica això. I per escoltar tots els meus drames quan només era una becària. Sort que sé que tornarem a coincidir en un futur, tot i que no sé ben bé quina de nosaltres serà la jefa.

A aquellas personas que pasaron por el IBMB brevemente, pero la amistad ha permanecido más tiempo. A Mónica, por esas charlas hasta las tantas en la terraza, pudiendo hablar de todo. Que pasen los años y esto siga igual. A Bea, por acogernos en Buffalo y hacernos sentir como en casa. Y por ser el gran ejemplo de la motivación por la ciencia. Y a Ester, por ser mi mejor estudiante. Porque apareciste

en el laboratorio en el momento adecuado y aunque no nos salió absolutamente nada, no sé como lo hubiera gestionado sin ti.

Y, en definitiva, agradecer a todas aquellas personas que han hecho que estos años hayan sido más fáciles: Alba A, Álex, Belén, Cris F, Elena, Galal, Joana, Jose, Juan, Isa, Lourdes, Marta V, Ofelia, Omar, Ramiro, Samuel y Yara.

Muchísimas gracias a todos.

A mis amigos de Lloret, mis divas virtuales. Por recordarme siempre de donde vengo y donde sé que siempre puedo volver. A Raúl, por conocerme como nadie y estar siempre dispuesto a entenderme, sobre todo con mis cosas no tan buenas. A Eva, por ser inseparables toda una vida y confiar tanto en mí, incluso cuando yo no lo he hecho. Por haber aprendido a explicar lo que hago porque sabes que me da vergüenza decirlo. A en Joel, per sempre tenir paraules de suport i els braços ben oberts quan l'he necessitat. A Anca y Gabriela, por estar siempre dispuestas a escuchar todas mis quejas (pero también alegrías), acompañadas de cafés, cañas o gintonics. A Óscar, porque no importa el tiempo que pase que las cosas siempre siguen igual. I a la Nora i la Carlota, per haver estat presents en tots els bons moments però també en els dolents. A todos, os quiero muchísimo y solo espero tenernos toda la vida.

A toda esa gente que ha estado a mi lado durante estos años y que no puedo encajar en una sola categoría. A Laura, por vernos cada mil años pero mantener la conexión de cuando nos veíamos cada día en la universidad. A la Sílvia, per entendre les frustracions que a vegades ha suposat aquesta etapa. Però per ser conscients també de les bones coses que ens ha donat. A la Congo, per aquells sopars dels dimecres que feien la setmana un xic més curta. A la Dolors, per sempre tenir les portes obertes de la que és pràcticament la meva segona casa.

I lògicament a la Marta, per ser una part indispensable d'aquesta etapa. Per tot el que hem viscut però, sobretot, per seguir cuidant-nos molt. Gran part de com soc ara és gràcies a tu i t'estaré eternament agraïda. Que quedi constància en aquesta tesi que seràs la millor psicòloga del món i que t'admiro moltíssim.

A la PhD Society, mi Consejo de Sabios. ¿Quién nos iba a decir hace 10 años que las cosas serían así? A en Rafa, per ser un exemple a seguir en tot el que fa. Perquè no puc estar més orgullosa de tu i sé que només és el principi. Et menjaràs el món i estic feliç de poder estar al teu costat per veure-ho. A Elena, por ser un apoyo imprescindible desde Barcelona, Ponferrada, Madrid o Santiago. Primero por acogerme en Madrid y ser mi profe particular de alemán. Pero especialmente por esta etapa final, en la que has sido mi (doble) doctora de confianza. Eternamente agradecida, ya lo sabes. Que sigamos celebrando éxitos en cada Sonorama.

## ACKNOWLEDGMENTS

A l'Ainhoa, per totes les nits de burreria que ens van donar la vida. Ens queda pendent una nit de Frozen a Estocolm. A tots tres, us estimo molt. Em sento realment afortunada de tenir-vos a la meva vida.

A la persona más importante que me llevo de esta tesis, a Marcos. Porque aunque suena a tópico, yo no podría haber llegado hasta aquí sin ti. Por estar siempre dispuesto a discutir cada experimento, cada frustración y cada duda, sin importar donde ni cuando. Y por siempre querer celebrar los éxitos del otro como si fueran propios. Por ser, sin lugar a dudas, el mejor co-tesis. Pero principalmente gracias por haberte convertido en una de las personas más importantes de mi vida. Por poder contarte todo y no juzgarme nunca. Ahora nos toca cambiar los cafés, las cervezas y las cenas por videollamadas, pero sé que nos tendremos siempre. Voy a echarte mucho de menos pero sé que lo harás genial allí donde vayas.

A l'Anna, per portar tant de temps al meu costat que no soc capaç d'imaginar-me el meu dia a dia sense ella. Perquè això també hagués estat impossible sense tu. Per estar al meu costat cada cop que he pensat en deixar-ho, per escoltar i confiar en cada experiment que semblava que no sortiria. I per celebrar cada petit èxit i animar-me sempre a tirar endavant. Va ser una sort trobar-nos ja fa deu anys i estic molt orgullosa de poder dir que ets la meva millor amiga.

A mi familia, que de pequeña no tiene nada. A mi yaya, por cada vez que me ha dicho por teléfono que me deseaba mucha suerte y que estaba orgullosa de mí. A mi tía Fina, por ser como una segunda madre para mí. Porque, como ella dice, "a ver quien te quiere más que yo!". A mis primos, Laura e Iván, por ser las mejores personas que conozco. Por estar a mi lado en todo momento. Estoy muy orgullosa de vosotros y os quiero infinito.

A mi madre, por ser la persona más fuerte que conozco. Por cuidarnos siempre tanto y estar siempre dispuesta a darlo todo. Aunque nunca te lo diga, te quiero mucho. Y a mi hermano Alberto, mi persona favorita en el mundo, por siempre preocuparse por cómo estoy y por estar siempre a mi lado. Ahora los dos podremos decir que hemos escrito un libro, pero "Bili 1" siempre será mejor. Estoy muy orgullosa de ti y de todo lo que vas a conseguir. Sé que te lo digo constantemente, pero eres el mejor.

Y por último, los agradecimientos más difíciles pero también los más importantes. A mi padre, quien sé que estaría muy orgulloso de verme llegar hasta aquí. Por enseñarme a trabajar duro por lo que quieres y por recordarme que los fallos no marcan lo que soy. Esta tesis va para ti. Ojalá estuvieras aquí para verla.







## **ABSTRACT**



Neurons are highly polarized cells that require protein synthesis in distal dendrites to fulfil local protein requirements on short timescales. The regulation of this process relies in two major sub-processes: the transport of mRNAs from the soma to dendritic spines, and the regulation of protein translation.

Studies on the regulation of protein translation have traditionally focused on the initiation step. There is, however, growing evidence that the elongation step is also tightly regulated to achieve a more robust and transient control of the translational machinery in response to synaptic activity. In the first chapter of this doctoral thesis, we have focused on the regulation of protein translation by the eukaryotic elongation factor 1A (eEF1A). We have demonstrated that the neuron-specific isoform eEF1A2 is regulated by phosphorylation in an activity-dependent manner to regulate synaptic plasticity. Specifically, we show that glutamatergic stimulation opens a time window in which eEF1A2 dissociates from both its GEF protein and F-actin, thus decreasing protein synthesis and increasing actin cytoskeleton remodeling. In summary, we propose that eEF1A2 establishes a crosstalk mechanism that coordinates translation and actin dynamics during spine remodeling.

In the second chapter, we have studied the molecular mechanisms involved in the local capture of RNA granules. To date, how neuronal RNA granules are locally anchored in response to neuronal activity to enable mRNA translation specifically in dendritic spines is unclear. We have hypothesized that proteins present in the postsynaptic density could respond to neuronal activity and interact with RNA granules components to anchor these membrane-less organelles within dendritic spines. To address this, we searched for protein candidates and identified the actin-binding protein DrebrinA as a potential candidate for attracting and anchoring RNA granules. Live-imaging microscopy combined with biochemical approaches suggest that DrebrinA is mediating RNA granules attraction to spines in a concentration-dependent manner through its low complexity region.

Together, our results provide new insights on the molecular mechanisms involved in the regulation of local translation at synapses.



## **RESUMEN**





Las neuronas son células altamente polarizadas que requieren síntesis de proteínas en dendritas distales para cumplir con los requisitos locales de proteínas en plazos cortos de tiempo. La regulación de este proceso se basa en dos subprocesos principales: el transporte de ARNm desde el soma hacia las espinas dendríticas y la regulación de la traducción de proteínas.

Los estudios sobre la regulación de la traducción tradicionalmente se han centrado en el paso de iniciación. Sin embargo, existe cada vez más evidencia de que el paso de elongación también está estrechamente regulado para lograr un control más sólido y transitorio de la maquinaria de traducción en respuesta a la actividad sináptica. En el primer capítulo de esta tesis doctoral, nos hemos enfocado en la regulación de la traducción de proteínas por el factor de elongación eucariota 1A (eEF1A). Hemos demostrado que la isoforma específica de neuronas, eEF1A2, está regulada por fosforilación de manera dependiente de actividad para regular la plasticidad sináptica. Específicamente, mostramos que la estimulación glutamatérgica abre una ventana temporal en la que eEF1A2 se disocia tanto de su proteína GEF como de la F-actina, disminuyendo así la síntesis de proteínas y aumentando la remodelación del citoesqueleto de actina. En resumen, proponemos que eEF1A2 establece un mecanismo de coordinación entre la traducción de proteínas y la dinámica de actina durante la remodelación de las espinas dendríticas.

En el segundo capítulo, hemos estudiado los mecanismos moleculares involucrados en la captura local de gránulos de ARN. Hasta la fecha, no está claro cómo se anclan localmente los gránulos de ARN neuronales en respuesta a la actividad neuronal para permitir la traducción de ARNm específicamente en las espinas dendríticas. Hipotetizamos que las proteínas presentes en la densidad postsináptica podrían responder a la actividad neuronal e interactuar con componentes de los gránulos de ARN para anclar estos complejos dentro de las espinas dendríticas. Para abordar esto, buscamos candidatos de proteínas e identificamos una proteína de unión a actina, DrebrinA, como candidata potencial para atraer y anclar gránulos de ARN. Aproximaciones de microscopía *in vivo* combinadas con enfoques bioquímicos sugieren que DrebrinA media la atracción de los gránulos de ARN hacia las espinas de manera dependiente de su concentración a través de su dominio desordenado.

En conjunto, nuestros resultados proporcionan nuevas perspectivas sobre los mecanismos moleculares involucrados en la regulación de la traducción local en las sinapsis.



## **ABBREVIATIONS**



## ABBREVIATIONS

<b>3'UTR</b>	3' untranslated region
<b>4E-BP</b>	eIF4e-binding protein
<b>5'UTR</b>	5' untranslated region
<b>AAP</b>	Actin associated proteins
<b>aa-tRNA</b>	Aminoacyl-tRNA
<b>AB</b>	Actin-binding domain
<b>ABP</b>	Actin-binding protein
<b>ADF</b>	Actin-depolymerizing factor
<b>ALS</b>	Amyotrophic lateral sclerosis
<b>AMPA</b>	$\alpha$ -amino-3-hydroxy-5-methyl-4-isoxazolepropionic acid
<b>AMPA</b>	$\alpha$ -amino-3-hydroxy-5-methyl-4-isoxazolepropionic acid receptors
<b>Arp2/3</b>	Actin-related protein 2/3
<b>ASD</b>	Autism spectrum disorder
<b>BDNF</b>	Brain-derived neurotrophic factor
<b>CaMKII</b>	Calcium/calmodulin-dependent kinase II
<b>cDNA</b>	Complementary DNA
<b>cLTP</b>	Chemical LTP
<b>CPEB</b>	Cytoplasmic polyadenylation element binding protein
<b>cpm</b>	Counts per million
<b>Cryo-EM</b>	Cryogenic electron microscopy
<b>DAKO</b>	DrebrinA knockout mice
<b>DBN</b>	DrebrinA
<b>DDX5</b>	DEAD-box helicase 5/Probable ATP-dependent RNA helicase
<b>DHPG</b>	3,5-dihydroxyphenylglycine
<b>DHX9</b>	DExH-box helicase 9/ATP-dependent RNA helicase A

## ABBREVIATIONS

<b>DIV</b>	Days <i>in vitro</i>
<b>DMEM</b>	Dulbecco's modified eagle's media
<b>dsRBD</b>	Double-strand RNA-binding domain
<b>EB</b>	End-binding protein
<b>eEF1A</b>	Eukaryotic elongation factor 1A
<b>eEF1B</b>	Eukaryotic elongation factor 1B
<b>eEF2</b>	Eukaryotic elongation factor 2
<b>eEF2K</b>	Eukaryotic elongation factor 2 kinase
<b>eIF</b>	Eukaryotic initiation factor
<b>EJC</b>	Exon junction complex
<b>ERK1/2</b>	Extracellular signal regulated kinase 1 and 2
<b>F-actin</b>	Filamentous actin
<b>FBS</b>	Fetal bovine serum
<b>FDR</b>	False discovery rate
<b>FMRP</b>	Fragile mental retardation protein
<b>FRAP</b>	Fluorescence recovery after photobleaching
<b>FRET</b>	Förster resonance energy transfer
<b>FRET-FLIM</b>	Förster resonance energy transfer lifetime imaging microscopy
<b>FTD</b>	Frontotemporal dementia
<b>FUNCAT</b>	Fluorescence non-canonical amino acid tagging
<b>FUS</b>	Fused in sarcoma
<b>FXS</b>	Fragile X syndrome
<b>G-actin</b>	Globular actin
<b>GCN2</b>	General control nonderepressible 2
<b>GDP</b>	Guanosine diphosphate

## ABBREVIATIONS

<b>GEF</b>	Guanine nucleotide exchange factor
<b>GO</b>	Gene ontology
<b>GSEA</b>	Gene set enrichment analysis
<b>GTP</b>	Guanosine triphosphate
<b>HBSS</b>	Hanks' balanced salts solution
<b>iBAQ</b>	Intensity-based absolute quantification
<b>IDP</b>	Intrinsically disordered protein
<b>IDR</b>	Intrinsically disordered region
<b>IF</b>	Immunofluorescence
<b>IGF2BP</b>	Insulin-like growth factor II mRNA-binding protein
<b>IP</b>	Immunoprecipitation
<b>JNK</b>	c-Jun N-terminal kinase
<b>KA</b>	Kainate
<b>KH</b>	K homology domain
<b>LC-MS/MS</b>	Liquid chromatography-tandem mass spectrometry
<b>LCR</b>	Low complexity region
<b>LE</b>	Localization element
<b>LLPS</b>	Liquid-liquid phase separation
<b>LTD</b>	Long-term depression
<b>LTP</b>	Long-term potentiation
<b>MAP</b>	Microtubule associated protein
<b>MAPK</b>	Mitogen-activated protein kinases
<b>MEM</b>	Minimum essential media
<b>Met-tRNAi</b>	Methionine-transfer RNA
<b>mGluR</b>	Metabotropic glutamate receptors

## ABBREVIATIONS

<b>MLOs</b>	Membrane-less organelles
<b>mRNA</b>	Messenger ribonucleic acid
<b>mRNP</b>	Messenger ribonucleoprotein particle
<b>MS/MS</b>	Mass spectrometry
<b>MT</b>	Microtubules
<b>NES</b>	Nuclear export signal
<b>NLS</b>	Nuclear localization signal
<b>NMDA</b>	N-methyl D-aspartate
<b>NMDAR</b>	N-methyl D-aspartate receptors
<b>PABP</b>	Polyadenylation binding protein
<b>P-bodies</b>	Processing-bodies
<b>PEI</b>	Polyethylenimine
<b>PFA</b>	Paraformaldehyde
<b>PI3K</b>	Phosphatidylinositol 3-kinase
<b>PKA</b>	Protein kinase A
<b>PKC</b>	Protein kinase C
<b>PKG</b>	protein kinase G
<b>PKM <math>\zeta</math></b>	Protein kinase M $\zeta$
<b>pLDDT</b>	Predicted local distance difference test
<b>poly(A)</b>	Polyadenylation
<b>PrLD</b>	Prion-like domain
<b>PSD</b>	Postsynaptic density
<b>PSD-95</b>	Postsynaptic density-95
<b>PTM</b>	Post-translational modification
<b>RBD</b>	RNA binding domain



## ABBREVIATIONS

<b>RBP</b>	RNA-binding protein
<b>RF</b>	Release factors
<b>RGG</b>	Arginine-glycine-glycine box
<b>RNA</b>	Ribonucleic acid
<b>RNAi</b>	RNA interference
<b>ROI</b>	Region of interest
<b>RRM</b>	RNA recognition motif
<b>RT-qPCR</b>	Quantitative real time polymerase chain reaction
<b>SG</b>	Stress granule
<b>shRNA</b>	Short hairpin RNA
<b>sLTP</b>	Structural long-term potentiation
<b>smFISH</b>	Single-molecule fluorescence in situ hybridization
<b>ssRNA</b>	Single-strand RNA
<b>Stau</b>	Staufen
<b>SUnSET</b>	Surface sensing of translation
<b>TAD</b>	Tandem Agenet domain
<b>TDP-43</b>	TAR DNA-binding protein 43
<b>tRNA</b>	Transfer RNA
<b>Val-RS</b>	Valine-tRNA synthetase
<b>WB</b>	Western blot
<b>wst</b>	Wasted
<b>ZBP1</b>	Zipcode binding protein 1
<b>+TIP</b>	Plus-end tracking protein



# **TABLE OF CONTENTS**



INTRODUCTION .....	3
1. History .....	3
2. Neuronal structure .....	4
2.1. Postsynaptic density (PSD) .....	6
2.2. Actin cytoskeleton .....	7
2.3. Microtubule cytoskeleton.....	13
3. Synaptic plasticity .....	13
3.1. What is synaptic plasticity? .....	13
3.2. Long-term potentiation (LTP).....	15
3.3. Long-term depression (LTD) .....	15
3.4. Structural plasticity.....	16
4. Mechanisms of protein translation .....	17
4.1. Protein synthesis initiation .....	17
4.2. Protein synthesis elongation .....	19
4.3. Protein synthesis termination .....	20
4.4. Local translation .....	21
5. eEF1A.....	22
5.1. eEF1A isoforms and structure .....	23
5.2. Non-canonical functions of eEF1A.....	24
5.3. eEF1A2 in neurons.....	26
5.4. Post-translational modifications of eEF1A2.....	26
6. Alterations of synaptic plasticity in disease.....	27
7. RNA localization in dendrites and axons .....	28
8. Mechanism of neuronal RNA granule assembly.....	29
8.1. Liquid-liquid phase separation (LLPS).....	29
8.2. Cis-acting elements .....	30
8.3. Trans-acting factors.....	32
8.4. Assembly of RNA granules.....	35

## TABLE OF CONTENTS

9. Transport of RNA granules.....	37
9.1. Sushi belt theory.....	38
10. Anchoring of RNA granules.....	39
11. Local translation of RNA granules.....	40
AIMS .....	43
METHODS.....	47
1. CELL CULTURES/CELL BIOLOGY .....	49
1.1. Primary dissociated cultures .....	49
1.2. Hippocampal slice culture .....	49
1.3. Cell lines.....	50
2. MOLECULAR BIOLOGY .....	50
2.1. DNA constructs.....	50
2.2. Gene transfection .....	52
2.3. Viral production / Lentiviral production .....	54
2.4. Quantitative RT-PCR (RT-qPCR).....	54
2.5. Western blot (WB) analysis .....	55
2.6. Immunoprecipitation (IP) .....	56
2.7. APEX-mediated biotinylation.....	56
3. MORPHOLOGICAL ANALYSIS.....	57
3.1. Immunofluorescence (IF).....	57
3.2. Puromycin incorporation .....	58
3.3. Fluorescence recovery after photobleaching (FRAP) imaging.....	58
3.4. Förster resonance energy transfer (FRET) imaging.....	59
3.5. Live-imaging mRNPs .....	59
4. BIOINFORMATICS, DATA ANALYSIS AND REPRESENTATION .....	60
4.1. Mass spectrometry-based interactomic analysis .....	60
4.2. Spine analysis.....	60
4.3. Gene Set Enrichment Analysis (GSEA) .....	60
4.4. Global yeast genetic interaction network.....	61
4.5. Distance of mRNPs to spines .....	61

4.6. APEX proteomics .....	62
4.7. Graphical representation and statistical analysis .....	63
RESULTS.....	65
Chapter 1: Molecular mechanisms regulating eEF1A2 in the synaptic function.....	67
1. eEF1A2 expression in primary neuronal cultures.....	69
2. Generation of eEF1A2 phospho-mutants.....	70
3. Role of eEF1A2 phosphorylation in dendritic spines.....	71
4. Interactome analysis of eEF1A2 phospho-mutants.....	73
5. eEF1A2 phosphorylation in regulating actin dynamics .....	75
6. The implication of eEF1A2 phosphorylation in protein translation .....	76
7. Role of eEF1A2 phosphorylation in synaptic plasticity.....	78
Chapter 2: Molecular mechanisms regulating RNA transport granules capture in dendritic spines.....	85
1. Looking for protein candidates responsible for RNA granule local capture	87
2. DrebrinA localization in primary hippocampal cultures .....	89
3. Analyzing the effect of postsynaptic proteins in RNA granules positioning	92
4. Determining proteins involved in RNA granule local capture by proximity labeling .....	95
DISCUSSION.....	107
Chapter 1: Molecular mechanisms regulating eEF1A2 in the synaptic function.....	109
1. A switch from eEF1A1 to eEF1A2: what is its purpose? .....	111
2. Is phosphorylation the answer? .....	112
3. The effect on actin dynamics.....	112
4. The effect on protein translation.....	114
4.1. The importance of the interaction between eEF1A and eEF1B .....	115
5. Role of the activity-dependent phosphorylation of eEF1A2 .....	116
6. Proposed model for the role of eEF1A2 in the synaptic function .....	117

## TABLE OF CONTENTS

Chapter 2: Molecular mechanisms regulating RNA transport granules capture in dendritic spines.....	121
1. DrebrinA attractive effect on RNA granules .....	123
1.1. RNA granules imaging.....	123
1.2. DrebrinA's attraction capacity depends on its disordered region ....	125
2. How does DrebrinA act as an attractor of mRNPs?.....	126
2.1. The role of PTMs.....	126
2.2. The role of Drebrin-interacting proteins.....	127
2.3. The attraction capacity is not an inherent property of PSD proteins	128
3. Is DrebrinA responsible for the anchoring process? .....	129
3.1. Is DrebrinA exodus necessary for interacting with RNA granules?...	129
3.2. Are there other proteins involved in the attraction and/or anchoring of RNA granules? .....	130
3.3. How DrebrinA mediates RNA granules anchoring?.....	132
4. The role of RNA helicases .....	133
5. Using APEX technology to determine RNA granules content.....	135
6. Proposed model or RNA transport granules local capture.....	136
CONCLUSIONS .....	139
REFERENCES .....	143
ANNEX.....	175







# **INTRODUCTION**



A central goal of neuroscience is to unravel the mysteries of how neuronal circuits in the brain control various aspects of human experience and behavior. These circuits are formed by neurons, the fundamental building blocks of the brain. Neurons communicate with each other through electrical and chemical signals. Their morphology is much more complex compared to many other cells, presenting elaborate branching structures known as dendritic trees, which resemble the branches of a tree and contribute significantly to the brain's processing power.

The dendrites serve as the primary receivers of incoming information from other neurons. When a neuron receives signals from its neighboring cells, these inputs are integrated at the dendritic tree. The integration process involves summing up the incoming signals, and if the collective input reaches a certain threshold, the neuron generates an electrical impulse called an action potential. This action potential travels down the neuron's axon, a long, cable-like projection, to transmit the information to other neurons or target cells.

Studying these neural circuits and their intricate connections is an ongoing challenge in neuroscience. Researchers use advanced techniques, such as electrophysiology, optogenetics, and brain imaging, to gain insights into how neurons communicate, how signals propagate through circuits, and how specific brain regions contribute to various cognitive functions.

## **1. History**

Dendritic spines were first described by Santiago Ramón y Cajal in 1888, when he published a monograph in which he applied the Golgi stain to the cerebellum of birds. Within this work, he observed that the surfaces of Purkinje cells were covered with small protrusions, that he named "spines". Although these protrusions have been observed before by other investigators, they were initially dismissed as fixation artifacts or silver precipitates. As a result, Cajal's proposal was met with skepticism. Additionally, in 1894, Cajal proposed that spines were points of contact between two neurons and that physical changes in these structures could be associated with neuronal function and learning. In the 1950s, De Robertis and Palay performed the first ultrastructural analysis of synapses and ten years later synapses were conclusively demonstrated on spines. This vindicated Cajal's assertions, and spines became a topic of interest for neurobiological studies (Yuste, 2015).

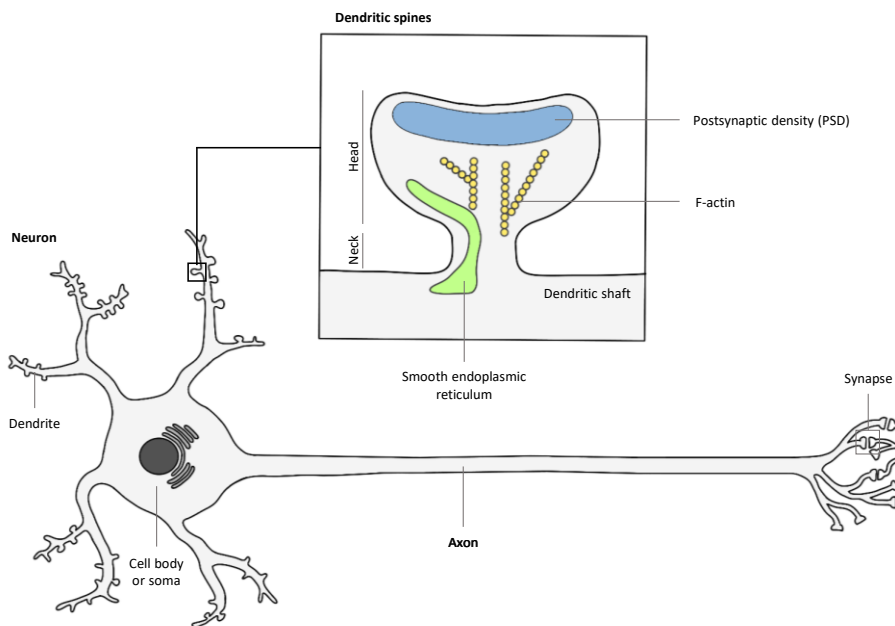
Cajal also used the term "neuronal plasticity" to describe nonpathological changes in the structure of adult brains. This statement was controversial, considering the "old dogma" that there is a fixed number of neurons in the adult brain that cannot be replaced when cells die. In the late 1960s, the term "neuroplasticity" was

## INTRODUCTION

introduced for describing morphological changes in neurons of adult brains. Many internal and external stimuli have been associated to changes in the morphology of neurons. One of the most studied ones is the stress-induced retraction of apical dendrites of CA3 pyramidal neurons in the hippocampus. The term neuroplasticity also included the formation of new neurons, known as neurogenesis. This phenomenon occurs in two specific regions, the subventricular zone and the dentate gyrus of the hippocampus. Nevertheless, it is crucial to note that the quantity of newly generated neurons is small compared to the total number of brain cells.

## 2. Neuronal structure

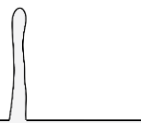

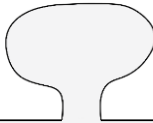
Neurons are highly polarized cells presenting a cell body from which a single axon and multiple dendrites extend. Axons can be extremely long, spanning hundreds of centimeters in length in vertebrates. Dendrites are highly branched and 13 mm-long on average (Holt et al., 2019; Magee, 2000). Dendrites contain specialized structures known as dendritic spines, which play a pivotal role in synaptic communication and plasticity (Fig. 1).



**Figure 1. Compartmentalization of subcellular domains in neurons.** Neurons are polarized cells with a cell body or soma from which extends a single axon and multiple dendrites. Dendrites contain small protrusions named dendritic spines, which are responsible for synaptic communication. Dendritic spines contain a postsynaptic density (PSD), filamentous actin (F-actin), and supporting organelles like the smooth endoplasmic reticulum. Dendritic spines can present different shapes depending on the size of the head and the neck.

Dendritic spines are small protrusions, typically 0.5 - 2  $\mu\text{m}$  in length, that contain the essential postsynaptic components such as the post synaptic density (PSD), the actin cytoskeleton, and supporting organelles like the smooth endoplasmic reticulum. Typical spines have a rounded head, which receives a single synapse, connected to the dendrite through the spine neck. The spine neck is a 50 - 400 nm thin membranous tube that prevents diffusion of molecules to and from the dendritic shaft. This spatial segregation facilitates the formation of microcompartments by acting as a diffusion barrier that isolates biochemical changes of one spine from the neighbor synapses of the same neuron (Adrian et al., 2014). Interestingly, it has been demonstrated that the neck of dendritic spines is a plastic structure which undergoes both shortening and widening upon induced spine potentiation (Hering & Sheng, 2001).

The standard dimensions for spines are  $\sim 1 \mu\text{m}$  for the head diameter, and a  $\sim 1 \mu\text{m}$  long and  $\sim 100 \text{ nm}$  wide spine neck. There are three shape categories based on the head and the spine neck sizes: (1) thin spines, when resemble thin, filopodia-like protrusions; (2) stubby spines, which are short without a well-defined spine neck; and (3) mushroom spines, characterized by a thin spine neck and a large head (Adrian et al., 2014)(Fig. 2).

			
	Thin spines	Stubby spines	Mushroom spines
Dynamic	Extremely	Very	Rarely
Average lifetime	Minutes to hours	$\sim 2$ days	$>1$ year
Prevalence	$\sim 2\text{-}3\%$ in mature brain $\sim 10\%$ at 1 month old $>25\%$ early postnatal	$\sim 20\%$ in young adults and probably more in development	$\sim 70\text{-}80\%$ in mature brain
Synaptic function	Little if any	Low AMPA to NMDA ratio	High AMPA to NMDA ratio
PSD-95	No	No	Yes

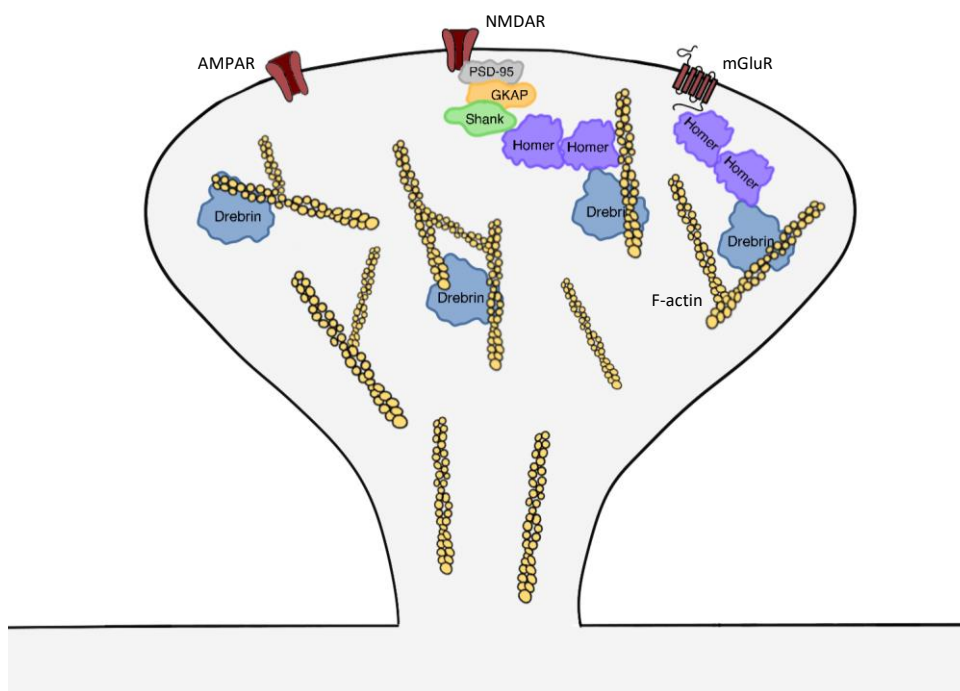
**Figure 2. Spines present different characteristics depending on their morphology.** Spines can be grouped in three categories (thin, stubby, and mushroom) depending on the spine head and spine neck sizes. Differences between the three types regarding dynamism, average lifetime, prevalence, synaptic function, and the presence of the protein Postsynaptic Density-95 (PSD-95) are shown. Adapted from Berry & Nedivi, 2017.

## INTRODUCTION

Spines may also be classified as: (1) type 1 asymmetric synapses, if they contain a prominent PSD; or (2) type 2 symmetric spines, if they lack a visible PSD. Type 1 are typically excitatory synapses, characteristics of glutamatergic synapses, whereas type 2 are typically inhibitory (Berry & Nedivi, 2017).

### 2.1. Postsynaptic density (PSD)

The PSD is abundant in proteins responsible for eliciting a response to neurotransmitters release. Ion channels and neurotransmitter receptors are found in the PSD membrane and maintained by scaffold proteins associated with cytoskeletal elements that guarantee their stability. The most relevant PSD scaffolds of excitatory synapses are Homer, GKAP, members of the membrane-associated guanylate kinases family (MAGUKs, such as PSD-95 and SAP97), and SH3 domain and ankyrin repeat domain proteins (SHANKs) (Hruska et al., 2018; MacGillavry et al., 2013) (Fig. 3). Protein kinases and signaling proteins are also constituents of the PSD. Proteomic studies have identified a vast range of 200 to 2000 different proteins in the PSD (Bayés et al., 2012; Dosemeci et al., 2007).



**Figure 3. Protein complex organization in the postsynaptic density (PSD).** The PSD of excitatory neurons is composed of glutamate receptors such as AMPAR, NMDAR and mGluR, among others (red), which are located in the postsynaptic membrane. Scaffolding proteins like PSD-95 (grey), GKAP (orange), Shank (green), and Homer (purple) are also present. Branched F-actin (yellow) maintains spine morphology together with actin-binding proteins like DrebrinA (blue) and Homer (purple).



Glutamate, the main excitatory neurotransmitter in the brain, is released from the excitatory presynaptic terminal and can bind to several postsynaptic receptors. Three types of ionotropic glutamate receptors exist:  $\alpha$ -amino-3-hydroxy-5-methyl-4-isoxazolepropionic acid (AMPA), N-methyl D-aspartate (NMDA) and kainate (KA) receptors. Although all are ligand-gated ion channels, they exhibit distinct ion permeabilities. On the one hand, NMDA receptors (NMDAR) are permeable to calcium, sodium, and potassium ions. However, they are characterized by a voltage-dependent  $Mg^{2+}$  block, necessitating postsynaptic membrane depolarization to facilitate  $Mg^{2+}$  removal and subsequent current conduction. On the other hand, AMPA receptors (AMPA) are permeable to sodium and potassium ions, and they lack voltage-dependent blockade. Consequently, they can be activated by ligands at resting potentials (Ho et al., 2011). Notably, the incorporation of AMPAR and NMDAR into spines occurs during the process of synapse maturation (Fig. 2).

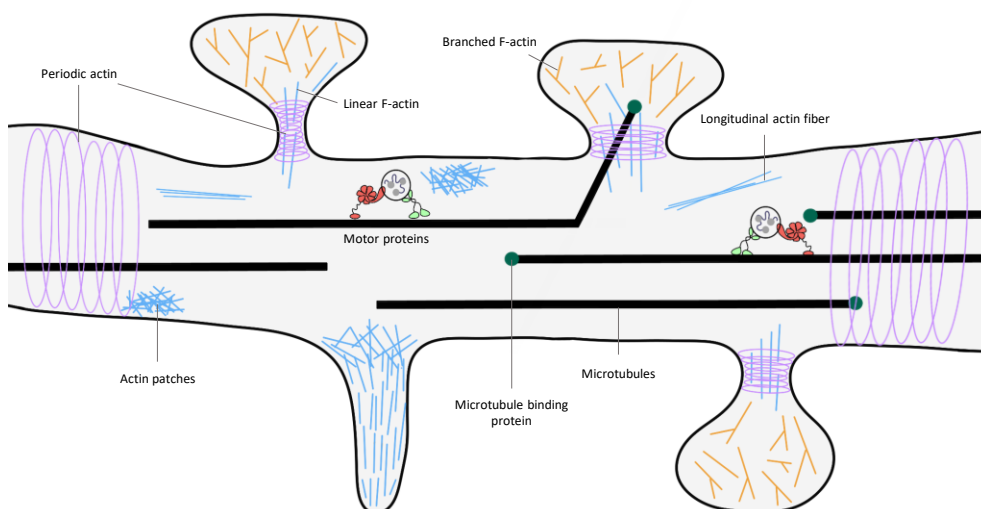
Glutamate is additionally capable of binding to metabotropic glutamate receptors (mGluRs), which are a class of G protein-coupled receptors. Unlike ionotropic glutamate receptors, mGluRs exert their effects indirectly through intracellular signaling pathways rather than mediating ion flux. This characteristic affords longer-lasting effects in comparison to ionotropic receptors (Niswender & Conn, 2010).

## **2.2. Actin cytoskeleton**

Filamentous-actin (F-actin) and microtubules (MTs) are the main orchestrators of neuronal polarity. Their organization is spatially and temporally controlled by actin-binding proteins (ABPs) and microtubule associated proteins (MAPs) by interacting with each other.

Dendritic spines are F-actin-based structures, but they are not the only ones. In addition, F-actin is also found within the shafts of dendrites forming structures like actin patches, longitudinal fibers, and actin rings. Actin patches are F-actin areas of a few microns-size, which are thought to serve as outgrowth points for filopodia. Longitudinal fibers are elongated bundles of F-actin that traverse the length of dendrites, but their function is still unknown. Actin rings are periodic cortical actin structures present in axons, dendrites, and the necks of dendritic spines. They are thought to maintain the shape of dendrites, and influence spine neck elasticity during the transport of organelles (Konietzny et al., 2017) (Fig. 4).

## INTRODUCTION



**Figure 4. The neuronal actin cytoskeleton.** Different actin structures are present in dendrites. Periodic actin (purple), linear actin (blue), and branched actin (orange) are shown. In the dendritic shaft, periodic actin forming actin rings is responsible for maintaining dendrite shape. Actin patches and longitudinal fibers formed by linear actin are also shown. Microtubules (black) and motor proteins (green and red) responsible for RNA granules transport are also shown. In the dendritic spine neck, periodic actin and linear F-actin are present. In the spine heads, branched F-actin maintains spine morphology and size. Adapted from Konietzny et al., 2017.

The actin cytoskeleton plays a key role in shaping dendritic spines. Its rapid polymerization and depolymerization produces protrusive forces that change neuronal morphology (Kessels et al., 2011). Actin filaments are highly accumulated in dendritic spine heads compared with the dendritic shaft. In the dendritic spine, there are two pools of F-actin: (1) a dynamic pool located at the tip of the spine; and (2) a stable pool located in the core. The dynamic pool appears to modulate spine size, shape, and plasticity, whereas the stable pool is needed to stabilize dendritic spines (Shaw et al., 2021). Interestingly, Honkura and colleagues (2008) demonstrated the emergence of a novel actin pool termed the “enlargement pool” following glutamate uncaging activation. This pool spans the entire spine head, consequently altering spine dimensions. Crucially, the maintenance or release of the enlargement pool onto the spine head or dendritic shaft depends on the constriction of the spine neck. If this release occurs, spines revert to their initial, smaller sizes, whereas if it is maintained, spines become bigger.

The actin cytoskeleton is associated to the abovementioned scaffolding proteins in dendritic spines through ABPs. These interactions are necessary for sustaining spine stability and flexibility, enabling a rapid response to synaptic activity to change spine morphology (Bosch et al., 2014; Mikhaylova et al., 2018).

In vertebrate cells, over a hundred ABPs may exist, but it remains unknown how many of them are present in dendritic spines. These ABPs present different functions: filament nucleation, severing, crosslinking, end capping, and monomer sequestering, as shown in Table 1 (adapted from Konietzny et al., 2017).

<b>Protein group</b>	<b>Function in neurons</b>
<b>Nucleators</b>	
Arp2/3-complex	F-actin branching in lamellipodia growth cones and spine heads
Formins	Synergize with other actin nucleators Role in filopodia, growth cones and axons
Cobl	Role in dendritic branching and growth cones
<b>Actin monomer (G-actin binding)</b>	
Profilin	Actin nucleotide exchange factor Maintain G/F-actin ratio together with capping proteins
CAP	Actin nucleotide exchange factor Sequester G-actin and severs F-actin Role in growth cone and dendrite development
<b>Elongation-promoting factors</b>	
VASP	Accelerate elongation and prevent capping Role in filopodia formation and neurite elaboration
<b>Barbed end capping</b>	
CapZ	Maintain G/F-actin ratio together with profilin Role in neurite elaboration
Adducin	Promote F-actin bundling and spectrin binding Component of actin rings
<b>Crosslinkers/Bundling</b>	
Spectrin	Couple F-actin cytoskeleton to plasma membrane Component of actin rings
$\alpha$ -actinin	Calcium sensitive Role in dendrite elaboration and branching
<b>Severing</b>	
ADF/Cofilin	Bind and sever F-actin Bind G-actin and enhance nucleation Enhance depolymerization and involved in LTP
Gelsolin	Sever F-actin Calcium sensitive Role in growth cone and spines
<b>Stabilizing</b>	
Cortactin	Stabilization of F-actin Activation of Arp2/3-complex Role in filopodia and growth cones
Abp1	Associate with newly formed F-actin Concentrated in PSD
Drebrin	Stabilizes actin Prevent F-actin from binding to tropomyosins, myosins, fascin and other ABPs Recruits MT into growth cones and dendritic spines

## INTRODUCTION

Actin-MT crosslinkers	
MAP1/2	Crosslink microtubules and F-actin Role in formation and stabilization of neurites
EB3	MT plus-end tracking protein (+TIP) Can simultaneously link to actin via Drebrin Role in neuritogenesis

**Table 1. Actin-binding proteins in neurons.** Main actin-binding proteins in neurons and their function in neurons are shown. Adapted from Konietzny et al., 2017.

### Nucleation of actin filaments proteins

Nucleation of actin filaments is the rate limiting step of filament formation and is mainly regulated by two protein families: the actin-related protein 2/3 complex (Arp2/3 complex) and formin molecules.

Arp2/3-complex nucleates actin filaments in a branched fashion from existing actin filaments. It is essential for distinct stages of both structural and functional maturation of excitatory spine synapses. Initially, the Arp2/3-complex inhibits the formation of dendritic filopodia, but as development progresses, it promotes the maturation from filopodia to mushroom-shaped spines (Spence et al., 2016).

Conversely, formins act as dimers to nucleate and extend unbranched actin filaments, binding to the fast-growing barbed ends of these filaments. It seems that formins play a pivotal role in generating linear F-actin from dendritic filopodia, while the Arp2/3 complex may be necessary in nucleating branched F-actin networks for spine head expansion (Lei et al., 2016). While dendritic spines predominantly harbor branched F-actin, the presence of unbranched filaments also exists, suggesting that formins might indeed contribute to the regulation of synaptic plasticity as well.

### Polymerization and depolymerization proteins

Actin polymerization requires the addition of globular actin (G-actin) monomers to growing filaments, a process mediated by ABPs like profilin. Profilin induces actin polymerization through binding to actin monomers and facilitating their addition to the growing end of actin filaments.

Actin dynamics are regulated not only through the polymerization of actin filaments, but also by the disassembly of the filaments by actin-depolymerizing factor (ADF)/cofilins, which sever and depolymerize aged actin filaments. Severing proteins carry the depolymerization of actin filaments by breaking down them into smaller pieces, providing G-actin reservoirs for new actin filaments formation (Kanellos & Frame, 2016). Cofilin activity is spatially and temporally regulated by different proteins to ensure efficient cell motility, considering that cells need to

move by expanding and retracting actin structures like filopodia and lamellipodia (Bravo-Cordero et al., 2013).

#### Actin crosslinking and stabilizing proteins

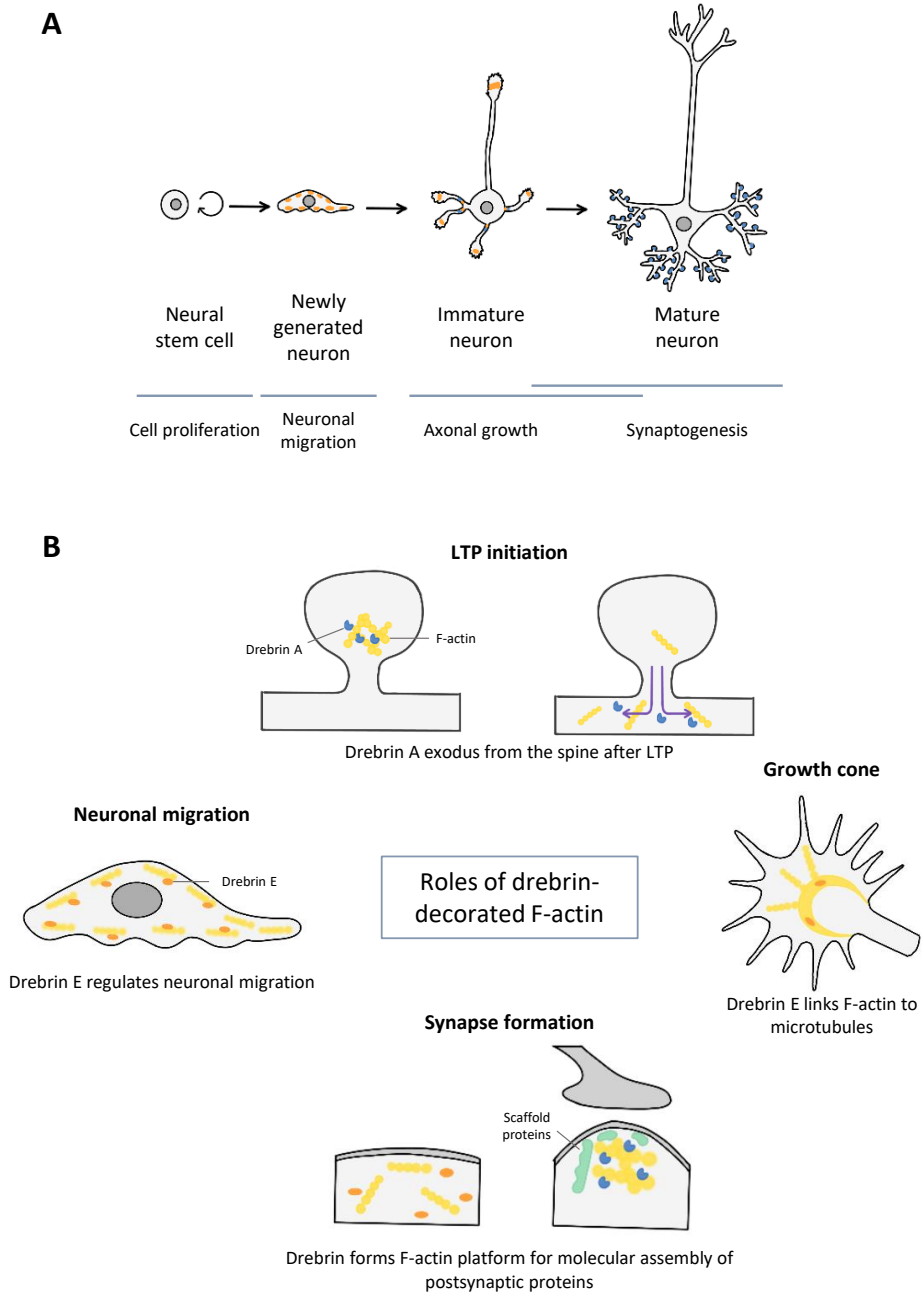
ABPs can remodel actin filaments without affecting the kinetics of actin polymerization, through proteins like  $\alpha$ -actinin, calponin, calcium/calmodulin-dependent kinase II  $\beta$  (CaMKII $\beta$ ), Neurabin I, or Drebrin by bundling or stabilizing actin filaments.

$\alpha$ -actinin, for example, localizes to the PSD and interacts with proteins related to synaptic strength, like NMDAR (Wyszynski et al., 1997). It has also been demonstrated that  $\alpha$ -actinin is necessary for PSD-95 and AMPAR anchoring in the PSD (Matt et al., 2018).

CaMKII is a serine/threonine protein kinase involved in synaptic plasticity and particularly concentrated in dendritic spines. Activation of CaMKII is sparked by calcium entry through NMDAR, which in turn triggers autophosphorylation of the kinase, thus enabling sustained activation until dephosphorylation of all subunits takes place. CaMKII activation governs synaptic plasticity through phosphorylation of several synaptic proteins, such as AMPAR (S. J. R. Lee et al., 2009; Lisman et al., 2002). Additionally, CaMKII $\beta$  bundles F-actin and is necessary for maintaining synaptic structure (Okamoto et al., 2007).

Another actor in this intricate interplay is the developmentally regulated brain protein known as Drebrin. Drebrin exerts control over actin bundling and prevents actin filaments from binding to other ABPs. Drebrin expression influences morphogenesis and maturation of dendritic spines (W.-H. Lin & Webb, 2009). Interestingly, Drebrin has two major isoforms resulting from alternative splicing of the *Dbn1* gene. The most abundant isoform of Drebrin switches from DrebrinE to DrebrinA during brain development in parallel with synapse formation (Fig. 5A). DrebrinA isoform is exclusively expressed in neurons, specifically in dendritic spines, and contains a neuron-specific region (Ins2) in the central part of the protein (Shirao et al., 2017).

## INTRODUCTION



**Figure 5. Drebrin localization and roles in neurons.** (A) Drebrin isoform-specific variations in subcellular distribution during neuronal development. DrebrinE (orange) is found through the entire cell of a migrating neuron. When neuron stops migrating, DrebrinE accumulates in axonal and dendritic growth cones. In parallel with synapse formation, DrebrinE switches to DrebrinA (blue) and it localizes to dendritic spines. (B) Drebrin-decorated F-actin is involved in many processes such as neuronal migration, growth cone development, synapse formation and long-term potentiation (LTP) initiation. Adapted from Shirao et al., 2017.

Previous research has demonstrated that inhibition of DrebrinA expression in hippocampal neurons leads to a delay in synapse formation, as well as a reduction in the accumulation of key postsynaptic proteins in the spine, which are crucial for synapse maturation (Takahashi et al., 2003). In mature neurons, DrebrinA is located at the core of dendritic spines decorating F-actin, although its localization is dependent on synaptic activity. Specifically, NMDAR activation and the subsequent calcium influx induces the exodus of DrebrinA (Mizui et al., 2014) (Fig. 5B). Given this intricate role of DrebrinA in synapse formation and maturation, it emerges as a key player in synaptic plasticity and neuronal connectivity.

### **2.3. Microtubule cytoskeleton**

In parallel with the actin cytoskeleton, the MT cytoskeleton must also undergo remodeling through neuronal development. MTs display several functions encompassing intracellular transport, organelle positioning, signal transduction, and structural maintenance.

MTs consist of heterodimers of  $\alpha$ - and  $\beta$ -tubulin, which bind in a head-to-tail manner creating polarized linear protofilaments. MTs can grow and depolymerize from both ends, though the dynamics differ at each end, with the plus end exhibiting faster growth. The plus end is responsible for regulating MT dynamics through plus-end tracking proteins (+TIPs). End-binding proteins (EB) are part of these +TIP complexes and facilitate MT growth. Furthermore, EB proteins can mediate the interaction with MT motors, actin-associated proteins (AAPs), and signaling factors, thereby orchestrating an intricate crosstalk (Kapitein & Hoogenraad, 2015).

MTs are found in the dendritic shaft and are typically excluded from dendritic spines. Nevertheless, MTs tips can transiently penetrate dendritic spines in an activity-dependent manner. This phenomenon correlates with spine enlargement, suggesting that it may be important for spine structural plasticity (Merriam et al., 2013). The targeting of MTs to spine has been linked to local actin remodeling at the base of the spine, demonstrating the need for a coordinated interplay between both cytoskeletal systems. This phenomenon offers a direct pathway for motor-driven transport of selective synaptic cargo into spines (Schätzle et al., 2018).

## **3. Synaptic plasticity**

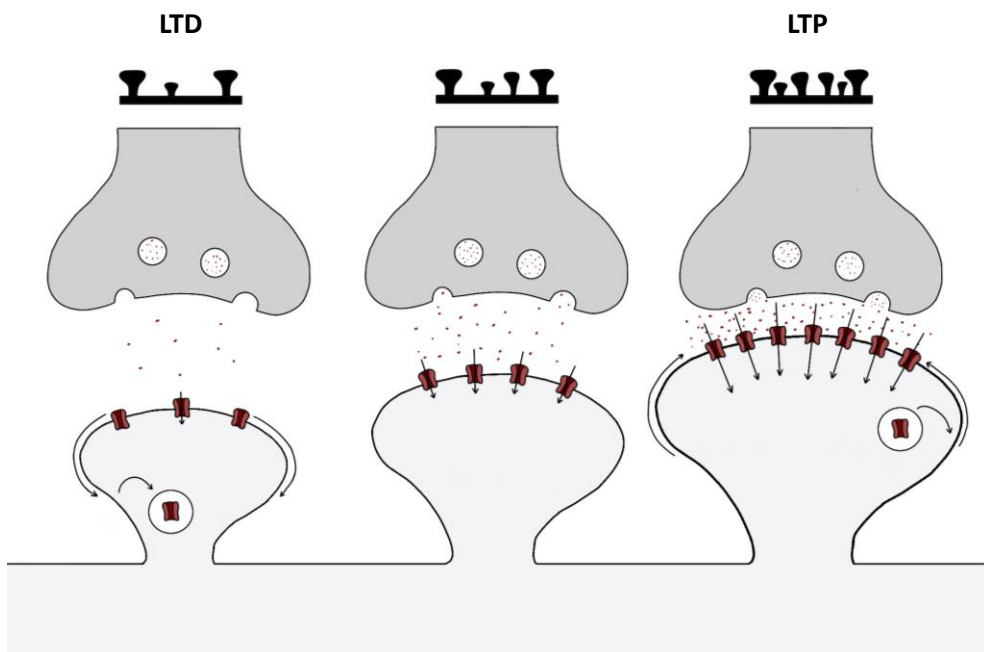
### **3.1. What is synaptic plasticity?**

The human brain is composed of a trillion ( $10^{12}$ ) neurons and a quadrillion ( $10^{15}$ ) synapses, and their interconnections underlie human perception, emotion, and behavior (Ho et al., 2011). Neuronal circuits are inherently plastic, allowing

## INTRODUCTION

individuals to adapt to a constantly changing environment. Synaptic plasticity is the experience-dependent change in connectivity between neurons and constitutes the pivotal cellular mechanism that underpins learning and memory (Pinho et al., 2020).

Cajal postulated that spines were dynamic, in the sense that they can emerge or be eliminated, and that such changes could underlie learning and memory. Later, in the mid-20<sup>th</sup> century, Donald Hebb formulated the Hebbian theory, proposing that synaptic connections are strengthened through correlated neuronal activity. This principle is often summarized as “*Cells that fire together, wire together*”. This concept led the preliminary work for understanding how connections between neurons can be reshaped by coordinated activity, forming the basis of learning and memory in the brain (Fauth & Tetzlaff, 2016).



**Figure 6. LTP and LTD affect synaptic transmission through different mechanisms.** Schematic diagram representing changes in dendritic spines after long-term potentiation (LTP) or long-term depression (LTD). In LTD, glutamate receptors (red) are internalized, conductance on the remaining receptors is diminished, presynaptic neurotransmitter release is decreased and, globally, spine density is reduced. On the other hand, in LTP, glutamate receptors are clustered in the PSD, synaptic transmission is strengthened, and presynaptic release is increased, as well as synaptic density.

Synaptic strength can be regulated by short- or long-lasting processes, which can in turn lead to either an enhancement or a decrease in synaptic strength. Short-term plasticity is achieved by changes that last from tens of milliseconds to several minutes. Conversely, long-term plasticity encompasses changes that last from hours



to months and includes both synaptic strengthening, termed as long-term potentiation (LTP), or synaptic weakening, referred as long-term depression (LTD).

Both LTP and LTD affect synaptic efficacy through different processes, as shown in figure 6: (1) trafficking of receptors to or from the postsynaptic membrane; (2) changing conductance of pre-existing receptors; (3) presynaptic modulation of neurotransmitter release; and (4) structural plasticity by changes in spine density, turnover, and morphology (Pinho et al., 2020).

### **3.2. Long-term potentiation (LTP)**

The initial stimulus for both LTP and LTD processes is the activation of NMDA receptors. Experimentally, LTP is induced by high-frequency bursts of stimulation, while LTD is prompted by low-frequency stimulation. Both processes are thought to be involved in information storage and therefore in learning and memory.

During LTP, calcium influx activates CaMKII (Lisman et al., 2002). Once activated, CaMKII undergoes autophosphorylation, which enables a calcium and calmodulin-independent kinase activity even after calcium levels return to baseline (Lou et al., 1986). Activated CaMKII phosphorylates several target proteins involved in synaptic function, including AMPA receptors. This phosphorylation event influences their insertion into the postsynaptic membrane, making the synapse more responsive to neurotransmitter release (Derkach et al., 1999; Ehlers, 2000). Furthermore, evidence exists that CaMKII contributes to structural modifications by interacting with the actin cytoskeleton of dendritic spines (K. Kim et al., 2015; Okamoto et al., 2007).

Beyond CaMKII, a multitude of other kinases have been recognized as pivotal players in LTP, encompassing SRC family tyrosine kinases, protein kinase A (PKA), protein kinase C (PKC), and mitogen-activated protein kinases (MAPK) (Soderling & Derkach, 2000). These kinases collectively orchestrate the intricate cascade of events underpinning the induction and maintenance of LTP.

### **3.3. Long-term depression (LTD)**

LTD is a form of synaptic plasticity characterized by the weakening of synaptic connections between neurons, functioning as the counterpart to long-term potentiation. Mechanisms underlying LTD involve changes in the number of neurotransmitter receptors, in synaptic structure, and modifications in the release of neurotransmitters. LTD plays a pivotal role in preserving the equilibrium of synaptic interconnections within neural networks by diminishing irrelevant or unused connections in memory consolidation (Diniz & Crestani, 2022).

## INTRODUCTION

In the hippocampus, two major forms of LTD have garnered attention: NMDAR-LTD and mGluR-LTD. NMDAR-LTD is usually triggered by low-frequency stimulation that induces neuronal depolarization (Collingridge et al., 2010). Activation of NMDAR occurs due to the coincident glutamate release and postsynaptic depolarization, facilitating calcium entry. This cascade triggers various intracellular signaling pathways leading to the internalization or removal of AMPAR from the postsynaptic membrane (H. K. Lee et al., 1998).

The second major form of LTD requires the activation of mGluRs, which is usually induced by single-shock low-frequency stimulation or the application of the group I mGluR agonist 3,5-dihydroxyphenylglycine (DHPG). Activation of mGluRs also leads to removal of AMPA receptors from the postsynaptic membrane, thereby diminishing synaptic strength. Although both forms of LTD rely on distinct receptors and signaling mechanisms, some instances of LTD require synergistic interactions between them (Palmer et al., 1997).

Traditionally, it was posited that LTP requires kinases like CaMKII, while LTD hinges on phosphatases. However, in 2014 it was demonstrated that LTD also requires CaMKII and its autophosphorylation activity. The distinguishing factor between these processes lies in the phosphorylation of the AMPA receptor subunit GluA1: in LTP, phosphorylation occurs at Ser<sup>831</sup>, while in LTD, phosphorylation happens on Ser<sup>567</sup>, resulting in diminished synaptic GluA1 localization (Coultrap et al., 2014).

### **3.4. Structural plasticity**

Synaptic plasticity undergoes continuous remodeling throughout life, facilitated by mechanisms of synapse formation, stabilization, and removal, collectively known as “structural plasticity”. This phenomenon needs molecular reorganization, primarily involving the actin cytoskeleton, and subsequently influencing the size of the PSD and abundance of glutamate receptors within it (Meyer et al., 2014). Notably, changes in spine structure affect synaptic function.

Dynamic spines cover a wide range of spine morphologies and sizes. Filopodia-like protrusions are highly unstable and can be added or pruned within hours. In contrast, mushroom-type spines tend to remain stable over extended periods from months to years (Grutzendler et al., 2002; Zuo et al., 2005). Small, highly dynamic spines or filopodia can mature into larger, stable spines, suggesting that they represent an early stage of spine development (Berry & Nedivi, 2017).

Around 70 - 80 % of spines in adult mouse neocortex present mature excitatory synapses scaffolded by PSD-95. These PSD-95 positive spines are generally stable. However, in rare instance, they lose PSD-95 and subsequently disappear (Cane et

al., 2014). This form of spine dynamics is most likely to represent permanent alterations in local circuit connectivity. Remarkably, spiny neurons are rarely found in lower organisms like *Drosophila melanogaster* and *Caenorhabditis elegans*, suggesting that the evolution of spines occurred to support the complexity of “advanced” nervous systems, such as the mammalian brain (Hering & Sheng, 2001).

In addition to the morphological changes that occur over hours or days, dendritic spines also display rapid motility. Changes in spine shape can happen within seconds to minutes in most spines, a process linked to the remodeling of the actin cytoskeleton within these protrusions. Although the precise molecular mechanisms underlying this process remain elusive, evidence suggests that such motility is more prominent during the critical developmental periods and decreases as neuronal maturation progresses (Hering & Sheng, 2001).

It is postulated that distinct spine shapes and sizes correspond to different developmental stages. Additionally, the volume of spine heads can increase in response to stimuli that strengthen synapses and decrease with stimuli that weaken synapses. In fact, spine size is proportional to the PSD size, to the number of postsynaptic receptors, and to the number of docked presynaptic vesicles. As a result, the enlargement of the spine head is likely to be correlated with the strengthening of synaptic transmission (Berry & Nedivi, 2017; Hering & Sheng, 2001).

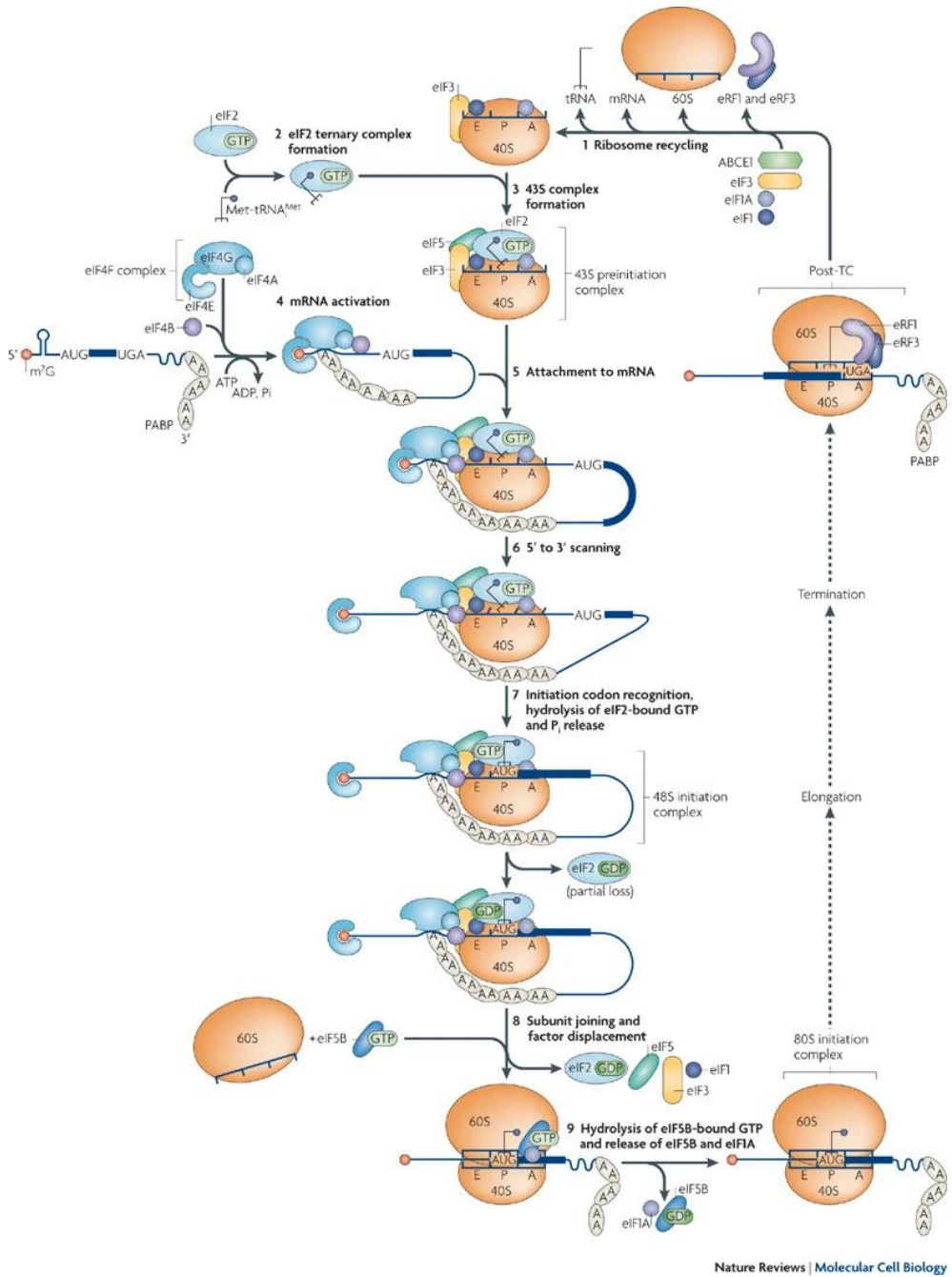
#### **4. Mechanisms of protein translation**

It is known that long-lasting changes in synaptic strength require *de novo* protein synthesis. In eukaryotes, protein translation is divided into three steps: initiation, elongation, and termination. Among these, protein translation initiation is the rate-limiting step, therefore is the major target for translational control (Costa-Mattioli et al., 2009). While protein translation initiation is widely acknowledged as a key regulatory point, emerging evidence indicates that the elongation step also undergoes intricate regulation (Graber et al., 2013).

##### **4.1. Protein synthesis initiation**

The initiation step aims to form an 80S ribosomal initiation complex, which involves the assembly of two separated 40S and 60S ribosomal subunits. In this process, the initiator tRNA, methionine-tRNA (Met-tRNA<sup>i</sup>), is base paired with the initiation codon in the ribosomal P site to subsequently start translation elongation stage. This stage is governed by an interplay of several eukaryotic initiation factors (eIFs) alongside the ribosomal subunits (Fig. 7).

# INTRODUCTION



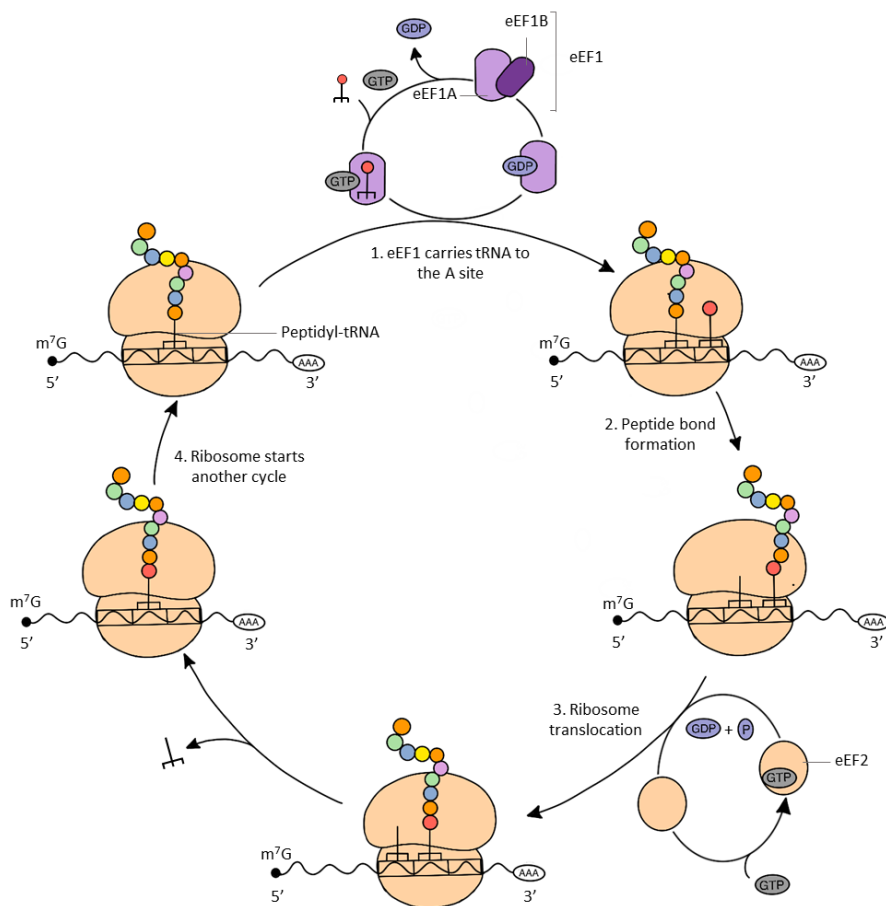
**Figure 7. The mechanisms of eukaryotic translation initiation.** From Jackson et al., 2010

First, the small subunit (40S) and several eIFs assemble the 43S preinitiation complex. Within this assembly is the Met-tRNA<sub>i</sub>. The messenger RNA (mRNA) is activated through the binding of the eIF4 complex, which subsequently attaches to the 43S preinitiation complex. The 43S-mRNA complex goes under a scanning

process along the mRNA molecule in a 5' to 3' direction until it recognizes the AUG codon. Upon encountering the start codon, the 43S complex transitions into the 48S initiation complex, in which the Met-tRNA<sub>i</sub> is correctly positioned onto the start codon within the ribosomal P site. The Met-tRNA<sub>i</sub> is associated with a ternary complex including GTP-bound eIF2. GTP hydrolysis prompts the release of eIF2-GDP and signals the assembly of the large ribosomal subunit (60S) with the small ribosomal subunit (40S), forming the 80S initiation complex (Jackson et al., 2010).

#### 4.2. Protein synthesis elongation

Translation elongation is the process mediating the growing of the polypeptide chain through eukaryotic elongation factors (eEFs) (Fig. 8).



**Figure 8. The mechanisms of eukaryotic translation elongation.** Adapted from Guerrero et al. (2015).

## INTRODUCTION

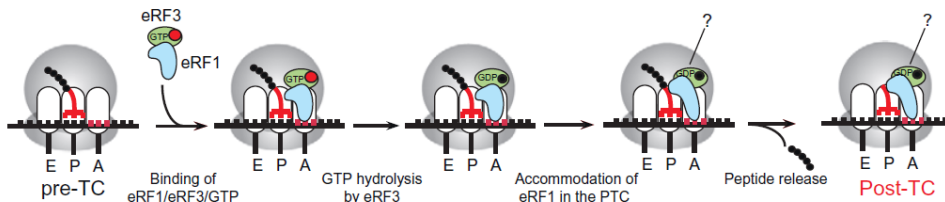
Eukaryotic elongation factor 1A (eEF1A), when bound to GTP, brings the aminoacyl-tRNAs (aa-tRNAs) (charged tRNAs carrying specific amino acids) to the ribosome's A site, positioning them for codon recognition. Once the codon-anticodon pairing is established, GTP hydrolysis is triggered and leads to the release of eEF1A from the A site. Concomitantly, the ribosome undergoes conformational changes that shift the position of the tRNA from A to P and P to E sites. This process enables the formation of a peptide bond between the growing polypeptide chain and the newly introduced amino acid. Subsequently, the eukaryotic elongation factor 2 (eEF2) enters the A site, hydrolyses GTP and resets the ribosome to a conformation able to receive the next aa- tRNA in the A site. This process repeats itself multiple times (Richter & Collier, 2015).

As just mentioned, eEF1A, in its GTP-bound form, binds and delivers aa-tRNAs to the A site of the ribosome. When a correct codon-anticodon pair is formed, a conformational change in the ribosome leads to GTP hydrolysis and the release of eEF1A-GDP. Due to the slow spontaneous dissociation rate of GDP from eEF1A, an active exchange of GDP for GTP is required (Pittman et al., 2006). This exchange is carried by the guanine nucleotide exchange factor (GEF), the eukaryotic elongation factor 1B (eEF1B), allowing the recycle of eEF1A to perform the next round of translation. In higher eukaryotes, the eEF1B complex encompasses four subunits: the structural protein eEF1B $\gamma$ , two nucleotide exchange factors eEF1B $\beta$  and eEF1B $\delta$ , and a tRNA synthetase termed valine-tRNA synthetase (Val-RS) (Le Sourd et al., 2006).

The elongation step of translation is also subjected to regulation in neurons. In this context, mRNAs travel through dendrites stalled in translation in structures called RNA granules. Cryogenic electron microscopy (Cryo-EM) analysis has demonstrated that ribosomes within these granules are stalled in a hybrid state. This means that the ribosome is partially engaged with both the incoming aa-tRNA and the growing peptide chain, indicating that the pause happened during the protein synthesis process, likely within the elongation step (Anadolu et al., 2023). This insight underscores the complexity of translational control mechanisms within neuronal contexts.

### **4.3. Protein synthesis termination**

The final stage of protein translation is termination, in which the ribosome stops adding amino acids to the growing polypeptide chain. This event happens when a stop codon (UAA, UAG, or UGA) in the mRNA is recognized in the A site of the ribosome.



**Figure 9. The mechanisms of eukaryotic translation termination.** From Jackson et al., 2012.

The stop codon itself does not correspond to any amino acid, thus its recognition triggers a signaling cascade prompting the ribosome to stop protein synthesis. Termination process requires two polypeptide release factors (RFs): eRF-1, which is codon-specific; and eRF-3, which is non-specific. These RFs bind to the A-site and form an eRF-1/eRF-3/GTP complex. Within this complex, eRF-1 is responsible for codon recognition. Subsequently, eRF-3 hydrolyses GTP, and eRF-1 hydrolyses the polypeptidyl-tRNA. Importantly, the ribosome remains bound to the mRNA and needs to be recycled to allow further rounds of translation (Jackson et al., 2012) (Fig. 9).

In essence, the termination step ensures the precise and controlled conclusion of the protein translation process, guaranteeing the fidelity of the final polypeptide product and preparing the ribosome for subsequent translation events.

#### 4.4. Local translation

In the past 30 years, it has become clear that protein translation is not confined solely to the neuronal soma, but rather, it occurs within decentralized local domains in a process known as “local translation”. The localization of mRNA, ribosomes and regulatory elements required for protein synthesis at distal dendrites enables fulfilment of local protein requirements on short timescales (Holt et al., 2019).

The existence of local translation in dendrites was first suggested by identification of polyribosomes under the base of dendritic spines in hippocampal neurons by electron microscopy (Steward & Levy, 1982). The initial findings suggested that only a limited number of mRNAs were present in synapses. However, the development of more sensitive technologies has allowed the identification of 2500 mRNAs within dendrites and axons of hippocampal pyramidal neurons (Cajigas et al., 2012).

Differentiation of local translation from somatic translation has been challenging. Most approaches have focused on physically isolate the synaptic neuropil from the cell-body. Using this, a requirement for local translation has been demonstrated for LTP (Vickers et al., 2005) and mGluR-LTD (Huber et al., 2000).

## INTRODUCTION

Considering that protein translation is essential for memory consolidation, a lot of efforts have been focused on determining how local translation is regulated at the synaptic level. For instance, one of the major pathways that regulate translation initiation is phosphorylation of eIF2 through the integrated stress response. Specifically, general translation is inhibited when eIF2 is phosphorylated. However, translation increases for some specific transcripts (Kapur et al., 2017; Sossin & Costa-Mattioli, 2019).

Several studies have revealed activity-dependent regulation of translation initiation and elongation. One of the most studied mechanisms involved the cytoplasmic polyadenylation element binding protein (CPEB). CPEB binds to the 3' untranslated regions (3'UTR) of mRNAs and represses their translation. However, upon neuronal activity, CPEB is phosphorylated and recruits other proteins that enhance the polyadenylation (poly(A)) tail length of the mRNAs. This extended poly(A) tail subsequently attracts the poly(A) binding protein (PABP), which recruits the eIF4G to interact with the eIF4E. This interaction facilitates the initiation of translation. Importantly, CPEB localizes to synapses and regulates the *CaMKII $\alpha$*  mRNA translation (Y. S. Huang et al., 2023; Wells et al., 2001; L. Wu et al., 1998).

Another activity-dependent mechanism of translation is the regulation by phosphorylation of eIF4E-binding protein (4E-BP). When 4E-BP is hypophosphorylated, it binds to eIF4E preventing translation initiation. However, neuronal activity induces 4E-BP phosphorylation, affecting its association with eIF4E, and relieving translational inhibition (Costa-Mattioli et al., 2009).

Regarding the elongation step, most studies have focused on the regulation of eEF2 (S. Park et al., 2008; Scheetz et al., 2000; Sutton et al., 2007). This would allow a more robust transient control of the translational machinery in response to synaptic activity (Fuchs & Flügge, 2014). Upon activation, the eukaryotic elongation factor 2 kinase (eEF2K) phosphorylates and inhibits eEF2, resulting in a decrease in general translation. However, some mRNAs like *Map1b*, *CaMKII* and *Arc* increase their translation levels. Since eEF2K is regulated by calcium, NMDAR and mGluR are both upstream to this process (Heise et al., 2014).

### 5. eEF1A

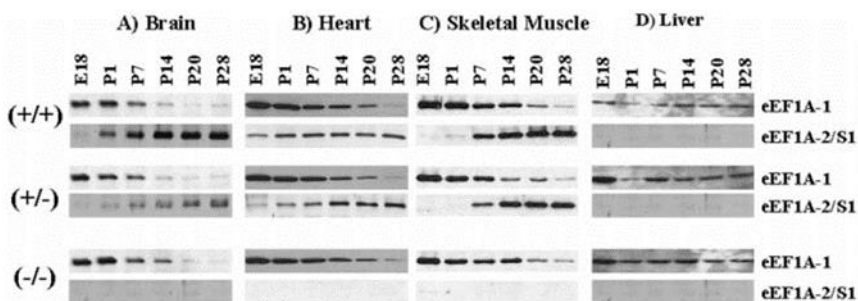
eEF1A is a classic G-protein that binds to the aa-tRNA in a GTP-dependent manner and then binds to the elongating ribosome. Recycling of the inactive eEF1A-GDP complex back to the active GTP-bound state is mediated by the eEF1B complex, which acts as a GEF (Negrutskii et al., 1996).



### 5.1. eEF1A isoforms and structure

Vertebrates have two eEF1A genes that encode two distinct isoforms, eEF1A1 and eEF1A2. In humans, *EEF1A1* and *EEF1A2* genes are located on chromosomes 6 and 8, respectively (Lund et al., 1996). Remarkably, these isoforms are 92 % identical and 98 % similar at the amino acid level (Soares et al., 2009) and yet they display very different expression patterns. Isoform eEF1A1 is expressed ubiquitously during development but is replaced by isoform eEF1A2 in neurons and muscle (skeletal and cardiac) cells over the course of postnatal development (Khalyfa et al., 2001). Other non-mammal species also present two different isoforms, like *Drosophila* and *Xenopus* (S. Lee et al., 1992).

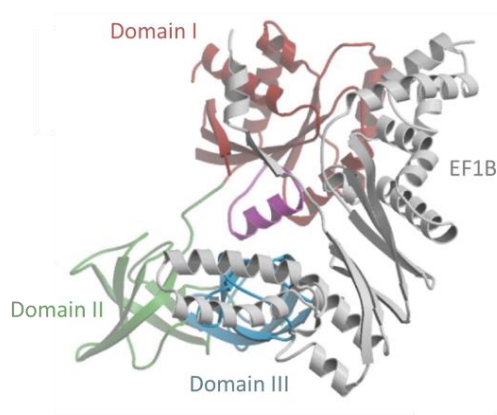
The switch from one isoform to another was well documented by Chambers and colleagues (1998), using the *Eef1a2*<sup>-/-</sup> mouse model, named as “wasted” (*wst*) mice. The autosomal recessive *wst* mutation appeared spontaneously in a mouse colony at the Jackson laboratory in 1972. Homozygous *wst/wst* mice appear completely normal until weaning age, approximately 21 days after birth. Then, they develop tremors and ataxia, followed by weight lost (probably due to muscle wasting), progressive paralysis, and die by 28 days after birth. Heterozygous mice (+/*wst*) do not display any phenotype and present a pattern of expression similar to the wild-type (+/+) animals. Later, Khalyfa and others (2001) carefully described that in neurons, eEF1A1 is the predominant isoform before postnatal day 7, later being succeeded by eEF1A2, which becomes the sole isoform by postnatal day 14 (Fig. 10). Hence, eEF1A2 is essential for mouse survival, and its absence in the *wst* mice may result in a loss of protein synthesis ability, leading to several defects culminating in the death of these mice.



**Figure 10. Differential expression of eEF1A1 and eEF1A2 proteins during development of wild-type, heterozygous, and homozygous *wst* mice.** Mouse tissue from (A) brain, (B) heart, (C) skeletal muscle, and (D) liver obtained at embryonic day 18 (E18) and postnatal (P) days 1, 7, 14, 20, and 28 were used for immunoblotting assays from wild-type (+/+), heterozygous (+/-) and homozygous *wst* (-/-) mice. eEF1A1 and eEF1A2 protein levels were assessed using specific antibodies. From Khalyfa et al., 2001.

## INTRODUCTION

eEF1A comprises three different domains, each contributing to specific facets of its function: (1) Domain I, which binds GTP; (2) Domain II, which binds aa-tRNA; and (3) Domain III, which binds actin cytoskeleton. Both domain I and II mediate association with the GEF eEF1B $\alpha$  (Jakobsson et al., 2018) (Fig. 11). Comparison of the 3D structure of both isoforms reveal two distinct sub-clusters of sequence variation. Non-conserved residues appear in discrete surface clusters that do not overlap with the binding site of GTP/GDP, eEF1B and aa-tRNA (Soares et al., 2009).



**Figure 11. Structure of bacterial elongation factor EF1A.** The EF1A-EF1B complex from *E. coli*. The different domains of EF1A are shown: domain I (red), domain II (green) and domain III (blue). EF1B is also shown (grey). The region that switches depending on GTP-binding is shown in magenta. From Andersen et al., 2003.

Both isoforms do not show differences during the elongation step of protein translation but have different relative affinities for GTP and GDP. eEF1A1 binds GTP more strongly than GDP, and eEF1A2 exhibits the opposite trend (Kahns et al., 1998).

### 5.2. Non-canonical functions of eEF1A

Besides its canonical function in protein translation, eEF1A has been implicated in many other cellular processes (Mateyak & Kinzy, 2010; Sasikumar et al., 2012). Nevertheless, the isoform eEF1A2 has been less studied at the biochemical level, so the specific functions undertaken by each eEF1A isoform and those functions that are shared between them remain elusive.

#### Actin cytoskeleton

eEF1A was first isolated in *Dictyostelium discoideum* as an ABP (F. Yang et al., 1990) and since then an extensive number of *in vitro* experiments have been performed to characterize this interaction. eEF1A can both bind and bundle actin filaments *in vitro* but this process cannot be performed as efficiently in the presence of aa-tRNA,

suggesting that both processes are mutually exclusive (G. Liu et al., 1996). In fact, mutants of eEF1A that reduced actin bundling activity, did not alter translation in *S. cerevisiae* (Gross & Kinzy, 2005).

An increasing number of studies support the idea that the actin cytoskeleton and the translation machinery are intrinsically connected and may show reciprocal regulation (De Rubeis et al., 2013; W. Huang et al., 2013; S. Kim & Coulombe, 2010). In fact, perturbations of the actin cytoskeleton are associated with a reduction in the rate of global protein synthesis in yeast (Gross & Kinzy, 2007; Munshi et al., 2001) and mammalian cells (Silva et al., 2016).

#### Nuclear export

The initial work on the role of eEF1A in nuclear export of tRNAs stemmed from a multicopy suppressor screening of mutants in *S. cerevisiae*. Specifically, it was observed that reduced levels or mutated forms of eEF1A correlated with tRNAs accumulation in the nuclei (Großhans et al., 2000). It seems that eEF1A facilitates the communication between nucleus and cytoplasm, enabling the nuclear tRNA export machinery to sense and react to defects in protein translation, and vice versa. Besides its role as mediator of tRNA export in yeast, eEF1A is also involved in the nuclear export of proteins in mammalian cells through Exportin-5 pathway (Bohnsack et al., 2002; Khacho et al., 2008; Mingot et al., 2013).

#### Proteolysis

It is intriguing that the same protein, eEF1A, could be involved in such opposing functions as protein translation and protein degradation. However, the fact that eEF1A is in high concentration next to the ribosome might facilitate a role in protein quality control and co-translational degradation. Some studies demonstrate that eEF1A interacts with unfolded proteins upon their release from the ribosome, assisting in their refolding or degradation (Gandin et al., 2013; Hotokezaka et al., 2002). In addition, eEF1A interacts with ubiquitinated proteins and the 26S proteasome in order to degrade proteins co-translationally (Chuang et al., 2005).

#### Apoptosis

Initial investigations regarding eEF1A and apoptosis yielded contrary effects (Duttaroy et al., 1998; Talapatra et al., 2002). Subsequent research revealed that the effect on apoptosis might be isoform-dependent. In myoblasts, eEF1A2 levels correlate with differentiation and possess anti-apoptotic properties, whereas expression of the isoform eEF1A1 leads to the opposite effect (Ruest et al., 2002).

## INTRODUCTION

### Viral propagation

Viruses depend on host cell proteins for replication and propagation, leading some viruses to incorporate eEF1A in their life cycle. eEF1A has been mostly implicated in the replication of positive single-strand RNA viruses (+ssRNA viruses), as its RNA can be directly translated by the cellular protein synthesis machinery. Examples of positive-strand RNA viruses linked to eEF1A include dengue virus, turnip yellow mosaic virus, tobacco mosaic virus, turnip crinkle virus, West Nile virus, and coronaviruses (D. Li et al., 2013; Sasikumar et al., 2012). Interestingly, negative single-strand RNA viruses (-ssRNA viruses), like the vesicular stomatitis virus, have also shown associations with eEF1A (T. Das et al., 1998).

Interestingly, a study published in 2020 suggested that eEF1A could be involved in the host cell's response to SARS-CoV-2 infection by impacting the host's antiviral response and protein translation machinery (White et al., 2021).

eEF1A's affinity for viral RNAs might stem from structural similarities between viral RNAs and tRNAs, as canonical partners of eEF1A. In some cases, eEF1A can also interact with viral polymerases and support the formation of virus replication complexes (D. Li et al., 2013).

### **5.3. eEF1A2 in neurons**

The presence of eEF1A2 within the excitatory PSD of rat cerebral cortex has been established. Notably, eEF1A2 demonstrates colocalization with postsynaptic proteins such as PSD-95 and SynGAP $\alpha$ , but does not exhibit colocalization with synaptophysin, a presynaptic marker (S.-J. Cho et al., 2004). The process of synaptic localization is orchestrated through the domain III of the protein, as highlighted by Cho and colleagues (2012).

### **5.4. Post-translational modifications of eEF1A2**

Several post-translational modifications (PTMs) have been described for eEF1A. For instance, numerous phosphorylation events have been reported. For instance, eEF1A1 is phosphorylated at Ser<sup>300</sup>, affecting its binding to aa-tRNA and leading to protein synthesis inhibition (K. Lin et al., 2010). Additionally, eEF1A2 has been identified as a target for phosphorylation at Ser<sup>205</sup> and Ser<sup>358</sup> by the stress-induced c-Jun N-terminal kinase (JNK). This phosphorylation promotes degradation of newly synthesized proteins by the proteasome (Gandin et al., 2013), thereby linking eEF1A2 to protein quality control mechanisms. Because Ser<sup>358</sup> is evolutionarily conserved but not present in isoform eEF1A1, its PTM could constitute a relevant difference in the physiological roles of the two isoforms.

In recent years, lysine methylation has emerged as a prominent PTM at both N- and C-terminal ends of eEF1A. This modification is particularly abundant, underscoring its potential significance in eEF1A regulation. For example, S. Liu and colleagues (2019) showed that demethylation of eEF1A stimulates protein synthesis in cancer cells and promotes tumorigenesis. However, it is worth noting that the effects of lysine methylation on eEF1A's function as elongation factor appears relatively subtle, as highlighted by other investigations (Jakobsson et al., 2018). This observation suggests that this PTM might primarily affect the non-canonical functions of eEF1A.

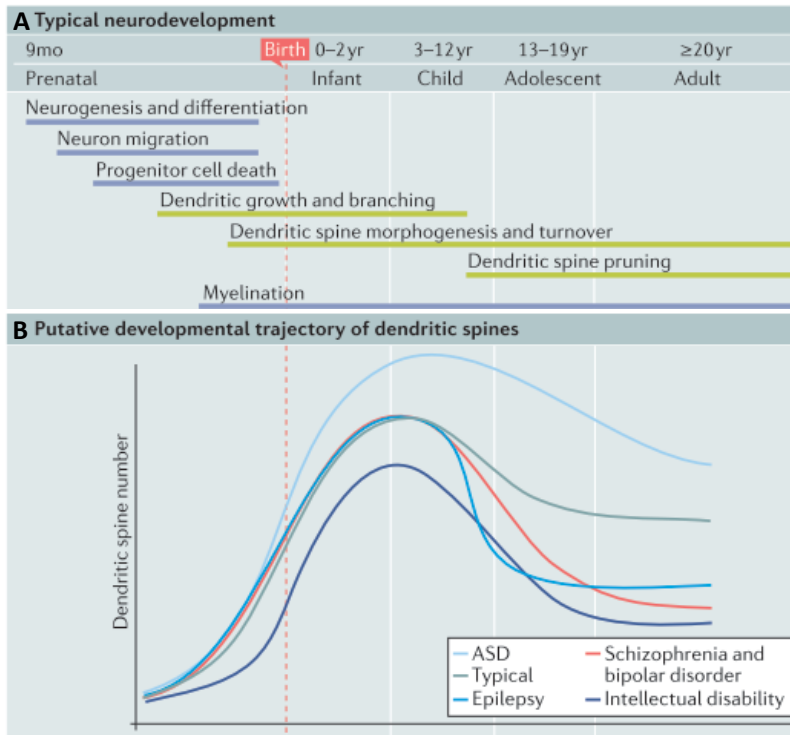
Consequently, further research is needed to unravel the intricate roles and functional consequences of eEF1A regulation by PTMs.

## **6. Alterations of synaptic plasticity in disease**

During human brain development, dendrites appear at 17 - 25 weeks of gestation, whereas spines appear late in the second trimester at 26 - 34 weeks. The number of spines increases rapidly and reaches its peak during childhood (1 - 2 years old). Then, the brain undergoes a process of synaptic pruning, which involves the elimination of excess and unused synaptic connections. This process continues into adolescence and adulthood and makes the brain more efficient by strengthening important connections and eliminating unnecessary ones. Spines are highly dynamic and can be maintained or eliminated as an experience-dependent optimization of neuronal circuits (Forrest et al., 2018).

Thus, alterations in these processes of spine formation and elimination could lead to neuropsychiatric disorders such as autism spectrum disorder (ASD), epilepsy, intellectual disability, schizophrenia, or bipolar disorder. Given the tight relationship between spine structure and function, even small alterations in spine structure may reveal a huge dysfunction at the cellular or circuit level. Understanding the molecular underpinnings of spine pathology may provide insights into the causes and treatments (Forrest et al., 2018; Penzes et al., 2011) (Fig. 12).

As an organism ages, it experiences a gradual decline in synaptic density and complexity that is considered a normal part of the aging process and is not associated with any pathological condition (Diniz & Crestani, 2022). These morphological changes may also be associated with changes in memory, learning, and other cognitive functions. However, the extent and impact can vary among individuals. Thus, recent research is also focused on understanding the underlying mechanisms of age-related synaptic changes and their relationship to cognitive decline to mitigate it.



**Figure 12. Spine and dendrite development in health and disease.** (A) Timeline of the main cellular events during human brain development. (B) Trajectories of dendritic spine development during typical development or in neuropsychiatric disorders including autism spectrum disorder (ASD), epilepsy, schizophrenia and bipolar disorder, and intellectual disability. From Forrest et al., 2018.

## 7. RNA localization in dendrites and axons

The spatial organization of mRNAs in subcellular compartments guarantees temporal and spatial control of gene expression, providing the basis for cell polarization. mRNA localization is essential for several processes, such as embryo development, establishing differences in cell fate, and for neuronal function (Chartrand et al., 2001).

mRNA localization is particularly relevant in polarized cells, including differentiated neurons, because the site of transcription can be distant from the ultimate destination of the protein. Local protein synthesis avoids transporting proteins through long distances, a process that could not be possible for proteins with short half-life times. Moreover, localizing mRNAs proves to be more cost-effective than transporting individual proteins.

In single-cell organisms, such as bacteria and fungi, asymmetric distribution of mRNA and proteins enables the modulation of gene expression and organization of cellular functions. In multicellular organisms, this process is particularly relevant

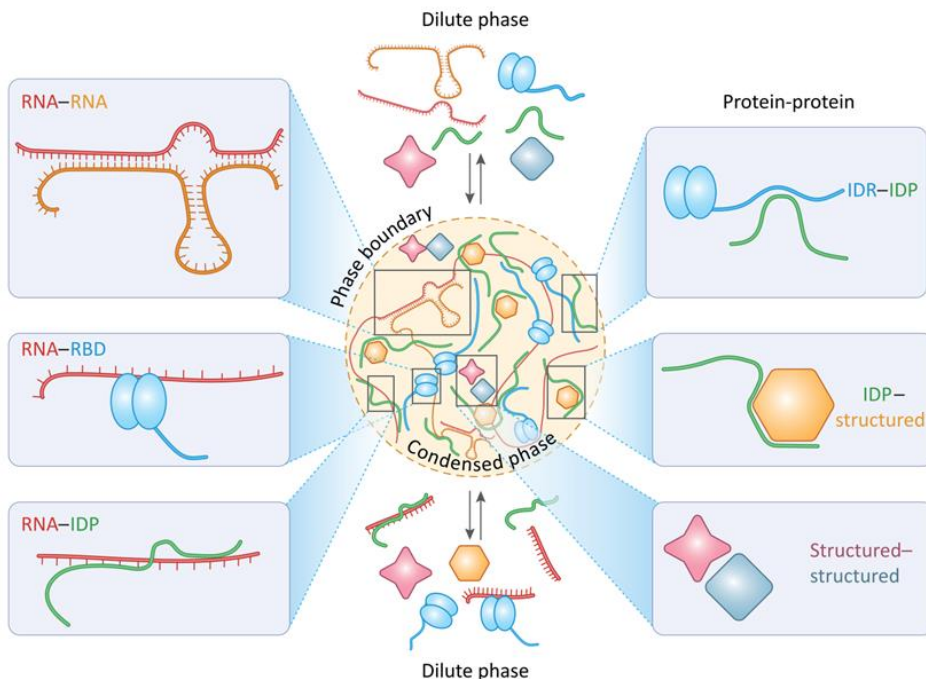
during developmental processes, such as embryonic patterning and asymmetric cell division (S. Das et al., 2021).

RNAs bind RNA-binding proteins (RBPs) and form RNA-protein complexes named RNA granules. The concept of RNA granules includes stress granules (SGs), processing-bodies (P-bodies), and transport granules. Transport granules are of particular interest to our study, which encompass RBPs, ribosomal components and mRNAs.

## 8. Mechanism of neuronal RNA granule assembly

### 8.1. Liquid-liquid phase separation (LLPS)

RNA granules are membrane-less organelles (MLOs) formed through LLPS. This phenomenon emerges from multivalent and dynamic interactions between RNA-RNA, RNA-protein and protein-protein components that enable the de-mixing of liquid droplets from the rest of the liquid cytosol. Notably, these structures can dynamically exchange components with the cytosol or other MLOs (Van Treeck et al., 2018) (Fig. 13).



**Figure 13. Interactions driving membrane-less organelle (MLO) formation.** Liquid-liquid phase separation (LLPS) is due to different types of interactions. These include RNA-RNA, RNA-protein through RNA binding domains (RBD), RNA-protein through intrinsically disordered regions/protein (IDR/IDP), and different protein-protein interactions such as IDR-IDP, IDP-structured or structured-structured. From Ryan and Fawzy, 2019.

## INTRODUCTION

There are several types of RNA granules: RNA transport granules, P-bodies and SGs, which present differences in their protein composition, intracellular distribution, and function. RNA transport granules are involved in the transport of specific mRNAs from the nucleus to specific subcellular locations. On the other hand, P-bodies are involved in mRNA degradation, storage, and translational repression. Finally, SGs appear in response to cellular stress conditions and are involved in sequestering and storing mRNAs temporarily until the stress disappears. Protein composition is different between them, although some proteins can be shared between the different structures (Putnam et al., 2023).

The fundamental principle underpinning LLPS is multivalency, a phenomenon in which a single biomolecule can interact simultaneously with multiple copies of itself or with various biomolecules. In the context of proteins, multivalency is often, but not exclusively, facilitated by IDRs. These IDRs are regions of polypeptide chains that lack a stable 3D structure but can adopt many non-globular conformations. This feature facilitates interactions by allowing interacting motifs to be presented in different orientations (Mittag & Parker, 2018; Protter et al., 2018).

Importantly, proteins condensed into liquid condensates maintain their native physiological conformation and functions, in contrast to protein aggregates that are usually misfolded and immobile (Hayashi et al., 2021). However, the high concentration of specific biomolecules within a condensate facilitates further transitions in the material properties, resulting in gelatinous or solid assemblies, as well as favoring fibrillar structures, that can be physiological or not (Bose et al., 2022; Elbaum-Garfinkle & Brangwynne, 2015). In fact, the liquidity of the granule determines the capability of exchanging its components with the surrounding cytosol and it can vary in physiological processes like aging (Pushpalatha et al., 2022) or even during development (Bose et al., 2022). For instance, mutations in RBPs like FUS and TDP-43 have also been linked to solidification of these structures that ultimately lead to altered mRNA trafficking and neuronal dysfunction (Gopal et al., 2017; Qamar et al., 2018).

### **8.2. Cis-acting elements**

Additionally to the coding sequence, eukaryotic mRNAs contain two UTRs at the 5' and 3' ends, which play a pivotal role in different aspects of post-transcriptional regulation. Most mRNA regulatory elements are present within the 5' and 3'UTRs, enabling binding of protein complexes that form messenger ribonucleoprotein particles (mRNPs). The 5'untranslated region (5'UTR) is mainly governing mRNA translation, whereas the 3'UTR participates in functions related to mRNA



metabolism, such as nuclear export, cytoplasmic localization, translation efficiency, and mRNA stability (Andreassi & Riccio, 2009).

mRNA localization is mostly determined by cis-acting elements present in the 3'UTR, also known as "zipcodes" or localization elements (LEs). These elements facilitate mRNA localization through several mechanisms: active and directed transport of the transcript to a subcellular region, regulation of mRNA stabilization and degradation, and localized trapping of diffusing mRNA within the cytoplasm (Martin & Ephrussi, 2009).

While some LEs, as well as their binding proteins, have been identified in neurons (as summarized in table 2, from Andreassi & Riccio, 2009), the knowledge about most zipcode sequences remains limited due to the low degree of conservation within 3'UTR sequences.

Transcript	Organism	Subcellular location	LE position	Minimum LE length (nt)	Binding proteins
$\beta$ -actin	Rat	Filopodia	3'UTR	54	ZBP1
Arc	Rat	Dendrites	3'UTR	350 (strong) 370 (weak)	
BDNF	Mouse, rat	Dendrites	3'UTR		
CamKII	Rat	Dendrites	3'UTR	1200, 30, CPE	CPEB
Dendrin	Rat	Dendrites	3'UTR	1000	
IP3RI	Mouse	Dendrites	3'UTR		Hfz
MAP2	Rat	Dendrites	3'UTR	640	MARTA1 MARTA2
Nanos	<i>Drosophila</i>	Dendrites	3'UTR		
Neurogranin	Rat	Dendrites	3'UTR	30	
NMDA receptor subunit NR1	Rat	Dendrites	5'UTR	24	60 and 70 kDa proteins
Protein kinase M $\zeta$	Rat	Dendrites	3'UTR	84	
RhoA	Rat	Axons	3'UTR		
Shank1	Rat	Dendrites	3'UTR	200	
Syntaxin	<i>Aplysia</i>	Axon hillock	3'UTR	CPE	CPEB
Tau	Rat	Axons	3'UTR	91	Ilf3 NF90
vasopressin	Rat	Dendrites	ORF+3'UTR		PABP

**Table 2. List of mRNAs whose localization elements (LE) have been characterized in neurons.** From Andreassi & Riccio, 2009.

In recent years, substantial efforts have been directed towards elucidating the sequences that function as zipcodes for various mRNAs. First approaches involved

## INTRODUCTION

constructing chimeric reporter gene constructs fused with putative LEs. This approach enabled the identification of specific sequences essential for mRNA localization. These studies have revealed that zipcodes can span from a few nucleotides to over 1 kilobase in length, with a prominent presence within 3'UTRs (Jambhekar & Derisi, 2007).

While thousands of localized mRNAs exist, only a limited number of zipcodes have been characterized to date. An innovative study from Chekulaeva's group recently described a new protocol for identifying neuronal zipcodes within 3'UTRs. This methodology yielded the discovery of two new zipcodes, contributing to our understanding of the intricate mechanisms guiding mRNA localization (Mendonça et al., 2023).

In summary, cis-acting elements guide the localization, stability, and translation of mRNAs enabling dynamic control of gene expression. While the understanding of zipcode sequences and their binding proteins is still unfolding, recent studies continue to expand our comprehension of these complex regulatory mechanisms.

### **8.3. Trans-acting factors**

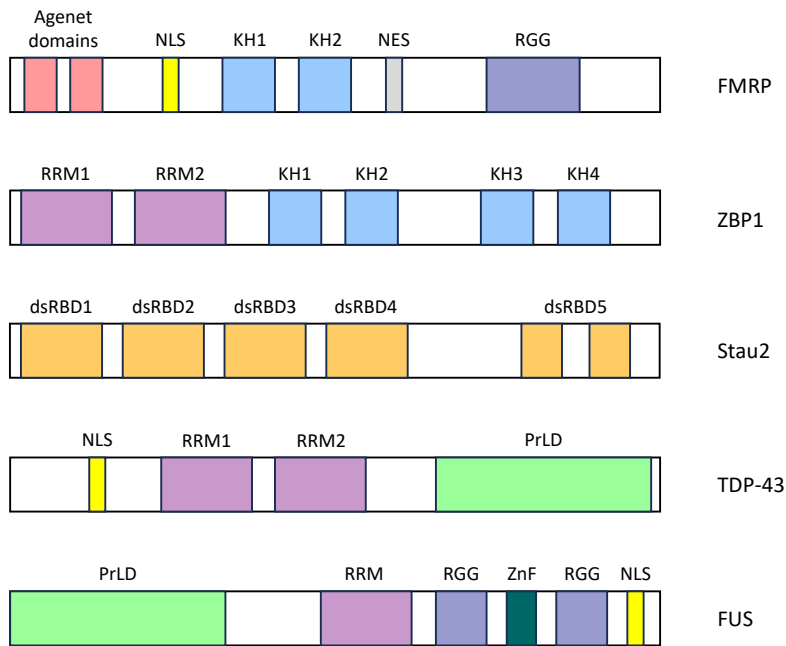
Cis-acting elements are recognized by RBPs that act as trans-elements. These RBPs can bind many different mRNA targets through different RNA binding domains. Typically, multiple binding domains co-exist in one RBP, to enhance specific RNA binding (Corley et al., 2020) (Fig. 14).

The human genome presents more than 2000 known RBPs. Among them, certain RBPs, like those from the ELAVL and RBFOX protein families, are exclusively expressed in neurons. A larger group is broadly expressed across different cell types but presents neuron-specific functions including FUS, ZBP1, and FMRP proteins (Darnell, 2013).

Trans-acting factors have been identified from two types of studies: from affinity purification of proteins that bind known LEs, and from genetic screenings for genes involved in mRNA localization. For instance, Staufén (Stau) was first identified in a genetic screening as a protein required for the localization of maternal determinants to the posterior pole of *Drosophila* eggs (St Johnston et al., 1991). Later, investigations revealed that most Stau2-co-purifying mRNAs in the hippocampus are present in neuronal processes, suggesting that Stau is implicated in dendritic mRNA regulation (Heraud-Farlow & Kiebler, 2014).

Importantly, several RBPs involved in mRNA transport also contribute to translational repression. For example, ZBP1-bound  $\beta$ -actin mRNA is silent during trafficking and its translation happens when ZBP1 is phosphorylated and

inactivated, as mentioned early. Similarly, FMRP also represses translation during transport (G. J. Bassell & Warren, 2008). In summary, trans-acting factors are necessary not only for mRNA transport but also for translational control.



**Figure 14. RNA-binding proteins display different RNA binding domains.** Scheme of five RBPs including FMRP, ZBP1, Stau2, TDP-43 and FUS, and their corresponding domains. Among these, the RNA binding domains correspond to: K Homology (KH), arginine-glycine-glycine box (RGG), RNA recognition motif (RRM), double-stranded RNA binding domain (dsRBD), and prion-like domain (PrLD). Non-RNA binding motifs like Agenet domains, Zinc finger (ZnF), and nuclear localization signal (NLS) are also shown.

### FMRP

Fragile Mental Retardation Protein (FMRP) is the resultant protein of the *Fmr1* gene. It functions as an RBP and represses local translation within dendrites. Loss-of-function mutations in *Fmr1* gene result in fragile X syndrome (FXS), a neurological disorder characterized by cognitive impairment. The absence of FMRP disrupts synaptic function and morphology, ultimately leading to defects in brain function. Intriguingly, in the absence of FMRP, global protein synthesis is increased by approximately 20 %, suggesting that an excess in protein translation may be a key contributor to the pathophysiology of FXS (Richter et al., 2015).

In mammals, the main isoform of FMRP is a 71-kDa protein with several evolutionary conserved functional domains. These domains encompass three RNA-binding motifs, including two K homology domains (KH1 and KH2), along with an arginine-glycine-glycine (RGG) box. FMRP further features nuclear localization and

## INTRODUCTION

export signals (NLS and NES, respectively) that mediate its shuttling into and out of the nucleus. Notably, it presents tandem Agenet domains (TAD) at the N-terminal part of the protein, likely contributing to its functional interactions (Santoro et al., 2012).

Remarkably, phosphorylation of FMRP does not affect its RNA binding capacity, but it does affect its association with ribosomes to inhibit translation. Specifically, phosphorylated FMRP appears to associate with stalled ribosomes, leading to translational inhibition. Conversely, when unphosphorylated, FMRP enables translation and contributes to the disassembly of RNA granules, potentially impacting local protein synthesis dynamics (Ceman et al., 2003; Tsang et al., 2018).

### ZBP1

Insulin-like Growth Factor II mRNA-Binding Protein (IGF2BP) was first identified from chicken and named Zipcode Binding Protein 1 (ZBP1). Homologs were later discovered in *Xenopus* and *Drosophila* and named RBP-Vg1/Vera and IMP1, respectively. In particular, mammals encode for three IGF2BP isoforms, referred as IGF2BP1, IGF2BP2, and IGF2BP3, which correspond to their gene names, respectively.

In neurons, ZBP1 regulates axonal growth, dendritic branching, as well as synaptic morphology (Eom et al., 2003; Perycz et al., 2011) through transport regulation, and translation and degradation of some neuronal mRNAs. The best studied target of ZBP1 is  $\beta$ -actin mRNA, as previously detailed in section “8.2. Cis-acting elements” (Hüttelmaier et al., 2005). Regulation of  $\beta$ -actin mRNA is particularly important to regulate cytoskeleton organization.

ZBP1 contains six putative RNA binding domains, two RNA recognition motifs (RRMs) and four KH domains. Studies suggest that RNA binding is mediated through either two (KH3-KH4) or four (KH1-KH2-KH3-KH4) of the KH domains, but not through the RRM domains (Nielsen et al., 2002). For instance, KH3 and KH4 are responsible for  $\beta$ -actin mRNA binding, granule formation and cytoskeletal association in chicken embryo fibroblasts (Farina et al., 2003).

Recent research has demonstrated that ZBP1 is essential for proper brain development and neonatal survival. In addition, the absence of ZBP1 results in a decreased anchoring and active transport of  $\beta$ -actin-containing mRNPs, demonstrating that this RBP plays an important role in mRNA transport and anchoring (Núñez et al., 2022).

### Staufen

Staufen (Stau) is a double-strand RNA-binding protein (dsRBP) mainly expressed in the brain, where it exerts regulatory functions on mRNA metabolism and translation. In mammals, there exist two orthologues of Stau, namely Stau1 and Stau2, both of which exhibit several splice isoforms. Stau1 is present in most cell types, including neurons, whereas Stau2 is only expressed in the brain (Monshausen et al., 2001). Although both Stau1 and Stau2 are found in the dendritic compartment, Stau2 is localized to more distal dendrites than Stau1. Furthermore, it is worth noting that these two proteins are not present in the same RNA granules (Duchaîne et al., 2002), suggesting distinct roles.

Stau2 has a crucial role in the morphogenesis of dendritic spines. Notably, it is involved in synaptic plasticity, specifically in mGluR-LTD and establishment of long-term memory formation (Heraud-Farlow & Kiebler, 2014).

### FUS and TDP-43

Fused in sarcoma (FUS) and TAR DNA-binding protein 43 (TDP-43) are DNA/RNA-binding proteins characterized by containing prion-like domains (PrLDs) that help the formation of RNA granules by LLPS. Both RBPs are involved in RNA metabolism, specifically in transcriptional regulation, pre-mRNA splicing, RNA processing, and RNA localization. Within their structure, they contain PrLDs as well as folded RRM and other RNA-binding domains such as RRG boxes, in the case of FUS (Portz et al., 2021).

Regulation of mRNAs encoding proteins required for neuronal maintenance, synaptic activity, and cytoskeleton function has been demonstrated for TDP-43 (Sephton et al., 2011) but also for FUS (Yokoi et al., 2017). Mutations in both proteins have been linked to amyotrophic lateral sclerosis (ALS) and frontotemporal dementia (FTD) (Prashad & Gopal, 2021).

*In vitro* condensates of PrLD-containing RBPs have shown a maturation process over time into less dynamic gels, fibers, and aggregates that is commonly named liquid-to-solid transition (Bose et al., 2022; Maharana et al., 2018). This phenomenon has been observed for FUS (Patel et al., 2015) and TDP-43 (Prasad et al., 2019) and enhanced by some ALS- and FTD-associated mutations.

## **8.4. Assembly of RNA granules**

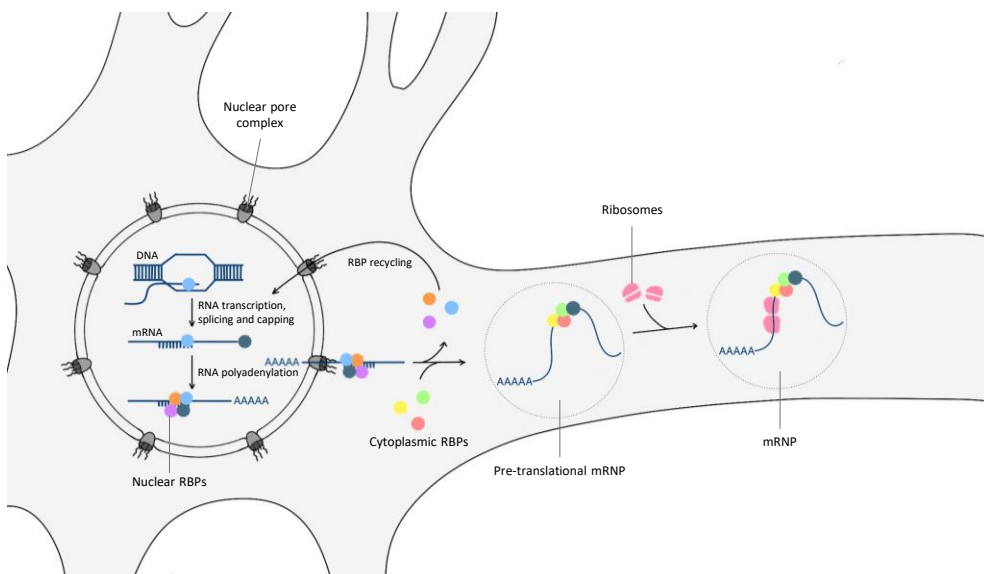
Nascent pre-mRNAs are capped, spliced, and polyadenylated co- and post-transcriptionally in the nucleus before they exit the nuclear pore as mature mRNAs. These processes ensure the formation of mature mRNAs that are ready for export through the nuclear pore complex.

## INTRODUCTION

As mRNAs make their way into the cytoplasm, they carry with them several RBPs or associated factors that were initially bound in the nucleus. One such example is the exon junction complex (EJC), which is retained by the mRNA even after nuclear export. Additionally, once exported, cytoplasmic RBPs can bind to specific sequences within the 3' and 5'UTRs of mRNAs. The ensemble of RBPs and mRNA forms a pre-translational mRNP complex, devoid of ribosomes at this stage (Fig. 15).

These cytoplasmic pre-translational mRNPs are primed for recruitment into the translational machinery and subsequently transported along dendrites through motor protein binding. During this transport, mRNPs travel stalled in translation. Upon reaching their destination, often near synapses, the mRNP complex is anchored. The precise molecular mechanisms underlying this anchoring process remain a subject of ongoing research; however, it is hypothesized that interactions with cytoskeletal elements or local scaffolding proteins play a role.

Once anchored in place, the mRNA within the mRNP can be sensitively responsive to local signals. When specific cues or stimuli are received, the localized mRNA can undergo translation, leading to the synthesis of proteins that are critically required near the synapses (Mateu-Regué et al., 2020; Turner-Bridger et al., 2020). This orchestration of events enables neurons to rapidly generate proteins in specific subcellular regions in response to their functional demands.



**Figure 15. Schematic overview of cytoplasmic mRNPs assembly in neurons.** Nascent mRNAs are transcribed, capped, spliced and polyadenylated before exiting the nucleus through the nuclear pore complex. Some nuclear RBPs remain bound in the cytoplasm, where cytoplasmic RBPs bind the exported mRNA. mRNAs bound to several RBPs form a pre-translational mRNP which lacks the translational machinery. When ribosomes are incorporated, the mRNP is completely formed.

Determining the constituents of RNA granules has been a long-standing interest. Researchers have pursued various strategies to unravel the composition of these dynamic cellular structures. One approach involved the isolation and purification of heavy granules using density gradient centrifugation coupled to mass spectrometry (El Fatimy et al., 2016; Elvira et al., 2006). In addition to the density gradient centrifugation approach, other research groups have employed immunoprecipitation techniques to selectively capture specific components of RNA granules. For instance, distinct RBPs, such as Barentsz and Stau2 have been immunoprecipitated from mouse brains to investigate their presence and partners within these granules (Fritzsche et al., 2013). Both approaches have consistently shown an enrichment of RBPs within these granules. The ongoing investigation into the composition of RNA granules continues to provide insights into the mechanisms governing localized translation and regulation of gene expression in a neuronal context.

Single-molecule FISH (smFISH) experiments have provided valuable insights into the spatial organization of dendritically localized mRNAs within neurons. These experiments have revealed that each mRNA specie exists as a single, independent RNA granule along dendrites (Batish et al., 2012; Turner-Bridger et al., 2018). For example, Mikl and colleagues (2011) showed that different mRNA species, such as *β-actin*, *CaMKIIα*, and *MAP2* transcripts, are present in distinct complexes within dendrites. The formation of homotypic clusters of specific mRNAs enables a fine-tuning of local translation of certain mRNAs without affecting other localized mRNAs.

## 9. Transport of RNA granules

Real-time imaging techniques have helped in the understanding of dynamic transport of RNA granules within neurons. RNA granules motility has been assessed through labeling of endogenous RNAs (Wong et al., 2017), by fluorescently tagging specific transcripts (Dictenberg et al., 2008; Dynes & Steward, 2012; Rook et al., 2000; Yoon et al., 2016) or by fluorescently tagging RBPs previously identified as granules components (Chu et al., 2019; El Fatimy et al., 2016; Tiruchinapalli et al., 2003).

Those studies have shown that transport of mRNPs is characterized by intermittent and stochastic motion, including “run” phases consisting of directed motion in anterograde or retrograde direction, and “rest” phases of slow diffusive movement, which constitutes more than the 80 % of the transport time. This behavior has been described for several mRNAs in neurons, such as *CaMKIIα* (Rook et al., 2000), *Arc* (Dynes & Steward, 2012), *β-actin* (H. Park et al., 2014), and *Rac1* (Chu et al., 2019).

## INTRODUCTION

The transport of RNA granules depends on MTs and their associated motor proteins. Kinesins are responsible for promoting anterograde transport (plus-end directed transport), while dyneins mediate retrograde transport (minus-end directed transport) (Broix et al., 2021). In contrast to membrane-bound organelles (e.g., mitochondria and lysosomes) transport, RNA granules are believed to be transported by molecular adaptors that facilitate interactions between motors and these membrane-less structures (H. Wu et al., 2020).

Interestingly, the same mRNA specie can be transported by different motors and associated adaptors, suggesting a complex regulation of transport directionality and speed. This transport is driven by the force-dependent kinetics of opposing motors (Hendricks et al., 2010). For instance,  *$\beta$ -actin* mRNA, as the best-characterized neuronal transport granule, moves at speeds of 0.5 - 2  $\mu\text{m/s}$  in both dendrites and axons (H. Park et al., 2014; Yoon et al., 2016). These speeds are similar for other MT-dependent dendritically localized mRNAs, such as *Arc* (S. Das et al., 2018).

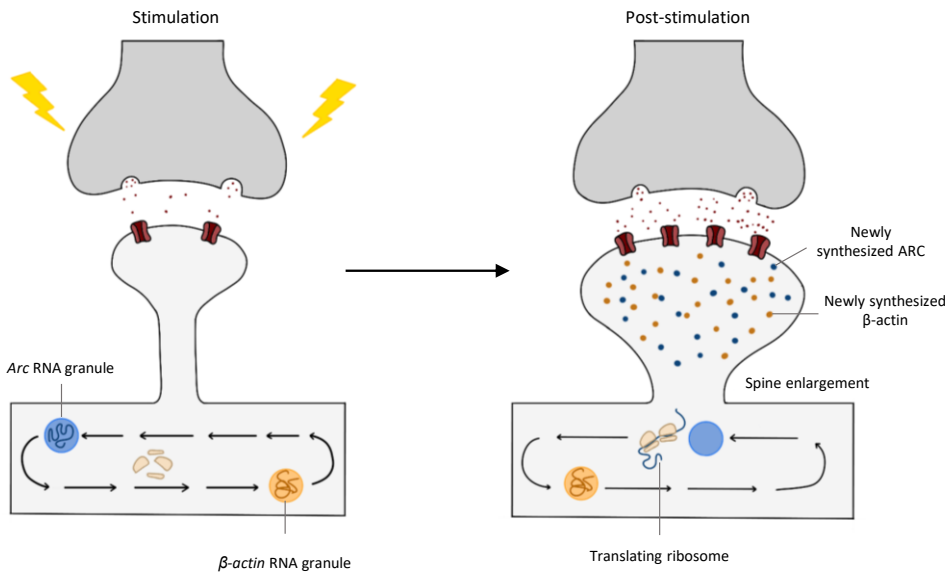
Recent evidence has highlighted additional mechanisms of long-range transport. "Hitchhiking" involves RNA granules attaching to motile membrane-bound organelles, like lysosomes, using adaptors like annexin A11 (Liao et al., 2019). This strategy enables long-distance transport by using the movement of other cellular components. Additionally, it has also been demonstrated that late endosomes carry RNA granules at their membrane and serve as locations to axonal local protein translation (Cioni et al., 2019).

Although motors are bound to mRNAs until they reach their final localization, it remains unclear if motor proteins are exchanged during transport, if they dissociate from mRNAs upon reaching their final localization, or if they are responsible for stopping mRNA transport. Continued research in this field promises to unveil further details about the mechanisms governing the transport of RNA granules.

### **9.1. Sushi belt theory**

The "sushi belt" theory is a metaphorical concept that links the movement of certain mRNAs within dendrites to the rotating conveyor belt used in sushi restaurants. Just as sushi plates move along the conveyor belt for customers to choose, this theory proposes that some mRNAs may move bidirectionally, patrolling multiple spines, waiting for cues like synaptic activity to induce local protein synthesis and influence synaptic function (Doyle & Kiebler, 2011) (Fig. 16).





**Figure 16. Sushi belt model.** RNAs like  $\beta$ -actin or *Arc* are transported along the MT cytoskeleton, as a sushi conveyor, bidirectionally within dendrites. RNAs are transported in membrane-less structures named RNA granules, where translation is stalled. In the sushi belt model, RNA granules patrol a group of synapses in dendrites waiting a synapse to become activated. Following stimulation, the RNA granules localize to the base of stimulated spines and undergo local translation to generate a new pool of proteins. The newly synthesized proteins (blue and orange dots) participate in enlarging the spine head and strengthening the synapse. Adapted from S. Das et al., 2021.

The concept is supported by experiments that have tracked the dynamics of specific mRNAs. For example, Bauer and colleagues (2019) provided evidence for this model by tracking *Rgs4* 3'UTR anterograde trafficking and synaptic recruitment dependent on neuronal activity. The “sushi belt theory” provides a conceptual framework to understand how dendritic mRNAs know where they are going and where they do need to be translated. However, deeper research is needed to confirm this theory for other mRNAs.

## 10. Anchoring of RNA granules

Anchoring mRNAs at its target site after transport is crucial for localized protein synthesis and proper synaptic function. Little is known about the molecular mechanisms underlying the anchoring process but there are several examples in various model systems that provide insights into this process.

In some cases, the protein encoded by the mRNA itself is responsible for its anchoring. For instance, in *S. cerevisiae*, the *ASH1* mRNA is anchored in the bud tip by the translated protein Ash1p (Beach et al., 1999). Similarly, in *Drosophila melanogaster*, the Oskar protein is also involved in the anchoring of its own mRNA in the posterior pole of the oocyte (Rongo et al., 1995).

## INTRODUCTION

For other mRNAs and in other cell models, the molecular mechanisms are less clear. In axon terminals of *Xenopus* embryos, it has been demonstrated that RNA granules are docked at sites of new branches emergence, indicating a potential anchoring mechanism (Wong et al., 2017). A similar behavior has been reported in dendrites of mature hippocampal neurons, where certain mRNAs, such as  $\beta$ -actin (Yoon et al., 2016) or *Arc* (Dynes & Steward, 2012), preferentially dock at the base of dendritic spines.

The precise and timed targeting of individual dendritic mRNAs to distinct synapses remains unknown. One theoretical concept is the “RNA signature” hypothesis, proposing that specific regulatory elements within each mRNA dictate its transport, localization, and translational control (Doyle & Kiebler, 2011).

Overall, while significant progress has been made in understanding the process of anchoring mRNAs, further research is needed to uncover the precise molecular mechanisms underpinning this process.

### **11. Local translation of RNA granules**

According to the prevailing model, mRNAs are not translated while being transported in RNA granules. This notion is primarily supported by proteomic studies of RNA granules, which have identified various translational repressors within these granules (El Fatimy et al., 2016; Elvira et al., 2006; Fritzsche et al., 2013).

Different studies have proposed varying degrees of translational repression within RNA granules. Some studies suggest that translation is stalled at the initiation phase (Fritzsche et al., 2013), meaning that the ribosome binds to the mRNA but does not progress to actual protein synthesis. Other studies claim that mRNAs are transported in stalled polysomes corresponding to the elongation phase (Graber et al., 2013, 2017; Langille et al., 2019).

These findings collectively suggest that the translational state of mRNAs within mRNPs probably involves a combination of initiation and elongation repression mechanisms. Regulation in both steps will ensure that mRNAs are translationally repressed during transport, allowing for precise control until the local translation is needed. Further research regarding the control of mRNA expression and localization is needed.





**AIMS**



The main objective of this project is to understand the molecular mechanisms involved in control of local mRNA expression in dendritic spines. To achieve this goal, we propose to tackle the following specific objectives:

- 1. To investigate the molecular mechanisms that regulate eEF1A2 in the synaptic function.**
  - 1.1. To analyze the role of eEF1A2 phosphorylation in dendritic spines.
  - 1.2. To analyze the putative functions of phosphorylated eEF1A2.
  - 1.3. To analyze the functional relevance of eEF1A2 phosphorylation in synaptic plasticity.
  
- 2. To investigate the molecular mechanisms that regulate the dissociation of mRNPs in dendritic spines.**
  - 2.1. To identify putative modulators of RNA granule entrapment and disaggregation.
  - 2.2. To study DrebrinA interactors and its functional relevance in RNA granules dynamics.





## **METHODS**



## 1. CELL CULTURES/CELL BIOLOGY

### 1.1. Primary dissociated cultures

Animal experimental procedures were approved by the ethics committee of the Research Council of Spain (Consejo Superior de Investigaciones Científicas). Hippocampi and cortex were dissected from embryonic day 17.5 (E17.5) CD1 mouse embryos (undetermined sex) in Hanks' Balanced Salts Solution (HBSS) (Biowest, X0507-500) containing 0.6 % glucose and 10 mM HEPES (Merck-Sigma, H3375). After dissection, tissues were digested with 0.05 % trypsin (Fisher, 15090046) and 0.02 % EDTA (Merck-Sigma, E9884) at 37 °C for 15 min. Enzymatic digestion was stopped by washing the tissue three times with Minimum Essential Media (MEM) (Fisher, 31095029) supplemented with 10 % Fetal Bovine Serum (FBS) (Biowest, S1810-500) and 0.6 % glucose. Hippocampi were left to sediment between washes, avoiding centrifugation, to keep cell viability. Trypsin-treated tissue was then mechanically disaggregated by using flame-polished Pasteur pipettes. Then, cells were plated on previously coated poly-D-lysine (Merck-Sigma, P7886) plates (0.5 mg/ml poly-D-lysine in borate buffer, pH 8.5) containing plating media (MEM supplemented with 10 % FBS, 0.6 % glucose, and penicillin-streptomycin (Fisher, 15140122)). For imaging experiments, hippocampal neurons were plated at a density of  $2 \times 10^4$  cells/cm<sup>2</sup> in 4-well plates (Fisher, 10507591) and ibidi  $\mu$ -Dish 35 mm (Inycom, 81156). For biochemistry experiments, cortical neurons were plated at a density of  $5 \times 10^4$  cells/cm<sup>2</sup> in 10-cm plates. Cells were plated in plating media for 2-4 h and then media was substituted for maintaining media consisting in Neurobasal (Fisher, 11570556) supplemented with 2 % B27 (Fisher, 11530536), 1 % GlutaMAX (Fisher, 35050061), and penicillin-streptomycin. Neurons were placed in incubators at 37 °C in 5 % CO<sub>2</sub>.

### 1.2. Hippocampal slice culture

Hippocampal organotypic slice cultures were prepared from postnatal day 6 to 7 rats as described (Bosch et al., 2014). Briefly, hippocampi were dissected from rat brains in partially frozen dissection media gassed with carbogen (5 % CO<sub>2</sub>/95 % O<sub>2</sub>) and 400  $\mu$ m-thick slices were prepared with a tissue chopper (Stoelting 51350) in sterile conditions. Individual slices were cultured at 35 °C on permeable cell culture inserts (Merck-Millipore, PTSP06H48) with MEM media supplemented with 20 % horse serum, 27 mM D-glucose, 6 mM NaHCO<sub>3</sub>, 2 mM CaCl<sub>2</sub>, 2 mM MgSO<sub>4</sub>, 30 mM HEPES, 0.01 % ascorbic acid, and 1  $\mu$ g/ml insulin. pH was adjusted to 7.3 and osmolality to 300-320 mOsm. Media was completely changed every 2 days.

## METHODS

### 1.3. Cell lines

HEK293T and Neuro-2a cells were grown in Dulbecco's Modified Eagle Media (DMEM) high glucose (Biowest, L0104-500) supplemented with 10 % FBS and penicillin-streptomycin. To generate the shEF1A2 stable cell line, Neuro-2a cells were infected with lentiviral particles expressing pLKO-shEF1A2 targeting eEF1A2 3'UTR sequence (5'-CAAAGTCCAGTGGAAATTCTT-3') (IRB Functional Genomics Facility). After infection, cells were subjected to puromycin (Sigma, P8833) treatment (5 µg/ml) for selection of stable cell lines.

## 2. MOLECULAR BIOLOGY

### 2.1. DNA constructs

eEF1A2, eEF1B2, actin, DrebrinA, and ZBP1 were amplified using primers shown in table 3 using Phusion High-Fidelity DNA Polymerase (Fisher, 10024537). Site-directed mutagenesis in complementary DNAs (cDNAs) were performed by In-Fusion HD (Takara, 638909) using primers shown in table 4. pcDNA3Flag5', pNBM470, pEGFP-C3, mEGFP-C3, and mScarlet-C1 were used as host vectors. Restriction enzyme digestion was performed following manufacturer's instructions. Dephosphorylation and ligation was performed using Rapid DNA Dephos & Ligation Kit (Roche, 4898117001). Ligation products were transformed into DH5α competent cells (Fisher, 18265017). Constructs were checked by restriction enzyme digestions, WB analysis, and/or sequencing in the case of point mutations.

Plasmids were prepared using a NucleoSpin Plasmid kit (Macherey-Nagel, 740588) for cell line transfections and NucleoBond Xtra Midi Plus EF kit (Macherey-Nagel, 740422) for neuron transfection.

Insert gene	Host vector		Oligonucleotide sequence (5'-3')
eEF1A2	FLAG (pcDNA3)	Fw	GCGCGGAATTCAAATGGGCAAGGAGAAGAC
		Rv	GCGCGCTCGAGTCACTTGCCCGCCTTC
eEF1A2	EGFP-C3	Fw	GCGCGCTCGAGTCACTTGCCCGCCTTC
		Rv	CGCGGAATTCTCACTTGCCCGCTTTC
eEF1B2	HA (pNBM470)	Fw	GCGCGGAATTCAAGGATTCGGAGACCTGAAA
		Rv	GCGCGCTCGAGTTAAATCTTGTTAAAAGCAGC
eEF1B2	mScarlet- C1	Fw	GATATCGAATTCTGGATTCGGAGACCTGAAAAC
		Rv	GATATCGGATCCTTAAATCTTGTTAAAAGCAGCCA
Actin	mScarlet- C1	Fw	GAATTCCTCGAGCTGATGACGATATCGCTGCGC
		Rv	GAATTCGGATCCCTAGAAGCACTTGCGGTGC
DrebrinA	FLAG-APEX	Fw	ATCGGCGCCGCTCGCCGGCGTCAGCTTCAG
		Rv	CGATCTCGAGCTAATCACCACCCTCGAAG

DrebrinA	mScarlet-C1	Fw	ATCGCTCGAGCTGCCGCGTCAGCTTCAG
		Rv	CGATGGATCCCTAATCACCACCCTCGAAG
DrebrinA ΔLCR	mScarlet-C1	Fw	ACTGCTCGAGGCGCGTCAGCTTCAG
		Rv	CGATGGATCCTTATGGGAGGGAGGAAGAGA
DrebrinA LCR	mScarlet-C1	Fw	ATCGCTCGAGCTTGACGCCACCTGGACAGC
		Rv	ATACGGATCCCTAATCACCACCCTCGAAG
ZBP1	FLAG-APEX	Fw	CGAGCATGCATCTAGAAACAAGCTTTACATCGGC AAC
		Rv	AATAGGGCCCTCTAGTCACTTCTCCGAGCCTG
ZBP1	mGFP-C3	Fw	GATATCCTCGAGAACAAGCTTTACATCGGCAAC
		Rv	GATATCGAATTCTCACTTCTCCGAGCCTG
ZBP1	mScarlet-C1	Fw	GATATCCTCGAGCTAACAAGCTTTACATCGGCAA C
		Rv	GATATCGAATTCTCACTTCTCCGAGCCTG
FLAG-APEX- NES	pFUW	Fw	GAGGATCAATTCGATGCCACCATGGACTACAAGG
		Rv	ATCGATAAGCTTGATCACTATAGAATAGGGCCCTC T
FLAG-APEX- DrebrinA	pFUW	Fw	GAGGATCAATTCGATGCCACCATGGACTACAAGG
		Rv	ATCGATAAGCTTGATCACTATAGAATAGGGCCCTC T
FLAG-APEX- ZBP1	pFUW	Fw	GAGGATCAATTCGATGCCACCATGGACTACAAGG
		Rv	ATCGATAAGCTTGATCACTATAGAATAGGGCCCTC T

**Table 3. Oligonucleotides used for DNA cloning.** Insert genes, host vectors, and forward (Fw) and reverse (Rv) oligonucleotides sequences are provided.

Mutation	Oligonucleotide sequence (5'-3')	
eEF1A2 S342A	Fw	GTTCCACCGCCCAGGTTATCATCCTGAACCACCCTG
	Rv	ACCTGGGCGGTGAACTGGGCAGCCTCCTGAGGCGG
eEF1A2 S342EE	Fw	CACCGAAGAGCAGGTTATCATCCTGAACCACCCTG
	Rv	ACCTGCTCTTCGGTGAAGTGGGCAGCCTCCTGAGG
eEF1A2 S358A	Fw	CGCTGGCTACGCCCCAGTCATCGACTGTCACACG
	Rv	GGGGCGTAGCCAGCGCTGATTTGCCAGGGTGG
eEF1A2 S358EE	Fw	TGGCTACGAAGAGCCAGTCATCGACTGTCACACGG
	Rv	TGGCTCTTCGTAGCCAGCGCTGATTTGCCAGGG
eEF1A2 S393A	Fw	CCCAAGGCCCTGAAGTCTGGTGATGCAGCCATTGT
	Rv	CTTCAGGGCCTTGGGGTTATCCTCCAGCTTCTTGC
eEF1A2 S393EE	Fw	AAGGAAGAGCTGAAGTCTGGTGATGCAGCCATTGT
	Rv	CTTCAGCTCTTCTTGGGGTTATCCTCCAGCTTCT
eEF1A2 S445A	Fw	AAGAAGGCCGCGGCGCAGGCAAGGTCACCAAGTC
	Rv	GCCGCCGGCCTTCTTCTCCACGTTCTTGATGACGC

## METHODS

eEF1A2 S445EE	Fw	AAGGAAGAGGGCGGCGCAGGCAAGGTCACCAAGTC
	Rv	GCCGCCCTCTCCTTCTTCTCCACGTTCTTGATGA
DrebrinA LCRmut (Mutation in Homer binding motif 1)	Fw	GAACTTCTAGCCACCCGCTGTGACCCAGAGGAGGAAGTAG
	Rv	CAGCGGGTGGCTAGAAGTTCTGGCAGCTCATCAAATTA
DrebrinA LCRmut (Mutation in Homer binding motif 2)	Fw	GTTCCGCTTCTTGACGTTA CAACAAGCCTCCAGAAATCG
	Rv	TAACGTACAAGAAGCGGAAC CTTTGCACATGGCTCTTCTG

**Table 4. Oligonucleotides for site-directed mutagenesis.** Protein mutation and forward (Fw) and reverse (Rv) oligonucleotide sequences are provided.

### 2.2. Gene transfection

Primary dissociated hippocampal neurons were transfected using CalPhos mammalian transfection kit (Takara, 631312). Briefly, hippocampal neurons original media was replaced by transfection media consisting in MEM supplemented with 15 mM HEPES, 1mM sodium pyruvate, 33 mM D-glucose, 2 % B27 at pH 7.45. To produce the DNA/CaP co-precipitate solution (or transfection solution), CaCl<sub>2</sub> solution was mixed with ddH<sub>2</sub>O, DNA plasmid solution and 2x HEPES-Buffered Saline (HBS) buffer. The reaction tube was thoroughly mixed (not vortexed) by blowing air bubbles five times with the pipette into the solution and then pipetted up and down once. Then, the precipitation solution was added to neurons. Cells were incubated with the transfection solution for 45 min in a 5 % CO<sub>2</sub> incubator at 37 °C. Longer incubation time increases the transfection efficiency but could be deleterious for cells. After incubation, the precipitate was visible on the microscope and was dissolved by incubating cells with wash buffer for 5 min consisting in 135 mM NaCl<sub>2</sub>, 20 mM HEPES, 1 mM Na<sub>2</sub>HPO<sub>4</sub>, 4 mM KCl, 2 mM CaCl<sub>2</sub>, 1 mM MgCl<sub>2</sub>, and 10 mM D-glucose at pH 7.3. Then, cells were incubated again with their original media (Neurobasal supplemented with 2 % B27 and 1 % GlutaMAX). Overexpression and viability were checked 16 hours post-transfection.

Organotypic slice cultures were biolistically transfected (Bio-rad, 1652431) at 5 to 7 days *in vitro* (DIV) and imaged 3 to 5 days later. “Bullets” containing DNA-coated gold particles were prepared according to the manufacturer’s protocol. Gold particles were shot at organotypic slices at 2 cm from the gun barrel by helium at a pressure of 100-150 psi. HEK293T and Neuro-2a cells were transfected using Lipofectamine 2000 (Invitrogen, 11668030) or FuGene-HD (Promega, E2311)

according to the manufacturer's protocol. All DNA constructs used in this thesis are shown in Table 5.

Plasmid name	Origin
FLAG (pcDNA3)	Stock from the lab
FLAG-APEX-NES	Addgene #49386
FLAG-eEF1A2 wt	This study
FLAG-eEF1A2 SA	This study
FLAG-eEF1A2 SE	This study
FLAG-eEF1A2 S358A	This study
FLAG-eEF1A2 S358E	This study
FLAG-eEF1A2 S393A	This study
FLAG-eEF1A2 S393E	This study
EGFP-C3	Stock from the lab
GFP-eEF1A2 wt	This study
GFP-eEF1A2 SA	This study
GFP-eEF1A2 SE	This study
GFP-Homer1b	Miquel Bosch's lab
HA (pNBM470)	Stock from the lab
HA-eEF1B2	This study
mGFP-C3	This study
mGFP-eEF1A2 wt	This study
mGFP-eEF1A2 SA	This study
mGFP-eEF1A2 SE	This study
mGFP-ZBP1	This study
mScarlet-C1	Addgene #85044
mScarlet-actin	This study
mScarlet-eEF1B2	This study
mScarlet-DrebrinA wt	This study
mScarlet-DrebrinA $\Delta$ LCR	This study
mScarlet-DrebrinA LCR	This study
mScarlet-DrebrinA LCRmut	This study
mScarlet-ZBP1	This study
pFUW	Michael Kiebler's lab
pFUW-FLAG-APEX-NES	This study
pFUW-FLAG-APEX-DrebrinA	This study
pFUW-FLAG-APEX-ZBP1	This study
pCMV-VSV-G	Addgene #138479
psPAX2	Addgene #12260

**Table 5. List of DNA plasmids used in this thesis.** Plasmid names and their origin are indicated.

## METHODS

### 2.3. Viral production / Lentiviral production

Lentivirus were produced in HEK293T cells as follows. HEK293T were grown on 10-cm tissue culture dishes (Fisher, 10075371) in standard HEK media (DMEM supplemented with 10 % FBS) until 70 % confluence was reached. HEK293T cells were transfected using polyethylenimine (PEI). Briefly, solution A was prepared containing the following plasmids: 6 µg of lentiviral transfer vector pFUW-FLAG-APEX, 1.5 µg VSV-G (containing vesicular stomatitis virus G-protein to mediate viral entry), and 4.5 µg psPAX2 (containing a Rev response element to enable nuclear export of viral mRNAs) in 750 µl of optiMEM (Fisher, 31985054). Next, we prepared solution B containing 120 µl PEI with 630 µl optiMEM for each condition. The PEI-optiMEM mix was added to the DNA-optiMEM tube and the total volume (1500 µl) was vortexed for 5 seconds. Following 10 minutes of incubation at room temperature, the solution was added dropwise to the plate of HEK293T cells. After 4 hours, the transfection media was replaced with 10 ml of neuronal maintaining media (Neurobasal supplemented with 2 % B27 and 1 % GlutaMAX) and plates were cultured at 37 °C and 5 % CO<sub>2</sub> during virus production. 48 hours post-transfection, the media was collected and passed through a 0.45 µm syringe filter (Fisher, 15216869) to remove cells but preserve lentiviral particles. Supernatants were used to transduce primary cortical neurons between 4 and 7 DIV by replacing half of their media for media containing lentiviral particles. 24 hours post-infection, media was completely changed by fresh neuronal maintaining media and cortical neurons were cultured until 18 DIV.

### 2.4. Quantitative RT-PCR (RT-qPCR)

RNA was obtained from indicated samples using E.Z.N.A total RNA purification kit (Omega Bio-tek, R3634-01) following the manufacturer's instructions. Then, samples were digested with ribonuclease-free deoxyribonuclease I (Roche, 11119915001) and 1 µg of RNA was reverse-transcribed into cDNA using the Prime Script RT Reagent kit (Takara, RR037B). qPCR was performed with Taqman probes (6xFAM-BQ1) on LightCycler@96 Real-Time PCR system (Roche) according to manufacturer's instructions. qPCR oligonucleotides are shown in Table 6.

Target gene	Gene full name		Oligonucleotide sequence (5'-3')
<i>Mm</i> <i>Eef1a1</i>	Eukaryotic	Sense	GAGCCAAGTGCTAATATG
	Elongation	Antisense	TGGTGGTAGGATAACAATC
	Factor 1 Alpha 1	Probe	AAAGTCACCCGCAAAGATGGC
<i>Mm</i> <i>Eef1a2</i>	Eukaryotic	Sense	CATGGTGACAACATGCTG
	Elongation	Antisense	GCTTGCATTTCCCTCCTTA
	Factor 1 Alpha 2	Probe	ATGGTTCAAGGGCTGGAAAGTAGA



<i>Mm Gapdh</i>	Glyceraldehyde- 3-Phosphate	Sense	CGTAGACAAAATGGTGAAG
		Antisense	CCATGTAGTTGAGGTCAA
	Dehydrogenase	Probe	TTGATGGCAACAATCTCCTT

**Table 6. List of qRT-PCR oligonucleotides used in this thesis.** Target gene, gene full name, and oligonucleotides sequences are provided.

## 2.5. Western blot (WB) analysis

Primary cortical neurons, Neuro-2a cells or HEK293T cells were lysed in 1x SR (2 % SDS and 0.125 M Tris-HCl pH 6.8) and sonicated to break cell membranes and genomic DNA. Next, 1 volume of 2x SS (10 % sucrose and 0.01 % bromophenol blue) was added. Protein samples were denatured by boiling them at 95 °C for 5 min and loaded into sodium dodecyl sulfate-polyacrylamide gel electrophoresis (SDS-PAGE). Proteins were separated based on their molecular weights as they migrated through the gel under an electric field.

Following electrophoresis, proteins were transferred from the SDS-PAGE gel onto a nitrocellulose membrane (Merck, GE10600002) using a semi-dry transfer system (Bio-Rad, 1703940). Next, to prevent non-specific binding, the membrane was blocked with non-fat dry milk during 1 h. Subsequently, the membrane was incubated with primary antibodies shown in table 7. After primary antibody incubation, the membrane was thoroughly washed to remove any unbound antibodies prior to incubation with the secondary fluorescent antibodies shown in table 7. The protein bands on the membrane were visualized using chemiluminescent or fluorescent substrates and analyzed using ImageJ software.

Antigen	Host	Dilution	Source	Identifier
eEF1A	Mouse	1:1000	Millipore	05-235
eEF1A2	Rabbit	1:1000	Abyntek	LS-C102299
p-eEF1A2 (Ser <sup>358</sup> )	Rabbit	1:400	PhosphoSolutions	P153-358-25
Actin	Rabbit	1:2000	Sigma-Aldrich	A2066
FLAG	Mouse	1:500	Sigma-Aldrich	F3165
HA (12CA5)	Mouse	1:400	Roche	11583816001
HRP- Conjugated Streptavidin	Streptomyces avidinii	1:1000	Thermo Scientific	N100
Anti-mouse IRDye800	Goat	1:10000	LI-COR	926-32211
Anti-rabbit IRDye 680	Goat	1:10000	LI-COR	926-68021

## METHODS

---

Anti-rabbit peroxidase- linked	Donkey	1:10000	Fisher	10379664
--------------------------------------	--------	---------	--------	----------

---

**Table 7. List of primary and secondary antibodies used for WB.** Details of antigen, host species, used dilutions, sources, and identifiers of each antibody are provided.

### 2.6. Immunoprecipitation (IP)

HEK293T cells were collected in lysis buffer (20 mM HEPES pH 7.5, 125 mM NaCl, 0.1 % NP-40, 1 mM EDTA pH 8, protease inhibitor (Roche, 05056489001), and phosphatase inhibitor (Roche, 04906837001)) on ice. Next, lysates were sonicated three times for 10 seconds each at 10 % amplitude. After sonication, lysates were centrifuged at 12000 rpm for 10 min to obtain the whole-cell protein extract, which was referred to as “input”. “Input” samples were incubated with  $\alpha$ -FLAG agarose beads (Merck-Sigma, A2220) at 4 °C for 2 h. Before incubation, the  $\alpha$ -FLAG agarose beads were washed with lysis buffer. Subsequently, beads were collected by centrifugation at 1000 rpm and washed thoroughly to remove any unbound or non-specifically bound proteins. The captured protein complexes were eluted from the beads adding 1 volume of 2x SDS- sample buffer and boiling at 95 °C for 5 min and referred as “IP”. Co-IP analyses were performed later by WB.

### 2.7. APEX-mediated biotinylation

Cortical neurons were infected between 4 and 7 DIV using pFUW-FLAG-APEX-NES, pFUW-FLAG-APEX-DrebrinA or pFUW-FLAG-APEX-ZBP1 plasmids. At 18 DIV, prior to APEX activation, neurons were incubated with 500  $\mu$ M biotin-phenol (BP) (Merck, SML2135) for 30 min at 37 °C. APEX labelling was performed by adding hydrogen peroxide (Sigma, 88597) to a final concentration of 1 mM for 1 min before quenching the biotinylation reaction by washing three times with STOP/Quench buffer (5 mM Trolox ((+/-)-6-Hydroxy-2,5,7,8-tetramethylchromane-2-carboxylic acid (Sigma, 238813), 10 mM sodium ascorbate (Sigma, A7631), 10 mM sodium azide (Sigma, S2002) , 1 mM CaCl<sub>2</sub>, and 0.5 mM MgCl<sub>2</sub> in phosphate-buffered saline (PBS) at pH 7.4). Samples were collected using cell scrappers and suspended in cold lysis buffer (4M urea, 50 mM Tris pH 8, 150 mM NaCl, 5 mM EDTA, 0.5 % sodium deoxycholate, 0.1 % SDS, 1 % Triton X-100, 5 mM Trolox, 10 mM sodium ascorbate, and 10 mM sodium azide). Samples were passed repeatedly through a syringe (26 G) ensure complete cell lysis. Then, 1 volume of 55 % trichloroacetic acid (Sigma, T6399) was added to the cells and samples were incubated on ice for 15 min. Proteins were precipitated in a tabletop centrifuge at 14000 rpm at 4 °C for 10 min. Pellets were washed with -20 °C-cold acetone (Sigma, 179124) three more times. Then, dry pellets were resuspended in cell lysis solution (8M urea, 100 mM sodium phosphate pH 8, 1% SDS, 100 mM NaHCO<sub>3</sub>, and 10 mM TCEP) until they were

completely dissolved. The resuspended protein solutions were centrifuged at 14000 rpm at room temperature for 10 min and supernatants were transferred to new microcentrifuge tubes.

Biotinylated proteins can be captured by streptavidin-coated beads because of the strong noncovalent interactions between streptavidin and biotin. For affinity purification, ~75  $\mu$ l of streptavidin magnetic beads (Fisher, 10150874) per condition were washed three times in 4 M urea and 0.5 % SDS and added to each sample. Beads were incubated overnight at 4  $^{\circ}$ C and then separated from solutions by using a strong magnetic rack. Then, beads were washed once with 4 M urea and 0.5 % SDS, and three times with 50 mM Tris pH 8. Beads were frozen at -80  $^{\circ}$ C prior to on-bead digestion of the IP samples. Biotinylation in the samples were detected by WB using a Streptavidin-HRP conjugate antibody as mentioned in “2.5. Western blot (WB)” section.

### **3. MORPHOLOGICAL ANALYSIS**

#### **3.1. Immunofluorescence (IF)**

Primary hippocampal neurons were obtained from embryonic day 17.5 (E17.5) CD1 mouse embryos and plated into 4-well plates containing coverslips (Fisher, 10507591) at a density of  $2 \times 10^4$  cells/cm<sup>2</sup>. Neurons at 14 DIV were fixed with 4 % paraformaldehyde (PFA) with 4 % sucrose at 4  $^{\circ}$ C for 20 min. After fixation, cells were washed with PBS and permeabilized using 0.1 % Triton-X (Sigma, 11332481001) in PBS at 4  $^{\circ}$ C for 5 min.

Non-specific binding sites were blocked with 5 % normal goat serum (Fisher, PCN5000) in PBS for 30 min at room temperature. Subsequently, neurons were incubated with the primary antibodies shown in table 8 for 2 h at room temperature. Primary antibodies were carefully selected to ensure specificity and minimize cross-reactivity. After incubation with primary antibodies, neurons were washed with PBS and incubated with suitable fluorescently labelled secondary antibodies for 1 h at room temperature. The secondary antibodies used are also shown in table 8. In some experiments, nuclear staining was performed using Hoechst (Fisher, 62249). Finally, coverslips were mounted onto glass slides using 80 % glycerol in PBS, to preserve fluorescence and prevent photobleaching. IF images were acquired with Zeiss LSM780 confocal microscope under a 40x 1.4-NA oil-immersion objective and processed using ImageJ for visualization.

To validate the specificity of the IF signals, negative controls omitting primary antibodies were assessed. IF experiments were replicated independently with different neuronal batches to ensure reproducibility of results.

## METHODS

Antigen	Host	Dilution	Source	Identifier
eEF1A2	Rabbit	1:500	Abyntek	LS-C102299
PSD-95	Mouse	1:400	Millipore	MABN68
MAP2	Mouse	1:500	Sigma	M1406
FLAG	Mouse	1:400	Sigma-Aldrich	F3165
Puromycin (12D10)	Mouse	1:400	Merck	MABE343
Streptavidin-488	<i>Streptomyces avidinii</i>	1:1000	Jackson ImmunoResearch	AB_2337249
AlexaFluor 568 Goat Anti-Rabbit IgG	Goat	1:1000	Invitrogen	A11008
AlexaFluor 488 Goat Anti-Mouse IgG	Goat	1:1000	Invitrogen	A11001
AlexaFluor 568 Donkey Anti- Mouse IgG	Donkey	1:1000	Invitrogen	A10037

**Table 8. List of primary and secondary antibodies used for IF.** Details of antigen, host species, used dilutions, sources, and identifiers of each antibody are provided.

### 3.2. Puromycin incorporation

Neuro-2a cells stably expressing a short hairpin RNA (shRNA) against endogenous eEF1A2 mRNA were cultured on glass coverslips and co-transfected with GFP and HA-eEF1A2 phospho-mutants. 24 hours post-transfection, cells were treated with puromycin (1  $\mu$ g/ml; Sigma-Aldrich, P8833) for 5 min and fixed in 4 % paraformaldehyde with 4 % sucrose. IF was performed using  $\alpha$ -puromycin (1:500; Sigma-Aldrich, MABE343) as primary antibody, and Alexa 568 donkey  $\alpha$ -mouse (1:1000; Life Technologies, A10037) as secondary antibody. Images were acquired with a Zeiss LSM780 confocal microscope and quantification was performed using ImageJ (Wayne Rasband, National Institutes of Health (NIH)). Puromycin incorporation was determined by measuring fluorescence intensity in the cell body of transfected cells.

### 3.3. Fluorescence recovery after photobleaching (FRAP) imaging

At 13 DIV, hippocampal neurons cultured on 35-mm glass-bottom dishes (Ibidi) at  $2 \times 10^5$  cells per dish were transfected with plasmids expressing mScarlet-actin and mGFP-eEF1A2 SA or SE phospho-mutants. Cells were live-imaged 24 hours later in a Zeiss LSM780 confocal microscope equipped with a 5 % CO<sub>2</sub>, 37 °C humidified chamber under a 40x 1.2-NA water-immersion objective. Photobleaching was achieved with three continuous scans at maximum laser (561 nm) power after three

baseline images. Images were taken in 1-s intervals during 1 min. FRAP efficiency was calculated using ImageJ. Regions of interest were placed on individual spines (bleached) and non-bleached dendritic sections as control. Also, background signal was subtracted, and intensity values were normalized to the average of the three pre-bleaching frames. Data were fitted to a single-term exponential recovery model as described (Koulouras et al., 2018).

### 3.4. Förster resonance energy transfer (FRET) imaging

Hippocampal neurons were transfected at 13 DIV with FRET biosensor plasmids expressing mGFP-eEF1A2 proteins and mScarlet-eEF1B2. Same plasmids were also used in Neuro-2a experiments. Time-lapse images were conducted the day after transfection. For neuronal stimulation experiments, hippocampal cultures were stimulated with 50  $\mu$ M DHPG (Sigma-Aldrich, D3689). Images to calculate FRET efficiency were recorded every 2 min during 15 min in a Zeiss LSM780 confocal microscope equipped with a 5 % CO<sub>2</sub>, 37 °C humidified chamber under a 40x 1.2-NA water-immersion objective. Images were 1024 x 1024 pixels, with a pixel width of 65 nm. Briefly, donor (mGFP-eEF1A2) proteins were excited at 488 nm, and their emission was measured at 490 to 532 nm ( $I_D$ ). Acceptor (mScarlet-eEF1B2) proteins were excited at 561 nm, and their emission was measured at 563 to 695 nm ( $I_A$ ). We also measured the total signal emitted at 563 to 695 nm when excited at 488 nm ( $I_F$ ) to obtain the FRET efficiency as

$$FRET \% = 100 * \frac{I_F - k_D * I_D - k_A * I_A}{I_A}$$

$k_D$  and  $k_A$  correspond to correcting acceptor cross-excitation and donor bleed-through, respectively. FRETmapJ (Mendoza et al., 2021) was used to obtain maps with the FRET signal as pixel value for local quantification.

### 3.5. Live-imaging mRNPs

Primary hippocampal neurons were co-transfected at 7 DIV with plasmids expressing mScarlet- or mGFP-tagged DrebrinA, mScarlet or mGFP-tagged ZBP1, and pRFP670, as indicated in the corresponding figure legends. At 14 DIV, neurons were live-imaged to analyze DrebrinA concentration and ZBP1 positioning through the dendrite. Cells were not fixed to avoid fixation artifacts in liquid condensates (Irgen-Giorgio et al., 2022). Images were taken using Andor Dragonfly 505 spinning-disk microscope equipped with a 5 % CO<sub>2</sub>, 37 °C humidified chamber. Stacks every 1  $\mu$ m were taken under a 63x 1.4-NA oil-immersion objective. Laser power was kept constant throughout images and conditions.

## **4. BIOINFORMATICS, DATA ANALYSIS AND REPRESENTATION**

### **4.1. Mass spectrometry-based interactomic analysis**

HEK293T cells were transfected with plasmids expressing FLAG-eEF1A2 SA and FLAG-eEF1A2 SE, and triplicate samples were immunoprecipitated using  $\alpha$ FLAG-agarose beads (Merck-Sigma, A2220). FLAG immunoprecipitates (~150  $\mu$ g protein) were reduced with 100 mM DTT at 95 °C for 10 min before digestion with trypsin using the Filter Aided Sample Preparation protocol (Hau et al., 2020). Peptides were analyzed using a Q Exactive Plus Orbitrap mass spectrometer (Barts Cancer Institute, London). MaxQuant (version 1.6.3.3) software was used for database search and label-free quantification of mass spectrometry raw files. The search was performed against a FASTA file of the *Mus musculus* proteome, extracted from uniprot.org. All downstream data was analyzed using Perseus (version 1.5.5.3).

### **4.2. Spine analysis**

Spine number and fluorescence were determined using SpineJ (Pedraza et al., 2014). To use SpineJ software, neurons must express a fluorescent protein in levels high-enough to clearly highlight neurites and spines above a darker background. Neurites were traced with a software-assisted tool, and then, a recurrent algorithm detects individual protrusions along each track to obtain morphological data and the corresponding fluorescence density values. To assess the spine/dendrite fluorescence ratio, regions of interest (ROI) were placed within dendritic spine heads and in the dendritic shaft below them, and mean fluorescence intensity was measured.

Images were acquired using a Zeiss LSM780 confocal microscope. Stacks of 10 slices were imaged every 0.37  $\mu$ m, with a pinhole value of 1 airy unit under a 63x objective at 0.11  $\mu$ m per pixel. Laser power and PMT values were kept constant throughout images and conditions.

### **4.3. Gene Set Enrichment Analysis (GSEA)**

GSEA was performed to determine if a predefined set of genes showed statistically significant differences between two biological conditions. In this study, GSEA was employed to analyze proteomic data from two interactomes: the protein interactors of eEF1A2 phospho-null SA, and the interactors of eEF1A2 phospho-mimetic SE. The aim was to determine the functional enrichment of these interactomes with respect to different Gene Ontology (GO) categories. The GSEA software version 4.2.3 was employed for this analysis.

For each GO category, a barcode plot was generated to visually represent the enrichment profile of proteins. Within this barcode plot, each line corresponds to a

single protein, positioned to the left or the right of the barcode axis depending on the enrichment within the interactome. Proteins enriched in the SA condition are depicted to the right in red, while SE-enriched proteins are shown to the left in blue.

Additionally, we performed a volcano plot displaying the log-fold change between both conditions as an indicative of the magnitude of change on the x-axis and the log of the p-value as an indicative of statistical significance on the y-axis for each protein.

#### **4.4. Global yeast genetic interaction network**

The global yeast genetic interaction network, as described by Usaj et al., (2017), was constructed through a systematic analysis of yeast mutants and the investigation of gene pairs to elucidate their genetic interactions. By integrating these genetic interactions, a comprehensive network was created to illustrate the functional and regulatory relationships among the studied genes in the budding yeast *Saccharomyces cerevisiae*. In this study, we focused on exploring the interactions of yeast orthologs of human eEF1A2-phospho-mutant interactors within the global yeast genetic interaction network. It was observed that subsets of genes with highly similar genetic interaction profiles often clustered together, indicating their belonging to the same biological process, pathway, or protein complex.

In the network representation, nodes correspond to deletion alleles of nonessential genes or temperature-sensitive alleles of essential genes. Edges between nodes are established when alleles share similar genetic interaction profiles beyond a defined Pearson correlation coefficient. The resulting network consists of 4909 nodes representing 4418 unique genes connected by 34468 edges.

#### **4.5. Distance of mRNPs to spines**

The ImageJ plugin DendFociJ was developed to quantify fluorescence levels of a synaptic protein within dendritic spines and measure the closest distance to a fluorescence-tagged RNA granule foci in the dendritic shaft. To use this software, neurons were required to express a fluorescence protein as tracker, such as pRFP670, encoding a far-red fluorescent protein. Neurites were traced using a software-assisted tool that detected fluorescence changes above 10 % of the background. Individual spines were identified in neurons expressing a fluorescent-tagged synaptic protein, such as mScarlet-DrebrinA or GFP-Homer1b. Individual protrusions were detected, and their fluorescence levels were measured. Tracker fluorescence in these protrusions was also detected to normalize the synaptic fluorescence signal and obtain protein concentration in relative units. Protrusions were detected based on changes above 55 % of the background signal.

## METHODS

Furthermore, RNA granules foci were detected in neurons expressing mScarlet- or mGFP-ZBP1. The software detected fluorescence intensities over 30 % compared to the background signal in the dendritic shaft. Foci positions were determined using pixel positioning, enabling the measurement of the distance to the nearest mGFP-ZBP1 foci from each individual mScarlet-DrebrinA foci.

The data were analyzed on RStudio. The displayed data were binned, with each point on the graph representing a bin size of 100 data points. Additionally, the trend line of the dataset and its deviation were also presented.

Images were acquired using Andor Dragonfly 505 spinning-disk microscope equipped with a 5 % CO<sub>2</sub>, 37 °C humidified chamber. Stacks every 1 µm were taken under a 63x 1.4-NA oil-immersion objective.

### **4.6. APEX proteomics**

APEX proximity labelling was performed as described in “2.7. APEX-mediated biotinylation”. We performed three independent biological replicates of three different conditions (FLAG-APEX-NES, FLAG-APEX-DrebrinA, and FLAG-APEX-ZBP1) to ensure the reproducibility and reliability of the obtained results. The inclusion of NES interactors served as spatial controls, allowing us to filter out non-specific interactors.

Using tandem mass spectrometry (MS/MS), we identified and quantified the peptides, enabling the determination of the relative abundance of the interacting proteins in each replicate. Samples were analyzed by BGI Genomics using mass spectrometer Q-Exactive HF X. Subsequently, we compiled a comprehensive list of putative interacting partners, with each protein associated with an intensity value expressed in iBAQ (Intensity-Based Absolute Quantification) units.

To ensure the reliability of our results, we considered putative interactors those proteins that were consistently detected in at least two of the three replicates for a specific condition. Conversely, proteins that appeared as interactors in only one of the replicates were considered false positives and excluded from further analysis.

To facilitate comparison across conditions, we normalized the iBAQ values to the total amount of proteins detected in each condition, following an iBAQ per million approximation (iBAQ normalized counts per million; cpm). For proteins that were not detected or were found in only one replicate, we assigned a minimum value equal to one tenth of the minimum iBAQ normalized value for that specific condition. iBAQ normalized cpm values were transformed to log<sub>2</sub> before performing the statistical analysis.



Next, we calculated the mean cpm and standard deviation for each protein in each condition. Using this information, we determined the fold enrichment of each protein in the DrebrinA/NES and ZBP1/NES conditions, along with the corresponding p-value.

To identify positive interactors, we considered proteins that exhibit significantly different enrichment in either the ZBP1 or DrebrinA condition compared to the NES condition. Specifically, proteins with a p-value < 0.05 and a fold change > 1.5 were considered as positive interactors. The estimated significance level (p-value) was corrected using Benjamini and Hochberg False Discovery Rate (FDR) adjustment. Proteins with FDR less than or equal to 0.05 were selected as differentially enriched and introduced into PANTHER to perform a GO Biological Process enrichment analysis (<http://geneontology.org>) (Ashburner et al., 2000; The Gene Ontology Consortium, 2023).

#### **4.7. Graphical representation and statistical analysis**

GSEA graphs were obtained with Excel as previously explained in “4.3. Gene Set Enrichment Analysis (GSEA)” section. Volcano plots were obtained with R software. All statistical analysis were performed with Graphpad Prism 8 Software (GraphPad Software) and statistical significance was determined where the p-value was <0.05 (\*), <0.01 (\*\*), <0.001 (\*\*\*) and <0.0001 (\*\*\*\*). Sample sizes are provided in figure legends.



# RESULTS

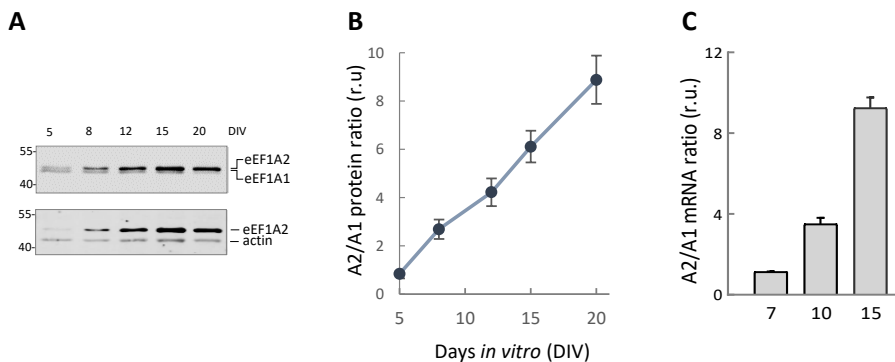


# **Chapter 1: Molecular mechanisms regulating eEF1A2 in the synaptic function**



## 1. eEF1A2 expression in primary neuronal cultures

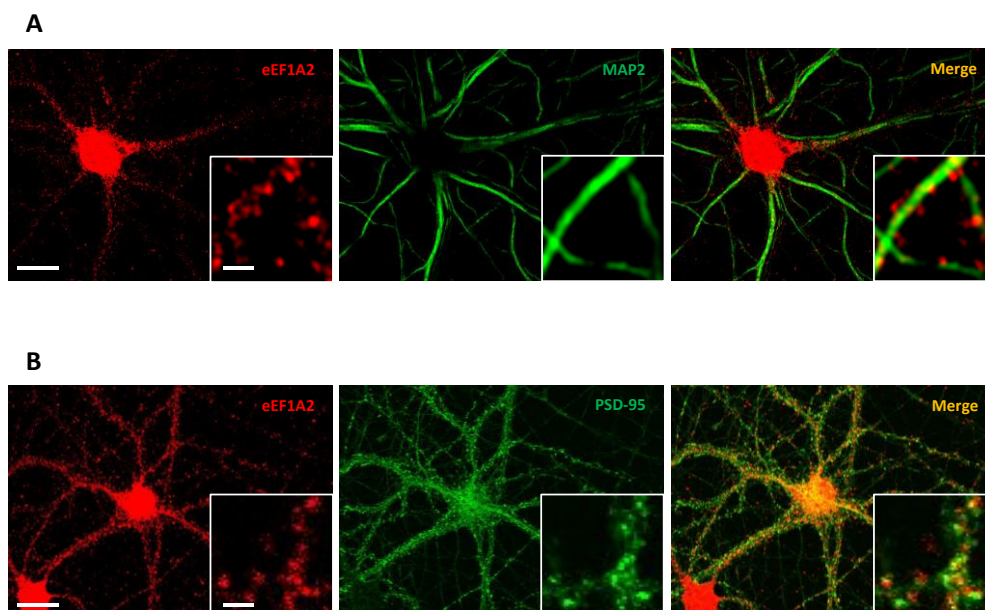
First, we wanted to test if the eEF1A isoform switch could be reproduced *in vitro*. As it has previously been described in mouse brains (Khalyfa et al., 2001), isoform eEF1A2 expression progressively increased in cultures of hippocampal neurons at the protein level, whereas eEF1A1 levels remained constant through all DIV (Fig. 17A-B). Although eEF1A1 and eEF1A2 contain 462 and 463 amino acid residues, respectively, isoform eEF1A1 migrated slightly faster as observed by immunoblot analysis with a specific antibody against eEF1A2 (Fig. 17A). Specific eEF1A1 antibodies did not work in our hands. Whereas eEF1A2 is expressed in neurons (Fig. 18), eEF1A1 is the main isoform in glial cells, which explains why we observed low levels of eEF1A1 by immunoblot analysis in long-term hippocampal cultures. Isoform switch was also determined at mRNA level by RT-qPCR using specific primers (Table 6) against each one of the isoforms and a progressive increase was also observed (Fig. 17C).



**Figure 17. eEF1A isoform switch can be reproduced *in vitro*.** (A) Differential expression of eEF1A isoforms in cultured hippocampal neurons from E17.5 mouse embryos. Samples were collected at different days in vitro (DIV) and analyzed by immunoblotting. Representative blot using a mouse monoclonal  $\alpha$ -eEF1A (top) or a rabbit polyclonal  $\alpha$ -eEF1A2 (bottom) is shown. eEF1A protein levels were normalized relative to actin. (B) Data from A represented as mean  $\pm$  SEM of n=3 experiments. (C) Quantification of eEF1A isoform mRNA ratios from cultured hippocampal neurons by qRT-PCR. Bars represent mean  $\pm$  SEM of n=3 experiments.

Next, we confirmed that eEF1A2 is expressed in mature hippocampal neurons at 14 DIV by double-IF using antibodies against  $\alpha$ -eEF1A2 and  $\alpha$ -MAP2 (Microtubule-Associated Protein 2), as a neuron-specific protein that stabilizes MTs in the dendrites (Fig. 18A). We also determined eEF1A2 presence in dendritic spines, by analyzing its colocalization with PSD-95, a pivotal postsynaptic scaffolding protein in excitatory neurons (Fig. 18B).

## RESULTS



**Figure 18. eEF1A2 localizes in dendritic spines of excitatory neurons.** Hippocampal neurons were fixed and analyzed by immunofluorescence and confocal microscopy. (A) From 25 neurons analyzed, a representative cell is shown with the corresponding images obtained with  $\alpha$ -eEF1A2 (red) and  $\alpha$ -MAP2 (green) antibodies. (B) From 20 neurons analyzed, a representative cell is shown with the corresponding images obtained with  $\alpha$ -eEF1A2 (red) and  $\alpha$ -PSD-95 (green) antibodies. Scale bar, 20  $\mu$ m. Insets show an enlarged region of the same cell; scale bar, 3  $\mu$ m.

These results support previously literature regarding eEF1A2 expression pattern and localization, confirming its expression in neuronal cell lines, specifically in the dendritic compartment.

### 2. Generation of eEF1A2 phospho-mutants

When comparing eEF1A1 and eEF1A2 sequences, we observed that both isoforms are 92 % identical at the amino acid level, as it has previously been described (Soares et al., 2009). eEF1A presents three different domains displaying multiple mutual interactions. Whereas domain I contains the GTP-binding site, domain II is implicated in the interaction with aa-tRNA. Both domains interact with eEF1B2 during the exchange of GDP for GTP. Last, domain II and domain III carry residues important for the interaction of eEF1A with the actin cytoskeleton (Jakobsson et al., 2018).

In domain III, isoform eEF1A2 presents four putative phosphorylation residues, Ser<sup>342</sup>, Ser<sup>358</sup>, Ser<sup>393</sup>, and Ser<sup>445</sup>, that are not present in isoform eEF1A1. Ser<sup>358</sup> is the most conserved and it is also present in chickens, xenopus, flies, and yeast (Fig. 19A). To test whether phosphorylation in domain III is relevant to eEF1A2 function in synaptic plasticity, we replaced the four eEF1A2-specific serine (S) residues with



alanine (A) or glutamic acid (E) to obtain phospho-null (SA) or phospho-mimetic (SE) mutants, respectively (Fig. 19B).

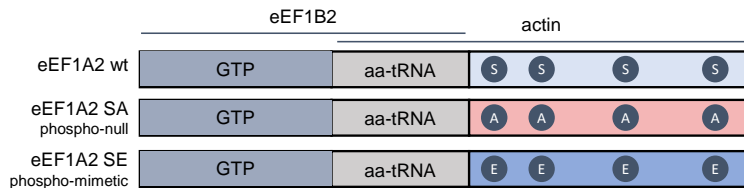
## A

```

          342                358                393
Mouse eEF1A2  AQFTSQV IILNHPGQISAGYSPVIDCHTAHIACKFAELKEKIDRRSGKKLEDNPKSLKSG
Mouse eEF1A1  AGFTAQVI IILNHPGQISAGYAPVLDCHTAHIACKFAELKEKIDRRSGKKLEDGPKFLKSG
Chicken eEF1A2 AQFTSQV IILNHPGQISAGYSPVIDCHTAHIACKFAELKEKIDRRSGKKLEDNPKSLKSG
Chicken eEF1A1 AGFTAQVI IILNHPGQISAGYAPVLDCHTAHIACKFAELKEKIDRRSGKKLEDGPKFLKSG
Xenopus EF1A2 AGFTSQV IILNHPGQISAGYSPVIDCHTAHIACKFAELKEKIDRRSGKKLEDNPKSLKSG
Xenopus EF1A1 GTFTAQVI IILNHPGQIGAGYAPVLDCHTAHIACKFAELKEKIDRRSGKKLEDNPKFLKSG
Fly eEF1A2    ADFTAQVI IIVLNHPGQIANGYTPVLDCHTAHIACKFSEIKEKCDRRTGKTTEPEPKAIKSG
Fly eEF1A1    ADFTAQVI IIVLNHPGQIANGYTPVLDCHTAHIACKFAEIKEKIDRRSGKTTTEENPKFIKSG
Yeast TEF2    ASFNATVI IIVLNHPGQISAGYSPVLDCHTAHIACRFDELLEKNDRRSGKKLEDHPKFLKSG
Yeast TEF1    ASFNATVI IIVLNHPGQISAGYSPVLDCHTAHIACRFDELLEKNDRRSGKKLEDHPKFLKSG
: * : ** :***** ** :* :***** : * : * : * : * : * : * : * : * : * : *
          345
Mouse eEF1A2  DAAIVEMVPGKPMCIVESFSQYPLGRFAVRDMRQTVAVGV IKNVEKKS GGAGKVTKSAQK
Mouse eEF1A1  DAAIVDMVPGKPMCIVESFSQYPLGRFAVRDMRQTVAVGV IKAVDKKAAGAGKVTKSAQK
Chicken eEF1A2 DAAIVDMI PGKPMCIVESFSQYPLGRFAVRDMRQTVAVGV IKNVEKKS GGAGKVTKSAQK
Chicken eEF1A1 DAAIVEMIPGKPMCIVESFSQYPLGRFAVRDMRQTVAVGV IKAVDKKAAGAGKVTKSAQK
Xenopus EF1A2 DAAIVEMIPGKPMCIVESFSQYPLGRFAVRDMRQTVAVGV IKNVEKKS GGAGKVTKSAQK
Xenopus EF1A1 DAAIVDMI PGKPMCIVESFSQYPLGRFAVRDMRQTVAVGV IKAVDKKAAGAGKVTKSAQK
Fly eEF1A2    DAAIIVLVPSKPLCVESFQEFPLGRFAVRDMRQTVAVGV IKS VNFKETTSGKVTKAAEK
Fly eEF1A1    DAAIVNLVPSKPLCVESFQEFPLGRFAVRDMRQTVAVGV IKA VNFK DASGGKVTKAAEK
Yeast TEF2    DAALVKFVPSKPMCVEAFSEYPLGRFAVRDMRQTVAVGV IKSVDKTEK-AAKVTKAAQK
Yeast TEF1    DAALVKFVPSKPMCVEAFSEYPLGRFAVRDMRQTVAVGV IKSVDKTEK-AAKVTKAAQK
***:: : * : * : * : * : * : * : * : * : * : * : * : * : * : * : * : * : * : * : *

```

## B



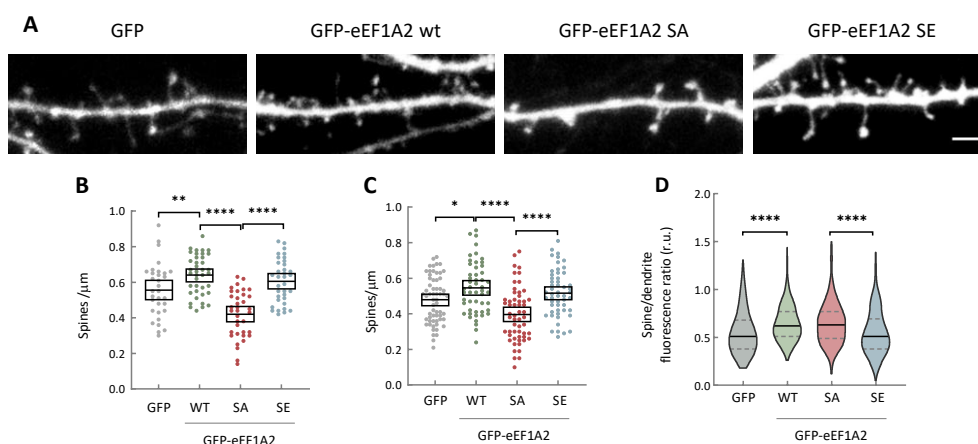
**Figure 19. Isoform eEF1A2 presents four putative phosphorylation residues.** (A) Sequence alignment of the eEF1A2 C-terminal domain from different species. Conserved serine residues mutated in this study are highlighted. (B) Scheme showing the three domains of eEF1A2 and relevant protein interactions. Blue dots represent phosphorylation sites (Ser<sup>342</sup>, Ser<sup>358</sup>, Ser<sup>393</sup>, and Ser<sup>445</sup>) in domain III that are not present in eEF1A1. Serine residues were replaced to alanine in the phospho-null SA mutant, and mutated to glutamic acid in the phospho-mimetic SE.

### 3. Role of eEF1A2 phosphorylation in dendritic spines

We hypothesized that eEF1A2 phosphorylation could be critical in synaptic-related processes like maintaining the density of dendritic spines. To address this point, we overexpressed GFP-eEF1A2 proteins [wild type (wt), SA, and SE] together with DsRed2 in CA1 pyramidal cells of rat hippocampal slice cultures (Fig. 20A,B,D) and in hippocampal dissociated neurons (Fig. 20C) to analyze spine density. For organotypic cultures, hippocampal slices were biolistically transfected at 5 to 7 DIV and imaged 3 to 5 days later, whereas dissociated hippocampal neurons were

## RESULTS

transfected at 13 DIV and imaged at 14 DIV. Spine density was assessed using the ImageJ plugin, SpineJ, which enables the semi-automatic detection of protrusions in dendrites. Both in organotypic slices (Fig. 20B) and primary dissociated hippocampal cultures (Fig. 20C), the phospho-null SA mutant showed a significant reduction in the number of dendritic spines compared to wt and phospho-mimetic SE mutant, suggesting that spine formation process requires eEF1A2 phosphorylation.

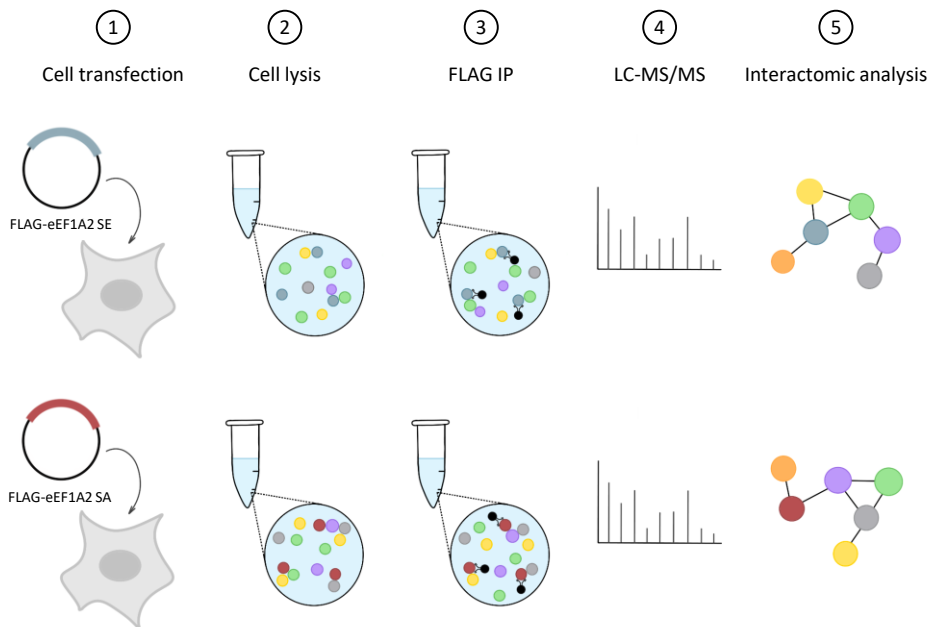


**Figure 20. eEF1A2 phosphosite configuration modulates spine growth.** Organotypic hippocampal slices (A, B and D) or dissociated hippocampal cultures (C) were transfected with plasmids expressing GFP or GFP fusions of WT, SA, or SE eEF1A2 proteins and plasmid expressing DsRed2 for dendritic tracing. (A) Representative dendrites of organotypic hippocampal slices expressing GFP or GFP-eEF1A2 WT and phospho-mutants. Scale bar, 2  $\mu\text{m}$ . (B) Spine densities (represented as spine/ $\mu\text{m}$ ) were assessed in GFP-positive neurons of (A). The total number of observations (spines/neurons) plotted is as follows: GFP, n = 834/32; WT, n = 1387/39; SA, n = 780/36; SE, n = 938/35. Single-neuron data (dots) from three independent experiments and median  $\pm$  Q values are plotted. \*\* $P < 0.01$  and \*\*\*\* $P < 0.0001$ ; by Kruskal-Wallis tests. (C) Spine densities (represented as spine/ $\mu\text{m}$ ) were assessed in GFP-positive hippocampal neurons from dissociated cultures. The total number of observations (spines/neurons) plotted is as follows: GFP, n = 1990/61; WT, n = 2040/51; SA, n = 1434/56; SE, n = 1952/53. Single-neuron data (dots) from three independent experiments and median  $\pm$  Q values are plotted. \* $P < 0.05$ , \*\* $P < 0.01$  and \*\*\*\* $P < 0.0001$ ; by Kruskal-Wallis tests. (D) Quantification of GFP-fused WT, SA, and SE eEF1A2 proteins in spines of CA1 pyramidal neurons from slices described in (A). GFP fluorescence in spines was normalized to that in corresponding dendritic shafts. The total number of observations (spines/neurons) plotted is as follows: GFP, n = 259/10; WT, n = 364/10; SA, n = 313/12; SE, n = 534/13. Median  $\pm$  Q values and the results of a Kruskal-Wallis test (\*\*\*\* $P < 0.0001$ ) are also shown.

We then estimated eEF1A2 distribution by comparing the GFP signal in spines versus the adjacent dendritic shafts. The GFP-eEF1A2 SE mutant showed a reduced accumulation in spines compared to the wt and SA mutant and similar to the GFP levels (Fig. 20D), suggesting that phosphorylation in domain III modulates eEF1A2 targeting to dendritic spines. These data indicate that phosphorylation is important for the regulation of structural synaptic plasticity.

#### 4. Interactome analysis of eEF1A2 phospho-mutants

To elucidate the role of eEF1A2 phosphorylation, we decided to examine the interactomes of both the SA and SE mutants. HEK293T cells were transfected with FLAG-eEF1A2 SA and FLAG-eEF1A2 SE cDNAs. 24 hours after transfection, cells were lysed and immunoprecipitated with  $\alpha$ -FLAG-agarose beads. Immunoprecipitates were analyzed by liquid chromatography-tandem mass spectrometry (LC-MS/MS) (Fig. 21).

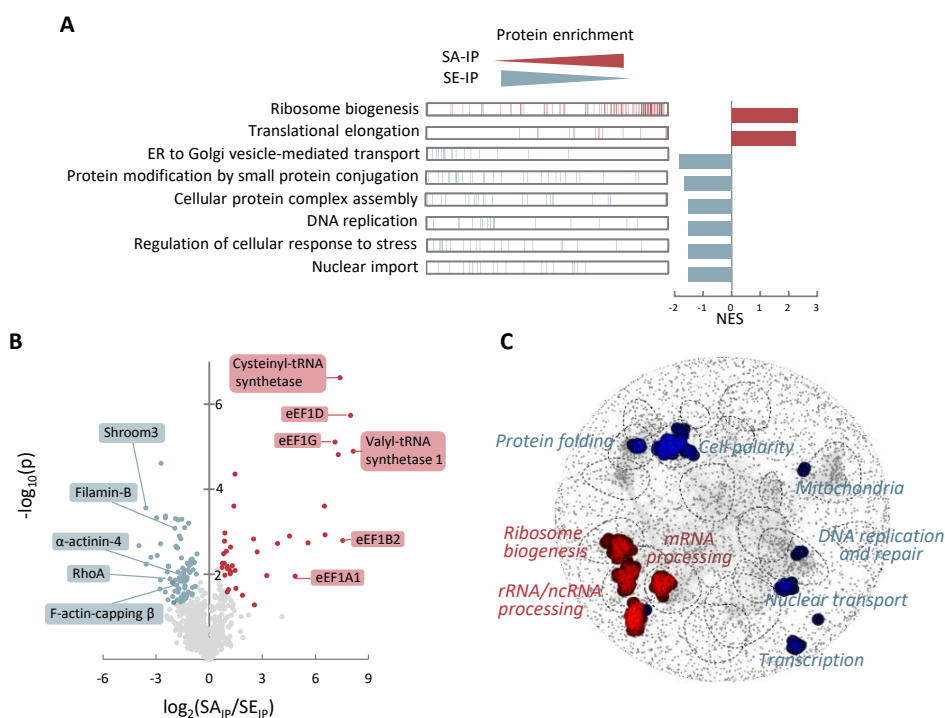


**Figure 21. Scheme for proteomic analysis of eEF1A2 phospho-mutants interactome.** HEK293T cells were transfected with plasmids codifying for FLAG-eEF1A2 SA and SE phospho-mutants. 24 h later, cells were lysed and immunoprecipitated using  $\alpha$ -FLAG agarose beads. Proteins were digested using trypsin and resulting peptides for each phospho-mutant were analyzed by quantitative LC-MS/MS. Then, interacting proteins were described for each phospho-mutant.

Of a total of 3026 proteins identified as putative interactors, 37 proteins were differentially enriched in SA immunoprecipitates (SA-IP) and 88 proteins in SE immunoprecipitates (SE-IP). GO enrichment analysis showed that SA-IP were enriched in proteins associated with ribosome biogenesis and translational elongation in comparison to SE-IP (Fig. 22A). Among translation-associated proteins, we found cysteinyl-tRNA synthetase, eEF1D, eEF1G, valyl-tRNA synthetase 1, eEF1B2, and eEF1A1 (Fig. 22B). By contrast, SE-IP were enriched in interactors involved in ER to Golgi vesicle-mediated transport, protein modification by small protein conjugation, protein complex assembly, DNA replication, regulation of cellular response to stress, and nuclear import (Fig. 22A). In addition to these

## RESULTS

categories, SE-IP showed statistically significant enrichment in a set of proteins involved in actin cytoskeleton dynamics – Shroom3, Filamin B,  $\alpha$ -actinin-4, RhoA, and F-actin-capping  $\beta$  – rather than actin itself (Fig. 22B). These results suggest that eEF1A2 phosphorylation could be involved in modulating actin dynamics as well as other non-canonical functions of eEF1A2. Interacting proteins enriched for each one of eEF1A2 phospho-mutants are shown in Supplementary Figure 1.



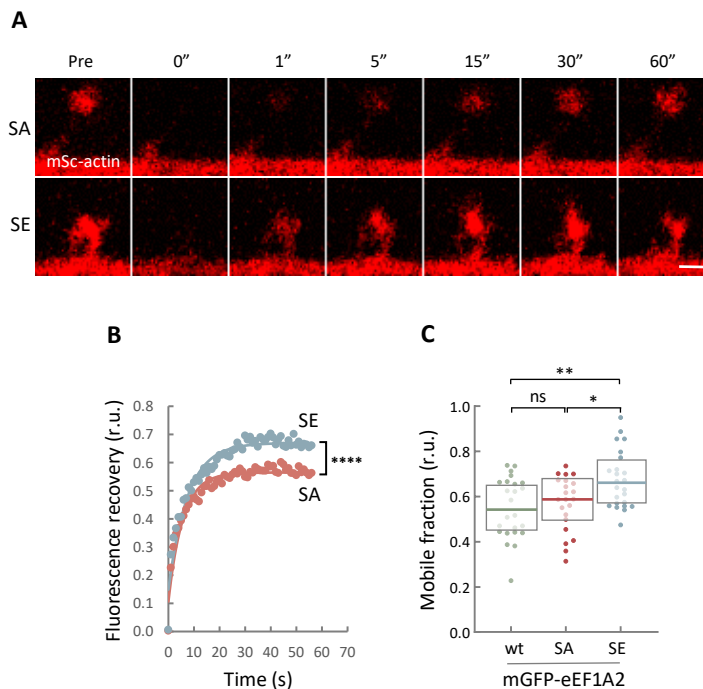
**Figure 22. Interactomic analysis of eEF1A2 phospho-mutants dissects translational and noncanonical functions.** (A) Triplicate immunoprecipitates from HEK293T cells expressing FLAG-tagged SA or SE eEF1A2 proteins were analyzed by LC-MS/MS. The results of a gene set enrichment analysis of FLAG immunoprecipitates are shown as barcode plots for the most significant GO terms (left). A bar chart with the corresponding normalized enrichment scores (NES) is also shown. SA-IP is shown in red; whereas SE-IP is shown in blue. (B) Volcano plot showing relative enrichment of identified interactors in immunoprecipitates of FLAG-tagged SA and SE eEF1A2 proteins (see also supplementary figure 1 for details). (C) Distribution of eEF1A2 SA (red) and SE (blue) interactor orthologs in the yeast global genetic interaction network. Categories enriched with the corresponding orthologs are indicated.

As a complement to the GO enrichment analysis, we examined how yeast orthologs of human eEF1A2-phospho-mutant interactors were grouped in the global yeast genetic interaction network (Usaj et al., 2017). Whereas phospho-null eEF1A2 SA interactors were found in clusters related to ribosome biogenesis and mRNA processing, phospho-mimetic eEF1A2 SE binding proteins displayed strong genetic

interactions in smaller clusters, many of them related to noncanonical functions such as endocytosis, nuclear processes, or actin cytoskeleton dynamics (Fig. 22C).

### 5. eEF1A2 phosphorylation in regulating actin dynamics

The first step of remodeling the spine actin network is the unbundling of actin filaments, which are usually cross-linked by different types of ABPs. Dissociation of these actin-cross-linking proteins would allow access to other ABPs to stimulate spatiotemporal flexibility of the actin filament network (Bosch et al., 2014; Mikhaylova et al., 2018).



**Figure 23. Phospho-mimetic residues in eEF1A2 increase actin dynamics in dendritic spines.**

(A) Hippocampal neurons were transfected with plasmids expressing mScarlet-actin and SA or SE mGFP-eEF1A2 proteins, and actin mobility in dendritic spines was analyzed by FRAP. Scale bar, 1  $\mu$ m. (B) FRAP profiles from dendritic spines as in (A). Mean values ( $n > 25$ ) and fitted lines are plotted. \*\*\*\* $P < 0.0001$  by paired t test. (C) Mobile fraction of mScarlet-actin in single dendritic spines from cells expressing mGFP fusions of WT (green), SA (red), or SE (blue) eEF1A2 proteins as in (A). Median  $\pm$  Q values are also plotted. \* $P < 0.05$  and \*\* $P < 0.01$  by Kruskal-Wallis test.

Previous results from our group showed that eEF1A2 phosphorylation influenced its association with F-actin by binding and bundling experiments (data not shown). However, the effect of phosphorylation in actin dynamics in dendritic spines has not been elucidated yet. We analyzed mScarlet-actin mobility by FRAP in dendritic spines of hippocampal neurons co-transfected with mGFP tagged eEF1A2 proteins [wt, SA, and SE] (Fig. 23A).

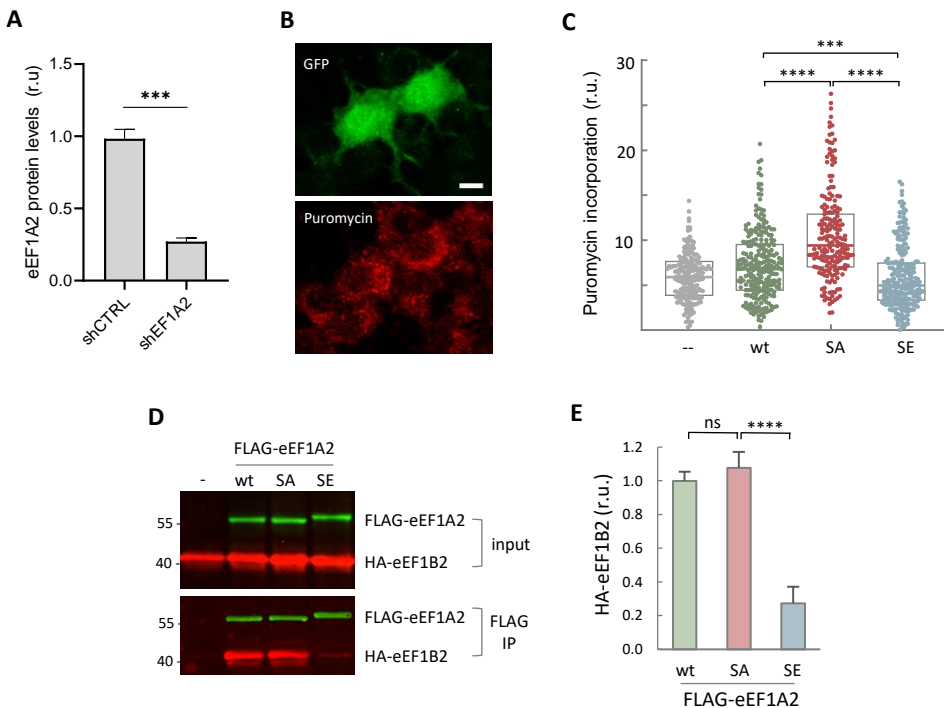
## RESULTS

Individual dendritic spines were photobleached and fluorescence recovery of mScarlet-actin was determined. We hypothesized that if eEF1A2 phospho-mutants bound actin differently, actin fluorescence recovery would be altered. Our results demonstrated that neurons expressing the phospho-mimetic SE mutant showed a faster recovery of mScarlet-actin fluorescence after photobleaching, in comparison to wt and SA-expressing neurons (Fig. 23B). Moreover, we detected an increase in the mobile fraction of mScarlet-actin (Fig. 23C). In all, these results support the idea that phosphorylation of eEF1A2 hinders its interaction with actin and increases actin dynamics.

### **6. The implication of eEF1A2 phosphorylation in protein translation**

eEF1A2 canonical function is related to protein translation, specifically translation elongation. As it has previously been mentioned, eEF1A2 phospho-null interactomes are significantly enriched in proteins related to translation (Fig. 22). For that reason, we hypothesized that phosphorylation of eEF1A2 could also regulate translation elongation in neurons.

To address that, we overexpressed HA-tagged eEF1A2 proteins in Neuro-2a cells. To maximize the effect of transfected eEF1A2 proteins, we created a stable Neuro-2a cell line expressing a shRNA against the 3'UTR of mRNA encoding endogenous eEF1A2. The Neuro-2a stably-expressing shEF1A2 presented a reduction of almost 80 % in endogenous eEF1A2 levels (Fig. 24A), tested by WB. Then, a puromycin incorporation assay was performed to visualize newly synthesized proteins (Fig. 24B, C). Puromycin is a tyrosyl-tRNA mimic that blocks translation by entering the A site of ribosomes and releases the elongating polypeptide chains from translating ribosomes, containing puromycin instead of a normal amino acid at the C-terminus. Neuro-2a stable shEF1A2 cells were co-transfected with GFP and HA-eEF1A2 phospho-mutants and 24 h later cells were treated with puromycin to assess translation efficiency. Puromycin incorporation was assessed by IF with an antibody  $\alpha$ -puromycin in GFP-positive cells in comparison to non-transfected cells from the same field. We found that the SA mutant was able to stimulate translation. In contrast, puromycin incorporation by the SE mutant was not significantly different from non-transfected cells (Fig. 24C). These results confirm the relevance of eEF1A2 phosphorylation in translation.

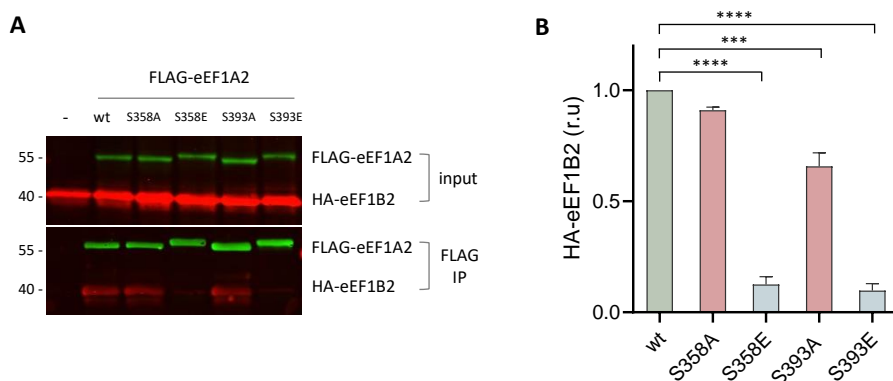


**Figure 24. eEF1A2 stimulates translation and interacts with its GEF in a phosphosite-dependent manner.** (A) Neuro-2a cells stably expressing an shRNA against the endogenous eEF1A2 mRNA were co-transfected with plasmids expressing GFP and wt, SA, or SE HA-eEF1A2 proteins, and protein synthesis was assessed by puromycin incorporation by immunostaining. Scale bar, 10  $\mu$ m. (B) eEF1A2 protein levels were assessed in Neuro2a shCTRL and Neuro2a shEF1A2 stable cell lines by WB using a rabbit polyclonal  $\alpha$ -eEF1A2. shEF1A2 downregulated proteins levels to 25% relative to shCTRL. Mean  $\pm$  SEM values (n=3) are plotted. Unpaired t-test: \*\*\*P < 0.001. (C) Quantification of puromycin incorporation in single Neuro-2a cells as in (A). Median  $\pm$  Q values (n > 200) are also plotted. Kruskal-Wallis test: \*\*\*P < 0.001 and \*\*\*\*P < 0.0001. (D) Interactions between eEF1A2 and eEF1B2. HEK293T cells were co-transfected with plasmids expressing HA-eEF1B2 and FLAG-tagged wt, SA, or SE eEF1A2 proteins. Immunoprecipitation (IP) was performed with  $\alpha$ FLAG beads, and HA-eEFB2 and FLAG-tagged eEF1A2 protein levels in lysates (input) and IP samples were simultaneously analyzed by immunoblotting. (E) Quantification of eEF1B2 levels in IP samples from immunoblot analysis as in (D). eEF1B2 protein levels were normalized relative to FLAG-tagged proteins in IP samples. Data are mean  $\pm$  SEM of n = 4 experiments; analyzed by one-way ANOVA: ns, non-significant; \*\*\*\*P < 0.0001.

Exchange of GDP for GTP is the first step in eEF1A2 recycling during translation, which is driven by eEF1B2. Thus, we decided to analyze the interaction between these two factors and performed IP analysis in HEK293T cells, which had been co-transfected with HA-eEF1B2 and FLAG-tagged eEF1A2 proteins. We observed that the phospho-mimetic SE mutant showed a fivefold decrease in levels of co-immunoprecipitated eEF1B2 protein. By contrast, the phospho-null SA mutant was as efficient as the wt eEF1A2 protein (Fig. 24D, E).

## RESULTS

Our phospho-mutants were quadruple considering all serine residues that change between isoform eEF1A1 and eEF1A2. However, it is possible that not all phosphorylation events happen at the same time or that some of them present opposite phenotypes. Thus, we wanted to test if single point phospho-mutants exhibit the same behavior as quadruple mutants. For that reason, we generated single point mutants on Ser<sup>358</sup> and Ser<sup>393</sup> and analyzed their interaction with the GEF eEF1B2 by co-IP (Fig. 25).



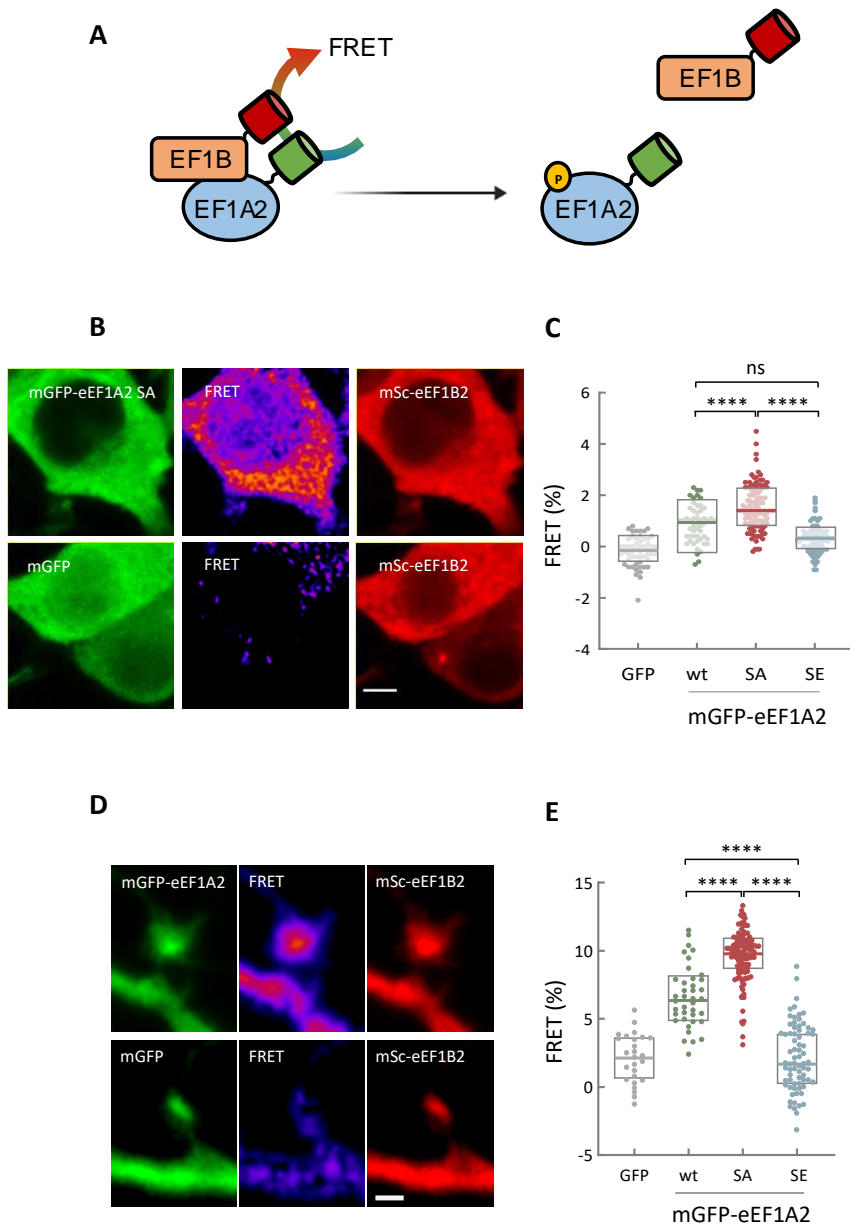
**Figure 25. Single point mutations for Ser<sup>358</sup> and Ser<sup>393</sup> present the same phenotype as the quadruple mutant when interacting with eEF1B2.** (A) Interactions between eEF1A2 single phospho-mutants and eEF1B2. HEK293T cells were co-transfected with plasmids expressing HA-eEF1B2 and FLAG-tagged wt, S358A, S358E, S393A or S393E eEF1A2 proteins. Immunoprecipitation (IP) was performed with  $\alpha$ FLAG beads, and HA-eEF1B2 and FLAG-tagged eEF1A2 protein levels in lysates (input) and IP samples were simultaneously analyzed by immunoblotting. (B) Quantification of eEF1B2 levels in IP samples from immunoblot analysis as in (A). eEF1B2 protein levels were normalized relative to FLAG-tagged proteins in IP samples. Data are mean  $\pm$  SEM of  $n = 2$  experiments; analyzed by one-way ANOVA. \*\*\*\* $P < 0.0001$ , \*\*\* $P < 0.001$ .

We observed that both phospho-mimetic mutants, S358E and S393E interact less with eEF1B2 in comparison to the phospho-null mutants S358A and S393A, as it happened with the quadruple mutant. This result supports the idea that at least both Ser<sup>358</sup> and Ser<sup>393</sup> phosphorylation are important in the interaction with the GEF eEF1B2, so the quadruple mutant is a good approach as it follows the same direction that both single mutants. For this reason, in the following experiments, only the quadruple phospho-mutants were used.

### 7. Role of eEF1A2 phosphorylation in synaptic plasticity

Next, we wanted to visualize this interaction in dendritic spines where local translation plays an important role in synaptic plasticity. To this end, we measured FRET between mGFP-eEF1A2 and mScarlet-eEF1B2.





**Figure 26. eEF1A2 interacts with its GEF in dendritic spines in a phosphosite-dependent manner.** (A) Schematic of the FRET strategy for quantifying the eEF1A2/eEF1B2 interaction. (B) Fluorescence and FRET images of representative Neuro-2a cells expressing mScarlet-eEF1B2 and mGFP-eEF1A2 SA or mGFP-eEF1A2 SE. Scale bar, 5  $\mu$ m. (C) FRET levels in Neuro-2a cells as in (B). The number of observations (cells) analyzed is as follows: mGFP,  $n = 55$ ; wt,  $n = 53$ ; SA,  $n = 60$ ; SE,  $n = 48$ . Median  $\pm$  Q values are plotted. Kruskal-Wallis test: \*\*\*\* $p < 0.001$ . (D) Fluorescence and FRET images of representative spines from hippocampal neurons expressing mScarlet-eEF1B2 and mGFP-eEF1A2 or mGFP as control. Scale bar, 1  $\mu$ m. (E) FRET levels in spines from hippocampal neurons as in (D) expressing mScarlet-eEF1B2 and mGFP or mGFP-tagged wt, SA, or SE eEF1A2 proteins. The total number of observations (spines/neurons) analyzed is as follows: mGFP,  $n = 30/5$ ; wt,  $n = 40/6$ ; SA,  $n = 118/8$ ; SE,  $n = 75/7$ . Median  $\pm$  Q values are plotted. Kruskal-Wallis test: \*\*\*\* $p < 0.001$ .

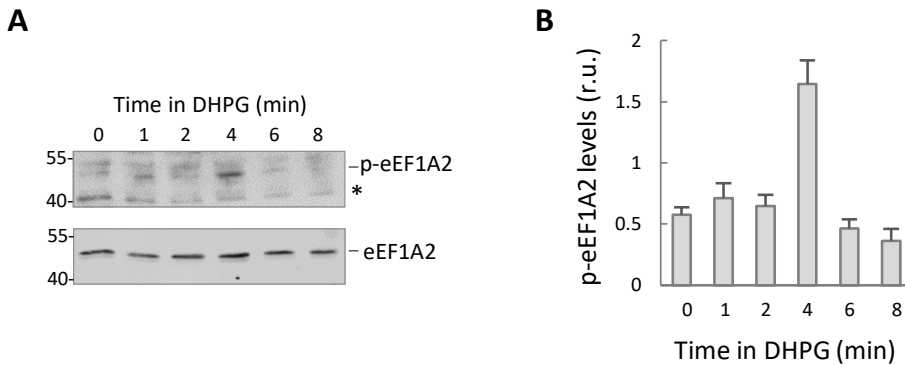
## RESULTS

We hypothesized that when eEF1A2 and eEF1B2 do interact, mGFP-eEF1A2 energy should transfer to mScarlet-eEF1B2 and FRET signal will be obtained. However, when both proteins do not interact, like observed with the phospho-mimetic mutant, energy could not be transferred, so FRET signal is lost (Fig. 26A).

First, we wanted to confirm the suitability of the approach by testing it in a cell line model which is easier to manipulate than primary hippocampal cultures. For that, we co-transfected Neuro-2a cells with plasmids codifying for mGFP-eEF1A2 and mScarlet-eEF1B2 and measured FRET levels in cell bodies. The SA mutant showed increased FRET levels in comparison to the SE mutant and wt conditions. However, no statistically significant differences were observed between wt and SE mutant (Fig. 26B, C). Subsequently, we co-transfected mGFP-eEF1A2 and mScarlet-eEF1B2 in 13 DIV hippocampal neurons and measured FRET levels in dendritic spines 24 hours after transfection. The SE mutant showed a significant reduction in FRET levels compared to the SA mutant and wt in dendritic spines. Accordingly, the phospho-null SA mutant showed the highest FRET levels, significantly higher than wt (Fig. 26D, E). These results support the idea that phosphorylation of eEF1A2 could regulate its association with its GEF, eEF1B2, and consequently modulate protein synthesis in hippocampal neurons.

Group 1 metabotropic glutamate receptors (mGluR1 and mGluR5) are implicated in different forms of mGluR-mediated synaptic plasticity that depend, partially, on the regulation of local protein synthesis (Bear et al., 2004; Di Prisco et al., 2014; Muddashetty et al., 2007; Waung & Huber, 2009). Activation of mGluR by DHPG stimulates the JNK pathway in cultured neurons (L. Yang et al., 2006) and has been linked to the phosphorylation of several synaptic proteins such as PSD-95 or elongation factor eEF2 (Nelson et al., 2013; S. Park et al., 2008). Moreover, polysome-associated JNK phosphorylates eEF1A2 at residues Ser<sup>205</sup> and Ser<sup>358</sup> in HEK293T cells (Gandin et al., 2013).

Taking all these data into consideration, we decided to analyze whether the activation of mGluRs with DHPG regulates eEF1A2 phosphorylation. First, we analyzed eEF1A2 phosphorylation levels by immunoblot using an antibody against phosphorylated eEF1A2 in Ser<sup>358</sup> residue (p-eEF1A2). 14 DIV cortical neurons were stimulated with 50  $\mu$ M DHPG and lysates were collected at different time points. Then, samples were immunoblotted using p-eEF1A2 and total eEF1A2 antibodies (Fig. 27A). Notably, DHPG provoked a transient phosphorylation of eEF1A2 that reached its peak 4 min after treatment (Fig. 27B).

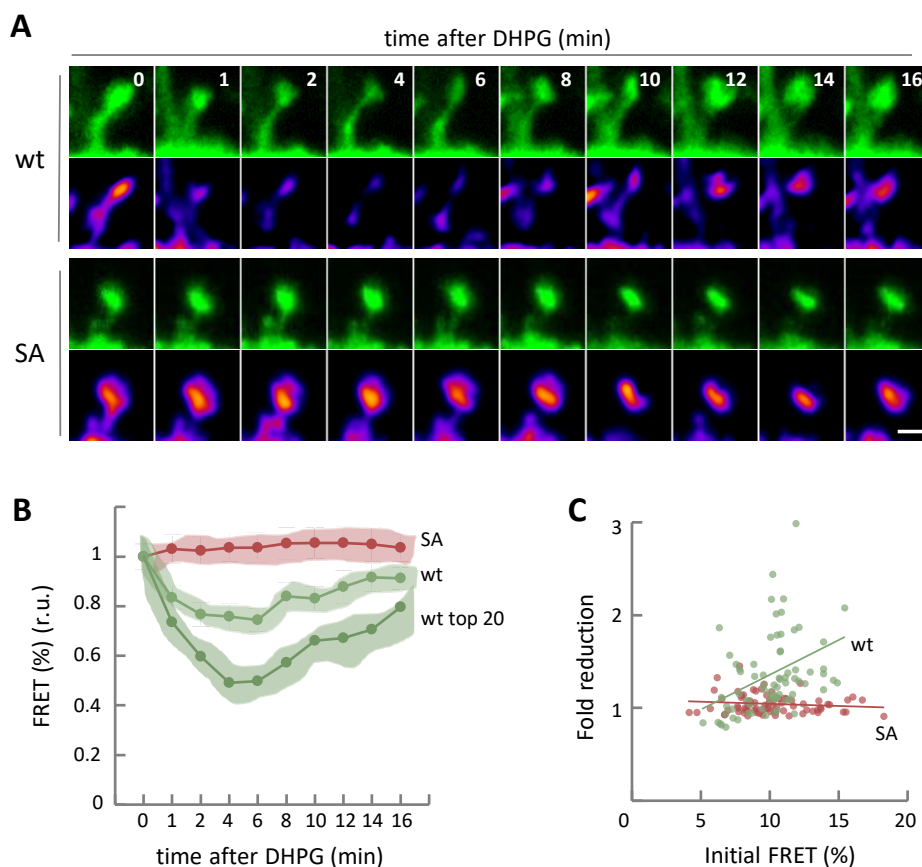


**Figure 27. DHPG induces transient phosphorylation of eEF1A2 in cortical neurons.** (A) Cortical cultured neurons were treated with DHPG, and lysates were obtained at different time points post stimulation for immunoblot analysis with phospho-eEF1A2 (p-eEF1A2) (upper panel) or total eEF1A2 (lower panel) antibodies. Asterisk indicates a non-specific band. (B) Quantification of phospho-eEF1A2 from immunoblot analysis as in (A). p-eEF1A2 levels were normalized relative to eEF1A2 protein levels. Data are represented as mean  $\pm$  SEM (n=4).

Then, we decided to use the above-mentioned FRET-based approach as an indicator of eEF1A2 phosphorylation status by analyzing the interaction of eEF1A2 and eEF1B2 *in vivo*. We hypothesized that non-phosphorylated status of wt mGFP-eEF1A2 would present FRET signal, whereas FRET levels would decrease when eEF1A2 gets phosphorylated after stimulation. Thus, we co-transfected mGFP-eEF1A2 and mScarlet-eEF1B2 in 13 DIV hippocampal neurons and live-imaged 24 hours post-transfection.

Neurons were stimulated with 50  $\mu$ M DHPG and images were taken every minute. We observed that FRET levels temporarily dropped during the first 4 min after DHPG addition, indicating that DHPG causes a reversible reduction in eEF1A2-eEF1B2 interaction within a narrow time window after stimulation (Fig. 28A, B). We noted that the fold change reduction was stronger in spines with higher initial FRET values (Fig. 28C). In sharp contrast, FRET levels produced by the phospho-null SA mutant were maintained during DHPG treatment and did not correlate with the initial status of the spine.

## RESULTS



**Figure 28. DHPG induces transient phosphosite-mediated dissociation of eEF1A2 from its GEF factor in dendritic spines.** (A) Fluorescence and FRET images of representative spines from hippocampal neurons expressing mScarlet-eEF1B2 and mGFP-tagged wt or SA eEF1A2 proteins at the indicated times after DHPG addition. Scale bar, 1  $\mu$ m. (B) FRET levels in spines from hippocampal neurons as in (A) expressing mScarlet-eEF1B2 and mGFP-tagged wt or SA eEF1A2 proteins as a function of time after DHPG addition. The total number of observations (spines/neurons) analyzed is as follows: wt, n = 76/10; SA, n = 131/12. FRET levels were made relative to time 0 and mean  $\pm$  CL ( $\alpha = 0.05$ ) values are plotted. Data from 20 spines with highest initial FRET values produced by wt eEF1A2 (wt top 20) are also shown. (C) Transient fold reduction in FRET as a function of initial FRET levels for mGFP-tagged wt (green) and SA (red) eEF1A2 proteins analyzed as in (B).

Thus, our results indicate that DHPG transiently downregulates the interaction between eEF1A2 and eEF1B2, thereby affecting the first step in the eEF1A2 activation cycle for translation elongation. Because the phospho-null mutant was totally unaffected, the observed modulation would link the activation of mGluRs, eEF1A2 phosphorylation, and local modulation of translation in dendritic spines.





## **Chapter 2: Molecular mechanisms regulating RNA transport granules capture in dendritic spines**





## **1. Looking for protein candidates responsible for RNA granule local capture**

RNAs are transcribed in the neuronal nucleus, exported to the cytoplasm, and transported along the MT cytoskeleton as a running sushi belt. These RNAs are bound to RBPs, adaptor proteins and molecular motors forming non-membrane structures named RNA granules or mRNPs. Some studies propose that mRNPs patrol a group of spines in dendrites until a particular synapse becomes activated and it may recruit these structures in order to translate the containing mRNAs. However, the molecular mechanisms underlying the attraction of mRNPs and their local capture are still unknown.

We hypothesized that proteins localized in the dendritic shaft or spine neck could play a role in capturing RNA transport granules. Therefore, we searched for protein candidates by data mining previously published datasets. Our criteria were as follows: (1) presence in the PSD compartment, (2) association with actin (AAPs), and (3) translocation to the spine during structural long-term potentiation (sLTP).

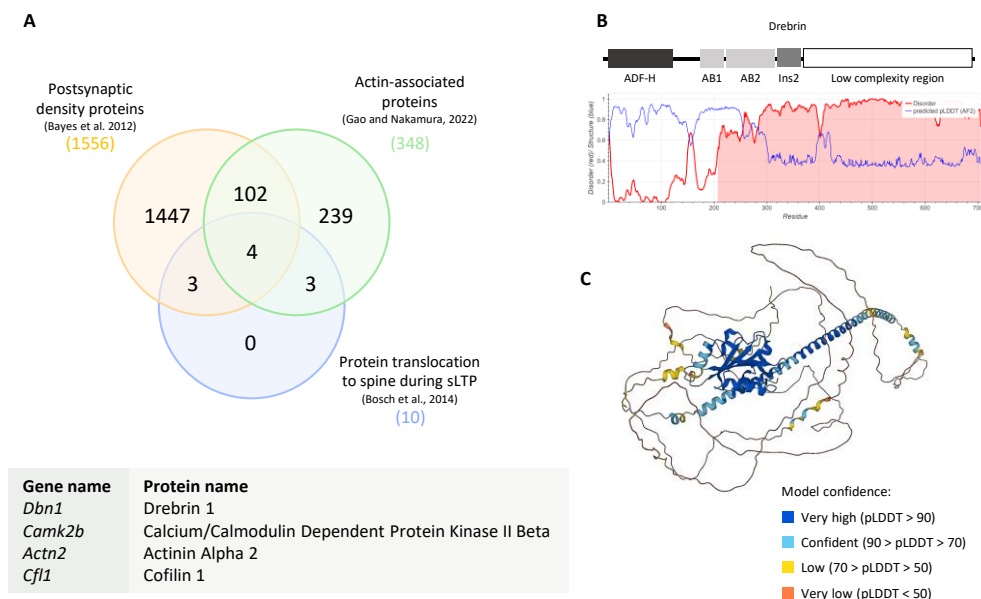
To identify proteins in the PSD, we used the dataset published by Bayés et al., (2012). They isolated synaptic plasma membranes from human and mouse cortex samples by ultracentrifugation on a sucrose density gradient, and subsequently analyzed the PSD fractions by LC-MS/MS. In our analysis, we considered the 1556 proteins identified in mouse PSD.

The second criterion in our data mining approach involved selecting actin-associated proteins. For this purpose, we referred to the dataset published in 2022 by Gao and Nakamura, which summarized 348 known AAPs. Prior literature in the field has posited that the actin cytoskeleton may play a crucial role in anchoring mRNA molecules prior to translation (G. Bassell & Singer, 1997). One of the proposed mechanisms involves the transfer of mRNA from the MT cytoskeleton to the actin cytoskeleton, although the precise molecular mechanisms governing this process remain elusive (Blower, 2013).

Lastly, we proposed that proteins involved in RNA granule capture might undergo delocalization from the dendritic spine head to the spine neck or the dendritic shaft, facilitating the interaction with RNA granules. Bosch et al., (2014) demonstrated that the induction of LTP in single dendritic spines could modify their protein composition. They analyzed 15 key postsynaptic proteins representing various aspects of synapse function and showed that 10 of these proteins efficiently translocated to the spine after long-term stimulation. These 10 proteins constitute our third dataset for data mining.

## RESULTS

Based on these criteria, only four proteins fulfilled all three requirements: Drebrin 1, CaMKII $\beta$ ,  $\alpha$ -actinin-2, and Cofilin 1 (Fig. 29A).



**Figure 29. The synaptic protein Drebrin is a putative candidate for RNA granules local capture.** (A) Venn diagram showing overlapping proteins among PSD proteins, actin associated proteins and proteins that translocate to dendritic spines during structural long-term potentiation (sLTP). Databases used are also illustrated. Proteins overlapping the three conditions are shown. (B) Sequence-based prediction of disorder for DrebrinA using Metapredict V2.3, a deep learning-based consensus predictor of intrinsic disorder. Red line shows predicted disorder. Blue line shows AlphaFold2-based predictions by producing a per-residue predicted local distance difference test (pLDDT) score. Some regions below 50 pLDDT may be unstructured in isolation. Disorder and pLDDT scores are anticorrelated. (C) AlphaFold2 structure prediction of DrebrinA (Uniprot: Q9QXS6) showing long IDRs. Each residue in the sequence is color-coded based on the model confidence score, pLDDT.

Protter and colleagues (2018) demonstrated that disordered regions could nonspecifically interact with other proteins and disrupt phase separation *in vitro*, as well as promote formation of higher-order structures due to the promiscuous protein-protein or protein-RNA interactions. IDRs interactions will be relatively indiscriminate with respect to binding partners, what would be helpful to enable the interaction with components of mRNPs, which are known to be highly heterogeneous (El Fatimy et al., 2016; Elvira et al., 2006; Fritzsche et al., 2013).

Out of the four proteins identified in the data mining analysis, we examined their structural characteristics, particularly focusing on the presence of disordered regions, using the AlphaFold2 (Jumper et al., 2021; Varadi et al., 2022) and Metapredict V2 (Emenecker et al., 2021) softwares. AlphaFold2 is an artificial intelligence system designed for predicting the three-dimensional structures of

proteins, including disordered regions. On the other hand, Metapredict V2 is a computational tool designed to predict protein intrinsic disorder by combining multiple disorder prediction methods.

Through the combined use of AlphaFold2 and Metapredict V2, we determined that of the four protein candidates, only Drebrin exhibited a significant disordered region. Metapredict V2 subjects the protein sequence of interest to distinct disorder prediction algorithms, each based on unique principles and methodologies. Considering amino acid composition, sequence motifs, physicochemical properties, and evolutionary conservation, it predicts which parts of a protein are disordered or structured. Then, it calculates a score from 0 to 1 reflecting the varying degrees of disorder. The disorder prediction provided by Metapredict in the Drebrin protein sequence is visualized in red, indicating that more than half of the residues comprising the protein are considered disordered (Fig. 29B).

Additionally, the predicted local distance difference test (pLDDT) values from AlphaFold2 are shown in blue (Fig. 29B). This parameter quantifies the accuracy of predicted distances between pairs of amino acids in a protein structure. Higher pLDDT scores indicate more reliable predictions. Disordered regions typically exhibit lower pLDDT values, generally below 0.5, as observed for Drebrin. Figure 29C illustrates that the disordered region of Drebrin corresponds to its C-terminal portion and displays very low-confidence values.

## **2. DrebrinA localization in primary hippocampal cultures**

Drebrin is an ABP with two major isoforms resulting from alternative splicing of the *Dbn1* gene. The most abundant isoform of Drebrin switches from DrebrinE to DrebrinA during brain development in parallel with synapse formation. DrebrinA isoform is exclusively expressed in neurons and contains a neuron-specific region (Ins2) in the central part of the protein. Drebrin distribution is limited to dendritic spines concurrently with isoform switch (Shirao et al., 2017).

First, we aimed to confirm DrebrinA enrichment in dendritic spines by tagging it with a red fluorescent protein (mScarlet-DrebrinA). Consistently with previous studies (Hanamura et al., 2018; Ivanov et al., 2009), we observed the accumulation of mScarlet-DrebrinA in dendritic spines of hippocampal neurons at 14 DIV.

Furthermore, we investigated the potential colocalization of DrebrinA with RNA transport granules. As mentioned earlier, RNA transport granules consist of mRNAs bound to RBPs. As an RNA granules marker, we overexpressed a mGFP-tagged RBP. Specifically, we used GFP-tagged zipcode binding protein 1 (mGFP-ZBP1), which is involved in the transport and translation of  $\beta$ -actin mRNA (Hüttelmaier et al., 2005).

## RESULTS

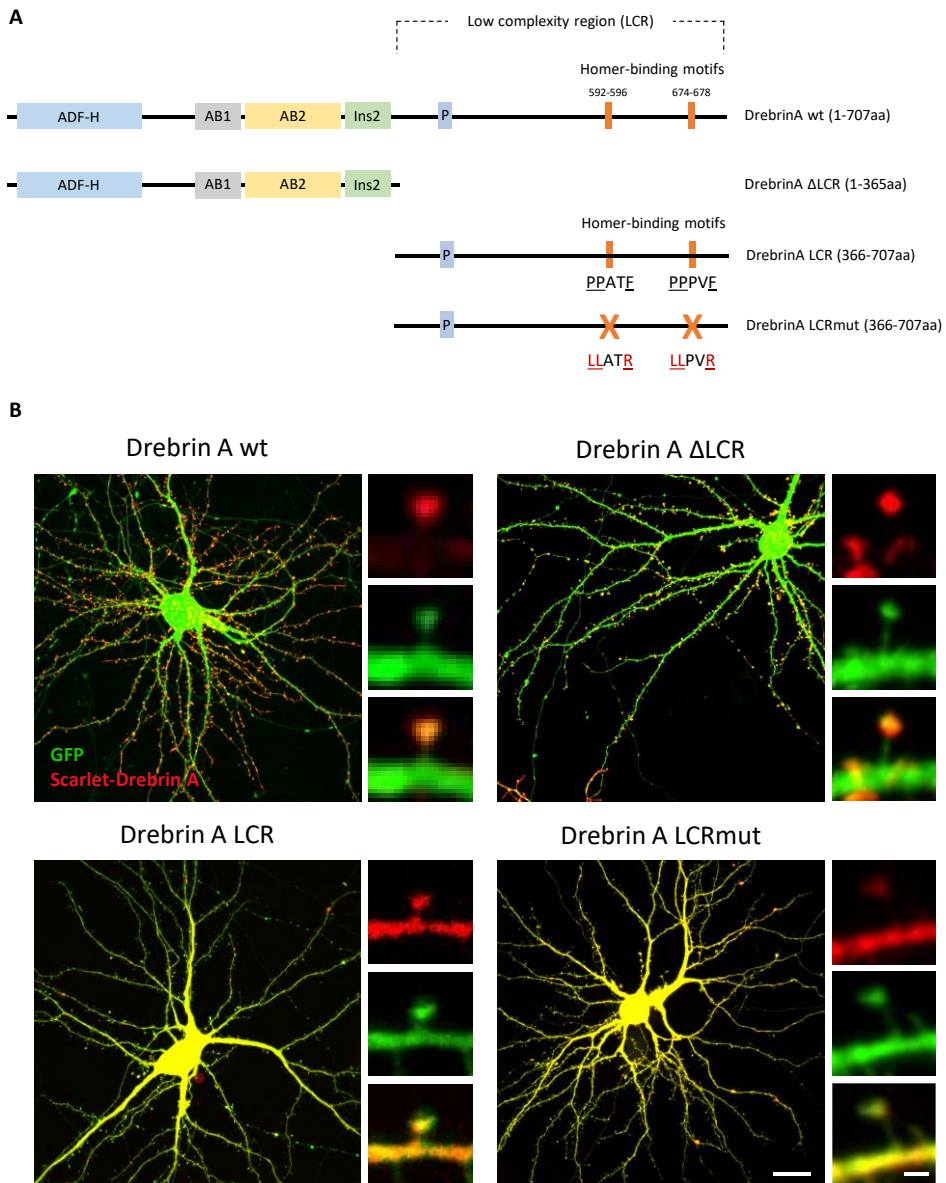
We co-transfected both plasmids into hippocampal neurons at 7 DIV and live-imaged cells at 14 DIV, a stage at which mature spines have already formed. As expected, mScarlet-DrebrinA was enriched in dendritic spines, whereas mGFP-ZBP1 was predominantly located in the dendritic shaft, and no colocalization was observed between the two. The distribution of mGFP-ZBP1 displayed a punctate pattern, representing individual RNA granules (Fig. 30).



**Figure 30. mScarlet-DrebrinA is enriched in dendritic spines whereas mGFP-ZBP1 is localized in the dendritic shaft of hippocampal neurons.** Hippocampal neurons were transfected at 7 DIV with plasmids codifying for mGFP-ZBP1, mScarlet-DrebrinA and pRFP670 (tracker) and fixed at 14 DIV. Representative images are shown. Scale bar, 20  $\mu\text{m}$ . Insets show an enlarged region of the same cell; scale bar, 2  $\mu\text{m}$ .

Both the neuron-specific DrebrinA and the ubiquitously expressed DrebrinE share an N-terminal ADF domain (actin-depolymerizing factor domain) followed by two actin-binding domains (AB1 and AB2). In the case of DrebrinA, it contains an additional 46-amino-acid domain known as Ins2, which is exclusive to the adult neuronal form. Finally, both isoforms share a C-terminal domain, which encompasses a large IDR, also referred to as low complexity region (LCR) and contains two Homer-binding motifs (Shirao et al., 2017).

To investigate which domains are responsible for the localization of DrebrinA in dendritic spines, we generated several DrebrinA mutants. One of the mutants, DrebrinA  $\Delta$ LCR, lacked the LCR but maintained the actin-related domains and the Ins2 domain. Additionally, we created DrebrinA LCR, which solely consisted of the LCR containing the two Homer-binding motifs. Finally, DrebrinA LCRmut mutant contained point mutations within the LCR which disrupt the Homer-DrebrinA interaction (Fig. 31A), as it has previously been described by H. Li et al. (2019). The Homer-binding motif is characterized by a PPXXF-like sequence motif (Y.M. Yang et al., 2014) which we modified by replacing proline (P) residues with leucine (L) residues and the phenylalanine (F) residue with an arginine (R) residue, resulting in a new motif, LLXXR.



**Figure 31. DrebrinA is enriched in dendritic spines through its actin-related domains.** (A) Scheme showing mScarlet-DrebrinA wt and mutants ( $\Delta$ LCR, LCR, and LCRmut). DrebrinA wt presents an actin depolymerizing domain (ADF-H, in blue), followed by two actin-binding domains (AB1 and AB2, in grey and yellow), the neuron-specific sequence (Ins2, in green), and the low complexity region (LCR) containing two Homer-binding motifs (in orange). DrebrinA  $\Delta$ LCR lacks the LCR, whereas DrebrinA LCR lacks the N-terminal part of the protein and only contains the LCR. DrebrinA LCRmut consist of the LCR but with mutations in Homer-binding regions impairing their interaction. Point mutations in Homer-binding motifs to disrupt Homer-DrebrinA interaction are shown, consisting in a change from PPxxF to LLxxR. Based on Y.M. Yang et al., 2014. (B) Hippocampal neurons at 14 DIV expressing mScarlet-DrebrinA mutants and GFP (tracker). DrebrinA wt and  $\Delta$ LCR are enriched in dendritic spines, whereas DrebrinA LCR and LCRmut are distributed homogeneously. Representative images are shown. Scale bar, 20  $\mu$ m. Insets show an enlarged region of the same cell; scale bar, 1  $\mu$ m.

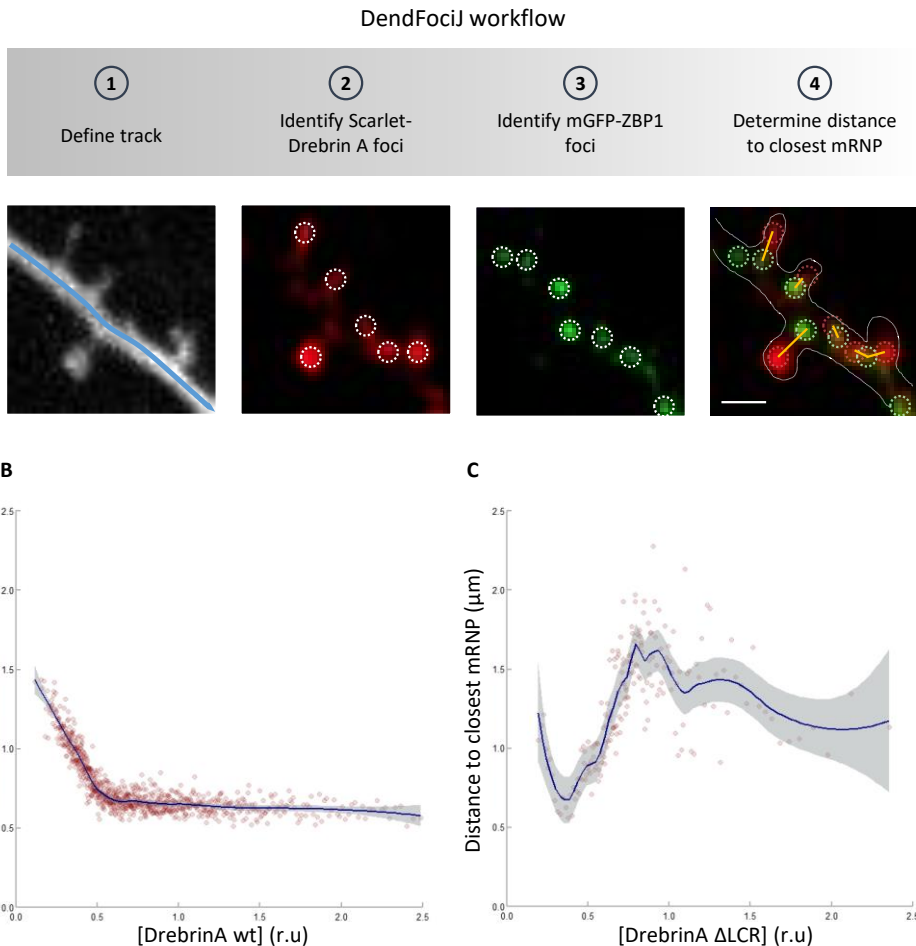
## RESULTS

We overexpressed mScarlet-DrebrinA mutants along with GFP as a tracker to examine the localization of DrebrinA based on the presence or absence of specific domains. Both DrebrinA wild-type (wt) and DrebrinA  $\Delta$ LCR were enriched in dendritic spines heads, indicating that actin-related domains are responsible for DrebrinA localization in dendritic spines. In contrast, DrebrinA LCR and LCRmut mutants displayed a homogeneous distribution throughout the neuron (Fig. 31B).

### **3. Analyzing the effect of postsynaptic proteins in RNA granules positioning**

To investigate whether DrebrinA could influence the trapping or attraction of mRNA transport granules (mRNPs), we co-transfected 7 DIV hippocampal neurons with plasmids encoding for mGFP-ZBP1, mScarlet-DrebrinA and pRFP670 as a tracker and live-imaged them at 14 DIV. We reasoned that if DrebrinA levels influenced mRNPs trapping, higher levels of DrebrinA within a single dendritic spine would correspond to a closer proximity of an mRNP. To analyze this, we developed an ImageJ plugin called DendFociJ, which allowed us to measure mScarlet-DrebrinA levels in individual dendritic spines and determine the closest distance to a mGFP-ZBP1 foci in the dendritic shaft (Fig. 32A).

The DendFociJ plugin first identified the dendritic track by detecting fluorescence changes above the background. Next, it detected mScarlet-DrebrinA foci based on a fluorescence change above 55 % of the background signal, primarily representing individual dendritic spines. Subsequently, it identified mGFP-ZBP1 foci presenting a fluorescence intensity of over 30 % compared to the background signal, corresponding to individual RNA transport granules predominantly present in the dendritic shaft. The plugin exported data on mScarlet-DrebrinA foci intensity levels and the distance to the nearest mGFP-ZBP1 foci. To standardize the data, mScarlet-DrebrinA fluorescence levels were normalized against the tracker fluorescence and referred to as DrebrinA concentration, represented as [DrebrinA]. This enabled us to measure the correlation between these variables and determine whether DrebrinA influenced the position of mRNPs within dendrites. As shown in Figure 32B, DrebrinA acts as an attractor for RNA granules in a concentration-dependent manner.

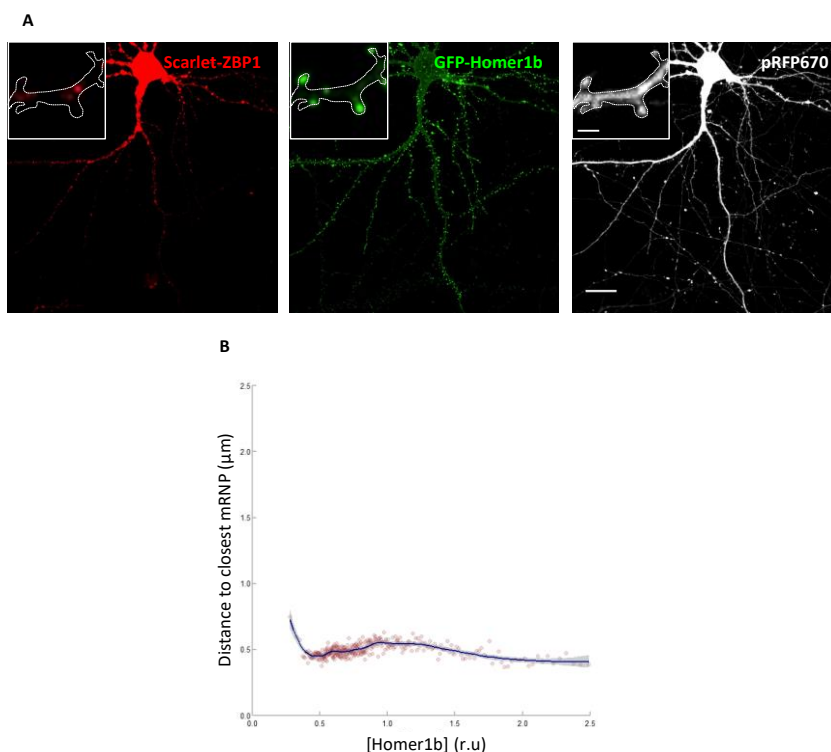


**Figure 32. DrebrinA acts as an attractor of RNA granules to dendritic spines through its LCR domain.** (A) Workflow of DendFociJ plugin of ImageJ. First, user defines the dendrite track. Next, software identifies one-pixel sized mScarlet-DrebrinA foci corresponding to dendritic spines. On third place, software identifies one-pixel sized mGFP-ZBP1 foci. Finally, the software determines the distance to the closest mGFP-ZBP1 foci for each mScarlet-DrebrinA foci intensity value. Graphs plotting distance to closest mRNP versus (B) DrebrinA wt or (C) DrebrinA  $\Delta$ LCR concentration (in relative units) are shown. Data is obtained from DendFociJ. Protein concentration was determined by dividing DrebrinA wt or  $\Delta$ LCR fluorescence intensity by pRFP670 tracker fluorescence intensity.

We hypothesized that the LCR of DrebrinA could interact with components of RNA transport granules, such as RBPs, even though evidence of direct interaction was lacking. We reasoned that this disordered region could be involved in DrebrinA's attraction capacity. To test this, we used the same abovementioned approach, but using mScarlet-DrebrinA  $\Delta$ LCR mutant instead of the wt protein. If the LCR was responsible for attracting granules, the mutant lacking this region would lose this capacity. As expected, DrebrinA  $\Delta$ LCR concentration levels did not influence the distance of mRNPs to spines (Fig. 32C).

## RESULTS

Since DrebrinA is found in mature dendritic spines, it is possible that its attraction capacity is not an inherent property of DrebrinA itself, but rather a property of other components of mature dendritic spines. Therefore, we decided to investigate whether other proteins present in the PSD also influenced granule attraction. We focused on Homer1, a PSD scaffold protein involved in regulating glutamatergic synapses and spine morphogenesis (Tao-Cheng et al., 2014).



**Figure 33. The minimal distance of mRNPs remains constant in a Homer concentration-independent manner.** (A) Hippocampal neurons were transfected at 7 DIV with plasmids codifying for mScarlet-ZBP1, GFP-Homer1b, and pRFP670 and imaged at 14 DIV. Representative images are shown. Scale bar, 20  $\mu\text{m}$ . Insets show an enlarged region of the same cell; scale bar, 2  $\mu\text{m}$ . (B) Graph plotting distance to closest mRNP versus Homer1b concentration (in relative units) is shown. Data is obtained from DendFociJ. Protein concentration was determined by dividing Homer1b fluorescence intensity by tracker fluorescence intensity.

We used a GFP-tagged Homer1b, one of the long isoforms of the Homer family, and evaluated its localization in mouse hippocampal neurons at 14 DIV. Accordingly to literature, GFP-Homer1b was enriched in dendritic spines (Hering & Sheng, 2001) (Fig. 33A). We co-transfected it with mScarlet-ZBP1 to verify that the overexpression pattern of ZBP1 was not affected by the fusion protein tag. mScarlet-ZBP1 exhibited a similar punctate pattern to mGFP-ZBP1 (Fig. 30). Moreover, no colocalization was observed between GFP-Homer1b and mScarlet-ZBP1 signals.



To assess if Homer1b had a similar attraction effect as DrebrinA, we employed the same approach described earlier, co-transfecting hippocampal neurons with plasmids encoding mScarlet-ZBP1, GFP-Homer1b and pRFP670. We analyzed the distance to the closest mRNP depending on the concentration of Homer1b. As observed in Figure 33B, the distance of RNA granules remained constant regardless of Homer concentration, demonstrating that Homer1b do not attract RNA granules within the dendrite. These results confirm that DrebrinA influences the positioning of mRNPs in dendrites, but this is not an inherent property of all PSD proteins.

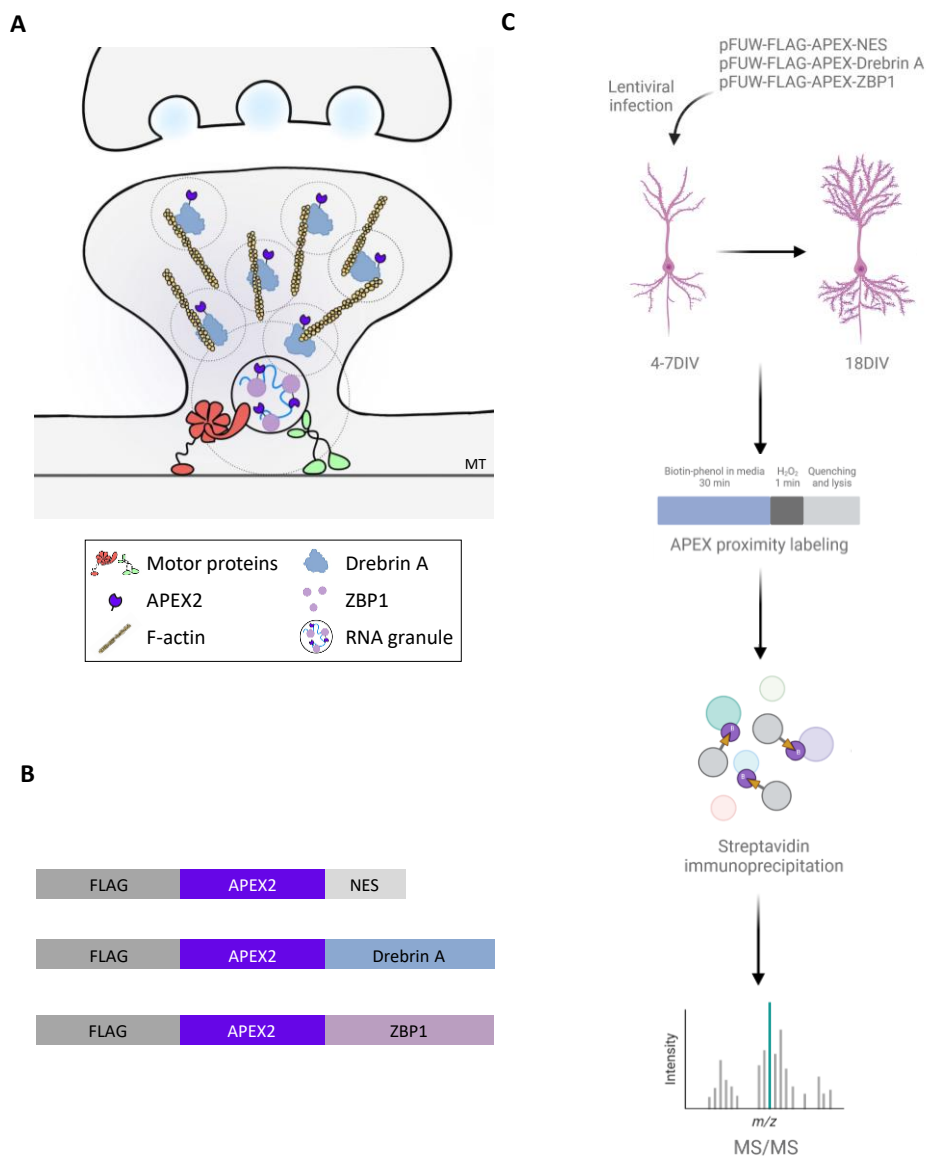
Our results demonstrate that DrebrinA is involved in the attraction of RNA granules to dendritic spines. However, the employed approach does not allow us to determine whether DrebrinA solely has an attracting effect or is also involved in the molecular mechanisms of RNA granule anchoring.

#### **4. Determining proteins involved in RNA granule local capture by proximity labeling**

There is a knowledge gap in the scientific literature regarding the molecular mechanisms underlying granule capture. It is hypothesized that molecules involved in this process interact, likely in response to specific signals, with proteins that are constituent components of the granules. These interactions are expected to be transient in nature, which poses challenges in their detection using conventional approaches that primarily focus on identifying strong protein-protein interactions. As a result, there is currently limited evidence available in the literature pertaining to these transient interactions.

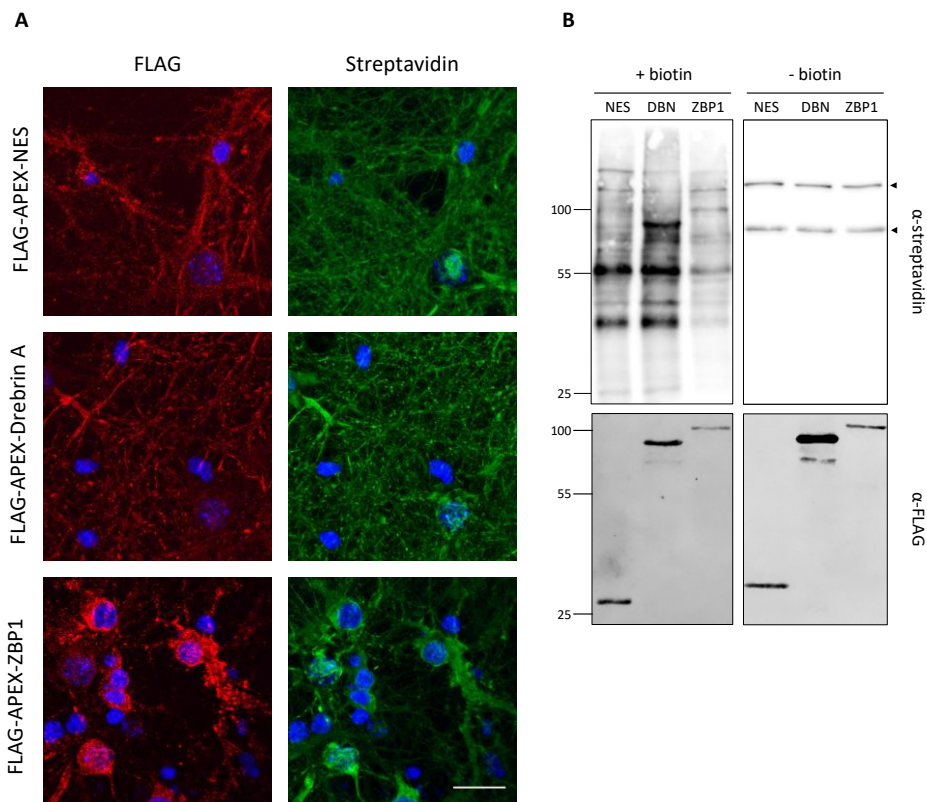
Proximity labeling proteomics approaches have emerged as valuable tools for studying protein interaction patterns and subcellular localization (Chung et al., 2017; Fazal et al., 2019; Frankenfield et al., 2020; Markmiller et al., 2018; Marmor-Kollet et al., 2020; Padrón et al., 2019). These techniques rely on enzyme-catalyzed *in vivo* reaction to label proteins in close proximity to the labeling enzyme, APEX2, which is typically fused to a query protein. The labeled proteins can then be analyzed *ex vivo*. To investigate which proteins are involved in RNA granules capture, we performed proximity labeling using APEX2, an enhanced ascorbate peroxidase 2, fused to two different proteins: (1) DrebrinA, considering its effect on the attraction of mRNPs through dendrites, and its candidacy as a key player in this process; and (2) ZBP1, as a well-established core component of RNA granules. To establish a spatial control, we also fused APEX2 with a nuclear export signal (NES) (Fig. 34A, B).

## RESULTS



**Figure 34. Live-cell proteomics using APEX.** (A) Schematic representation of the APEX proximity labeling approach used to determine the interactors of DrebrinA and ZBP1 proteins. Dashed circles show APEX2 proximity labeling within 20 nm distance from the bait proteins. (B) Scheme of the three different plasmids used: FLAG-APEX-NES (Nuclear Export Signal), FLAG-APEX-DrebrinA, and FLAG-APEX-ZBP1. Bait proteins are tagged with FLAG and APEX2, an enhanced ascorbate peroxidase 2 that enables proximity labelling. (C) Illustration of the workflow used in the APEX proximity labeling approach. Primary cortical neurons were infected between 4 and 7 DIV using lentiviral particles codifying for pFUW-FLAG-APEX-NES, pFUW-FLAG-APEX-DrebrinA or pFUW-FLAG-APEX-ZBP1. At 18 DIV, APEX proximity labelling assay was performed. For that, biotin-phenol was added to the media for 30 min. Then, hydrogen peroxide (H<sub>2</sub>O<sub>2</sub>) was added for 1 min for APEX activation. Finally, the reaction was quenched, and cells were lysed. Biotinylated proteins were enriched through streptavidin immunoprecipitation and sent to mass spectrometry (MS/MS).

Cortical neurons between 4 and 7 DIV were infected with pFUW-FLAG-APEX-NES, DrebrinA, or ZBP1. Neurons were cultured until 18 DIV, to ensure proper maturation of dendritic spines. Subsequently, APEX proximity labeling was performed. Neurons were incubated in media containing biotin-phenol for at least 30 min, to ensure incorporation of the biotin into the cell. Following this, labeling was performed by adding hydrogen peroxide (H<sub>2</sub>O<sub>2</sub>) for 1 min. To stop the reaction, quenching buffers were used before lysing cells. Biotinylated proteins were enriched using streptavidin magnetic beads. For each experimental condition, we conducted biologically independent triplicate labeling reactions followed by individual streptavidin purification of biotinylated proteins. Affinity-purified samples were analyzed by quantitative MS/MS (Fig. 34C).



**Figure 35. Validation of expression of APEX2 in mouse cortical neurons.** Primary cortical neurons at 18 DIV expressing FLAG-APEX-NES, FLAG-APEX-DrebrinA or FLAG-APEX-ZBP1. (A) Confocal microscope imaging of the biotin-labeling patterns of APEX2 transgenes. Red fluorescence represents immunofluorescence of enzyme expression (Alexa Fluor 561 anti-mouse conjugate/anti-FLAG detection), and green fluorescence detects biotin-labeled proteins (Alexa Fluor 488 streptavidin conjugate detection). Labeling was conducted in living cells, and imaging was performed after fixation and permeabilization. Hoechst (blue) was used for nuclear staining. Scale bar, 20  $\mu$ m. (B) Streptavidin-HRP detection of biotinylated proteins of APEX2 by WB analysis. FLAG epitope tag detection of the expressed enzyme is shown to the bottom. Arrows indicate endogenous biotinylated proteins.

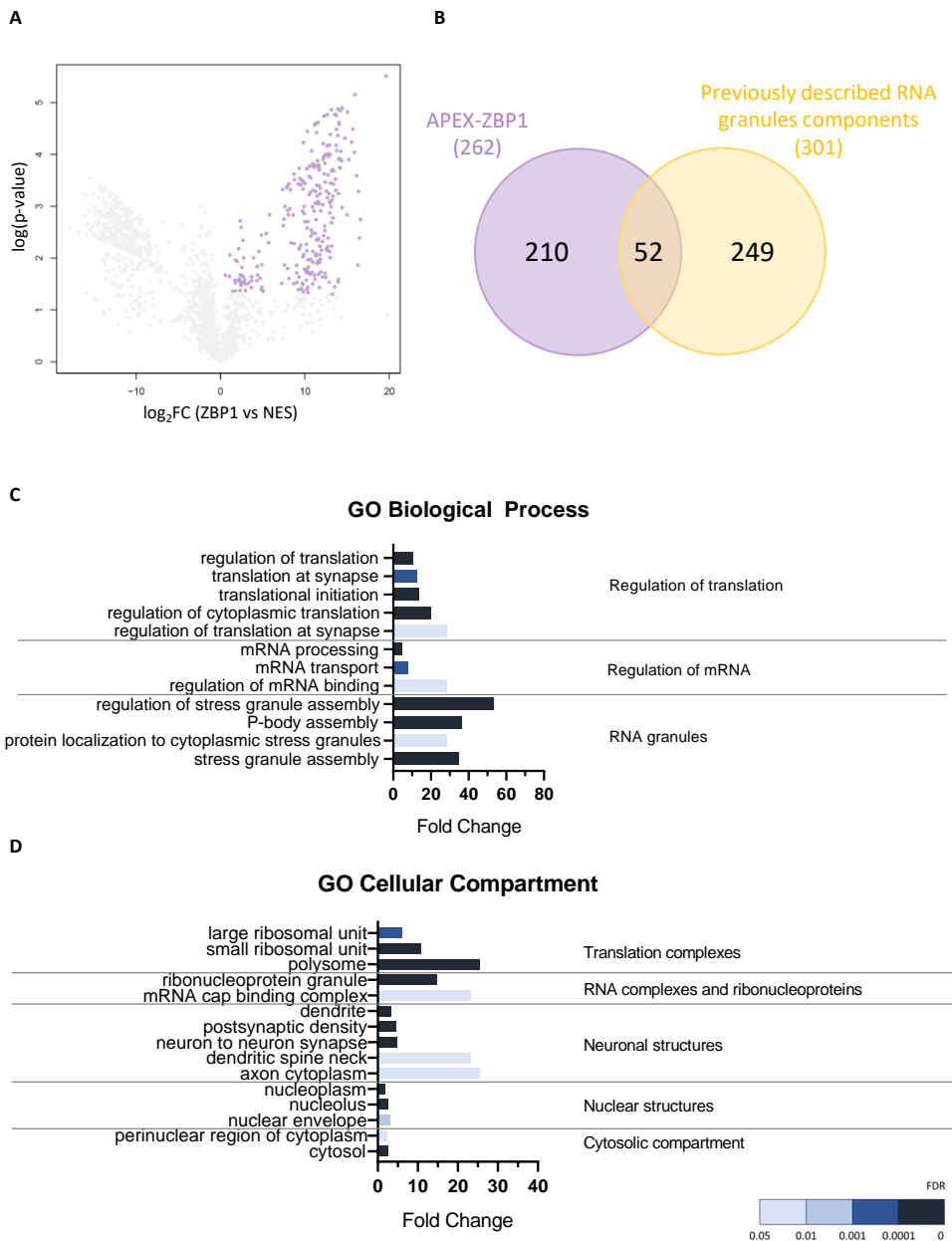
## RESULTS

In parallel, we assessed the proper expression of FLAG-APEX constructs in 18 DIV cortical neurons by IF and WB techniques. Immunostaining against FLAG demonstrated expression of the constructs in infected cortical neurons. Biotinylated proteins were detected using an antibody against streptavidin. FLAG-positive cells showed streptavidin labeling, confirming the functionality of APEX2 (Fig. 35A). In the absence of biotin-phenol or hydrogen peroxide exposure, no streptavidin signal was observed (data not shown). WB analysis also confirmed the expression of FLAG-APEX plasmids and the occurrence of biotinylation (Fig. 35B).

Regarding the mass spectrometry results, for the DrebrinA condition, a total of 1352 proteins were detected, out of which 787 were found in at least two out of three replicates, and thus considered as genuine interactions. On the other hand, for the ZBP1 condition, a total of 1197 proteins were detected, but only 652 were found in at least two replicates. Finally, for the NES condition, used as spatial control, 1356 proteins were identified but only 845 appeared in more than two replicates. Notably, DrebrinA interactors exhibited a correlation of 46.4 % with NES interactors, while ZBP1 interactors showed a correlation of 23 % with the NES condition.

The proximity labeling mediated by APEX2 biotinylated the surrounding proteins. To exclude some proteins that would be biotinylated considering its cytosolic distribution, ZBP1 interactors were compared to NES interactors. As mentioned before, we also fused the peroxidase APEX2 to a NES that could allow the biotinylation of cytoplasmic proteins to exclude false positive interactors of ZBP1 or DrebrinA. As shown in figure 36A, we found 262 proteins that were enriched in ZBP1 condition, using an adjust  $P < 0.05$  and a fold change  $> 1.5$ , as shown in Supplementary Table 1.

We decided to compare ZBP1 interactors from our dataset (referred as “APEX-ZBP1”) with other datasets that have described RNA granules composition in the literature (referred as “Previously described RNA granules components”). We used 5 different datasets as shown in table 9. As observed in figure 36B, 52 of the identified proteins have previously been described in the literature as transport RNA granules. This result reinforces the idea that APEX2 technology is suitable to determine the composition of these non-membrane bound structures.



**Figure 36. FLAG-APEX-ZBP1 interacting proteins are mostly RNA granules and neuronal structural proteins.** (A) Volcano plot of the differently enriched proteins between ZBP1 and NES conditions. Dark purple dots highlight the significantly enriched proteins in FLAG-APEX-ZBP1 interacting proteins in cortical neurons ( $\log_2$ fold change > 1.5 and adjusted  $P < 0.05$ ). Grey dots show non significantly enriched proteins and proteins enriched for the FLAG-APEX-NES condition. (B) Venn diagram showing the overlap between FLAG-APEX-ZBP1 interacting proteins from this study (APEX-ZBP1) and previously described RNA granules components from five different studies (detailed in table 9). (C) Gene Ontology Biological Process analysis showing the hallmarks that were significantly upregulated in FLAG-APEX-ZBP1 interacting proteins. (D) Gene Ontology Cellular Compartment analysis showing the hallmarks that were significantly upregulated in FLAG-APEX-ZBP1 interacting proteins.

## RESULTS

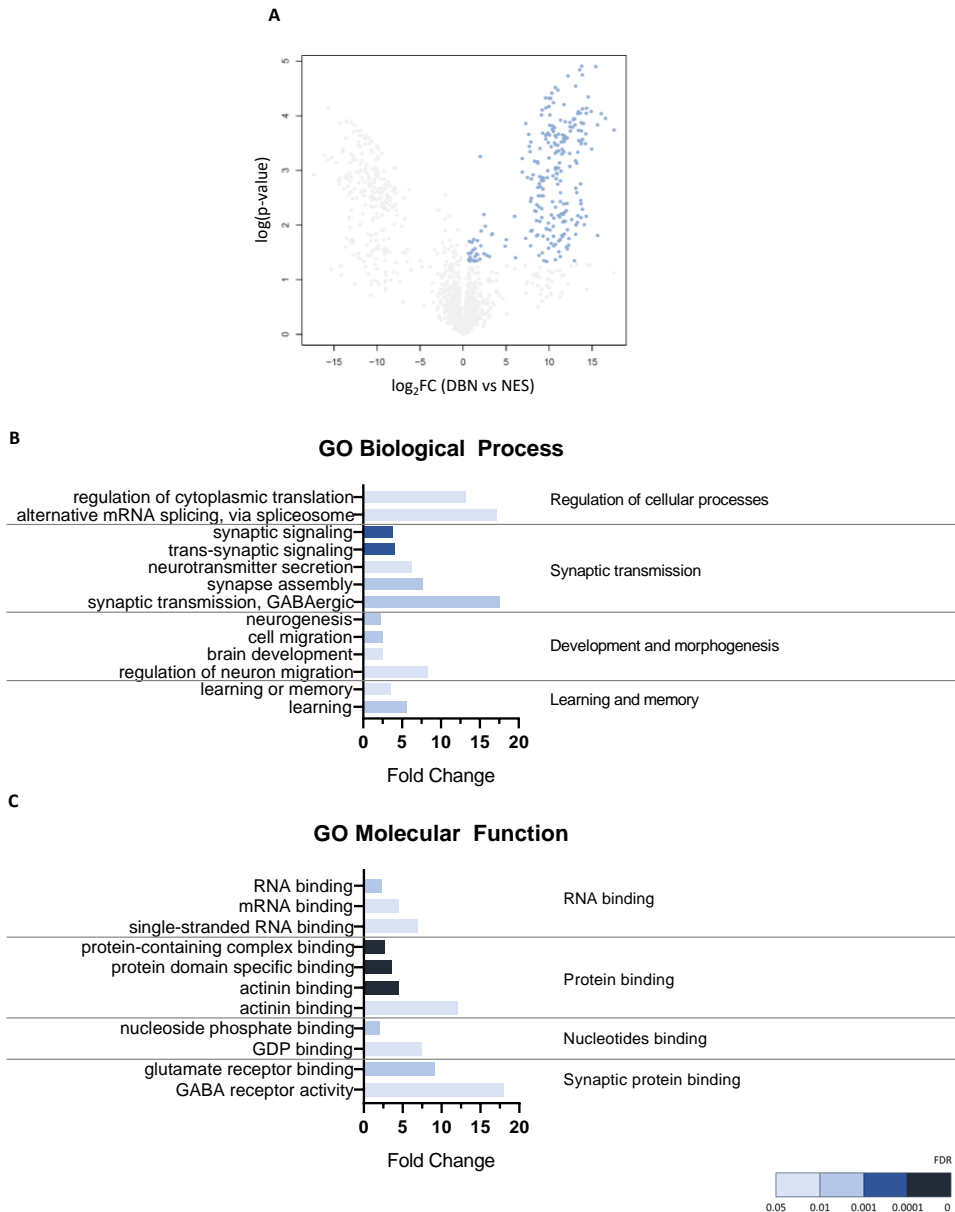
Reference	Isolation method	Tissue / Cell line	# of identified proteins
Fritzsche et al., 2013	Centrifugation in sucrose gradient and IP $\alpha$ -Btz and $\alpha$ -Stau2	Rat E17 brain	115
Jønson et al., 2007	IP $\alpha$ -FLAG-ZBP1	HEK293T cells	30
Kanai et al., 2005	Centrifugation in sucrose gradient, incubation with GST-KIF5 and IP $\alpha$ -GST	Mouse adult brain	41
Kurosaki et al., 2022	IP $\alpha$ -FMRP	SH-SY5Y cells	46
Mukherjee et al., 2019	BioID of $\beta$ -actin mRNA	HEK293T cells	136

**Table 9. Datasets of RNA granules proteomics.** Reference paper, isolation method of RNA granules, tissue or cell line used, and number of proteins identified are shown.

Next, we conducted a GO analysis to elucidate the functional attributes of ZBP1-interacting proteins. Our investigation included an exploration of their involvement in key biological processes. Among these, notable emphasis was placed on the regulation of protein translation, mRNA regulation and the orchestration of RNA granules (Fig. 36C). Additionally, a dissection of the cellular localization of these interacting proteins, undertaken via GO analysis, yielded profound insights. These proteins were predominantly associated with translation complexes, RNA assemblies as ribonucleoproteins, structural constituents of neuronal architecture, as well as nuclear and cytoplasmic proteins (Fig. 36D).

We conducted a parallel analysis for interactors of DrebrinA, referred as DBN, mirroring our approach to that of ZBP1. Upon juxtaposing the DrebrinA condition with the NES condition, we found an enrichment of 227 proteins under the DBN condition, meeting stringent criteria of adjusted  $P < 0.05$  and a fold change  $> 1.5$  (Fig. 37A), as shown in Supplementary Table 2. Our findings could not be aligned with external datasets because of the absence of mass spectrometry data delineating DrebrinA interactors, thereby limiting comparative analysis.

GO analysis regarding the biological processes of the interacting proteins showed an enrichment in proteins involved in the regulation of cellular processes such as protein translation, mRNA splicing, synaptic transmission, developmental morphogenesis, as well as learning and memory (Fig. 37B). These results can be explained by understanding the important role of DrebrinA in the structure of the actin cytoskeleton and its significant presence in the PSD (Hanamura et al., 2018; Ivanov et al., 2009; Takahashi et al., 2003).

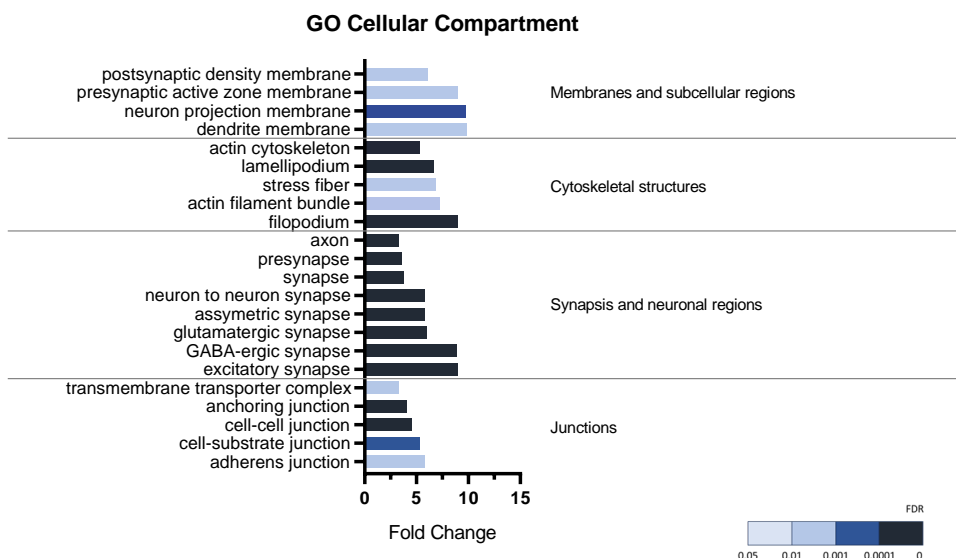


**Figure 37. FLAG-APEX-DrebrinA interacting proteins are mostly involved in synaptic function.** (A) Volcano plot of the differently enriched proteins between DrebrinA (DBN) and NES conditions. Blue dots highlight the significantly enriched proteins in FLAG-APEX-DBN interacting proteins in cortical neurons ( $\log_2$ fold change > 1.5 and adjusted P < 0.05). Grey dots show non significantly enriched proteins and proteins enriched for the FLAG-APEX-NES condition. (B) Gene Ontology Biological Process analysis showing the hallmarks that were significantly upregulated in FLAG-APEX-DBN interacting proteins. (C) Gene Ontology Molecular Function analysis showing the hallmarks that were significantly upregulated in FLAG-APEX-DBN interacting proteins.

## RESULTS

Furthermore, an analysis of the molecular functions exhibited by DrebrinA-interactors revealed an enrichment in entities associated with RNA binding, and protein binding, among others (Fig. 37C). A subset of these RBPs has previously been characterized as constituents of RNA granules (see references in Table 9).

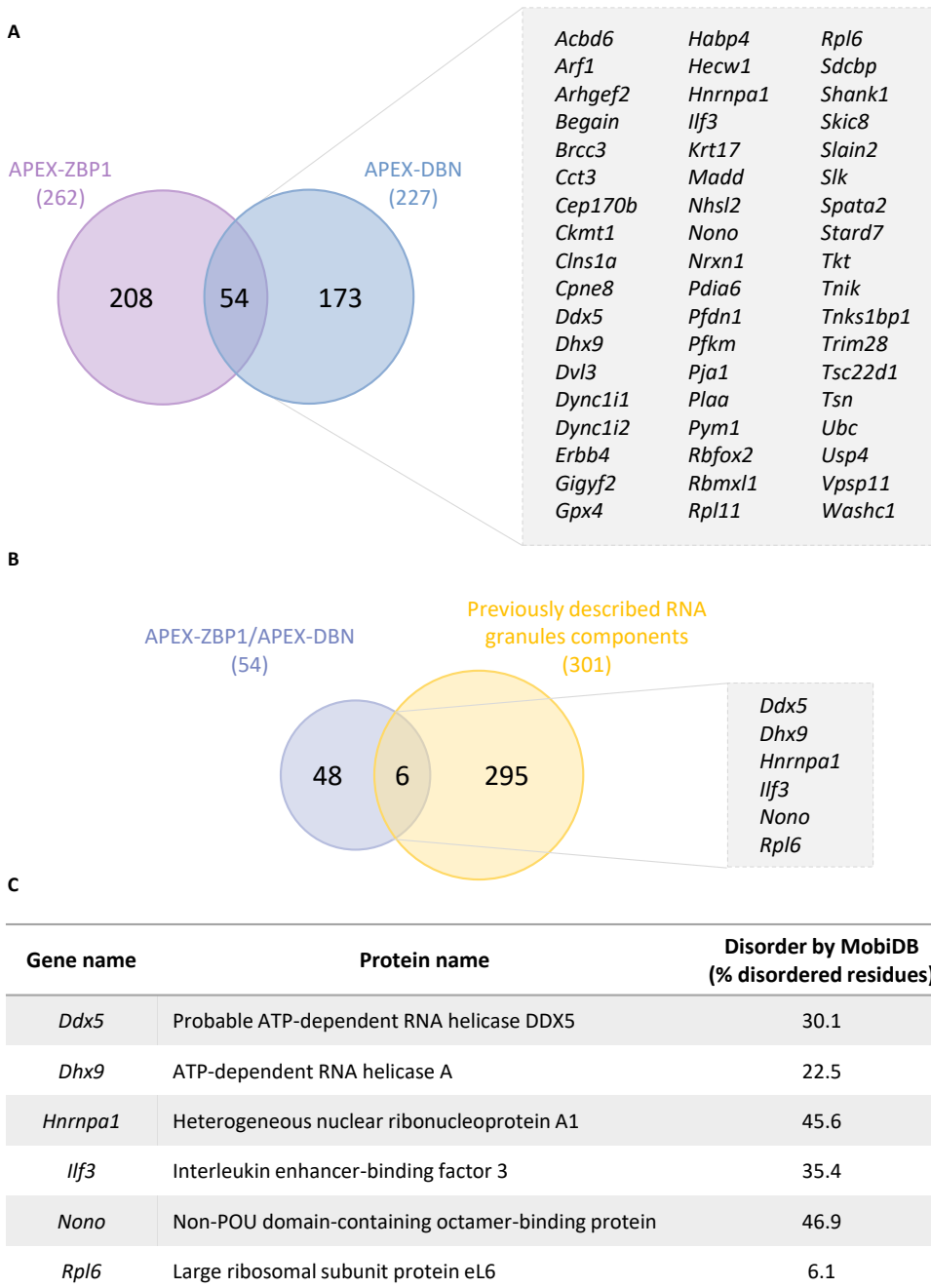
Lastly, we examined the cellular compartmentalization of DrebrinA interactors, unraveling an enrichment in membranes and subcellular regions, cytoskeletal structures, synapses and neuronal regions, and junctions (Fig. 38).



**Figure 38. FLAG-APEX-DrebrinA interacting proteins are mostly actin cytoskeleton and synaptic proteins.** Gene Ontology Cellular Compartment analysis showing the hallmarks that were significantly upregulated in FLAG-APEX-DBN interacting proteins.

As already mentioned, our main objective was to determine which proteins are involved in RNA granules capture. We hypothesized that RNA granules anchoring was mediated by synaptic proteins that interact with RNA granules proteins. Our initial candidate was DrebrinA, considering its attraction capacity of RNA granules dependent on DrebrinA dendritic spine levels. DrebrinA interacts with several RNA granules constituents, such as several hnRNPs, some ribosomal proteins, and RNA helicases. However, it does not directly interact with core RBPs such as ZBP1 or FMRP (Fig. 39A). All proteins interacting with both FLAG-APEX-ZBP1 and FLAG-APEX-DrebrinA are detailed in Supplementary Table 3.





**Figure 39. Proteins interacting with ZBP1 and DrebrinA present disordered regions in their structure.** (A) Venn diagram showing the overlap between FLAG-APEX-ZBP1 (APEX-ZBP1) and FLAG-APEX-DrebrinA (APEX-DBN) interacting proteins from this study. Gene names of the 54 overlapping proteins are also shown. (B) Venn diagram showing the overlap between shared interacting proteins between FLAG-APEX-ZBP1 and FLAG-APEX-DrebrinA interactors (APEX-ZBP1/APEX-DBN) and previously described RNA granules components from five different studies (detailed in Table 9). Gene names of the 6 overlapping proteins are also shown. (C) Gene names, protein names, and predicted disorder using MobiDB software for the 6 genes showed in (B) are shown.

## RESULTS

We hypothesized that RNA granule anchoring should be a promiscuous mechanism that will not depend on the RBPs forming the RNA granule. Considering the huge heterogeneity within RNA granules composition, we decided to compare our DBN-ZBP1 interacting proteins with previously reported RNA granules proteins to elucidate which proteins are essential constituents of these mRNPs and probably responsible for the anchoring process. We found that only 6 proteins exhibit these characteristics: probable ATP-dependent RNA helicase (DDX5), ATP-dependent RNA helicase A (DHX9), heterogeneous nuclear ribonucleoprotein A1 (hnRNPA1), interleukin enhancer-binding factor 3 (ILF3), Non-POU domain-containing octamer-binding protein (NonO), and large ribosomal subunit protein eL6 (RPL6) (Fig. 39B).

As mentioned at the beginning of this chapter, we thought that DrebrinA could interact with RNA granules proteins because of its C-terminal disordered region. These promiscuous protein-protein interactions would be higher when interacting with other disordered proteins. Thus, we analyzed the presence of intrinsically disordered regions in these proteins using MobiDB software. MobiDB is a bioinformatic tool that employs various algorithms and machine learning techniques to predict the disorder of each residue of a protein. It considers factors such as amino acid composition, sequence patterns, physicochemical properties, and disorder prediction algorithms to assess the likelihood of a given residue being part of a disordered region. Residues predicted to be disordered are assigned a value of 1, while those predicted to be ordered receive a value of 0. At the end, the software provides you a percentage of disordered of the whole protein. As shown in figure 39C, these putative anchoring-mediating proteins are mostly disordered, except for large ribosomal subunit protein eL6.

Interestingly, two out of these six proteins are RNA helicases, DDX5 and DHX9. Several studies have demonstrated the significant role of this protein family in disassembling RNA granules (Hubstenberger et al., 2013; Mugler et al., 2016), but little is known about the underlying molecular mechanisms. Nevertheless, our findings suggest that these proteins could potentially play a crucial role in granule anchoring and perhaps in their disassembly.





# **DISCUSSION**



# **Chapter 1: Molecular mechanisms regulating eEF1A2 in the synaptic function**





### 1. A switch from eEF1A1 to eEF1A2: what is its purpose?

In this study, we aim to elucidate the physiological relevance of eEF1A2 isoform in the context of synaptic plasticity. Vertebrates have two eEF1A genes that encode two different isoforms, eEF1A1 and eEF1A2, which are 98 % similar at the amino acid level and yet exhibit different expression patterns. While the eEF1A1 isoform is ubiquitously expressed, it is replaced by the eEF1A2 isoform in neurons and muscle tissues (Soares et al., 2009). Given their near-identical nature, the necessity of switching between these isoforms for proper development is indeed intriguing.

Notably, mice lacking the isoform eEF1A2 die 28 days after birth, underscoring the indispensable role of eEF1A2 (Khalyfa et al., 2001). This is understandable considering that eEF1A is the protein responsible for delivering aa-tRNAs to the elongating ribosome. The loss of this protein leads to deficiencies in protein translation, resulting in the death of mice. Surprisingly, heterozygous mice with a presumed 50 % reduction in eEF1A2 expression appeared phenotypically normal (Griffiths et al., 2012). However, there is a lack of data regarding what occurs if eEF1A1 substitutes eEF1A2. Investigating this phenomenon will aid in determining which functions are exclusively carried out by eEF1A2 and whether there are any differences between these isoforms that explain the switch between them, specifically in certain tissues.

A recent study analyzing the expression of eEF1A1 and eEF1A2 suggests that eEF1A2 is expressed as early as E11.5 in the developing neural tube. Furthermore, it was previously believed that eEF1A1 was completely replaced for eEF1A2 in neurons. However, a recent study postulates that eEF1A1 may still be present in axons, implying that both isoforms are transcribed in neurons but exhibit different subcellular localizations at the protein level (Davies et al., 2023). Intriguingly, a study conducted by Wefers and colleagues revealed that *eEF1A1* mRNA is more abundant in dendrites than *eEF1A2* mRNA, suggesting that eEF1A1 may have a role in developing hippocampal neurons, contrary to our findings. Several groups have conducted RNAseq analyses from somas and neurites of neuronal cells, yet the presence or absence of *eEF1A1* mRNA remains inconclusive, as documented by Middleton et al. (2019).

In our results, we presumed that the remaining eEF1A1 levels detected in our primary cultures originated from glial cells, in which eEF1A1 is the predominant isoform (Wefers et al., 2022). Hence, conducting IF experiments using specific antibodies for each cell type and eEF1A isoforms is necessary to corroborate the localizations suggested by Davies and Wefers. Additionally, obtaining pure neuronal primary cultures instead of the mixed cultures currently used in this study would be

## DISCUSSION

advantageous in determining if the remaining levels of eEF1A1 that we detect correspond to glial cells or neurons. Treatment with low concentrations of cytarabino furanoside (AraC) or 5-fluoro-20-deoxyuridine (FUdR) could aid in this regard, as these compounds specifically affect dividing cells (Lesslich et al., 2022).

### **2. Is phosphorylation the answer?**

When comparing amino acid sequences of both isoforms, we identified four putative phosphorylation residues exclusive to eEF1A2. These residues are Ser<sup>342</sup>, Ser<sup>358</sup>, Ser<sup>393</sup>, and Ser<sup>445</sup>. To investigate the potential significance of phosphorylation of these residues, we generated phospho-null and phospho-mimetic mutants. While phospho-mutants usually focus on individual residues, it has also been demonstrated in other studies that simultaneous mutation of multiple residues can be employed (K. Kim et al., 2015). This approach offers the advantage of investigating whether the phosphorylation of more than one residue is necessary to fulfil a particular function, a scenario that might go unnoticed when using single mutants. Nevertheless, it is essential to acknowledge the possibility that some of the selected residues may not undergo phosphorylation *in vivo*, potentially leading to artefactual phenotypes.

To elucidate the role of eEF1A2 phosphorylation, we conducted interactome analyses of both phospho-mutants in HEK293T cells. Comparing the interactors between these phospho-mutants provides insights into how the phosphorylation state of a protein affects its interaction with their partner molecules and, consequently, its various functions. In our study's context, the interactomic analysis of eEF1A2 phospho-mutants dissected translational and non-canonical functions of the elongation factor. Notably, the phospho-null SA mutant exhibited significant interactions with proteins associated with protein translation, which represents the canonical function of eEF1A2. On the other hand, the phospho-mimetic SE mutant interacted with proteins involved in a wide array of functions, encompassing ER-to-Golgi vesicle-mediated transport, protein modification, response to stress, nuclear import, among others. Some of these functions have previously been described as non-canonical functions of eEF1A. However, it is important to note that most of these non-canonical functions were previously analyzed in immortalized cell lines expressing both eEF1A1 and eEF1A2, without distinguishing between isoforms. Additionally, our study is the first evidence linking different functions depending on the phosphorylation state of eEF1A2.

### **3. The effect on actin dynamics**

F-actin in spines can be divided into a dynamic pool, with a turnover time less than 1 min, and a stable F-actin pool, with a constant turnover time of approximately 17

min (Koskinen & Hotulainen, 2014). Furthermore, it has been described that roughly 80 % of all spinous actin is in the filamentous form, with only around 5-15 % of it being in a stable form (Honkura et al., 2008b; Star et al., 2002).

Previous experiments from the group demonstrated that the phospho-mimetic mutant eEF1A2 SE was seriously compromised in its ability to bind actin and produce actin bundles. Similar to the approach followed in other studies (Mikhaylova et al., 2018; Shaw et al., 2021), we performed FRAP analysis on fluorescently tagged actin to test whether the presence of the phospho-null or the phospho-mimetic mutant impacted the proportions of dynamic versus stable actin content of the spine. As shown in figure 23, neurons expressing the phospho-mimetic SE mutant showed a faster recovery of mScarlet-actin fluorescence after photobleaching along with an increased mobile fraction. These results demonstrate that phosphorylation of eEF1A2 impacts actin dynamics within dendritic spines.

It is worth mentioning that some studies claim a direct correlation between spine-head volume and the total amount of F-actin in the spine, as well as to the amount of stable F-actin (Honkura et al., 2008a). Hence, in our approximation, only mushroom-like dendritic spines with similar sizes were analyzed to maintain a consistent approach.

Our findings suggest that phosphorylation of eEF1A2 enables its dissociation from F-actin. Supporting this notion, our proteomics analysis showed a clear enrichment of ABPs in SE-IP. ABPs are involved in many different aspects of actin dynamics: nucleation, severing, crosslinking, capping, polymerization, depolymerization, and trafficking (Konietzny et al., 2017). According to previous studies in yeast, it is possible that eEF1A acts as a bridge between translation and actin cytoskeleton (Gross & Kinzy, 2007; Perez & Kinzy, 2014). In line with our findings, a recent study by Romaus-Sanjurjo et al. (2022) found that overexpressing eEF1A2, but not eEF1A1 or both proteins simultaneously, increased protein synthesis and actin rearrangement in corticospinal tract neurons. This study parallels our research by demonstrating that eEF1A2 coordinates protein translation and actin dynamics.

As one of the proteins enriched in SE-IP, we identified  $\alpha$ -actinin-4, a  $\text{Ca}^{2+}$ -sensitive actin-binding protein that interacts with mGluR1s and regulates spine morphogenesis in primary neurons (Kalinowska et al., 2015). Regarding the functional consequences of these interactions, we hypothesize that phosphorylation of eEF1A2 binds and sequesters F-actin bundles and crosslinkers. This would open a time window where actin-modifying proteins could access and remodel F-actin.

## DISCUSSION

Consistent with a role in structural plasticity, the eEF1A2 isoform has been implicated in metastasis (Abbas et al., 2015; Scaggiante et al., 2012; Tomlinson et al., 2005). It has been shown that eEF1A2 stimulates actin remodeling, cell invasion, and migration (Amiri et al., 2007). A previous investigation in adenocarcinoma cell lines showed that eEF1A from metastatic cells has reduced F-actin affinity (Edmonds et al., 1996). Additionally, isoform eEF1A2 was found to be more enriched than eEF1A1 in cell protrusions of breast cancer cells (Mardakheh et al., 2015). Collectively, these findings support our proposal that localized eEF1A2 phosphorylation weakens its association with actin, increasing cytoskeleton reorganization, cell motility, and ultimately, metastatic growth.

### **4. The effect on protein translation**

The primary function of elongation factor eEF1A is to facilitate protein translation elongation, as it has been reported for both isoforms eEF1A1 and eEF1A2. While both proteins show similar translation activities, they display different relative affinities for GTP and GDP as well as different dissociation rate constants (Kahns et al., 1998).

Given that eEF1A2 is the only expressed isoform in adult neurons, it has been assumed that this protein's role is to enable protein translation elongation in these cells. However, our interactomic analysis yielded surprising results. We observed that the phospho-null mutant interacts with proteins involved in the translation machinery, but this is not the case for the phospho-mimetic mutant. This suggests that when eEF1A2 is in a phosphorylated state, translation is transiently inhibited, as there are no other proteins performing redundant functions.

To evaluate the functional relevance of the phospho-mutants in protein translation, we considered the necessity of downregulating the endogenous protein. After testing several shRNA sequences, we successfully reduced endogenous levels by almost 80 % (Fig. 24A). Subsequently, we assessed translation efficiency using puromycin incorporation. The antibiotic puromycin is incorporated into peptide chains at the A site of the ribosome as it is an analog of aa-tRNAs. Upon incorporation, it participates in the peptide bond formation with the nascent polypeptide chain and results in irreversible premature termination of translation. This reaction enables labeling of newly synthesized proteins, which can later be detected *in situ* by puromycin-specific antibodies. Thus, the presence of puromycin-labeled peptides serves as an indicator of translation activity in a given cell or system.

In our study, we showed that Neuro-2a cells expressing HA-tagged eEF1A2 phospho-mutants exhibited differences in puromycin incorporation. Specifically, we found that the phospho-mimetic mutant did not facilitate translation as efficiently as the wt or SA eEF1A2.

We chose Neuro-2a cells, a mouse neuroblastoma cell line, as our working model for practical reasons. Firstly, downregulation of eEF1A2 in primary neuronal cultures is not feasible since it severely impacts translation to the extent that neurons undergo cell death. Secondly, the overexpression of eEF1A2 mutants is more straightforward in Neuro-2a cells due to the higher efficiency of lentiviral infection compared to primary cultures. Consequently, puromycin incorporation was assessed in this cell line instead of using primary cultures. However, it is essential to note that the main limitation of this cellular model is that local translation cannot be assessed, as puromycin is incorporated in the entire cell body of the cell.

Evaluating local translation in neurons presents its own set of challenges. Currently, the most used techniques are FUNCAT (Fluorescent non-canonical amino acid tagging) and SUnSET (Surface sensing of translation). FUNCAT involves the use of the non-canonical amino acid azidohomoalanine (AHA), which is incorporated into nascent protein chains and subsequently tagged with a fluorophore by a click chemistry reaction (Dieterich et al., 2007). On the other hand, SUnSET relies on puromycin incorporation, as early mentioned. Nevertheless, both techniques face limitations due to the relatively low amount of locally synthesized proteins within the dendritic compartment. While some efforts have been made to address this issue, achieving dendritic spine resolution remains challenging, particularly in spines located on distal dendrites (Dieterich et al., 2010; Gamarra et al., 2020; Sun et al., 2021).

#### **4.1. The importance of the interaction between eEF1A and eEF1B**

The initial step in the recycling of eEF1A during translation involves the exchange of GDP for GTP and it is driven by the eEF1B complex. Our interactomic analysis revealed that eEF1A2 phospho-null mutant interacted more with eEF1B2, a finding subsequently validated through IP in HEK293T cells and FRET experiments in Neuro-2a cells and neurons.

We hypothesized that eEF1A2 phosphorylation might be a transient event occurring within a narrow time window and in a confined cellular location. For that reason, we required tools capable of analyzing rapid changes *in vivo*. FRET-based reporters had been extensively used to determine CaMKII activity based on its close or open conformations (Ardestani et al., 2019; Mower et al., 2011; Takao et al., 2005).

## DISCUSSION

Interestingly, in 2015, Kim and colleagues published a study in which they elegantly demonstrated that the transient activation of CaMKII $\beta$  during synaptic plasticity temporally regulates the activity-dependent modification of the actin cytoskeleton (K. Kim et al., 2015). In this report, they employed Förster-resonance energy transfer-fluorescence-lifetime imaging microscopy (FRET-FLIM) to measure the detachment of CaMKII $\beta$  from F-actin.

Similarly, we GFP-tagged eEF1A2 wild-type and mutants and mScarlet-tagged eEF1B2. Both plasmids were expressed in neurons and the interaction between both proteins was assessed. This methodology enabled us to confirm that this interaction occurs at the dendritic spine level, where local translation is mediated. Additionally, time-lapse experiments revealed that LTD induction results in the transient phosphosite-mediated dissociation of eEF1A2 and eEF1B2.

Our FRET analysis to visualize the interaction between eEF1A2 and its GEF, the most upstream step in the translation elongation cycle, provides direct evidence of a locally modulated translation event in synaptic spines. When eEF1A2 is phosphorylated, it does not interact with eEF1B2, preventing the exchange of GDP for GTP. Consequently, eEF1A2 cannot be recycled and translation cannot proceed. Hence, this approach has the potential to monitor translation *in vivo* in a neuronal context.

Other FRET-based approaches have been proposed for monitoring translation. For instance, Koltun and colleagues proposed a method in which bulk yeast fluorescently labeled tRNAs were introduced in cortical primary neurons and were able to assemble ribosomes in dendritic spines. In this method, two tRNA populations are labelled with Cy3 and Cy5 dyes and FRET can be measured when two-differently labelled tRNAs are located at the A and P sites of an active ribosome (Koltun et al., 2020).

### **5. Role of the activity-dependent phosphorylation of eEF1A2**

Activation of mGluRs by DHPG stimulates the JNK pathway (L. Yang et al., 2006), and polysome-associated JNK phosphorylates eEF1A2 at Ser<sup>358</sup> as a response to DHPG in primary striatal neurons (Gandin et al., 2013). Thus, our data on the behavior of phospho-null and phospho-mimetic mutants point to the notion that phosphorylation of eEF1A2 by JNK and/or other kinases mediating synaptic signals is a crucial mechanism for the regulation of local translation in dendritic spines.

While the precise *in vivo* demonstration of eEF1A2 phosphorylation local effects has not been demonstrated yet, a similar scenario has been described for eEF2 and translational suppression in cultured neurons (Marin et al., 1997; S. Park et al.,

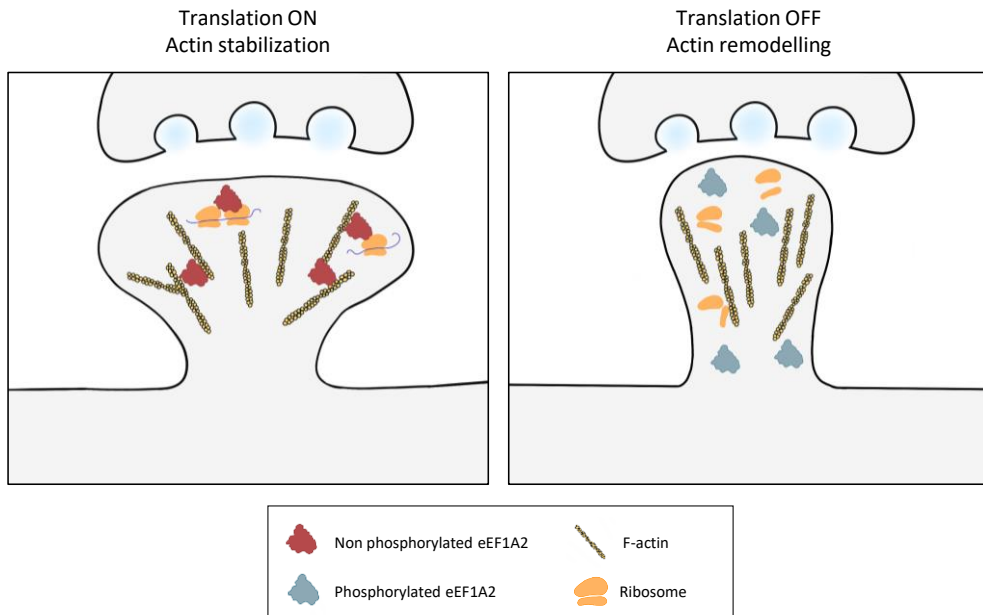
2008; Sutton et al., 2007), synaptic biochemical fractions (Scheetz et al., 2000), and hippocampal slices (Chotiner et al., 2003) after synaptic stimulation. This raises the question of whether the inhibition of protein synthesis by the two elongation factors eEF1A2 and eEF2 are redundant mechanisms. Both mechanisms have been observed under similar mGluR stimulation conditions, suggesting that phosphorylation of these two factors could be modulated by specific secondary signals. In the case of eEF2 phosphorylation, it has been demonstrated that although global translation is inhibited, some poorly initiated mRNAs in basal conditions increase their translation rates, like *Arc/Arg3.1* mRNA (Chotiner et al., 2003; S. Park et al., 2008; Scheetz et al., 2000). Whether this phenomenon is also happening after eEF1A2 phosphorylation remains to be determined.

However, there is growing evidence that eEF1A also has a profound impact at the initiation step of protein synthesis. In yeast, mutations in eEF1A that affect aa-tRNA binding simultaneously cause actin binding and/or bundling defects but, intriguingly, increase phosphorylation of eIF2A by general control nonderepressible 2 (GCN2), the eIF2A kinase (Gross & Kinzy, 2007; Perez & Kinzy, 2014). Phosphorylation at Ser<sup>51</sup>, which is conserved from yeast to mammals, by GCN2 converts eIF2A into an inhibitor of its own GEF, eIF2B, leading to the attenuation of general protein synthesis (Sonenberg & Hinnebusch, 2009). Therefore, the regulation of eEF1A2 would offer at least two substantial advantages compared to the eEF2 factor. First, the modulation of GTP loading through eEF1A2 phosphorylation provides a mechanism to regulate the most upstream step in translation elongation. Second, phosphorylation of eEF1A2 could provide feedback on translation initiation and efficiently downregulate protein synthesis.

## **6. Proposed model for the role of eEF1A2 in the synaptic function**

Our findings identify a previously unknown mechanism by which metabotropic signaling modulates structural plasticity. The stimulation of mGluR increases Ca<sup>2+</sup> levels, subsequently triggering activation of JNK and other Ca<sup>2+</sup> signaling kinases (Giese & Mizuno, 2013). Here, we show that receptor stimulation opens a time window in which elongation factor eEF1A2 dissociates from both its GEF protein and F-actin, thus decreasing protein synthesis and increasing actin cytoskeleton remodeling. This translational state could be common to the different forms of synaptic plasticity, including LTP, LTD, and homeostatic plasticity, in which activity-dependent spine remodeling is an essential initial event.

## DISCUSSION



**Figure 40. Proposed role of eEF1A2 in dendritic spine remodeling.** Two subpopulations of non-phosphorylated eEF1A2 would exist in stable spines, one involved in translation, and the other participating in F-actin bundles. As a result of synaptic stimulation, phosphorylation would dissociate eEF1A2 from F-actin and facilitate remodeling of the spine cytoskeleton. At the same time, eEF1A2 phosphorylation would cause its inactivation as a translation elongation factor, thus transiently preventing undesired protein accumulation before superimposed signals establish longer-term decisions as varied as LTP or LTD.

In summary, our work uncovers a crosstalk mechanism between local translation and actin dynamics in fast response to synaptic stimulation in neurons. As muscle cells also display a developmental eEF1A switch, we propose that eEF1A2 may be a general effector of structural plasticity to attain long-term physical and physiological changes at the subcellular level.







## **Chapter 2: Molecular mechanisms regulating RNA transport granules capture in dendritic spines**



## 1. DrebrinA attractive effect on RNA granules

The spatial and temporal organization of mRNAs in subcellular compartments controls gene expression and plays a fundamental role in cell polarization. This process is particularly essential in neurons, where the large length of axons and dendrites makes the transport of proteins over such distances unfeasible (S. Das et al., 2021). mRNA localization encompasses multiple processes, including the formation of RNA granules through LLPS, their subsequent transport, and ultimately, their anchoring to enable local translation. However, the precise molecular mechanisms governing where mRNAs are directed and how they are retained remain elusive.

The “sushi belt theory” proposes that RNA granules travel bidirectionally within dendrites and are stopped in the base of those spines that have been activated by stimulation (Doyle & Kiebler, 2011). If this theory is valid, it is reasonable to postulate the existence of sensory mechanisms within spines that detect neuronal activation and mediate the attraction of RNA granules to these activated sites. Our findings mark the first identification of a dendritic spine component capable of attracting RNA granules, the ABP DrebrinA.

### 1.1. RNA granules imaging

Through live-imaging experiments, we have demonstrated that DrebrinA acts as an attractor for RNA granules in a concentration-dependent manner (Fig. 32B). Imaging mRNA granules has been a challenge in the past decades for some technical limitations. For instance, Wong et al., (2017) used Cy5-UTP to label endogenous RNA in *Xenopus* embryos. This approach labels all RNA species in the cell, making it difficult to distinguish between different types of RNAs. Alternative methods have focused on fluorescently tagging specific transcripts, either employing the MS2 approach (Dictenberg et al., 2008; Dynes & Steward, 2012; Rook et al., 2000; Yoon et al., 2016) or molecular beacons (Donlin-Asp et al., 2021; Turner-Bridger et al., 2018). On the one hand, the MS2 system has been particularly used for studying dynamic processes because of its single-molecule precision in live cells, but it requires genetic manipulation to introduce the MS2 stem-loop sequences into the target RNA, potentially affecting RNA structure. On the other hand, molecular beacons are highly specific to their target sequences and do not require the overexpression of the targeted mRNA. However, their design can be intricate, and they are sensitive to environmental conditions. Both approaches are limited in that they analyze a single mRNA species-containing granule, thereby hindering the extrapolation of results as a general mechanism for RNA granules. Some groups have taken the approach of fluorescently tagging specific RBPs, considering that one

## DISCUSSION

RBP may bind different mRNA species. CRISPR-mediated endogenous tagging has been employed in mESC-derived pyramidal neurons (Chu et al., 2019). This technique, however, has limitations in primary neuronal cultures, where overexpression of GFP-tagged RBPs via transfection has been utilized (El Fatimy et al., 2016; Tiruchinapalli et al., 2003). Overexpression can lead to non-physiological protein levels, potentially resulting in aberrant granule behaviors or interactions, not faithfully representing the physiological conditions of RNA transport granules, as it has been mainly analyzed for SGs and P-bodies (Kedersha et al., 2016; Thomas et al., 2011). Nevertheless, it is a simpler approach in comparison to the methods mentioned earlier.

By GFP-tagging the RNA granule protein ZBP1, we analyzed the positioning of RNA granules within dendrites depending on DrebrinA levels within dendritic spines. The overexpression of mScarlet-DrebrinA mimics the endogenous protein localization, with an enrichment in the heads of dendritic spines (Fig. 30). Our observations indicate that higher levels of DrebrinA in dendritic spines are associated with a closer proximity of an RNA granule, suggesting an attractive effect. To our knowledge, these findings represent the first evidence of a protein involved in the attraction of RNA granules to a specific subset of dendritic spines.

However, mRNA dynamics over time have not been assessed. Time-lapse experiments are required to determine whether spines exhibiting high DrebrinA levels can attract more RNA granules to their base over a time window, using a similar approach to the one followed by Yoon and colleagues (2016). Furthermore, we have yet to establish whether this phenomenon is applicable to all RNA transport granules or exclusively to those containing ZBP1. To address these questions, other approaches for analyzing RNA granule dynamics, such as those mentioned above, should be considered, including tagging different RBPs or specific mRNA species. Additionally, to circumvent technical issues related to overexpression in neuronal cultures, the assessment of DrebrinA's endogenous levels by IF, coupled with fluorescence *in situ* hybridization (FISH) of specific mRNAs, could validate the obtained results.

It is noteworthy that our experiments were conducted using live-imaging microscopy instead of fixation methods, avoiding potential alterations associated with fixation. Indeed, Irgen-Giorgio et al., (2022) have demonstrated that PFA fixation can either enhance or diminish putative LLPS behavior.

## 1.2. DrebrinA's attraction capacity depends on its disordered region

Our results demonstrated that the influence of DrebrinA on RNA positioning followed a reverse plateau. Beyond a certain concentration of DrebrinA, the distance to the closest RNA granule remained constant. This suggests that a specific threshold of DrebrinA molecules within the spine may be required to initiate a signaling pathway.

Furthermore, we demonstrated that this attraction capacity is mediated through the LCR of the DrebrinA protein. This was confirmed by analyzing the same phenotype using a DrebrinA mutant lacking this region, referred to as DrebrinA  $\Delta$ LCR.

As depicted in figure 32, the reverse plateau tendency is lost when DrebrinA  $\Delta$ LCR is expressed. Notably, at low DrebrinA  $\Delta$ LCR concentration levels, the distance to the nearest mRNP decreases proportionally to the quantity of DrebrinA  $\Delta$ LCR present, as it happens for DrebrinA wt. Our hypothesis is that at low  $\Delta$ LCR mutant expression levels, spines contain endogenous DrebrinA, which is responsible for attracting mRNPs. However, as DrebrinA  $\Delta$ LCR levels increase, it exerts a dominant negative effect, leading to the loss of attraction capacity. It is probable that spines with high levels of DrebrinA  $\Delta$ LCR mutant lose their endogenous DrebrinA. Consequently, endogenous DrebrinA becomes predominantly localized in spines with low  $\Delta$ LCR levels.

To validate this hypothesis, we are considering two approaches. Firstly, the ratio of endogenous-mutant levels within individual spines could be assessed using antibodies specific to the LCR of DrebrinA. This would enable the detection of endogenous protein but not the overexpressed mutant. An available antibody (Abcam, #60932) could be employed for this purpose. Secondly, primary neurons can be co-transfected with mGFP-DrebrinA wild-type and mScarlet-DrebrinA  $\Delta$ LCR. In cells where both proteins are expressed at similar levels in the soma, individual spines should be analyzed to determine the ratio of wild type to  $\Delta$ LCR DrebrinA proteins.

In conclusion, our study sheds light on the intricate role of DrebrinA in RNA granules attraction in spines. We have revealed a reverse plateau effect, suggesting that a specific concentration threshold of DrebrinA molecules is essential to trigger a signaling pathway related to RNA positioning. Moreover, our investigation highlights the crucial role of the LCR of the DrebrinA protein in this process, as evidenced by the loss of the reverse plateau tendency in the DrebrinA  $\Delta$ LCR mutant. These findings have broader implications for understanding the molecular mechanisms

## DISCUSSION

governing synaptic function and plasticity and offer potential insights into neurological disorders characterized by dysregulated RNA transport and localization in neurons. Moving forward, our ongoing efforts to validate our hypothesis promise to deepen our understanding of the interplay between DrebrinA and RNA transport granules.

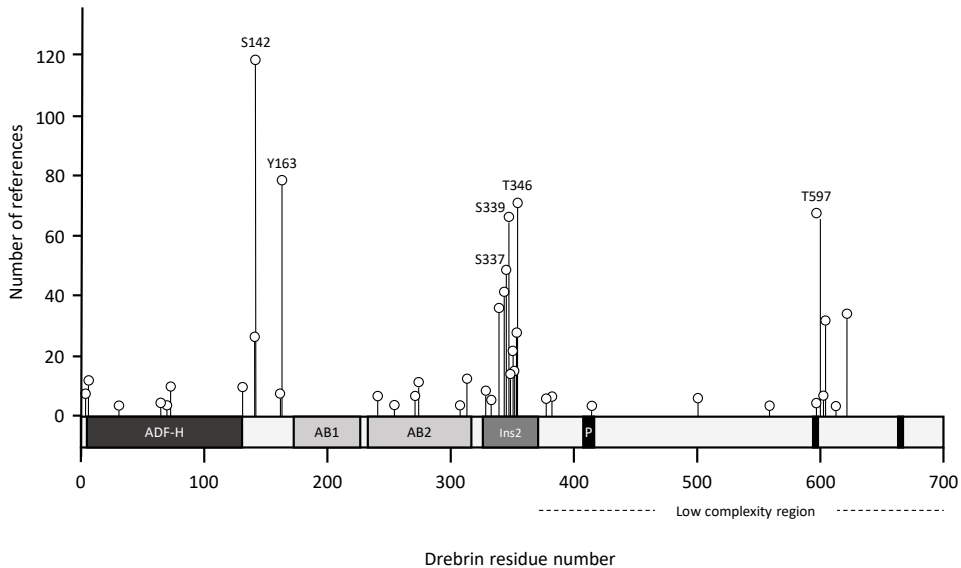
### **2. How does DrebrinA act as an attractor of mRNPs?**

#### **2.1. The role of PTMs**

In our study, we have yet to elucidate the molecular mechanisms underlying DrebrinA's attraction capacity. Our initial hypothesis is based on PTMs. It is well-established that LTP activates several kinases, initiating various signaling pathways in the brain. While more than 250 protein kinases are expressed in the adult mammalian brain, only a subset has been associated with learning and memory. The most well-characterized are CaMKII family, extracellular signal regulated kinase 1 and 2 (ERK 1/2), PKA, protein kinase G (PKG), the phosphatidylinositol 3-kinase (PI3K), and the protein kinase M  $\zeta$  (PKM  $\zeta$ ) (Giese & Mizuno, 2013). However, there is currently no direct evidence of DrebrinA phosphorylation by any of these kinases.

Several PTMs have been described for Drebrin, being phosphorylation at Ser<sup>142</sup> the most extensively studied (Hornbeck et al., 2015). Other phosphorylation sites include Tyr<sup>163</sup>, Thr<sup>346</sup>, Tyr<sup>597</sup>, Ser<sup>339</sup>, and Ser<sup>337</sup>, among others (Fig. 41). In the case of Ser<sup>142</sup>, the kinase CDK5 has been identified as the enzyme responsible for this PTM, although other kinases may be also involved. Drebrin phosphorylation by CDK5 has been reported in isolated actin gels from mouse brain extracts (Tanabe et al., 2014). In this context, Ser<sup>142</sup> was identified as a common phosphorylation site for both DrebrinE and A, whereas Ser<sup>342</sup> was described as a DrebrinA-specific site due to its location in the neuronal-specific domain Ins2. Notably, Drebrin-Ser<sup>142</sup> phosphorylation has also been observed in response to Brain-Derived Neurotrophic Factor (BDNF) treatment in axonal growth cones of hippocampal neurons. Specifically, this phosphorylation event modulates growth cone movement on soft substrates (Chen et al., 2022). BDNF is known to play a pivotal role in synaptic plasticity, including facilitating LTP (Kang & Schuman, 1996), enhancing learning and memory (Cunha et al., 2010), and neuroprotection (Mattson et al., 2004; Nagahara et al., 2009). Additionally, Ser<sup>142</sup> phosphorylation has been associated to Drebrin's role in linking F-actin to MTs through the interaction with the +TIP protein EB3. This interaction is dependent on Ser<sup>142</sup>-phosphorylation, as it induces conformational changes in Drebrin (Worth et al., 2013).





**Figure 41. Phosphorylation events described for Drebrin protein.** Scheme illustrating phosphorylation events reported for Drebrin in the literature. The x-axis represents Drebrin residue numbers and domains, including ADF-H, AB1, AB2, Ins2, and the low complexity region. The y-axis indicates the number of references in which each phosphorylation has been detected. Six specific phosphorylated residues which have been consistently reported in multiple research papers, are highlighted in the figure. Adapted from PhosphoSitePlus® (PSP).

Among all the PTMs described for Drebrin, approximately 75 % involve phosphorylation events. Interestingly, the 28 % of these phosphorylation events are localized in the neuronal-specific domain Ins2, underscoring the significance of post-translational regulation in adult DrebrinA. Based on this collective data, we hypothesize that DrebrinA's attraction capacity may be influenced by PTMs.

## 2.2. The role of Drebrin-interacting proteins

RNA granules are transported within dendrites through the MT cytoskeleton and its associated motor proteins, including kinesins and dyneins. Initially, it was believed that while MT were primarily located in the dendritic shaft, the actin cytoskeleton was concentrated in dendritic spines, maintaining separate domains (Kaech et al., 1997, 2001). However, subsequent studies have revealed the presence of MTs in dendritic spines. In fact, several independent studies demonstrated that MTs enter dendritic spines in a synaptic activity-dependent manner (Gu et al., 2008; Hu et al., 2008; Jaworski et al., 2009). Notably, numerous studies also suggest that MT dynamics play important roles in LTP. In fact, pharmacological stabilization of MTs or inhibition of its polymerization affects LTP (Barnes et al., 2010; Jaworski et al., 2009; Shumyatsky et al., 2005).

## DISCUSSION

It appears that MTs target spines undergoing activity-dependent changes rather than randomly polymerizing into a small subset of spines, as demonstrated by Merriam et al. (2013). Additionally, calcium signaling and actin polymerization in the spine are necessary for MT polymerization within these spines. Interestingly, MTs and actin do not directly interact. Instead, the +TIP protein EB3 interacts with Drebrin, as demonstrated in PSDs (Jaworski et al., 2009) and axonal growth cones (Geraldo et al., 2008).

The entry of MTs into dendritic spines may function as a mechanism to transport cargos into these spines (Dent, 2017), such as RNA granules. Considering that only activated synapses are likely entered by MT tips and that the interaction between actin and MTs is dependent on DrebrinA, it would make sense that DrebrinA-enriched spines were responsible of the attraction of RNA granules and subsequently anchor them through MAPs. When analyzing DrebrinA interactors in our APEX dataset (Fig. 37), we identified proteins involved in molecular motors, such as the cytoplasmic dynein 1 intermediate chain 1 and 2, the dynactin subunit 6, the kinesin-like protein KIF21B, and a MT stabilizer protein named stathmin-2. However, we did not find enriched interactions with +TIP such as EB1 or EB3.

As demonstrated by Schätzle and colleagues (2018), NMDA receptor activation triggers MT entry in spines. Indeed, they observed a strong correlation between activated spines and MT targeting events in uncaging experiments. These experiments were conducted using the calcium sensor GCaMP6, which allows the detection of calcium entry in activated spines (Bauer et al., 2022; Metzbower et al., 2019; Schätzle et al., 2018). In the context of our study, it would be interesting to analyze whether those spines containing higher levels of DrebrinA protein correspond to activated spines, which in turn can be detected using the abovementioned sensor.

### **2.3. The attraction capacity is not an inherent property of PSD proteins**

Our findings demonstrate that the PSD protein Homer1b did not attract RNA granules in a concentration-dependent manner (Fig. 33). This result confirms that DrebrinA's attraction capacity is not an inherent property of all PSD proteins. However, as mentioned earlier, it is probable that other proteins in the synapse play redundant roles in this process. This leads us to question what differentiates the "attracting" proteins from the "not attracting" ones, like Homer1.

The Homer family consists of several proteins encoded by *Homer 1*, *2*, and *3* genes. Homer1 long isoforms are constitutively expressed in neurons and present two major domains: (1) the EVH1-like domain, which enables interactions with other

PSD proteins like Drebrin; and (2) the carboxy-terminal region, which mediates homomeric or heteromeric interactions between long Homer isoforms. Homer1 has been demonstrated to interact with synaptic proteins involved in calcium dynamics, the actin cytoskeleton, receptor trafficking, and signal transduction (de Bartolomeis et al., 2022).

In contrast to DrebrinA, Homer1 does not present a LCR, and only a few PTMs have been described (Hornbeck et al., 2015). Interestingly, Stillman and colleagues showed that Homer1 interactome changes following neuronal depolarization, as it detaches from mGluR5 and Shank3 (Stillman et al., 2022). Although there is no evidence of interaction with RNA granule protein constituents, changes in its interactors may play a role in the triggered signaling pathway.

### **3. Is DrebrinA responsible for the anchoring process?**

#### **3.1. Is DrebrinA exodus necessary for interacting with RNA granules?**

While DrebrinA is highly accumulated in dendritic spines, approximately 20 % of spines do not contain detectable Drebrin *in vivo* (Aoki et al., 2005). In 2006, it was demonstrated that DrebrinA content in dendritic spines is regulated by synaptic activity. Specifically, glutamate stimulation induces DrebrinA exodus from the spine head to the dendritic shaft (Sekino et al., 2006; Yamazaki et al., 2023). This phenomenon has been linked to actin remodeling in the spine.

Glutamate uncaging experiments have allowed the determination of the specific time window of DrebrinA exodus. This is a rapid process, as described by Bosch and colleagues (2014): one minute after glutamate uncaging, DrebrinA exits the spine, but it returns to the spine within the following four minutes. Other groups have demonstrated DrebrinA exodus after chemical LTP (cLTP) stimulation (Mizui et al., 2014). Using this approach, DrebrinA exodus from dendritic spines appears to be prominent at five minutes after stimulation and requires more time to return to the original levels within the spine.

As earlier mentioned, our initial hypothesis was that the synaptic protein involved in RNA granules anchoring might change its localization after stimulation. The study by Bosch and colleagues (2014) elegantly demonstrated that some proteins exit the spine to the dendritic shaft after LTP stimulation, including DrebrinA. Our idea was that this change in localization could be facilitating interactions with proteins present in RNA granules. Therefore, it is plausible that dendritic spines highly enriched in DrebrinA protein would undergo synaptic activation, leading to DrebrinA exodus. The exodus of DrebrinA would result in changes to its interactors, as evidenced by the abolishment of its interaction with CaMKII $\beta$  upon NMDA

## DISCUSSION

activation (Yamazaki et al., 2023). The newly interacting proteins may encompass RNA granule constituents.

To test this hypothesis, we are planning to analyze DrebrinA interactors using APEX technology after cLTP stimulation. Specifically, primary cortical neurons will be infected with pFUW-FLAG-APEX-DrebrinA and pFUW-FLAG-APEX-NES, as spatial control. At 18 DIV, the APEX proximity ligation assay will be performed. Neurons will be cultured with biotin-phenol for 30 min. Then, neurons will be stimulated for 10 min, followed by treatment with hydrogen peroxide to biotin-label DrebrinA interactors. Based on the study by Mizui et al. (2014), we would use a 10-minute time window to allow DrebrinA to completely exit the spine and interact with the RNA granules located at the base of the spines. Initially, this timepoint would be verified through live-imaging experiments using fluorescent tagged DrebrinA. This approach will shed light on determining the involvement of DrebrinA in the anchoring process and elucidate if its role is purely in attraction or also in anchoring, through direct or indirect interactions with RNA granule constituents.

### **3.2. Are there other proteins involved in the attraction and/or anchoring of RNA granules?**

The study of Bosch et al. (2014) identified ten proteins out of fifteen analyzed that exhibited a translocation from the spine to the shaft after stimulation. These proteins included GluA1, CaMKII $\alpha$ , CaMKII $\beta$ ,  $\beta$ -actin, cofilin-1, Aip1, Arp2/3, profilin IIa, Drebrin, and  $\alpha$ -actinin-2. Other ABPs, like cortactin, which were not analyzed in Bosch's study, have also been shown to translocate to the spine base after glutamate uncaging (Hering & Sheng, 2003; Schätzle et al., 2018). Interestingly, Schätzle and colleagues reported that exclusively downregulating cortactin, but not Drebrin, reduced the number of MTs entries per hour into spines (Schätzle et al., 2018). On the other hand, in the study by Merriam and colleagues, Drebrin knockdown did affect MT invasions to spines (Merriam et al., 2013). These findings lead us to hypothesize that it is possible that other synaptic proteins, such as cortactin, may also play a role in RNA granule attraction. Additionally, cortactin also presents a substantial, disordered region that could mediate promiscuous interactions, as hypothesized for Drebrin.

If DrebrinA was the sole protein involved in such a crucial process, its downregulation would have a tremendous impact on neuronal function. However, DrebrinA knockout mice (DAKO) are viable. DAKO mice were generated by a targeted knockout of the exon 11A, encoding the DrebrinA-specific domain. Consequently, despite lacking DrebrinA, DrebrinE remains expressed in these animals throughout their lives (Aoki et al., 2009). DAKO mice exhibit abnormal

dendritic spine morphogenesis, impaired LTP and LTD, as well as hippocampus-dependent memory impairment (Kojima et al., 2016; Yasuda et al., 2018). Total knockout (drebrin-KO) animals also remain viable and present a similar phenotype to DAKO mice (Jung et al., 2015).

Knockdown experiments using RNA interference (RNAi) and antisense oligonucleotides have demonstrated that Drebrin is involved in spine morphogenesis. Downregulation of Drebrin levels results in alterations in spine morphology, specifically leading to an increase in filopodia-like protrusions and shorter neurites (Geraldo et al., 2008; Mizui et al., 2009; Takahashi et al., 2003, 2006).

Regarding cortactin, there is also a knockout mouse (Ctnn-KO) that is viable but exhibits defects in synaptic plasticity (Cornelius et al., 2021). These results suggest that DrebrinA or cortactin could be involved in similar processes regarding synaptic plasticity. However, it would be interesting to assess the effect of knocking down Drebrin in neuronal cultures and evaluate its impact on RNA granules positioning within dendrites. If there were no redundant proteins performing Drebrin function, in knocked down neurons, RNA granules would probably travel bidirectionally without stopping at specific locations or randomly stopping through the dendrite. Therefore, time-lapse experiments would probably be necessary to precisely determine RNA granule dynamics in comparison to wild-type neurons.

In our data mining analysis, three additional proteins met the three conditions required besides Drebrin: CaMKII $\beta$ ,  $\alpha$ -actinin-2, and cofilin-1. These proteins were not studied in detail because they do not exhibit a disordered structure (Fig. 29). However, exploring their interactors could be interesting to determine if they are also involved in the local capture of RNA granules.

We also considered the possibility that the actin cytoskeleton itself may sense and attract RNA granules instead of a single protein. It is likely that DrebrinA-enriched spines also contain more F-actin, as mature spines typically do. In addition, Mizui et al. (2014) demonstrated that F-actin also exits the spine after cLTP stimulation, facilitating interactions with RNA granules. However, we ruled out the idea that actin is the attracting mechanism for RNA granules based on the experiments using the DrebrinA  $\Delta$ LCR mutant. As shown in figure 31B, both wt and DrebrinA  $\Delta$ LCR mutant present similar distribution within spines. In parallel, spine morphology is not affected by DrebrinA  $\Delta$ LCR mutant. Therefore, we hypothesize that the F-actin cytoskeleton in those spines should not be altered either. If the actin cytoskeleton

## DISCUSSION

was responsible for RNA granules attraction, the expression of DrebrinA  $\Delta$ LCR would not have the observed effect on RNA granules positioning within dendrites (Fig. 32).

In summary, our investigation has revealed potential candidates in the RNA granule attraction process. While the exact mechanisms underlying RNA granule localization remain to be fully elucidated, these findings open the door to further research.

### **3.3. How DrebrinA mediates RNA granules anchoring?**

Anchoring mRNAs at their target sites after transport is crucial for localized protein synthesis and proper synaptic function. Considering our findings in the key role of DrebrinA in the RNA granules attraction, we hypothesized that the same protein could also be involved in their anchoring.

We speculated that if DrebrinA is responsible for RNA granules anchoring, it would likely interact with proteins that constitute RNA granules. However, these interactions are probably transient, which could explain why they have not previously been identified using other approaches like immunoprecipitation. For that reason, we decided to employ APEX proximity labeling, a technique that enables the detection of transient interactors (Chung et al., 2017; Fazal et al., 2019; Frankenfield et al., 2020; Markmiller et al., 2018; Marmor-Kollet et al., 2020; Padrón et al., 2019). As fully detailed in the results section, 18 DIV cortical neurons expressing FLAG-APEX-DrebrinA transgenes were used to determine DrebrinA interactors in a neuronal context. To eliminate false positive interactors, the resulting proteins were compared to the interactome of a NES that served as a spatial control.

As shown in figures 37 and 38, DrebrinA interacts with proteins involved in various molecular functions and localized in several cellular compartments. Given its function as an ABP, most of its interactors are actin-related proteins. However, a subset of interactors is consistent with proteins that have been linked to RNA granules. Surprisingly, none of them correspond to typical RNA granules core proteins such as FMRP, ZBP1, or Stau2. These results suggest that the anchoring process may involve other proteins present on RNA granules, rather than direct binding of DrebrinA to core RBPs.

The content of RNA granules has been determined by various groups using different approaches. While some components appear to be independent of the isolation method, others strictly depend on the specific purification techniques employed (El Fatimy et al., 2016; Elvira et al., 2006; Fritzsche et al., 2013; Jøanson et al., 2007; Kanai et al., 2004; Kurosaki et al., 2022; Mukherjee et al., 2019). Additionally, some purifications have been achieved by IP of specific RBPs (Fritzsche et al., 2013; Jøanson

et al., 2007; Kurosaki et al., 2022), demonstrating the existence of different types of RNA granules containing particular compositions.

Hence, we aimed to elucidate the RNA granule content within ZBP1-positive granules. ZBP1 is known to bind  $\beta$ -actin mRNAs and transport them through dendrites while inhibiting its translation. Using the abovementioned APEX technology, we investigated the interactors of ZBP1 in mature cortical neurons. Through this approach, we identified some interactors that have previously been described as RNA granules components (Fig. 36B), although the majority were novel findings. Notably, many of the ZBP1 interactors are associated with RNA binding-related functions and appear to play roles in several aspects of RNA granules biology (Fig. 36C, D).

Interestingly, APEX technology can be used not only to label protein interactors but also RNA. Indeed, Fazal and colleagues (2019) used this technique, called APEX-seq, to determine the transcriptome of nine different subcellular locations. For our study, this approach could be useful for determining not only protein constituents of RNA granules, but also mRNA composition within them.

To pinpoint which proteins may mediate the anchoring process between DrebrinA and RNA granules, we conducted a comparative analysis of the interactomes of DrebrinA and ZBP1 to identify shared partners that could potentially mediate this function. We identified fifty-four proteins that were shared between the significantly enriched interactors of both DrebrinA and ZBP1 (Fig. 39A). Our hypothesis states that the anchoring process is likely independent on the RBPs constituents of the RNA granules. To test this, we reasoned that the putative anchoring protein should also appear in previously reported datasets related to mRNPs composition. When comparing this information, only six proteins emerged as putative candidates (Fig. 39B, C). These proteins include DDX5, DHX9, hnRNPA1, ILF3, NonO, and RPL6.

#### **4. The role of RNA helicases**

It is noteworthy that two out of these six proteins are RNA helicases, namely DDX5 (also known as p68) and DHX9. RNA helicases play a pivotal role in rearranging RNA secondary structures and RNA-protein interactions through an ATP-dependent reaction. This family of proteins is involved in a wide range of functions, including translation inhibition or activation, mRNA degradation, transport and storage, nuclear export, and splicing (Jankowsky, 2011).

RNA helicases are key players in the dynamics of RNA granules and contribute to the interplay between mRNA storage, translation, and decay. Indeed, mRNAs are

## DISCUSSION

sequestered within RNA granules, where their translation is stalled to protect them from degradation. It is postulated that RNA helicases may disassemble RNA-RNA interactions and thereby limit mRNP granule formation (Van Treeck et al., 2018).

Numerous studies have highlighted the role of RNA helicases in RNA granules. For instance, the RNA helicase CGH-1 in *C. elegans* prevents the formation of non-dynamic solid structures and regulates the dynamics of mRNP during development (Hubstenberger et al., 2013). Similarly, mutations in the DEAD-box ATPase Dhh1 prevent P-body disassembly in *S. cerevisiae* (Mugler et al., 2016). Additionally, RNA helicases can also play roles in mRNP granule assembly, like it has been shown for Ded1/DDX3, by nucleating protein-protein interactions (Hilliker et al., 2011).

In most cases, the recruitment mechanism of RNA helicases to granules remains unclear. Several studies utilizing RNA helicase mutants have shown that ATPase activity is not crucial for their recruitment to RNA granules, while ATP binding plays a pivotal role. Emerging evidence suggests that RNA helicases often have dual roles. Initially, they promote granule formation in an ATP-independent manner. Subsequently, these helicases can act in an ATP-dependent manner to remodel and disassemble the RNA granule (Hooper & Hilliker, 2013).

The role of RNA helicases in neurons has been relatively unexplored. In 2009, Banerjee and colleagues identified the RNA helicase MOV10 in the synaptic compartment, where it underwent rapid proteasomal degradation in an activity-dependent manner to facilitate the translation of a subset of mRNAs (Banerjee et al., 2009). In 2012, the RNA helicase DDX1 was identified as a constituent in Stau2- and Pum2-containing RNA granules. This complex was responsible for the localization and expression of target mRNAs like  $\beta$ -actin and *prox1* (Vessey et al., 2012).

These findings suggest that RNA helicases may have a key role in RNA granules disassembly after stimulation, being the anchoring mechanism potentially initiated by DrebrinA. However, further experiments are required to confirm our hypothesis. Analyzing the interactomes of DrebrinA after stimulation might shed light on this hypothesis by building upon the results observed in non-stimulated conditions.

Our results imply that the attraction capacity of DrebrinA relies on the LCR domain. It is plausible that this domain also mediates interactions with anchoring proteins, such as RNA helicases. Our plan is to compare DrebrinA interactors found in our APEX dataset with a new dataset of DrebrinA  $\Delta$ LCR interactors, also obtained through the APEX proximity labeling technique.



## 5. Using APEX technology to determine RNA granules content

Proximity labeling proteomic approaches have previously been employed to determine the composition of SGs (Markmiller et al., 2018; Marmor-Kollet et al., 2020; Padrón et al., 2019). However, to the best of our knowledge, our study represents the first attempt to employ this technique to elucidate the composition of RNA granules in neurons. Specifically, APEX technology was used to determine the composition of ZBP1-positive RNA granules.

The interactors of ZBP1 have previously been identified in HEK293 cells by IP of FLAG-ZBP1 overexpressed protein (Jøanson et al., 2007). Additionally, other interactors have been indirectly detected by Mukherjee and colleagues (2019), when they determined the interactors of  $\beta$ -actin mRNA, a known target of ZBP1 (Hüttelmaier et al., 2005), also in HEK293 cells.

Most experiments aimed at comprehending the composition of RNA granules by proximity labeling techniques have been conducted in cell lines like HEK293 (Fazal et al., 2019; Markmiller et al., 2018; Padrón et al., 2019; Qin et al., 2023), primarily for technical reasons. Immortalized cell lines offer advantages in terms of transfection and infection efficiencies, facilitating the generation of stable cell lines that can yield more reproducible results. Conversely, neuronal cultures present unique challenges when it comes to overexpressing proteins in the context of complex experiments like the one described herein. It is worth noting that there is only one prior study employing APEX technology in rat cortical neurons, where researchers successfully identified the interactors of  $\alpha$ -synuclein (Chung et al., 2017).

Using the APEX approach, we identified 262 interacting proteins of ZBP1. Among these, 52 proteins have also previously been identified as RNA granules components (Fig. 36B). Moreover, other key RBPs have been identified in ZBP1 interactomes, such as FMRP and Stau1. The enrichment in translation initiation factors suggests that mRNAs are mainly stopped at the initiation step within ZBP1-positive RNA granules.

APEX technology has emerged as a powerful tool for elucidating the composition of RNA transport granules in neurons. This proximity labeling technique provides several advantages. Firstly, it offers precise spatial resolution. Secondly, it is suitable to live-cell applications, enabling the detection of dynamic interactions. In addition, it is compatible with primary cultures. However, it also presents some limitations. Firstly, it requires the overexpression of a fusion protein, which could potentially introduce artifacts and non-physiological interactions. Secondly, it presents a

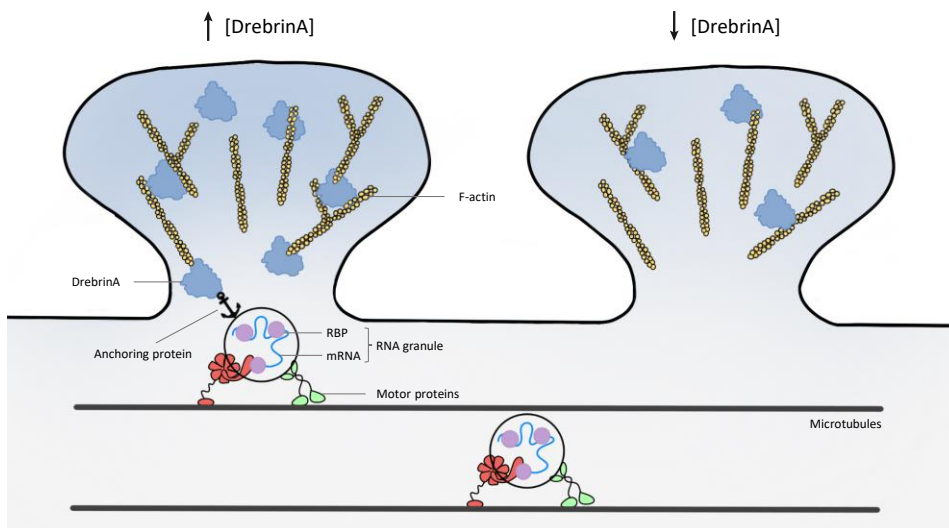
## DISCUSSION

limited detection range, which reduces the occurrence of false positive interactors but may result in the omission of some proteins. Finally, it is necessary to carefully design controls to accurately interpret the results.

Taking all these factors into consideration, we firmly believe that this approach is the most suitable for determining the content of RNA transport granules. This study not only opens the door to further investigations seeking to elucidate the composition of RNA granules under physiological conditions, but also in various neurological disorders in which components of RNA granules are affected.

### 6. Proposed model of RNA transport granules local capture

In summary, our findings support the idea that DrebrinA concentration levels within spines affect RNA positioning along dendrites. High levels of DrebrinA in dendritic spines would attract RNA granules to the base of this spines. Subsequently, RNA granules will be anchored by unknown mechanisms to enable its dissociation for further local translation. We hypothesize that RNA helicases could be involved in RNA anchoring by interacting with DrebrinA and RNA granules core components, such as ZBP1.



**Figure 42. DrebrinA concentration levels within spines determine RNA granules positioning within dendrites.** Proposed model of the attractive role of DrebrinA on RNA granules. High DrebrinA concentration levels within spines would attract RNA granules to their bases. Subsequently, these granules will be anchored by unknown mechanisms that will enable their local capture and translation.

These results represent the first evidence of a synaptic protein involved in attracting RNA granules. Elucidating the molecular mechanisms underlying RNA granules transport and anchoring is crucial to understand how local translation is regulated in neurons.





## **CONCLUSIONS**



## **Chapter 1: Molecular mechanisms regulating eEF1A2 in the synaptic function**

1. The neuron-specific isoform eEF1A2 is regulated by phosphorylation to control spine growth, actin dynamics, and protein translation.
2. Phosphorylation of eEF1A2 hinders its association with F-actin and increases actin dynamics likely by sequestering actin crosslinkers.
3. Activation of metabotropic glutamate receptors induces transient eEF1A2 dissociation from its GEF in dendritic spines, affecting the recycling process of eEF1A2. This opens a time window during which protein synthesis is decreased and actin cytoskeleton remodelling is increased.

## **Chapter 2: Molecular mechanisms regulating RNA transport granules capture in dendritic spines**

1. DrebrinA acts as an attractor of RNA granules to dendritic spines in a concentration-dependent manner through its low complexity region.
2. DrebrinA interacts with some constituent proteins of RNA granules to mediate the anchoring of these membrane-less structures. RNA helicases are potential candidates, considering its known role in affecting the dynamics of RNA granules.
3. The APEX proximity labelling technique is a useful tool for determining the composition of ZBP1-containing RNA granules.





## **REFERENCES**



- Abbas, W., Kumar, A., & Herbein, G. (2015). The eEF1A proteins: at the crossroads of oncogenesis, apoptosis, and viral infections. *Frontiers in Oncology*, 5(April), 1–10. <https://doi.org/10.3389/fonc.2015.00075>
- Adrian, M., Kusters, R., Wierenga, C. J., Storm, C., Hoogenraad, C. C., & Kapitein, L. C. (2014). Barriers in the brain: Resolving dendritic spine morphology and compartmentalization. *Frontiers in Neuroanatomy*, 8(DEC), 1–12. <https://doi.org/10.3389/fnana.2014.00142>
- Amiri, A., Noei, F., Jeganathan, S., Kulkarni, G., Pinke, D. E., & Lee, J. M. (2007). eEF1A2 activates Akt and stimulates Akt-dependent actin remodeling, invasion and migration. *Oncogene*, 26(21), 3027–3040. <https://doi.org/10.1038/sj.onc.1210101>
- Anadolu, M. N., Sun, J., Kailasam, S., Chalkiadaki, K., Krimbacher, K., Li, J. T. Y., Markova, T., Jafarnejad, S. M., Lefebvre, F., Ortega, J., Gkogkas, C. G., & Sossin, W. S. (2023). Ribosomes in RNA Granules Are Stalled on mRNA Sequences That Are Consensus Sites for FMRP Association. *Journal of Neuroscience*, 43(14), 2440–2459. <https://doi.org/10.1523/JNEUROSCI.1002-22.2023>
- Andersen, G. R., Nissen, P., & Nyborg, J. (2003). Elongation factors in protein biosynthesis. *Trends in Biochemical Sciences*, 28(8), 434–441. [https://doi.org/10.1016/S0968-0004\(03\)00162-2](https://doi.org/10.1016/S0968-0004(03)00162-2)
- Andreassi, C., & Riccio, A. (2009). To localize or not to localize: mRNA fate is in 3'UTR ends. *Trends in Cell Biology*, 19(9), 465–474. <https://doi.org/10.1016/j.tcb.2009.06.001>
- Aoki, C., Kojima, N., Sabaliauskas, N., Shah, L., Ahmed, T. H., Oakford, J., Ahmed, T., Yamazaki, H., Hanamura, K., & Shirao, T. (2009). Drebrin a knockout eliminates the rapid form of homeostatic synaptic plasticity at excitatory synapses of intact adult cerebral cortex. *Journal of Comparative Neurology*, 517(1), 105–121. <https://doi.org/10.1002/cne.22137>
- Aoki, C., Sekino, Y., Hanamura, K., Fujisawa, S., Mahadomrongkul, V., Ren, Y., & Shirao, T. (2005). Drebrin A is a postsynaptic protein that localizes in vivo to the submembranous surface of dendritic sites forming excitatory synapses. *Journal of Comparative Neurology*, 483(4), 383–402. <https://doi.org/10.1002/cne.20449>
- Ardestani, G., West, M. C., Maresca, T. J., Fissore, R. A., & Stratton, M. M. (2019). FRET-based sensor for CaMKII activity (FRESCA): A useful tool for assessing CaMKII activity in response to Ca<sup>2+</sup> oscillations in live cells. *Journal of Biological Chemistry*, 294(31), 11876–11891. <https://doi.org/10.1074/jbc.RA119.009235>
- Ashburner, M., Ball, C. A., Blake, J. A., Botstein, D., Butler, H., Cherry, J. M., David, A. P., Dolinski, K., Dwight, S. S., Eppig, J. T., Harris, M. A., Hill, D. P., Issel-Tarver, L., Kasarskis, A., Lewis, S., Matese, J. C., Richardson, J. E., Ringwald, M., Rubin, G. M., & Sherlock, G. (2000). Gene Ontology: tool for the unification of biology. *Nature Genetics*, 25(0), 25–29. <https://doi.org/10.2174/1381612824666180522105202>

## REFERENCES

- Banerjee, S., Neveu, P., & Kosik, K. S. (2009). A Coordinated Local Translational Control Point at the Synapse Involving Relief from Silencing and MOV10 Degradation. *Neuron*, *64*(6), 871–884. <https://doi.org/10.1016/j.neuron.2009.11.023>
- Barnes, S. J., Opitz, T., Merkens, M., Kelly, T., Von Der Brelie, C., Krueppel, R., & Beck, H. (2010). Stable mossy fiber long-term potentiation requires calcium influx at the granule cell soma, protein synthesis, and microtubule-dependent axonal transport. *Journal of Neuroscience*, *30*(39), 12996–13004. <https://doi.org/10.1523/JNEUROSCI.1847-10.2010>
- Bassell, G. J., & Warren, S. T. (2008). Fragile X Syndrome: Loss of Local mRNA Regulation Alters Synaptic Development and Function. *Neuron*, *60*(2), 201–214. <https://doi.org/10.1016/j.neuron.2008.10.004>
- Bassell, G., & Singer, R. H. (1997). mRNA and cytoskeletal filaments. *Current Opinion in Cell Biology*, *9*(1), 109–115. [https://doi.org/10.1016/S0955-0674\(97\)80159-7](https://doi.org/10.1016/S0955-0674(97)80159-7)
- Batish, M., Van Den Bogaard, P., Kramer, F. R., & Tyagi, S. (2012). Neuronal mRNAs travel singly into dendrites. *Proceedings of the National Academy of Sciences of the United States of America*, *109*(12), 4645–4650. <https://doi.org/10.1073/pnas.1111226109>
- Bauer, K. E., Bargenda, N., Schieweck, R., Illig, C., Segura, I., Harner, M., & Kiebler, M. A. (2022). RNA supply drives physiological granule assembly in neurons. *Nature Communications*, *13*(1), 1–12. <https://doi.org/10.1038/s41467-022-30067-3>
- Bauer, K. E., Segura, I., Gaspar, I., Scheuss, V., Illig, C., Ammer, G., Hutten, S., Basyuk, E., Fernández-Moya, S. M., Ehses, J., Bertrand, E., & Kiebler, M. A. (2019). Live cell imaging reveals 3'-UTR dependent mRNA sorting to synapses. *Nature Communications*, *10*(1). <https://doi.org/10.1038/s41467-019-11123-x>
- Bayés, À., Collins, M. O., Croning, M. D. R., van de Lagemaat, L. N., Choudhary, J. S., & Grant, S. G. N. (2012). Comparative Study of Human and Mouse Postsynaptic Proteomes Finds High Compositional Conservation and Abundance Differences for Key Synaptic Proteins. *PLoS ONE*, *7*(10). <https://doi.org/10.1371/journal.pone.0046683>
- Beach, D. L., Salmon, E. D., & Bloom, K. (1999). Localization and anchoring of mRNA in budding yeast. *Current Biology*, *9*(11), 569–578. [https://doi.org/10.1016/S0960-9822\(99\)80260-7](https://doi.org/10.1016/S0960-9822(99)80260-7)
- Bear, M. F., Huber, K. M., & Warren, S. T. (2004). The mGluR theory of fragile X mental retardation. *Trends in Neurosciences*, *27*(7), 370–377. <https://doi.org/10.1016/j.tins.2004.04.009>
- Berry, K. P., & Nedivi, E. (2017). Spine Dynamics: Are They All the Same? *Neuron*, *96*(1), 43–55. <https://doi.org/10.1016/j.neuron.2017.08.008>
- Blower, M. D. (2013). Molecular insights into intracellular RNA localization. *Int Rev Cell Mol Biol*, *302*(1), 1–39. <https://doi.org/10.1016/B978-0-12-407699-0.00001-7>

- Bohnsack, M. T., Regener, K., Schwappach, B., Saffrich, R., Paraskeva, E., Hartmann, E., & Görlich, D. (2002). Exp5 exports eEF1A via tRNA from nuclei and synergizes with other transport pathways to confine translation to the cytoplasm. *The EMBO Journal*, *21*(22), 6205–6215. <https://doi.org/10.1093/emboj/cdf613>
- Bosch, M., Castro, J., Saneyoshi, T., Matsuno, H., Sur, M., & Hayashi, Y. (2014). Structural and molecular remodeling of dendritic spine substructures during long-term potentiation. *Neuron*, *82*(2), 444–459. <https://doi.org/10.1016/j.neuron.2014.03.021>
- Bose, M., Lampe, M., Mahamid, J., & Ephrussi, A. (2022). Liquid-to-solid phase transition of oskar ribonucleoprotein granules is essential for their function in Drosophila embryonic development. *Cell*, *185*(8), 1308-1324.e23. <https://doi.org/10.1016/j.cell.2022.02.022>
- Bravo-Cordero, J. J., Magalhaes, M. A. O., Eddy, R. J., Hodgson, L., & Condeelis, J. (2013). Functions of cofilin in cell locomotion and invasion. *Nature Reviews Molecular Cell Biology*, *14*(7), 405–417. <https://doi.org/10.1038/nrm3609>
- Broix, L., Turchetto, S., & Nguyen, L. (2021). Coordination between Transport and Local Translation in Neurons. *Trends in Cell Biology*, *31*(5), 372–386. <https://doi.org/10.1016/j.tcb.2021.01.001>
- Cajigas, I. J., Tushev, G., Will, T. J., Tom Dieck, S., Fuerst, N., & Schuman, E. M. (2012). The Local Transcriptome in the Synaptic Neuropil Revealed by Deep Sequencing and High-Resolution Imaging. *Neuron*, *74*(3), 453–466. <https://doi.org/10.1016/j.neuron.2012.02.036>
- Cane, M., Maco, B., Knott, G., & Holtmaat, A. (2014). The relationship between PSD-95 clustering and spine stability In Vivo. *Journal of Neuroscience*, *34*(6), 2075–2086. <https://doi.org/10.1523/JNEUROSCI.3353-13.2014>
- Ceman, S., O'Donnell, W. T., Reed, M., Patton, S., Pohl, J., & Warren, S. T. (2003). Phosphorylation influences the translation state of FMRP-associated polyribosomes. *Human Molecular Genetics*, *12*(24), 3295–3305. <https://doi.org/10.1093/hmg/ddg350>
- Chambers, D. M., Peters, J., & Abbott, C. M. (1998). The lethal mutation of the mouse wasted (wst) is a deletion that abolishes expression of a tissue-specific isoform of translation elongation factor 1, encoded by the Eef1a2 gene. *Proceedings of the National Academy of Sciences*, *95*(8), 4463–4468. <https://doi.org/10.1073/pnas.95.8.4463>
- Chartrand, P., Singer, R. H., & Long, R. M. (2001). RNP localization and transport in yeast. *Annu Rev Cell Dev Biol*, *17*, 297–310. <https://doi.org/10.1146/annurev.cellbio.17.1.297>
- Chen, C., Chu, C. H., Chu, Y., Chang, T. Y., Chen, S. W., Liang, S. Y., Tsai, Y. C., Chen, B. C., Tu, H. L., & Cheng, P. L. (2022). Neuronal paxillin and drebrin mediate BDNF-induced force transduction and growth cone turning in a soft-tissue-like environment. *Cell Reports*, *40*(7), 111188. <https://doi.org/10.1016/j.celrep.2022.111188>

## REFERENCES

- Cho, S. J., Lee, H. S., Dutta, S., Seog, D. H., & Moon, I. S. (2012). Translation elongation factor-1A1 (eEF1A1) localizes to the spine by domain III. *BMB Reports*, *45*(4), 227–232. <https://doi.org/10.5483/BMBRep.2012.45.4.227>
- Cho, S.-J., Jung, J.-S., Ko, B. H., Jin, I., & Moon, I. S. (2004). Presence of translation elongation factor-1A (eEF1A) in the excitatory postsynaptic density of rat cerebral cortex. *Neuroscience Letters*, *366*, 29–33. <https://doi.org/10.1016/j.neulet.2004.05.036>
- Chotiner, J. K., Khorasani, H., Nairn, A. C., O'Dell, T. J., & Watson, J. B. (2003). Adenylyl cyclase-dependent form of chemical long-term potentiation triggers translational regulation at the elongation step. *Neuroscience*, *116*(3), 743–752. [https://doi.org/10.1016/S0306-4522\(02\)00797-2](https://doi.org/10.1016/S0306-4522(02)00797-2)
- Chu, J. F., Majumder, P., Chatterjee, B., Huang, S. L., & Shen, C. K. J. (2019). TDP-43 Regulates Coupled Dendritic mRNA Transport-Translation Processes in Co-operation with FMRP and Staufen1. *Cell Reports*, *29*(10), 3118–3133.e6. <https://doi.org/10.1016/j.celrep.2019.10.061>
- Chuang, S., Chen, L., Lambertson, D., Anand, M., Kinzy, T. G., & Madura, K. (2005). Proteasome-Mediated Degradation of Cotranslationally Damaged Proteins Involves Translation Elongation Factor 1A. *Molecular and Cellular Biology*, *25*(1), 403–413. <https://doi.org/10.1128/MCB.25.1.403>
- Chung, C. Y., Khurana, V., Yi, S., Sahni, N., Loh, K. H., Auluck, P. K., Baru, V., Udeshi, N. D., Freyzon, Y., Carr, S. A., Hill, D. E., Vidal, M., Ting, A. Y., & Lindquist, S. (2017). In Situ Peroxidase Labeling and Mass-Spectrometry Connects Alpha-Synuclein Directly to Endocytic Trafficking and mRNA Metabolism in Neurons. *Cell Systems*, *4*(2), 242–250.e4. <https://doi.org/10.1016/j.cels.2017.01.002>
- Cioni, J. M., Lin, J. Q., Holtermann, A. V., Koppers, M., Jakobs, M. A. H., Azizi, A., Turner-Bridger, B., Shigeoka, T., Franze, K., Harris, W. A., & Holt, C. E. (2019). Late Endosomes Act as mRNA Translation Platforms and Sustain Mitochondria in Axons. *Cell*, *176*(1–2), 56–72.e15. <https://doi.org/10.1016/j.cell.2018.11.030>
- Collingridge, G. L., Peineau, S., Howland, J. G., & Wang, Y. T. (2010). Long-term depression in the CNS. *Nature Reviews Neuroscience*, *11*(7), 459–473. <https://doi.org/10.1038/nrn2867>
- Consortium, T. G. O. (2023). The Gene Ontology knowledgebase in 2023. *Genetics*, *224*(1), 1–14. <https://doi.org/10.1093/genetics/iyad031>
- Corley, M., Burns, M. C., & Yeo, G. W. (2020). How RNA-Binding Proteins Interact with RNA: Molecules and Mechanisms. *Molecular Cell*, *78*(1), 9–29. <https://doi.org/10.1016/j.molcel.2020.03.011>
- Cornelius, J., Rottner, K., Korte, M., & Michaelsen-Preusse, K. (2021). Cortactin contributes to activity-dependent modulation of spine actin dynamics and spatial memory formation. *Cells*, *10*(7), 1–13. <https://doi.org/10.3390/cells10071835>

- Costa-Mattioli, M., Sossin, W. S., Klann, E., & Sonenberg, N. (2009). Translational Control of Long-Lasting Synaptic Plasticity and Memory. *Neuron*, *61*(1), 10–26. <https://doi.org/10.1016/j.neuron.2008.10.055>
- Coultrap, S. J., Freund, R. K., O’Leary, H., Sanderson, J. L., Roche, K. W., Dell’Acqua, M. L., & Bayer, K. U. (2014). Autonomous CaMKII mediates both LTP and LTD using a mechanism for differential substrate site selection. *Cell Reports*, *6*(3), 431–437. <https://doi.org/10.1016/j.celrep.2014.01.005>
- Cunha, C., Brambilla, R., & Thomas, K. L. (2010). A simple role for BDNF in learning and memory? *Frontiers in Molecular Neuroscience*, *3*(February), 1–14. <https://doi.org/10.3389/neuro.02.001.2010>
- Darnell, R. (2013). RNA Protein Interaction in Neurons. *Annu Rev Neurosci*, *36*, 243–270. <https://doi.org/10.1146/annurev-neuro-062912-114322>
- Das, S., Moon, H. C., Singer, R. H., & Park, H. Y. (2018). A transgenic mouse for imaging activity-dependent dynamics of endogenous arc mRNA in live neurons. *Science Advances*, *4*(6). <https://doi.org/10.1126/sciadv.aar3448>
- Das, S., Vera, M., Gandin, V., Singer, R. H., & Tutucci, E. (2021). Intracellular mRNA transport and localized translation. *Nature Reviews Molecular Cell Biology*, *22*(7), 483–504. <https://doi.org/10.1038/s41580-021-00356-8>
- Das, T., Mathur, M., Gupta, A. K., Janssen, G. M. C., & Banerjee, A. K. (1998). RNA polymerase of vesicular stomatitis virus specifically associates with translation elongation factor-1  $\alpha\beta$  for its activity. *Proceedings of the National Academy of Sciences of the United States of America*, *95*(4), 1449–1454. <https://doi.org/10.1073/pnas.95.4.1449>
- Davies, F. C. J., Marshall, G. F., Pegram, E., Gadd, D., & Abbott, C. M. (2023). Endogenous epitope tagging of eEF1A2 in mice reveals early embryonic expression of eEF1A2 and subcellular compartmentalisation of neuronal eEF1A1 and eEF1A2. *Molecular and Cellular Neuroscience*, *126*(June), 103879. <https://doi.org/10.1016/j.mcn.2023.103879>
- de Bartolomeis, A., Barone, A., Buonaguro, E. F., Tomasetti, C., Vellucci, L., & Iasevoli, F. (2022). The Homer1 family of proteins at the crossroad of dopamine-glutamate signaling: An emerging molecular “Lego” in the pathophysiology of psychiatric disorders. A systematic review and translational insight. *Neuroscience and Biobehavioral Reviews*, *136*(March), 104596. <https://doi.org/10.1016/j.neubiorev.2022.104596>
- De Rubeis, S., Pasciuto, E., Li, K. W., Fernández, E., DiMarino, D., Buzzi, A., Ostroff, L. E., Klann, E., Zwartkruis, F. J. T., Komiyama, N. H., Grant, S. G. N., Pujol, C., Choquet, D., Achsel, T., Posthuma, D., Smit, A. B., & Bagni, C. (2013). CYFIP1 coordinates mRNA translation and cytoskeleton remodeling to ensure proper dendritic Spine formation. *Neuron*, *79*(6), 1169–1182. <https://doi.org/10.1016/j.neuron.2013.06.039>

## REFERENCES

- Dent, E. W. (2017). Of microtubules and memory: Implications for microtubule dynamics in dendrites and spines. *Molecular Biology of the Cell*, 28(1), 1–8. <https://doi.org/10.1091/mbc.E15-11-0769>
- Derkach, V., Barria, A., & Soderling, T. R. (1999). Ca<sup>2+</sup>/calmodulin-kinase II enhances channel conductance of  $\alpha$ -amino-3-hydroxy-5-methyl-4-isoxazolepropionate type glutamate receptors. *Proceedings of the National Academy of Sciences of the United States of America*, 96(6), 3269–3274. <https://doi.org/10.1073/pnas.96.6.3269>
- Di Prisco, G. V., Huang, W., Buffington, S. A., Hsu, C. C., Bonnen, P. E., Placzek, A. N., Sidrauski, C., Krnjević, K., Kaufman, R. J., Walter, P., & Costa-Mattioli, M. (2014). Translational control of mGluR-dependent long-term depression and object-place learning by eIF2 $\alpha$ . *Nature Neuroscience*, 17(8), 1073–1082. <https://doi.org/10.1038/nn.3754>
- Dicthenberg, J. B., Swanger, S. A., Antar, L. N., Singer, R. H., & Bassell, G. J. (2008). A Direct Role for FMRP in Activity-Dependent Dendritic mRNA Transport Links Filopodial-Spine Morphogenesis to Fragile X Syndrome. *Developmental Cell*, 14(6), 926–939. <https://doi.org/10.1016/j.devcel.2008.04.003>
- Dieterich, D. C., Hodas, J. J. L., Gouzer, G., Shadrin, I. Y., Ngo, J. T., Triller, A., Tirrell, D. A., & Schuman, E. M. (2010). In situ visualization and dynamics of newly synthesized proteins in rat hippocampal neurons. *Nature Neuroscience*, 13(7), 897–905. <https://doi.org/10.1038/nn.2580>
- Dieterich, D. C., Lee, J. J., Link, A. J., Graumann, J., Tirrell, D. A., & Schuman, E. M. (2007). Labeling, detection and identification of newly synthesized proteomes with bioorthogonal non-canonical amino-acid tagging. *Nature Protocols*, 2(3), 532–540. <https://doi.org/10.1038/nprot.2007.52>
- Diniz, C. R. A. F., & Crestani, A. P. (2022). The times they are a-changin’: a proposal on how brain flexibility goes beyond the obvious to include the concepts of “upward” and “downward” to neuroplasticity. *Molecular Psychiatry*, 28(3), 977–992. <https://doi.org/10.1038/s41380-022-01931-x>
- Donlin-Asp, P. G., Polisseni, C., Klimek, R., Heckel, A., & Schuman, E. M. (2021). Differential regulation of local mRNA dynamics and translation following long-term potentiation and depression. *Proceedings of the National Academy of Sciences of the United States of America*, 118(13). <https://doi.org/10.1073/PNAS.2017578118>
- Dosemeci, A., Makusky, A. J., Jankowska-Stephens, E., Yang, X., Slotta, D. J., & Markey, S. P. (2007). Composition of the Synaptic PSD-95 Complex. *Mol Cell Proteomics*, 6(10), 1748–1760. <https://doi.org/10.1074/mcp.M700040-MCP200>
- Doyle, M., & Kiebler, M. A. (2011). Mechanisms of dendritic mRNA transport and its role in synaptic tagging. *EMBO Journal*, 30(17), 3540–3552. <https://doi.org/10.1038/emboj.2011.278>
- Duchaîne, T. F., Hemraj, I., Furic, L., Deitinghoff, A., Kiebler, M. A., & DesGroseillers, L. (2002). Staufen2 isoforms localize to the somatodendritic domain of neurons and interact



- with different organelles. *Journal of Cell Science*, *115*(16), 3285–3295. <https://doi.org/10.1242/jcs.115.16.3285>
- Duttaroy, A., Bourbeau, D., Wang, X. L., & Wang, E. (1998). Apoptosis rate can be accelerated or decelerated by overexpression or reduction of the level of elongation factor-1 $\alpha$ . *Experimental Cell Research*, *238*(1), 168–176. <https://doi.org/10.1006/excr.1997.3819>
- Dynes, J. L., & Steward, O. (2012). Arc mRNA docks precisely at the base of individual dendritic spines indicating the existence of a specialized microdomain for synapse-specific mRNA translation. *Journal of Comparative Neurology*, *520*(14), 3105–3119. <https://doi.org/10.1002/cne.23073>
- Edmonds, B. T., Wyckoff, J., Yeung, Y. G., Wang, Y., Stanley, E. R., Jones, J., Segall, J., & Condeelis, J. (1996). Elongation factor-1 $\alpha$  is an overexpressed actin binding protein in metastatic rat mammary adenocarcinoma. *Journal of Cell Science*, *109*(11), 2705–2714. <https://doi.org/10.1242/jcs.109.11.2705>
- Ehlers, M. D. (2000). Reinsertion or Degradation of AMPA Receptors Determined by Activity-Dependent Endocytic Sorting. *Neuron*, *28*, 511–525. [https://doi.org/10.1016/s0896-6273\(00\)00129-x](https://doi.org/10.1016/s0896-6273(00)00129-x)
- El Fatimy, R., Davidovic, L., Tremblay, S., Jaglin, X., Dury, A., Robert, C., De Koninck, P., & Khandjian, E. W. (2016). Tracking the Fragile X Mental Retardation Protein in a Highly Ordered Neuronal RiboNucleoParticles Population: A Link between Stalled Polyribosomes and RNA Granules. *PLoS Genetics*, *12*(7), 1–31. <https://doi.org/10.1371/journal.pgen.1006192>
- Elbaum-Garfinkle, S., & Brangwynne, C. P. (2015). Liquids, Fibers, and Gels: The Many Phases of Neurodegeneration. *Developmental Cell*, *35*(5), 531–532. <https://doi.org/10.1016/j.devcel.2015.11.014>
- Elvira, G., Wasiak, S., Blandford, V., Tong, X. K., Serrano, A., Fan, X., del Rayo Sánchez-Carbente, M., Servant, F., Bell, A. W., Boismenu, D., Lacaille, J. C., McPherson, P. S., DesGroseillers, L., & Sossin, W. S. (2006). Characterization of an RNA granule from developing brain. *Molecular and Cellular Proteomics*, *5*(4), 635–651. <https://doi.org/10.1074/mcp.M500255-MCP200>
- Emenecker, R. J., Griffith, D., & Holehouse, A. S. (2021). Metapredict: a fast, accurate, and easy-to-use predictor of consensus disorder and structure. *Biophysical Journal*, *120*(20), 4312–4319. <https://doi.org/10.1016/j.bpj.2021.08.039>
- Eom, T., Antar, L. N., Singer, R. H., & Bassell, G. J. (2003). Localization of a B-Actin Messenger Ribonucleoprotein Complex with Zipcode-Binding Protein Modulates the Density of Dendritic Filopodia and Filopodial Synapses. *Journal of Neuroscience*, *23*(32), 10433–10444. <https://doi.org/10.1523/jneurosci.23-32-10433.2003>
- Farina, K. L., Hüttelmaier, S., Musunuru, K., Darnell, R., & Singer, R. H. (2003). Two ZBP1 KH domains facilitate  $\beta$ -actin mRNA localization, granule formation, and cytoskeletal

## REFERENCES

- attachment. *Journal of Cell Biology*, 160(1), 77–87.  
<https://doi.org/10.1083/jcb.200206003>
- Fauth, M., & Tetzlaff, C. (2016). Opposing effects of neuronal activity on structural plasticity. *Frontiers in Neuroanatomy*, 10(JUNE), 1–18.  
<https://doi.org/10.3389/fnana.2016.00075>
- Fazal, F. M., Han, S., Parker, K. R., Kaewsapsak, P., Xu, J., Boettiger, A. N., Chang, H. Y., & Ting, A. Y. (2019). Atlas of Subcellular RNA Localization Revealed by APEX-Seq. *Cell*, 178(2), 473–490.e26. <https://doi.org/10.1016/j.cell.2019.05.027>
- Forrest, M. P., Parnell, E., & Penzes, P. (2018). Dendritic structural plasticity and neuropsychiatric disease. *Nature Reviews Neuroscience*, 19(4), 215–234.  
<https://doi.org/10.1038/nrn.2018.16>
- Frankenfield, A. M., Fernandopulle, M. S., Hasan, S., Ward, M. E., & Hao, L. (2020). Development and Comparative Evaluation of Endolysosomal Proximity Labeling-Based Proteomic Methods in Human iPSC-Derived Neurons. *Analytical Chemistry*, 92(23), 15437–15444. <https://doi.org/10.1021/acs.analchem.0c03107>
- Fritzsche, R., Karra, D., Bennett, K. L., Ang, F., Heraud-Farlow, J. E., Tolino, M., Doyle, M., Bauer, K. E., Thomas, S., Planyavsky, M., Arn, E., Bakosova, A., Jungwirth, K., Hörmann, A., Palfi, Z., Sandholzer, J., Schwarz, M., Macchi, P., Colinge, J., ... Kiebler, M. A. (2013). Interactome of two diverse RNA granules links mRNA localization to translational repression in neurons. *Cell Reports*, 5(6), 1749–1762.  
<https://doi.org/10.1016/j.celrep.2013.11.023>
- Fuchs, E., & Flügge, G. (2014). Adult neuroplasticity: More than 40 years of research. *Neural Plasticity*, 2014. <https://doi.org/10.1155/2014/541870>
- Gamarra, M., Blanco-Urrejola, M., Batista, A. F. R., Imaz, J., & Baleriola, J. (2020). Object-Based Analyses in FIJI/ImageJ to Measure Local RNA Translation Sites in Neurites in Response to A $\beta$ 1-42 Oligomers. *Frontiers in Neuroscience*, 14(June), 1–18.  
<https://doi.org/10.3389/fnins.2020.00547>
- Gandin, V., Gutierrez, G. J., Brill, L. M., Varsano, T., Feng, Y., Aza-Blanc, P., Au, Q., McLaughlan, S., Ferreira, T. A., Alain, T., Sonenberg, N., Topisirovic, I., & Ronai, Z. A. (2013). Degradation of Newly Synthesized Polypeptides by Ribosome-Associated RACK1/c-Jun N-Terminal Kinase/Eukaryotic Elongation Factor 1A2 Complex. *Molecular and Cellular Biology*, 33(13), 2510–2526. <https://doi.org/10.1128/mcb.01362-12>
- Gao, J., & Nakamura, F. (2022). Actin-Associated Proteins and Small Molecules Targeting the Actin Cytoskeleton. *International Journal of Molecular Sciences*, 23(4).  
<https://doi.org/10.3390/ijms23042118>
- Geraldo, S., Khanzada, U. K., Parsons, M., Chilton, J. K., & Gordon-Weeks, P. R. (2008). Targeting of the F-actin-binding protein drebrin by the microtubule plus-tip protein EB3 is required for neuriteogenesis. *Nature Cell Biology*, 10(10), 1181–1189.  
<https://doi.org/10.1038/ncb1778>

- Giese, K. P., & Mizuno, K. (2013). The roles of protein kinases in learning and memory. *Learning and Memory*, *20*(10), 540–552. <https://doi.org/10.1101/lm.028449>.112
- Gopal, P. P., Nirschl, J. J., Klinman, E., & Holzbaur, E. L. F. (2017). Amyotrophic lateral sclerosis-linked mutations increase the viscosity of liquid-like TDP-43 RNP granules in neurons. *Proceedings of the National Academy of Sciences of the United States of America*, *114*(12), E2466–E2475. <https://doi.org/10.1073/pnas.1614462114>
- Graber, T. E., Freemantle, E., Anadolu, M. N., Hébert-Seropian, S., Macadam, R. L., Shin, U., Hoang, H. D., Alain, T., Lacaille, J. C., & Sossin, W. S. (2017). UPF1 governs synaptic plasticity through association with a STAU2 RNA granule. *Journal of Neuroscience*, *37*(38), 9116–9131. <https://doi.org/10.1523/JNEUROSCI.0088-17.2017>
- Graber, T. E., Hébert-seropian, S., Khoutorsky, A., David, A., Yewdell, J. W., Lacaille, J.-C., & Sossin, W. S. (2013). Reactivation of stalled polyribosomes in synaptic plasticity. *PNAS*, *110*(40), 16205–16210. <https://doi.org/10.1073/pnas.1307747110>
- Griffiths, L. A., Doig, J., Churchhouse, A. M. D., Davies, F. C. J., Squires, C. E., Newbery, H. J., & Abbott, C. M. (2012). Haploinsufficiency for translation elongation factor eEF1A2 in aged mouse muscle and neurons is compatible with normal function. *PLoS ONE*, *7*(7). <https://doi.org/10.1371/journal.pone.0041917>
- Gross, S. R., & Kinzy, T. G. (2005). Translation elongation factor 1A is essential for regulation of the actin cytoskeleton and cell morphology. *Nature Structural and Molecular Biology*, *12*(9), 772–778. <https://doi.org/10.1038/nsmb979>
- Gross, S. R., & Kinzy, T. G. (2007). Improper Organization of the Actin Cytoskeleton Affects Protein Synthesis at Initiation. *Molecular and Cellular Biology*, *27*(5), 1974–1989. <https://doi.org/10.1128/mcb.00832-06>
- Großhans, H., Simos, G., & Hurt, E. (2000). Review: Transport of tRNA out of the nucleus - Direct channeling to the ribosome? *Journal of Structural Biology*, *129*(2–3), 288–294. <https://doi.org/10.1006/jsbi.2000.4226>
- Grutzendler, J., Kasthuri, N., & Gan, W. B. (2002). Long-term dendritic spine stability in the adult cortex. *Nature*, *420*(6917), 812–816. <https://doi.org/10.1038/nature01276>
- Gu, J., Firestein, B. L., & Zheng, J. Q. (2008). Microtubules in dendritic spine development. *Journal of Neuroscience*, *28*(46), 12120–12124. <https://doi.org/10.1523/JNEUROSCI.2509-08.2008>
- Guerrero, S., Batisse, J., Libre, C., Bernacchi, S., Marquet, R., & Paillart, J. C. (2015). Hiv-1 replication and the cellular eukaryotic translation apparatus. *Viruses*, *7*(1), 199–218. <https://doi.org/10.3390/v7010199>
- Hanamura, K., Kamata, Y., Yamazaki, H., Kojima, N., & Shirao, T. (2018). Isoform-dependent Regulation of Drebrin Dynamics in Dendritic Spines. *Neuroscience*, *379*, 67–76. <https://doi.org/10.1016/j.neuroscience.2018.02.038>

## REFERENCES

- Hau, H. T. A., Ogundele, O., Hibbert, A. H., Monfries, C. A. L., Exelby, K., Wood, N. J., Nevarez-Mejia, J., Carbajal, M. A., Fleck, R. A., Dermit, M., Mardakheh, F. K., Williams-Ward, V. C., Pipalia, T. G., Conte, M. R., & Hughes, S. M. (2020). Maternal *Larp6* controls oocyte development, chorion formation and elevation. *Development (Cambridge)*, *147*(4), 1–14. <https://doi.org/10.1242/dev.187385>
- Hayashi, Y., Ford, L. K., Fioriti, L., McGurk, L., & Zhang, M. (2021). Liquid-liquid phase separation in physiology and pathophysiology of the nervous system. *Journal of Neuroscience*, *41*(5), 834–844. <https://doi.org/10.1523/JNEUROSCI.1656-20.2020>
- Heise, C., Gardoni, F., Culotta, L., di Luca, M., Verpelli, C., & Sala, C. (2014). Elongation factor-2 phosphorylation in dendrites and the regulation of dendritic mRNA translation in neurons. *Frontiers in Cellular Neuroscience*, *8*(February), 1–8. <https://doi.org/10.3389/fncel.2014.00035>
- Hendricks, A. G., Perlson, E., Ross, J. L., Schroeder, H. W., Tokito, M., & Holzbaur, E. L. F. (2010). Motor Coordination via a Tug-of-War Mechanism Drives Bidirectional Vesicle Transport. *Current Biology*, *20*(8), 697–702. <https://doi.org/10.1016/j.cub.2010.02.058>
- Heraud-Farlow, J. E., & Kiebler, M. A. (2014). The multifunctional Staufen proteins: Conserved roles from neurogenesis to synaptic plasticity. *Trends in Neurosciences*, *37*(9), 470–479. <https://doi.org/10.1016/j.tins.2014.05.009>
- Hering, H., & Sheng, M. (2001). Dendritic spines: structure, function and regulation. *Nature Reviews Neuroscience*, *2*(December), 880–888. <https://doi.org/10.1038/35104061>
- Hering, H., & Sheng, M. (2003). Activity-Dependent Redistribution and Essential Role of Cortactin in Dendritic Spine Morphogenesis. *Journal of Neuroscience*, *23*(37), 11759–11769. <https://doi.org/10.1523/jneurosci.23-37-11759.2003>
- Hilliker, A., Gao, Z., Jankowsky, E., & Parker, R. (2011). The DEAD-Box Protein Ded1 Modulates Translation by the Formation and Resolution of an eIF4F-mRNA Complex. *Molecular Cell*, *43*(6), 962–972. <https://doi.org/10.1016/j.molcel.2011.08.008>
- Ho, V. M., Lee, J. A., & Martin, K. C. (2011). The cell biology of synaptic plasticity. *Science*, *334*(6056), 623–628. <https://doi.org/10.1126/science.1209236>
- Holt, C. E., Martin, K. C., & Schuman, E. M. (2019). Local translation in neurons: visualization and function. *Nature Structural and Molecular Biology*, *26*(7), 557–566. <https://doi.org/10.1038/s41594-019-0263-5>
- Honkura, N., Matsuzaki, M., Noguchi, J., Ellis-Davies, G. C. R., & Kasai, H. (2008a). The Subspine Organization of Actin Fibers Regulates the Structure and Plasticity of Dendritic Spines. *Neuron*, *57*(5), 719–729. <https://doi.org/10.1016/j.neuron.2008.01.013>

- Honkura, N., Matsuzaki, M., Noguchi, J., Ellis-Davies, G. C. R., & Kasai, H. (2008b). *The Subspine Organization of Actin Fibers Regulates the Structure and Plasticity of Dendritic Spines Suppl Fig. 57*, 1–9.
- Hooper, C., & Hilliker, A. (2013). Packing them up and dusting them off: RNA helicases and mRNA storage. *Biochimica et Biophysica Acta - Gene Regulatory Mechanisms*, *1829*(8), 824–834. <https://doi.org/10.1016/j.bbagr.2013.03.008>
- Hornbeck, P. V., Zhang, B., Murray, B., Kornhauser, J. M., Latham, V., & Skrzypek, E. (2015). PhosphoSitePlus, 2014: Mutations, PTMs and recalibrations. *Nucleic Acids Research*, *43*(D1), D512–D520. <https://doi.org/10.1093/nar/gku1267>
- Hotokezaka, Y., Bben, U. T., Hotokezaka, H., Van Leyen, K., Beatrix, B., Smith, D. H., Nakamura, T., & Wiedmann, M. (2002). Interaction of the eukaryotic elongation factor 1A with newly synthesized polypeptides. *Journal of Biological Chemistry*, *277*(21), 18545–18551. <https://doi.org/10.1074/jbc.M201022200>
- Hruska, M., Henderson, N., Le Marchand, S. J., Jafri, H., & Dalva, M. B. (2018). Synaptic nanomodules underlie the organization and plasticity of spine synapses. *Nature Neuroscience*, *21*(5), 671–682. <https://doi.org/10.1038/s41593-018-0138-9>
- Hu, X., Viessmann, C., Nam, S., Merriam, E., & Dent, E. W. (2008). Activity-dependent dynamic microtubule invasion of dendritic spines. *Journal of Neuroscience*, *28*(49), 13094–13105. <https://doi.org/10.1523/JNEUROSCI.3074-08.2008>
- Huang, W., Zhu, P. J., Zhang, S., Zhou, H., Stoica, L., Galiano, M., Krnjević, K., Roman, G., & Costa-Mattioli, M. (2013). mTORC2 controls actin polymerization required for consolidation of long-term memory. *Nature Neuroscience*, *16*(4), 441–448. <https://doi.org/10.1038/nn.3351>
- Huang, Y. S., Mendez, R., Fernandez, M., & Richter, J. D. (2023). CPEB and translational control by cytoplasmic polyadenylation: impact on synaptic plasticity, learning, and memory. *Molecular Psychiatry*, *January*, 1–9. <https://doi.org/10.1038/s41380-023-02088-x>
- Huber, K. M., Kayser, M. S., & Bear, M. F. (2000). Role for rapid dendritic protein synthesis in hippocampal mGluR- dependent long-term depression. *Science*, *288*(5469), 1254–1256. <https://doi.org/10.1126/science.288.5469.1254>
- Hubstenberger, A., Noble, S. L., Cameron, C., & Evans, T. C. (2013). Translation repressors, an RNA helicase, and developmental cues control RNP phase transitions during early development. *Developmental Cell*, *27*(2), 161–173. <https://doi.org/10.1016/j.devcel.2013.09.024>
- Hüttelmaier, S., Zenklusen, D., Lederer, M., Dichtenberg, J., Lorenz, M., Meng, X. H., Bassell, G. J., Condeelis, J., & Singer, R. H. (2005). Spatial regulation of  $\beta$ -actin translation by Src-dependent phosphorylation of ZBP1. *Nature*, *438*(7067), 512–515. <https://doi.org/10.1038/nature04115>

## REFERENCES

- Irgen-Giorgio, S., Yoshida, S., Walling, V., & Chong, S. (2022). Fixation can change the appearance of phase separation in living cells. *ELife*, *11*, 1–24. <https://doi.org/10.7554/eLife.79903>
- Ivanov, A., Esclapez, M., Pellegrino, C., Shirao, T., & Ferhat, L. (2009). Drebrin A regulates dendritic spine plasticity and synaptic function in mature cultured hippocampal neurons. *Journal of Cell Science*, *122*(4), 524–534. <https://doi.org/10.1242/jcs.033464>
- Jackson, R. J., Hellen, C. U. T., & Pestova, T. V. (2010). The mechanism of eukaryotic translation initiation and principles of its regulation. *Nature Reviews Molecular Cell Biology*, *11*(2), 113–127. <https://doi.org/10.1038/nrm2838>
- Jackson, R. J., Hellen, C. U. T., & Pestova, T. V. (2012). Termination and post-termination events in eukaryotic translation. In *Advances in Protein Chemistry and Structural Biology* (1st ed., Vol. 86). Elsevier Inc. <https://doi.org/10.1016/B978-0-12-386497-0.00002-5>
- Jakobsson, M. E., Matecki, J., & Falnes, P. Ø. (2018). Regulation of eukaryotic elongation factor 1 alpha (eEF1A) by dynamic lysine methylation. *RNA Biology*, *6286*. <https://doi.org/10.1080/15476286.2018.1440875>
- Jambhekar, A., & Derisi, J. L. (2007). Cis-acting determinants of asymmetric, cytoplasmic RNA transport. *Rna*, *13*(5), 625–642. <https://doi.org/10.1261/rna.262607>
- Jankowsky, E. (2011). RNA helicases at work: Binding and rearranging. *Trends in Biochemical Sciences*, *36*(1), 19–29. <https://doi.org/10.1016/j.tibs.2010.07.008>
- Jaworski, J., Kapitein, L. C., Gouveia, S. M., Dortland, B. R., Wulf, P. S., Grigoriev, I., Camera, P., Spangler, S. A., Di Stefano, P., Demmers, J., Krugers, H., Defilippi, P., Akhmanova, A., & Hoogenraad, C. C. (2009). Dynamic Microtubules Regulate Dendritic Spine Morphology and Synaptic Plasticity. *Neuron*, *61*(1), 85–100. <https://doi.org/10.1016/j.neuron.2008.11.013>
- Jønson, L., Vikesaa, J., Krogh, A., Nielsen, L. K., Hansen, T. v. O., Borup, R., Johnsen, A. H., Christiansen, J., & Nielsen, F. C. (2007). Molecular composition of IMP1 ribonucleoprotein granules. *Molecular and Cellular Proteomics*, *6*(5), 798–811. <https://doi.org/10.1074/mcp.M600346-MCP200>
- Jumper, J., Evans, R., Pritzel, A., Green, T., Figurnov, M., Ronneberger, O., Tunyasuvunakool, K., Bates, R., Židek, A., Potapenko, A., Bridgland, A., Meyer, C., Kohl, S. A. A., Ballard, A. J., Cowie, A., Romera-Paredes, B., Nikolov, S., Jain, R., Adler, J., ... Hassabis, D. (2021). Highly accurate protein structure prediction with AlphaFold. *Nature*, *596*(7873), 583–589. <https://doi.org/10.1038/s41586-021-03819-2>
- Jung, G., Kim, E. J., Cicvaric, A., Sase, S., Gröger, M., Höger, H., Sialana, F. J., Berger, J., Monje, F. J., & Lubec, G. (2015). Drebrin depletion alters neurotransmitter receptor levels in protein complexes, dendritic spine morphogenesis and memory-related synaptic plasticity in the mouse hippocampus. *Journal of Neurochemistry*, *134*(2), 327–339. <https://doi.org/10.1111/jnc.13119>

- Kaech, S., Fischer, M., Doll, T., & Matus, A. (1997). Isoform specificity in the relationship of actin to dendritic spines. *Journal of Neuroscience*, *17*(24), 9565–9572. <https://doi.org/10.1523/jneurosci.17-24-09565.1997>
- Kaech, S., Parmar, H., Roelandse, M., Bornmann, C., & Matus, A. (2001). Cytoskeletal microdifferentiation: A mechanism for organizing morphological plasticity in dendrites. *Proceedings of the National Academy of Sciences of the United States of America*, *98*(13), 7086–7092. <https://doi.org/10.1073/pnas.111146798>
- Kahns, S., Lund, A., Kristensen, P., Knudsen, C. R., Clark, B. F. C., Cavallius, J., & Merrick, W. C. (1998). The elongation factor 1 A-2 isoform from rabbit: Cloning of the cDNA and characterization of the protein. *Nucleic Acids Research*, *26*(8), 1884–1890. <https://doi.org/10.1093/nar/26.8.1884>
- Kalinowska, M., Chávez, A. E., Lutz, S., Castillo, P. E., Bukauskas, F. F., & Francesconi, A. (2015). *Actinin-4 Governs Dendritic Spine Dynamics and Promotes Their Remodeling by Metabotropic Glutamate Receptors*. *290*(26), 15909–15920. <https://doi.org/10.1074/jbc.M115.640136>
- Kanai, Y., Dohmae, N., & Hirokawa, N. (2004). Kinesin transports RNA: Isolation and characterization of an RNA-transporting granule. *Neuron*, *43*(4), 513–525. <https://doi.org/10.1016/j.neuron.2004.07.022>
- Kanellos, G., & Frame, M. C. (2016). Cellular functions of the ADF/cofilin family at a glance. *Journal of Cell Science*, *129*(17), 3211–3218. <https://doi.org/10.1242/jcs.187849>
- Kang, H., & Schuman, E. M. (1996). *A requirement for local protein synthesis in neurotrophin-induced hippocampal synaptic plasticity*. *273*, 1402–1406.
- Kapitein, L. C., & Hoogenraad, C. C. (2015). Building the Neuronal Microtubule Cytoskeleton. *Neuron*, *87*(3), 492–506. <https://doi.org/10.1016/j.neuron.2015.05.046>
- Kapur, M., Monaghan, C. E., & Ackerman, S. L. (2017). Regulation of mRNA Translation in Neurons—A Matter of Life and Death. *Neuron*, *96*(3), 616–637. <https://doi.org/10.1016/j.neuron.2017.09.057>
- Kedersha, N., Panas, M. D., Achorn, C. A., Lyons, S., Tisdale, S., Hickman, T., Thomas, M., Lieberman, J., McInerney, G. M., Ivanov, P., & Anderson, P. (2016). G3BP-Caprin1-USP10 complexes mediate stress granule condensation and associate with 40S subunits. *Journal of Cell Biology*, *212*(7), 845–860. <https://doi.org/10.1083/jcb.201508028>
- Kessels, M. M., Schwintzer, L., Schlobinski, D., & Qualmann, B. (2011). Controlling actin cytoskeletal organization and dynamics during neuronal morphogenesis. *European Journal of Cell Biology*, *90*(11), 926–933. <https://doi.org/10.1016/j.ejcb.2010.08.011>
- Khacho, M., Mekhail, K., Pilon-Larose, K., Pause, A., Côté, J., & Lee, S. (2008). eEF1A is a novel component of the mammalian nuclear protein export machinery. *Molecular Biology of the Cell*, *19*(2), 5296–5308. <https://doi.org/10.1091/mbc.E08>

## REFERENCES

- Khalyfa, A., Bourbeau, D., Chen, E., Petroulakis, E., Pan, J., Xu, S., & Wang, E. (2001). Characterization of Elongation Factor-1A (eEF1A-1) and eEF1A-2/S1 Protein Expression in Normal and wasted Mice \*. *The Journal of Biological Chemistry*, 276(25), 22915–22922. <https://doi.org/10.1074/jbc.M101011200>
- Kim, K., Lakhanpal, G., Lu, H. E., Khan, M., Suzuki, A., Kato-Hayashi, M., Narayanan, R., Luyben, T. T., Matsuda, T., Nagai, T., Blanpied, T. A., Hayashi, Y., & Okamoto, K. (2015). A Temporary Gating of Actin Remodeling during Synaptic Plasticity Consists of the Interplay between the Kinase and Structural Functions of CaMKII. *Neuron*, 87(4), 813–826. <https://doi.org/10.1016/j.neuron.2015.07.023>
- Kim, S., & Coulombe, P. A. (2010). Emerging role for the cytoskeleton as an organizer and regulator of translation. *Nature Reviews Molecular Cell Biology*, 11(1), 75–81. <https://doi.org/10.1038/nrm2818>
- Kojima, N., Yasuda, H., Hanamura, K., Ishizuka, Y., Sekino, Y., & Shirao, T. (2016). Drebrin A regulates hippocampal LTP and hippocampus-dependent fear learning in adult mice. *Neuroscience*, 324, 218–226. <https://doi.org/10.1016/j.neuroscience.2016.03.015>
- Koltun, B., Ironi, S., Gershoni-Emek, N., Barrera, I., Hleihil, M., Nanguneri, S., Sasmal, R., Agasti, S. S., Nair, D., & Rosenblum, K. (2020). Measuring mRNA translation in neuronal processes and somata by tRNA-FRET. *Nucleic Acids Research*, 48(6), E32–E32. <https://doi.org/10.1093/nar/gkaa042>
- Konietzny, A., Bär, J., & Mikhaylova, M. (2017). Dendritic Actin Cytoskeleton: Structure, Functions, and Regulations. *Frontiers in Cellular Neuroscience*, 11(May), 1–10. <https://doi.org/10.3389/fncel.2017.00147>
- Koskinen, M., & Hotulainen, P. (2014). Measuring F-actin properties in dendritic spines. *Frontiers in Neuroanatomy*, 8(AUG), 1–14. <https://doi.org/10.3389/fnana.2014.00074>
- Koulouras, G., Panagopoulos, A., Rapsomaniki, M. A., Giakoumakis, N. N., Taraviras, S., & Lygerou, Z. (2018). EasyFRAP-web: A web-based tool for the analysis of fluorescence recovery after photobleaching data. *Nucleic Acids Research*, 46(W1), W467–W472. <https://doi.org/10.1093/nar/gky508>
- Kuroski, T., Mitsutomi, S., Hewko, A., Akimitsu, N., & Maquat, L. E. (2022). Integrative omics indicate FMRP sequesters mRNA from translation and deadenylation in human neuronal cells. *Molecular Cell*, 1–18. <https://doi.org/10.1016/j.molcel.2022.10.018>
- Langille, J. J., Ginzberg, K., & Sossin, W. S. (2019). Polysomes identified by live imaging of nascent peptides are stalled in hippocampal and cortical neurites. *Learning and Memory*, 26(9), 351–362. <https://doi.org/10.1101/lm.049965.119>
- Le Sourd, F., Boulben, S., Le Bouffant, R., Cormier, P., Morales, J., Belle, R., & Mulner-Lorillon, O. (2006). eEF1B: At the dawn of the 21st century. *Biochimica et Biophysica Acta - Gene Structure and Expression*, 1759(1–2), 13–31. <https://doi.org/10.1016/j.bbaexp.2006.02.003>



- Lee, H. K., Kameyama, K., Huganir, R. L., & Bear, M. F. (1998). NMDA induces long-term synaptic depression and dephosphorylation of the GluR1 subunit of AMPA receptors in hippocampus. *Neuron*, *21*(5), 1151–1162. [https://doi.org/10.1016/S0896-6273\(00\)80632-7](https://doi.org/10.1016/S0896-6273(00)80632-7)
- Lee, S., Francoeur, A.-M., Liu, S., & Wang, E. (1992). Tissue-specific Expression in Mammalian Brain, Heart, and Muscle of S1, A Member of the Elongation Factor-1a Gene Family \*. *The Journal of Biological Chemistry*, *267*(33), 24064–24068. [https://doi.org/10.1016/S0021-9258\(18\)35946-5](https://doi.org/10.1016/S0021-9258(18)35946-5)
- Lee, S. J. R., Escobedo-Lozoya, Y., Szatmari, E. M., & Yasuda, R. (2009). Activation of CaMKII in single dendritic spines during long-term potentiation. *Nature*, *458*(7236), 299–304. <https://doi.org/10.1038/nature07842>
- Lei, W., Omotade, O. F., Myers, K. R., & Zheng, J. Q. (2016). Actin cytoskeleton in dendritic spine development and plasticity. *Current Opinion in Neurobiology*, *39*, 86–92. <https://doi.org/10.1016/j.conb.2016.04.010>
- Lesslich, H. M., Klapal, L., Wilke, J., Haak, A., & Dietzel, I. D. (2022). Adjusting the neuron to astrocyte ratio with cyostatics in hippocampal cell cultures from postnatal rats: A comparison of cytarabino furanoside (AraC) and 5-fluoro-2'-deoxyuridine (FUDR). *PLoS ONE*, *17*(3 March), 1–16. <https://doi.org/10.1371/journal.pone.0265084>
- Li, D., Wei, T., Abbott, C. M., & Harrich, D. (2013). The Unexpected Roles of Eukaryotic Translation Elongation Factors in RNA Virus Replication and Pathogenesis. *Microbiology and Molecular Biology Reviews*, *77*(2), 253–266. <https://doi.org/10.1128/membr.00059-12>
- Li, Z., Liu, H., Li, J., Yang, Q., Feng, Z., Li, Y., Yang, H., Yu, C., Wan, J., Liu, W., & Zhang, M. (2019). Homer Tetramer Promotes Actin Bundling Activity of Drebrin. *Structure*, *27*(1), 27–38.e4. <https://doi.org/10.1016/j.str.2018.10.011>
- Liao, Y. C., Fernandopulle, M. S., Wang, G., Choi, H., Hao, L., Drerup, C. M., Patel, R., Qamar, S., Nixon-Abell, J., Shen, Y., Meadows, W., Vendruscolo, M., Knowles, T. P. J., Nelson, M., Czekalska, M. A., Musteikyte, G., Gachechiladze, M. A., Stephens, C. A., Pasolli, H. A., ... Ward, M. E. (2019). RNA Granules Hitchhike on Lysosomes for Long-Distance Transport, Using Annexin A11 as a Molecular Tether. *Cell*, *179*(1), 147–164.e20. <https://doi.org/10.1016/j.cell.2019.08.050>
- Lin, K. W., Yakymovych, I., Jia, M., Yakymovych, M., & Souchelnytskyi, S. (2010). Phosphorylation of eEF1A1 at Ser300 by TbR-I Results in Inhibition of mRNA Translation. *Current Biology*, *20*(18), 1615–1625. <https://doi.org/10.1016/j.cub.2010.08.017>
- Lin, W.-H., & Webb, D. J. (2009). Actin and Actin-Binding Proteins: Masters of Dendritic Spine Formation, Morphology, and Function. *Open Neurosci J.*, *3*, 54–66. <https://doi.org/10.2174/1874082000903020054>

## REFERENCES

- Lisman, J., Schulman, H., & Cline, H. (2002). The molecular basis of CaMKII function in synaptic and behavioural memory. *Nature Reviews Neuroscience*, 3(3), 175–190. <https://doi.org/10.1038/nrn753>
- Liu, G., Tang, J., Edmonds, B. T., Murray, J., Levin, S., & Condeelis, J. (1996). F-actin sequesters elongation factor 1 $\alpha$  from interaction with aminoacyl-tRNA in a pH-dependent reaction. *Journal of Cell Biology*, 135(4), 953–963. <https://doi.org/10.1083/jcb.135.4.953>
- Liu, S., Hausmann, S., Carlson, S. M., Fuentes, M. E., Francis, J. W., Pillai, R., Lofgren, S. M., Hulea, L., Tandoc, K., Lu, J., Li, A., Nguyen, N. D., Caporicci, M., Kim, M. P., Maitra, A., Wang, H., Wistuba, I. I., Porco, J. A., Bassik, M. C., ... Gozani, O. (2019). METTL13 Methylation of eEF1A Increases Translational Output to Promote Tumorigenesis. *Cell*, 176(3), 491-504.e21. <https://doi.org/10.1016/j.cell.2018.11.038>
- Lou, L. L., Lloyd, S. J., & Schulman, H. (1986). Activation of the multifunctional Ca<sup>2+</sup>/calmodulin-dependent protein kinase by autophosphorylation: ATP modulates production of an autonomous enzyme. *Proceedings of the National Academy of Sciences of the United States of America*, 83(24), 9497–9501. <https://doi.org/10.1073/pnas.83.24.9497>
- Lund, A., Knudsen, S. M., Vissing, H., Clark, B., & Tommerup, N. (1996). Assignment of human elongation factor 1 $\alpha$  genes: EEF1A maps to chromosome 6q14 and EEF1A2 to 20q13.3. *Genomics*, 36(2), 359–361. <https://doi.org/10.1006/geno.1996.0475>
- MacGillavry, H. D., Song, Y., Raghavachari, S., & Blanpied, T. A. (2013). Nanoscale scaffolding domains within the postsynaptic density concentrate synaptic ampa receptors. *Neuron*, 78(4), 615–622. <https://doi.org/10.1016/j.neuron.2013.03.009>
- Magee, J. C. (2000). Dendritic integration of excitatory synaptic input. *Nature Reviews Neuroscience*, 1(December), 181–190. <https://doi.org/10.1038/35044552>
- Maharana, S., Wang, J., Papadopoulos, D. K., Richter, D., Pozniakovsky, A., Poser, I., Bickle, M., Rizk, S., Guillén-boixet, J., Franzmann, T. M., Jahnel, M., Marrone, L., Chang, Y., Sternecker, J., Tomancak, P., Hyman, A. A., & Alberti, S. (2018). RNA buffers the phase separation behavior of prion-like RNA binding proteins. *Science*, 360(6391), 918–921. <https://doi.org/10.1126/science.aar736>
- Mardakheh, F. K., Paul, A., Kümper, S., Sadok, A., Paterson, H., McCarthy, A., Yuan, Y., & Marshall, C. J. (2015). Global Analysis of mRNA, Translation, and Protein Localization: Local Translation Is a Key Regulator of Cell Protrusions. *Developmental Cell*, 35(3), 344–357. <https://doi.org/10.1016/j.devcel.2015.10.005>
- Marin, P., Nastiuk, K. L., Daniel, N., Girault, J. A., Czernik, A. J., Glowinski, J., Nairn, A. C., & Prémont, J. (1997). Glutamate-dependent phosphorylation of elongation factor-2 and inhibition of protein synthesis in neurons. *Journal of Neuroscience*, 17(10), 3445–3454. <https://doi.org/10.1523/jneurosci.17-10-03445.1997>

- Markmiller, S., Soltanieh, S., Server, K. L., Mak, R., Jin, W., Fang, M. Y., Luo, E. C., Krach, F., Yang, D., Sen, A., Fulzele, A., Wozniak, J. M., Gonzalez, D. J., Kankel, M. W., Gao, F. B., Bennett, E. J., Lécuycer, E., & Yeo, G. W. (2018). Context-Dependent and Disease-Specific Diversity in Protein Interactions within Stress Granules. *Cell*, *172*(3), 590-604.e13. <https://doi.org/10.1016/j.cell.2017.12.032>
- Marmor-Kollet, H., Siany, A., Kedersha, N., Knafo, N., Rivkin, N., Danino, Y. M., Moens, T. G., Olender, T., Sheban, D., Cohen, N., Dadosh, T., Addadi, Y., Ravid, R., Eitan, C., Toth Cohen, B., Hofmann, S., Riggs, C. L., Advani, V. M., Higginbottom, A., ... Hornstein, E. (2020). Spatiotemporal Proteomic Analysis of Stress Granule Disassembly Using APEX Reveals Regulation by SUMOylation and Links to ALS Pathogenesis. *Molecular Cell*, *80*(5), 876-891.e6. <https://doi.org/10.1016/j.molcel.2020.10.032>
- Martin, K. C., & Ephrussi, A. (2009). mRNA Localization: Gene Expression in the Spatial Dimension. *Cell*, *136*(4), 719-730. <https://doi.org/10.1016/j.cell.2009.01.044>
- Mateu-Regué, À., Nielsen, F. C., & Christiansen, J. (2020). Cytoplasmic mRNPs revisited: Singletons and condensates. *BioEssays*, *42*(12), 1-13. <https://doi.org/10.1002/bies.202000097>
- Mateyak, M. K., & Kinzy, T. G. (2010). eEF1A: Thinking outside the ribosome. *Journal of Biological Chemistry*, *285*(28), 21209-21213. <https://doi.org/10.1074/jbc.R110.113795>
- Matt, L., Kim, K., Hergarden, A. C., Patriarchi, T., Malik, Z. A., Park, D. K., Chowdhury, D., Buonarati, O. R., Henderson, P. B., Gökçek Saraç, Ç., Zhang, Y., Mohapatra, D., Horne, M. C., Ames, J. B., & Hell, J. W. (2018).  $\alpha$ -Actinin Anchors PSD-95 at Postsynaptic Sites. *Neuron*, *97*(5), 1094-1109.e9. <https://doi.org/10.1016/j.neuron.2018.01.036>
- Mattson, M. P., Maudsley, S., & Martin, B. (2004). BDNF and 5-HT: A dynamic duo in age-related neuronal plasticity and neurodegenerative disorders. *Trends in Neurosciences*, *27*(10), 589-594. <https://doi.org/10.1016/j.tins.2004.08.001>
- Mendonça, S., von Kügelgen, N., Dantsuji, S., Ron, M., Breimann, L., Baranovskii, A., Lödige, I., Kirchner, M., Fischer, M., Zerna, N., Bujanic, L., Mertins, P., Ulitsky, I., & Chekulaeva, M. (2023). Massively parallel identification of mRNA localization elements in primary cortical neurons. In *Nature Neuroscience* (Vol. 26, Issue 3). Springer US. <https://doi.org/10.1038/s41593-022-01243-x>
- Mendoza, M. B., Gutierrez, S., Ortiz, R., Moreno, D. F., Dermitt, M., Dodel, M., Rebollo, E., Bosch, M., Mardakheh, F. K., & Gallego, C. (2021). The elongation factor eEF1A2 controls translation and actin dynamics in dendritic spines. *Science Signaling*, *14*(691). <https://doi.org/10.1126/SCISIGNAL.ABF5594>
- Merriam, E. B., Millette, M., Lumbard, D. C., Saengsawang, W., Fothergill, T., Hu, X., Ferhat, L., & Dent, E. W. (2013). Synaptic regulation of microtubule dynamics in dendritic spines by calcium, F-actin, and Drebrin. *Journal of Neuroscience*, *33*(42), 16471-16482. <https://doi.org/10.1523/JNEUROSCI.0661-13.2013>

## REFERENCES

- Metzbower, S. R., Joo, Y., Benavides, D. R., & Blanpied, T. A. (2019). Properties of individual hippocampal synapses influencing NMDA-receptor activation by spontaneous neurotransmission. *ENeuro*, *6*(3). <https://doi.org/10.1523/ENEURO.0419-18.2019>
- Meyer, D., Bonhoeffer, T., & Scheuss, V. (2014). Balance and stability of synaptic structures during synaptic plasticity. *Neuron*, *82*(2), 430–443. <https://doi.org/10.1016/j.neuron.2014.02.031>
- Middleton, S. A., Eberwine, J., & Kim, J. (2019). Comprehensive catalog of dendritically localized mRNA isoforms from sub-cellular sequencing of single mouse neurons. *BMC Biology*, *17*(1), 1–16. <https://doi.org/10.1186/s12915-019-0630-z>
- Mikhaylova, M., Bär, J., van Bommel, B., Schätzle, P., YuanXiang, P. A., Raman, R., Hradsky, J., Konietzny, A., Loktionov, E. Y., Reddy, P. P., Lopez-Rojas, J., Spilker, C., Kobler, O., Raza, S. A., Stork, O., Hoogenraad, C. C., & Kreutz, M. R. (2018). Caldendrin Directly Couples Postsynaptic Calcium Signals to Actin Remodeling in Dendritic Spines. *Neuron*, *97*(5), 1110–1125.e14. <https://doi.org/10.1016/j.neuron.2018.01.046>
- Mikl, M., Vendra, G., & Kiebler, M. A. (2011). Independent localization of MAP2, CaMKII $\alpha$  and  $\beta$ -actin RNAs in low copy numbers. *EMBO Reports*, *12*(10), 1077–1084. <https://doi.org/10.1038/embor.2011.149>
- Mingot, M., Vega, S., Cano, A., Portillo, F., & Nieto, M. A. (2013). eEF1A Mediates the Nuclear Export of SNAG-Containing Proteins via the Exportin5-Aminoacyl-tRNA Complex. *Cell Reports*, *7*27–737. <https://doi.org/10.1016/j.celrep.2013.09.030>
- Mittag, T., & Parker, R. (2018). Multiple Modes of Protein–Protein Interactions Promote RNP Granule Assembly. *Journal of Molecular Biology*, *430*(23), 4636–4649. <https://doi.org/10.1016/j.jmb.2018.08.005>
- Mizui, T., Kojima, N., Yamazaki, H., Katayama, M., Hanamura, K., & Shirao, T. (2009). Drebrin is involved in the regulation of axonal growth through actin-myosin interactions. *Journal of Neurochemistry*, *109*(2), 611–622. <https://doi.org/10.1111/j.1471-4159.2009.05993.x>
- Mizui, T., Sekino, Y., Yamazaki, H., Ishizuka, Y., Takahashi, H., Kojima, N., Kojima, M., & Shirao, T. (2014). Myosin II ATPase activity mediates the long-term potentiation-induced exodus of stable F-actin bound by drebrin from dendritic spines. *PLoS ONE*, *9*(1). <https://doi.org/10.1371/journal.pone.0085367>
- Monshausen, M., Putz, U., Rehbein, M., Schweizer, M., Desgroseillers, L., Kuhl, D., Richter, D., & Kindler, S. (2001). Two rat brain Staufen isoforms differentially bind RNA. *Journal of Neurochemistry*, *76*(1), 155–165. <https://doi.org/10.1046/j.1471-4159.2001.00061.x>
- Mower, A. F., Kwok, S., Yu, H., Majewska, A. K., Okamoto, K. I., Hayashi, Y., & Sur, M. (2011). Experience-dependent regulation of CaMKII activity within single visual cortex synapses in vivo. *Proceedings of the National Academy of Sciences of the United States of America*, *108*(52), 21241–21246. <https://doi.org/10.1073/pnas.1108261109>

- Muddashetty, R. S., Kelić, S., Gross, C., Xu, M., & Bassell, G. J. (2007). Dysregulated metabotropic glutamate receptor-dependent translation of AMPA receptor and postsynaptic density-95 mRNAs at synapses in a mouse model of fragile X syndrome. *Journal of Neuroscience*, *27*(20), 5338–5348. <https://doi.org/10.1523/JNEUROSCI.0937-07.2007>
- Mugler, C. F., Hondele, M., Heinrich, S., Sachdev, R., Vallotton, P., Koek, A. Y., Chan, L. Y., & Weis, K. (2016). ATPase activity of the DEAD-box protein Dhh1 controls processing body formation. *ELife*, *5*(OCTOBER2016). <https://doi.org/10.7554/eLife.18746>
- Mukherjee, J., Hermesh, O., Eliscovich, C., Nalpas, N., Franz-Wachtel, M., Maček, B., & Jansen, R. P. (2019).  $\beta$ -Actin mRNA interactome mapping by proximity biotinylation. *Proceedings of the National Academy of Sciences of the United States of America*, *116*(26), 12863–12872. <https://doi.org/10.1073/pnas.1820737116>
- Munshi, R., Kandl, K. A., Carr-Schmid, A., Whitacre, J. L., Adams, A. E. M., & Kinzy, T. G. (2001). Overexpression of translation elongation factor 1A affects the organization and function of the actin cytoskeleton in yeast. *Genetics*, *157*(4), 1425–1436. <https://doi.org/10.1093/genetics/157.4.1425>
- Nagahara, A. H., Merrill, D. A., Coppola, G., Tsukada, S., Schroeder, B. E., Shaked, G. M., Wang, L., Blesch, A., Kim, A., Conner, J. M., Rockenstein, E., Chao, M. V., Koo, E. H., Geschwind, D., Masliah, E., Chiba, A. A., & Tuszynski, M. H. (2009). Neuroprotective effects of brain-derived neurotrophic factor in rodent and primate models of Alzheimer's disease. *Nature Medicine*, *15*(3), 331–337. <https://doi.org/10.1038/nm.1912>
- Negrutskii, B. S., Budkevich, T. V., Shalak, V. F., Turkovskaya, G. V., & El'skaya, A. V. (1996). Rabbit translation elongation factor 1 $\alpha$  stimulates the activity of homologous aminoacyl-tRNA synthetase. *FEBS Letters*, *382*(1–2), 18–20. [https://doi.org/10.1016/0014-5793\(96\)00128-7](https://doi.org/10.1016/0014-5793(96)00128-7)
- Nelson, C. D., Kim, M. J., Hsin, H., Chen, Y., & Sheng, M. (2013). Phosphorylation of threonine-19 of PSD-95 by GSK-3 $\beta$  is required for PSD-95 mobilization and long-term depression. *Journal of Neuroscience*, *33*(29), 12122–12135. <https://doi.org/10.1523/JNEUROSCI.0131-13.2013>
- Nielsen, F. C., Nielsen, J., Kristensen, M. A., Koch, G., & Christiansen, J. (2002). Cytoplasmic trafficking of IGF-II mRNA-binding protein by conserved KH domains. *Journal of Cell Science*, *115*(10), 2087–2097. <https://doi.org/10.1242/jcs.115.10.2087>
- Niswender, C. M., & Conn, P. J. (2010). Metabotropic glutamate receptors: Physiology, pharmacology, and disease. *Annual Review of Pharmacology and Toxicology*, *50*, 295–322. <https://doi.org/10.1146/annurev.pharmtox.011008.145533>
- Núñez, L., Buxbaum, A. R., Katz, Z. B., Lopez-Jones, M., Nwokafor, C., Czaplinski, K., Pan, F., Rosenberg, J., Monday, H. R., & Singer, R. H. (2022). Tagged actin mRNA dysregulation

## REFERENCES

- in IGF2BP1<sup>-/-</sup> mice. *Proceedings of the National Academy of Sciences of the United States of America*, 119(37), 1–7. <https://doi.org/10.1073/pnas.2208465119>
- Okamoto, K. I., Narayanan, R., Lee, S. H., Murata, K., & Hayashi, Y. (2007). The role of CaMKII as an F-actin-bundling protein crucial for maintenance of dendritic spine structure. *Proceedings of the National Academy of Sciences of the United States of America*, 104(15), 6418–6423. <https://doi.org/10.1073/pnas.0701656104>
- Padrón, A., Iwasaki, S., & Ingolia, N. T. (2019). Proximity RNA Labeling by APEX-Seq Reveals the Organization of Translation Initiation Complexes and Repressive RNA Granules. *Molecular Cell*, 75(4), 875–887.e5. <https://doi.org/10.1016/j.molcel.2019.07.030>
- Palmer, M. J., Irving, A. J., Seabrook, G. R., Jane, D. E., & Collingridge, G. L. (1997). The group I mGlu receptor agonist DHPG induces a novel form of LTD in the CA1 region of the hippocampus. *Neuropharmacology*, 36(11–12), 1517–1532. [https://doi.org/10.1016/S0028-3908\(97\)00181-0](https://doi.org/10.1016/S0028-3908(97)00181-0)
- Park, H. Y., Hyungsik, L., Yoon, Y. J., Follenzi, A., Nwokafor, C., Lopez-Jones, M., Meng, X., & Singer, R. H. (2014). Visualization of Dynamics of Single Endogenous mRNA Labeled in Live Mouse. *Science*, 343(January), 422–424. <https://doi.org/10.1126/science.1239200>
- Park, S., Park, J. M., Kim, S., Kim, J. A., Shepherd, J. D., Smith-Hicks, C. L., Chowdhury, S., Kaufmann, W., Kuhl, D., Ryazanov, A. G., Huganir, R. L., Linden, D. J., & Worley, P. F. (2008). Elongation Factor 2 and Fragile X Mental Retardation Protein Control the Dynamic Translation of Arc/Arg3.1 Essential for mGluR-LTD. *Neuron*, 59(1), 70–83. <https://doi.org/10.1016/j.neuron.2008.05.023>
- Patel, A., Lee, H. O., Jawerth, L., Maharana, S., Jahnel, M., Hein, M. Y., Stoynev, S., Mahamid, J., Saha, S., Franzmann, T. M., Pozniakovski, A., Poser, I., Maghelli, N., Royer, L. A., Weigert, M., Myers, E. W., Grill, S., Drechsel, D., Hyman, A. A., & Alberti, S. (2015). A Liquid-to-Solid Phase Transition of the ALS Protein FUS Accelerated by Disease Mutation. *Cell*, 162(5), 1066–1077. <https://doi.org/10.1016/j.cell.2015.07.047>
- Pedraza, N., Ortiz, R., Cornado, A., Llobet, A., Aldea, M., & Gallego, C. (2014). KIS, a Kinase Associated with Microtubule Regulators, Enhances Translation of AMPA Receptors and Stimulates Dendritic Spine Remodeling. *Journal of Neuroscience*, 34(42), 13988–13997. <https://doi.org/10.1523/JNEUROSCI.1573-14.2014>
- Penzes, P., Cahill, M. E., Jones, K. A., Vanleeuwen, J. E., & Woolfrey, K. M. (2011). Dendritic spine pathology in neuropsychiatric disorders. *Nature Neuroscience*, 14(3), 285–293. <https://doi.org/10.1038/nn.2741>
- Perez, W. B., & Kinzy, T. G. (2014). Translation elongation factor 1A mutants with altered actin bundling activity show reduced aminoacyl-tRNA binding and alter initiation via eIF2 $\alpha$  phosphorylation. *Journal of Biological Chemistry*, 289(30), 20928–20938. <https://doi.org/10.1074/jbc.M114.570077>

- Perycz, M., Urbanska, A. S., Krawczyk, P. S., Parobczak, K., & Jaworski, J. (2011). Zipcode binding protein 1 regulates the development of dendritic arbors in hippocampal neurons. *Journal of Neuroscience*, *31*(14), 5271–5285. <https://doi.org/10.1523/JNEUROSCI.2387-10.2011>
- Pinho, J., Marcut, C., & Fonseca, R. (2020). Actin remodeling, the synaptic tag and the maintenance of synaptic plasticity. *IUBMB Life*, *72*(4), 577–589. <https://doi.org/10.1002/iub.2261>
- Pittman, Y. R., Valente, L., Jeppesen, M. G., Andersen, G. R., Patel, S., & Kinzy, T. G. (2006). Mg<sup>2+</sup> and a key lysine modulate exchange activity of eukaryotic translation elongation factor 1B $\alpha$ . *Journal of Biological Chemistry*, *281*(28), 19457–19468. <https://doi.org/10.1074/jbc.M601076200>
- Portz, B., Lee, B. L., & Shorter, J. (2021). FUS and TDP-43 Phases in Health and Disease. *Trends in Biochemical Sciences*, *46*(7), 550–563. <https://doi.org/10.1016/j.tibs.2020.12.005>
- Prasad, A., Bharathi, V., Sivalingam, V., Girdhar, A., & Patel, B. K. (2019). Molecular mechanisms of TDP-43 misfolding and pathology in amyotrophic lateral sclerosis. *Frontiers in Molecular Neuroscience*, *12*(February), 1–36. <https://doi.org/10.3389/fnmol.2019.00025>
- Prashad, S., & Gopal, P. P. (2021). RNA-binding proteins in neurological development and disease. *RNA Biology*, *18*(7), 972–987. <https://doi.org/10.1080/15476286.2020.1809186>
- Protter, D. S. W., Rao, B. S., Van Treeck, B., Lin, Y., Mizoue, L., Rosen, M. K., & Parker, R. (2018). Intrinsically Disordered Regions Can Contribute Promiscuous Interactions to RNP Granule Assembly. *Cell Reports*, *22*(6), 1401–1412. <https://doi.org/10.1016/j.celrep.2018.01.036>
- Pushpalatha, K. V., Solyga, M., Nakamura, A., & Besse, F. (2022). RNP components condense into repressive RNP granules in the aging brain. *Nature Communications*, *13*(1), 1–15. <https://doi.org/10.1038/s41467-022-30066-4>
- Putnam, A., Thomas, L., & Seydoux, G. (2023). RNA granules: functional compartments or incidental condensates? *Genes & Development*, *37*(9–10), 354–376. <https://doi.org/10.1101/gad.350518.123>
- Qamar, S., Wang, G. Z., Randle, S. J., Ruggeri, F. S., Varela, J. A., Lin, J. Q., Phillips, E. C., Miyashita, A., Williams, D., Ströhl, F., Meadows, W., Ferry, R., Dardov, V. J., Tartaglia, G. G., Farrer, L. A., Kaminski Schierle, G. S., Kaminski, C. F., Holt, C. E., Fraser, P. E., ... St George-Hyslop, P. (2018). FUS Phase Separation Is Modulated by a Molecular Chaperone and Methylation of Arginine Cation- $\pi$  Interactions. *Cell*, *173*(3), 720–734.e15. <https://doi.org/10.1016/j.cell.2018.03.056>
- Qin, W., Cheah, J. S., Xu, C., Messing, J., Freibaum, B. D., Boeynaems, S., Taylor, J. P., Udeshi, N. D., Carr, S. A., & Ting, A. Y. (2023). Dynamic mapping of proteome trafficking within

## REFERENCES

- and between living cells by TransitID. *Cell*, 186(15), 3307–3324.e30. <https://doi.org/10.1016/j.cell.2023.05.044>
- Richter, J. D., Bassell, G. J., & Klann, E. (2015). Dysregulation and restoration of translational homeostasis in fragile X syndrome. *Nature Reviews Neuroscience*, 16(10), 595–605. <https://doi.org/10.1038/nrn4001>
- Richter, J. D., & Collier, J. (2015). Pausing on Polyribosomes: Make Way for Elongation in Translational Control. *Cell*, 163(2), 292–300. <https://doi.org/10.1016/j.cell.2015.09.041>
- Romaus-Sanjurjo, D., Saikia, J. M., Kim, H. J., Tsai, K. M., Le, G. Q., & Zheng, B. (2022). Overexpressing eukaryotic elongation factor 1 alpha (eEF1A) proteins to promote corticospinal axon repair after injury. *Cell Death Discovery*, 8(1), 1–13. <https://doi.org/10.1038/s41420-022-01186-z>
- Rongo, C., Gavis, E. R., & Lehmann, R. (1995). Localization of oskar RNA regulates oskar translation and requires Oskar protein. *Development*, 121(9), 2737–2746. <https://doi.org/10.1242/dev.121.9.2737>
- Rook, M. S., Lu, M., & Kosik, K. S. (2000). CaMKIIa 3' Untranslated Region-Directed mRNA Translocation in Living Neurons: Visualization by GFP Linkage. *The Journal of Neuroscience*, 20(17), 6385–6393. <https://doi.org/10.1523/JNEUROSCI.20-17-06385.2000>
- Ruest, L. B., Marcotte, R., & Wang, E. (2002). Peptide elongation factor eEF1A-2/S1 expression in cultured differentiated myotubes and its protective effect against caspase-3-mediated apoptosis. *Journal of Biological Chemistry*, 277(7), 5418–5425. <https://doi.org/10.1074/jbc.M110685200>
- Santoro, M. R., Bray, S. M., & Warren, S. T. (2012). Molecular mechanisms of fragile X syndrome: A twenty-year perspective. *Annual Review of Pathology: Mechanisms of Disease*, 7, 219–245. <https://doi.org/10.1146/annurev-pathol-011811-132457>
- Sasikumar, A. N., Perez, W. B., & Kinzy, T. G. (2012). The many roles of the eukaryotic elongation factor 1 complex. *Wiley Interdisciplinary Reviews: RNA*, 3(4), 543–555. <https://doi.org/10.1002/wrna.1118>
- Scaggiante, B., Dapas, B., Bonin, S., Grassi, M., Zennaro, C., Farra, R., Cristiano, L., Siracusano, S., Zanconati, F., Giansante, C., & Grassi, G. (2012). Dissecting the expression of EEF1A1/2 genes in human prostate cancer cells: The potential of EEF1A2 as a hallmark for prostate transformation and progression. *British Journal of Cancer*, 106(1), 166–173. <https://doi.org/10.1038/bjc.2011.500>
- Schätzle, P., Esteves da Silva, M., Tas, R. P., Katrukha, E. A., Hu, H. Y., Wierenga, C. J., Kapitein, L. C., & Hoogenraad, C. C. (2018). Activity-Dependent Actin Remodeling at the Base of Dendritic Spines Promotes Microtubule Entry. *Current Biology*, 28(13), 2081–2093.e6. <https://doi.org/10.1016/j.cub.2018.05.004>



- Scheetz, A. J., Nairn, A. C., & Constantine-Paton, M. (2000). NMDA receptor-mediated control of protein synthesis at developing synapses. *Nature Neuroscience*, 3(3), 211–216. <https://doi.org/10.1038/72915>
- Sekino, Y., Tanaka, S., Hanamura, K., Yamazaki, H., Sasagawa, Y., Xue, Y., Hayashi, K., & Shirao, T. (2006). Activation of N-methyl-d-aspartate receptor induces a shift of drebrin distribution: Disappearance from dendritic spines and appearance in dendritic shafts. *Molecular and Cellular Neuroscience*, 31(3), 493–504. <https://doi.org/10.1016/j.mcn.2005.11.003>
- Sephton, C. F., Cenik, C., Kucukural, A., Dammer, E. B., Cenik, B., Han, Y. H., Dewey, C. M., Roth, F. P., Herz, J., Peng, J., Moore, M. J., & Yu, G. (2011). Identification of neuronal RNA targets of TDP-43-containing ribonucleoprotein complexes. *Journal of Biological Chemistry*, 286(2), 1204–1215. <https://doi.org/10.1074/jbc.M110.190884>
- Shaw, J. E., Kilander, M. B. C., Lin, Y. C., & Koleske, A. J. (2021). Abl2: Cortactin interactions regulate dendritic spine stability via control of a stable filamentous actin pool. *Journal of Neuroscience*, 41(14), 3068–3081. <https://doi.org/10.1523/JNEUROSCI.2472-20.2021>
- Shirao, T., Hanamura, K., Koganezawa, N., Ishizuka, Y., Yamazaki, H., & Sekino, Y. (2017). The role of drebrin in neurons. *Journal of Neurochemistry*, 141(6), 819–834. <https://doi.org/10.1111/jnc.13988>
- Shumyatsky, G. P., Malleret, G., Shin, R. M., Takizawa, S., Tully, K., Tsvetkov, E., Zakharenko, S. S., Joseph, J., Vronskaya, S., Yin, D. Q., Schubart, U. K., Kandel, E. R., & Bolshakov, V. Y. (2005). Stathmin, a Gene Enriched in the Amygdala, Controls Both Learned and Innate Fear. *Cell*, 123(4), 697–709. <https://doi.org/10.1016/j.cell.2005.08.038>
- Silva, R. C., Sattlegger, E., & Castilho, B. A. (2016). Perturbations in actin dynamics reconfigure protein complexes that modulate GCN2 activity and promote an eIF2 response. *Journal of Cell Science*, 129(24), 4521–4533. <https://doi.org/10.1242/jcs.194738>
- Soares, D. C., Barlow, P. N., Newbery, H. J., Porteous, D. J., & Abbott, C. M. (2009). Structural models of human eEF1A1 and eEF1A2 reveal two distinct surface clusters of sequence variation and potential differences in phosphorylation. *PLoS ONE*, 4(7). <https://doi.org/10.1371/journal.pone.0006315>
- Soderling, T. R., & Derkach, V. A. (2000). Postsynaptic protein phosphorylation and LTP. *Trends in Neurosciences*, 23(2), 75–80. [https://doi.org/10.1016/S0166-2236\(99\)01490-3](https://doi.org/10.1016/S0166-2236(99)01490-3)
- Sonenberg, N., & Hinnebusch, A. G. (2009). Regulation of Translation Initiation in Eukaryotes: Mechanisms and Biological Targets. *Cell*, 136(4), 731–745. <https://doi.org/10.1016/j.cell.2009.01.042>

## REFERENCES

- Sossin, W. S., & Costa-Mattioli, M. (2019). Translational control in the brain in health and disease. *Cold Spring Harbor Perspectives in Biology*, *11*(8), 1–18. <https://doi.org/10.1101/cshperspect.a032912>
- Spence, E. F., Kanak, D. J., Carlson, B. R., & Soderling, S. H. (2016). The Arp2/3 complex is essential for distinct stages of spine synapse maturation, including synapse unsilencing. *Journal of Neuroscience*, *36*(37), 9696–9709. <https://doi.org/10.1523/JNEUROSCI.0876-16.2016>
- St Johnston, D., Beuchle, D., & Nüsslein-Volhard, C. (1991). Staufen, a gene required to localize maternal RNAs in the Drosophila egg. *Cell*, *66*(1), 51–63. [https://doi.org/10.1016/0092-8674\(91\)90138-O](https://doi.org/10.1016/0092-8674(91)90138-O)
- Star, E. N., Kwiatkowski, D. J., & Murthy, V. N. (2002). Rapid turnover of actin in dendritic spines and its regulation by activity. *Nature Neuroscience*, *5*(3), 239–246. <https://doi.org/10.1038/nn811>
- Steward, O., & Levy, W. B. (1982). Preferential localization of polyribosomes under the base of dendritic spines in granule cells of the dentate gyrus. *Journal of Neuroscience*, *2*(3), 284–291. <https://doi.org/10.1523/jneurosci.02-03-00284.1982>
- Stillman, M., Lautz, J. D., Johnson, R. S., MacCoss, M. J., & Smith, S. E. P. (2022). Activity dependent dissociation of the Homer1 interactome. *Scientific Reports*, *12*(1), 1–10. <https://doi.org/10.1038/s41598-022-07179-3>
- Sun, C., Nold, A., Fusco, C. M., Rangaraju, V., Tchumatchenko, T., Heilemann, M., & Schuman, E. M. (2021). The prevalence and specificity of local protein synthesis during neuronal synaptic plasticity. *Science Advances*, *7*(38), 1–14. <https://doi.org/10.1126/sciadv.abj0790>
- Sutton, M. A., Taylor, A. M., Ito, H. T., Pham, A., & Schuman, E. M. (2007). Postsynaptic Decoding of Neural Activity: eEF2 as a Biochemical Sensor Coupling Miniature Synaptic Transmission to Local Protein Synthesis. *Neuron*, *55*(4), 648–661. <https://doi.org/10.1016/j.neuron.2007.07.030>
- Takahashi, H., Mizui, T., & Shirao, T. (2006). Down-regulation of drebrin A expression suppresses synaptic targeting of NMDA receptors in developing hippocampal neurones. *Journal of Neurochemistry*, *97 Suppl 1*, 110–115. <https://doi.org/10.1111/j.1471-4159.2005.03536.x>
- Takahashi, H., Sekino, Y., Tanaka, S., Mizui, T., Kishi, S., & Shirao, T. (2003). Drebrin-dependent actin clustering in dendritic filopodia governs synaptic targeting of postsynaptic density-95 and dendritic spine morphogenesis. *Journal of Neuroscience*, *23*(16), 6586–6595. <https://doi.org/10.1523/jneurosci.23-16-06586.2003>
- Takao, K., Okamoto, K. I., Nakagawa, T., Neve, R. L., Nagai, T., Miyawaki, A., Hashikawa, T., Kobayashi, S., & Hayashi, Y. (2005). Visualization of synaptic Ca<sup>2+</sup>/calmodulin-dependent protein kinase II activity in living neurons. *Journal of Neuroscience*, *25*(12), 3107–3112. <https://doi.org/10.1523/JNEUROSCI.0085-05.2005>

- Talapatra, S., Wagner, J. D. O., & Thompson, C. B. (2002). Elongation factor-1 alpha is a selective regulator of growth factor withdrawal and ER stress-induced apoptosis. *Cell Death and Differentiation*, *9*(8), 856–861. <https://doi.org/10.1038/sj.cdd.4401078>
- Tanabe, K., Yamazaki, H., Inaguma, Y., Asada, A., Kimura, T., Takahashi, J., Taoka, M., Ohshima, T., Furuichi, T., Isobe, T., Nagata, K. I., Shirao, T., & Hisanaga, S. I. (2014). Phosphorylation of Drebrin by Cyclin-dependent Kinase 5 and Its role in neuronal migration. *PLoS ONE*, *9*(3). <https://doi.org/10.1371/journal.pone.0092291>
- Tao-Cheng, J. H., Thein, S., Yang, Y., Reese, T. S., & Gallant, P. E. (2014). Homer is concentrated at the postsynaptic density and does not redistribute after acute synaptic stimulation. *Neuroscience*, *266*(301), 80–90. <https://doi.org/10.1016/j.neuroscience.2014.01.066>
- Thomas, M. G., Loschi, M., Desbats, M. A., & Boccaccio, G. L. (2011). RNA granules: The good, the bad and the ugly. *Cellular Signalling*, *23*(2), 324–334. <https://doi.org/10.1016/j.cellsig.2010.08.011>
- Tiruchinapalli, D. M., Oleynikov, Y., Kelič, S., Shenoy, S. M., Hartley, A., Stanton, P. K., Singer, R. H., & Bassell, G. J. (2003). Activity-dependent trafficking and dynamic localization of zipcode binding protein 1 and  $\beta$ -actin mRNA in dendrites and spines of hippocampal neurons. *Journal of Neuroscience*, *23*(8), 3251–3261. <https://doi.org/10.1523/jneurosci.23-08-03251.2003>
- Tomlinson, V. A. L., Newbery, H. J., Wray, N. R., Jackson, J., Larionov, A., Miller, W. R., Dixon, J. M., & Abbott, C. M. (2005). Translation elongation factor eEF1A2 is a potential oncoprotein that is overexpressed in two-thirds of breast tumours. *BMC Cancer*, *5*, 1–7. <https://doi.org/10.1186/1471-2407-5-113>
- Tsang, B., Arsenault, J., Vernon, R. M., Lin, H., Sonenberg, N., Wang, L., & Bah, A. (2018). *Phosphoregulated FMRP phase separation models activity-dependent translation through bidirectional control of mRNA granule formation*. <https://doi.org/10.1073/pnas.1814385116>
- Turner-Bridger, B., Caterino, C., & Cioni, J. M. (2020). Molecular mechanisms behind mRNA localization in axons: Axonal mRNA Localisation. *Open Biology*, *10*(9). <https://doi.org/10.1098/rsob.200177>
- Turner-Bridger, B., Jakobs, M., Muresan, L., Wong, H. H. W., Franze, K., Harris, W. A., & Holt, C. E. (2018). Single-molecule analysis of endogenous  $\beta$ -actin mRNA trafficking reveals a mechanism for compartmentalized mRNA localization in axons. *Proceedings of the National Academy of Sciences of the United States of America*, *115*(41), E9697–E9706. <https://doi.org/10.1073/pnas.1806189115>
- Usaj, M., Tan, Y., Wang, W., VanderSluis, B., Zou, A., Myers, C. L., Costanzo, M., Andrews, B., & Boone, C. (2017). TheCellMap.org: A web-accessible database for visualizing and mining the global yeast genetic interaction network. *G3: Genes, Genomes, Genetics*, *7*(5), 1539–1549. <https://doi.org/10.1534/g3.117.040220>

## REFERENCES

- Van Treeck, B., Protter, D. S. W., Matheny, T., Khong, A., Link, C. D., & Parker, R. (2018). RNA self-assembly contributes to stress granule formation and defining the stress granule transcriptome. *Proceedings of the National Academy of Sciences of the United States of America*, *115*(11), 2734–2739. <https://doi.org/10.1073/pnas.1800038115>
- Varadi, M., Anyango, S., Deshpande, M., Nair, S., Natassia, C., Yordanova, G., Yuan, D., Stroe, O., Wood, G., Laydon, A., Zidek, A., Green, T., Tunyasuvunakool, K., Petersen, S., Jumper, J., Clancy, E., Green, R., Vora, A., Lutfi, M., ... Velankar, S. (2022). AlphaFold Protein Structure Database: Massively expanding the structural coverage of protein-sequence space with high-accuracy models. *Nucleic Acids Research*, *50*(D1), D439–D444. <https://doi.org/10.1093/nar/gkab1061>
- Vessey, J. P., Amadei, G., Burns, S. E., Kiebler, M. A., Kaplan, D. R., & Miller, F. D. (2012). An asymmetrically localized Staufen2-dependent RNA complex regulates maintenance of mammalian neural stem cells. *Cell Stem Cell*, *11*(4), 517–528. <https://doi.org/10.1016/j.stem.2012.06.010>
- Vickers, C. A., Dickson, K. S., & Wyllie, D. J. A. (2005). Induction and maintenance of late-phase long-term potentiation in isolated dendrites of rat hippocampal CA1 pyramidal neurones. *Journal of Physiology*, *568*(3), 803–813. <https://doi.org/10.1113/jphysiol.2005.092924>
- Waung, M. W., & Huber, K. M. (2009). Protein translation in synaptic plasticity: mGluR-LTD, Fragile X. *Current Opinion in Neurobiology*, *19*(3), 319–326. <https://doi.org/10.1016/j.conb.2009.03.011>
- Wefers, Z., Alecki, C., Huang, R., Jacob-Tomas, S., & Vera, M. (2022). Analysis of the Expression and Subcellular Distribution of eEF1A1 and eEF1A2 mRNAs during Neurodevelopment. *Cells*, *11*(12), 1–20. <https://doi.org/10.3390/cells11121877>
- Wells, D. G., Dong, X., Quinlan, E. M., Huang, Y. S., Bear, M. F., Richter, J. D., & Fallon, J. R. (2001). A role for the cytoplasmic polyadenylation element in NMDA receptor-regulated mRNA translation in neurons. *Journal of Neuroscience*, *21*(24), 9541–9548. <https://doi.org/10.1523/jneurosci.21-24-09541.2001>
- White, K. M., Rosales, R., Yildiz, S., Kehrer, T., Miorin, L., Moreno, E., Jangra, S., Uccellini, M. B., Rathnasinghe, R., Coughlan, L., Martinez-Romero, C., Batra, J., Rojc, A., Bouhaddou, M., Fabius, J. M., Obernier, K., Dejoze, M., Guillén, M. J., Losada, A., ... García-Sastre, A. (2021). Plitidepsin has potent preclinical efficacy against SARS-CoV-2 by targeting the host protein eEF1A. *Science*, *371*(6532), 926–931. <https://doi.org/10.1126/science.abf4058>
- Wong, H. H. W., Lin, J. Q., Ströhl, F., Roque, C. G., Cioni, J. M., Cagnetta, R., Turner-Bridger, B., Laine, R. F., Harris, W. A., Kaminski, C. F., & Holt, C. E. (2017). RNA Docking and Local Translation Regulate Site-Specific Axon Remodeling In Vivo. *Neuron*, *95*(4), 852–868.e8. <https://doi.org/10.1016/j.neuron.2017.07.016>

- Worth, D. C., Daly, C. N., Geraldo, S., Oozeer, F., & Gordon-Weeks, P. R. (2013). Drebrin contains a cryptic F-actin-bundling activity regulated by Cdk5 phosphorylation. *Journal of Cell Biology*, *202*(5), 793–806. <https://doi.org/10.1083/jcb.201303005>
- Wu, H., Zhou, J., Zhu, T., Cohen, I., & DICTENBERG, J. (2020). A kinesin adapter directly mediates dendritic mRNA localization during neural development in mice. *Journal of Biological Chemistry*, *295*(19), 6605–6628. <https://doi.org/10.1074/jbc.RA118.005616>
- Wu, L., Wells, D., Tay, J., Mendis, D., Abbott, M. A., Barnitt, A., Quinlan, E., Heynen, A., Fallon, J. R., & Richter, J. D. (1998). CPEB-mediated cytoplasmic polyadenylation and the regulation of experience-dependent translation of  $\alpha$ -CaMKII mRNA at synapses. *Neuron*, *21*(5), 1129–1139. [https://doi.org/10.1016/S0896-6273\(00\)80630-3](https://doi.org/10.1016/S0896-6273(00)80630-3)
- Wyszynski, M., Lin, J., Rao, A., Nigh, E., Beggs, A. H., Craig, A. M., & Sheng, M. (1997). Competitive binding of  $\alpha$ -actinin and calmodulin to the NMDA receptor. *Nature*, *385*, 439–442. <https://doi.org/10.1038/385439a0>
- Yamazaki, H., Koganezawa, N., Yokoo, H., Sekino, Y., & Shirao, T. (2023). Super-resolution imaging reveals the relationship between CaMKII $\beta$  and drebrin within dendritic spines. *Neuroscience Research*, *August*, 1–6. <https://doi.org/10.1016/j.neures.2023.08.002>
- Yang, F., Demma, M., Warren, V., Dharmawardhane, S., & Condeelis, J. (1990). Identification of an actin-binding protein from Dictyostelium as elongation factor 1a. *Nature*, *347*, 494–496. <https://doi.org/10.1038/347494a0>
- Yang, L., Mao, L., Chen, H., Catavsan, M., Kozinn, J., Arora, A., Liu, X., & Wang, J. Q. (2006). A signaling mechanism from G $\alpha_q$ -protein-coupled metabotropic glutamate receptors to gene expression: Role of the c-Jun N-Terminal kinase pathway. *Journal of Neuroscience*, *26*(3), 971–980. <https://doi.org/10.1523/JNEUROSCI.4423-05.2006>
- Yang, Y. M., Lee, J., Jo, H., Park, S., Chang, I., Muallem, S., & Shin, D. M. (2014). Homer2 protein regulates plasma membrane Ca<sup>2+</sup>-ATPase-mediated Ca<sup>2+</sup> signaling in mouse parotid gland acinar cells. *Journal of Biological Chemistry*, *289*(36), 24971–24979. <https://doi.org/10.1074/jbc.M114.577221>
- Yasuda, H., Kojima, N., Hanamura, K., Yamazaki, H., Sakimura, K., & Shirao, T. (2018). Drebrin isoforms critically regulate NMDAR- and mGluR-dependent LTD induction. *Frontiers in Cellular Neuroscience*, *12*(October), 1–10. <https://doi.org/10.3389/fncel.2018.00330>
- Yokoi, S., Udagawa, T., Fujioka, Y., Honda, D., Okado, H., Watanabe, H., Katsuno, M., Ishigaki, S., & Sobue, G. (2017). 3'UTR Length-Dependent Control of SynGAP Isoform  $\alpha 2$  mRNA by FUS and ELAV-like Proteins Promotes Dendritic Spine Maturation and Cognitive Function. *Cell Reports*, *20*(13), 3071–3084. <https://doi.org/10.1016/j.celrep.2017.08.100>
- Yoon, Y. J., Wu, B., Buxbaum, A. R., Das, S., Tsai, A., English, B. P., Grimm, J. B., Lavis, L. D., & Singer, R. H. (2016). Glutamate-induced RNA localization and translation in neurons.

## REFERENCES

- Proceedings of the National Academy of Sciences of the United States of America*, 113(44), E6877–E6886. <https://doi.org/10.1073/pnas.1614267113>
- Yuste, R. (2015). The discovery of dendritic spines by Cajal. *Frontiers in Neuroanatomy*, 9(APR), 1–6. <https://doi.org/10.3389/fnana.2015.00018>
- Zuo, Y., Lin, A., Chang, P., & Gan, W. B. (2005). Development of long-term dendritic spine stability in diverse regions of cerebral cortex. *Neuron*, 46(2), 181–189. <https://doi.org/10.1016/j.neuron.2005.04.001>



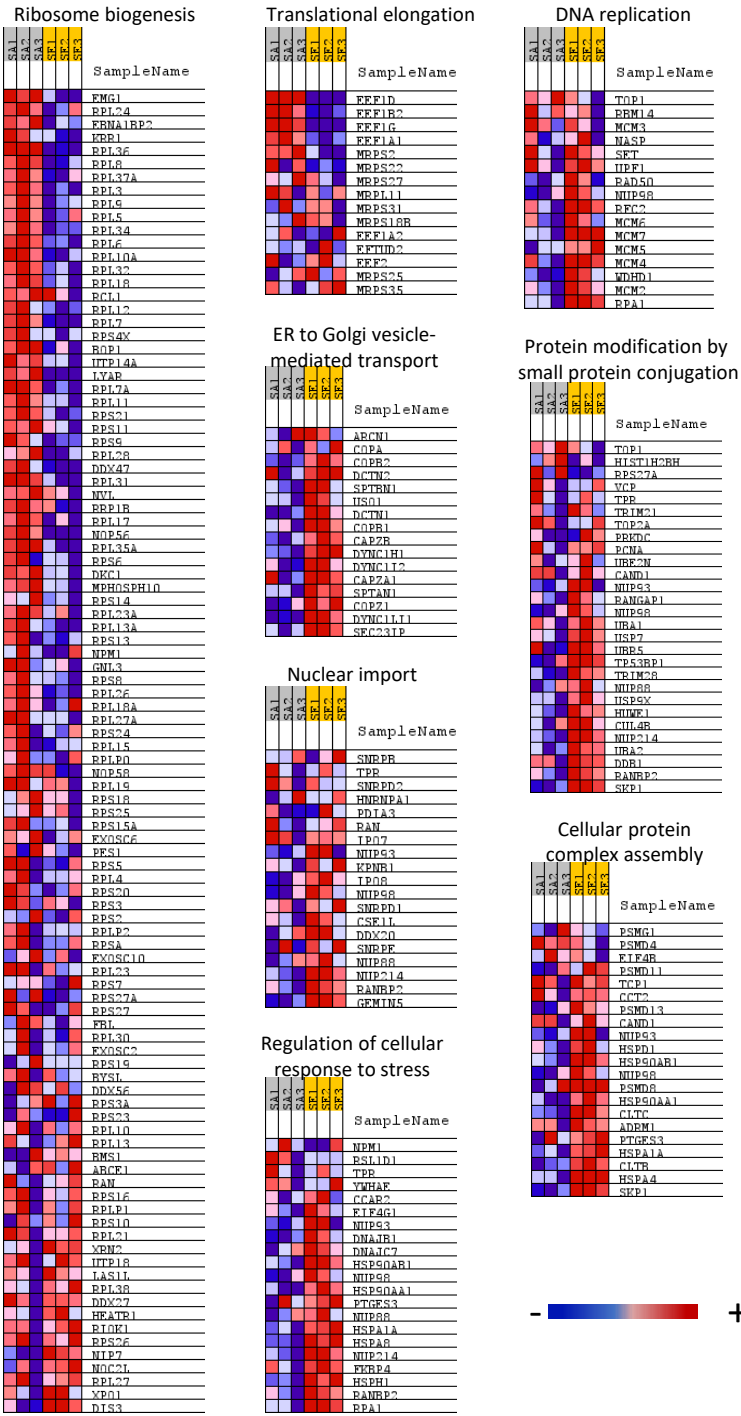




**ANNEX**



**Supplementary Figure 1. Interactomic analysis of eEF1A2 phospho-mutants dissects translational and non-canonical functions.** Triplicate immunoprecipitates from HEK293T cells expressing FLAG-tagged SA and SE eEF1A2 proteins were analyzed by LC-MS/MS. Colors in the heatmap denote high (red) to low (blue) normalized enrichment scores of individual proteins in the corresponding GO terms.



**Supplementary Table 1. FLAG-APEX-ZBP1 significantly enriched interacting proteins.** FLAG-APEX-ZBP1 interacting proteins with log<sub>2</sub> fold change values > 1.5 and p-value < 0.05 are shown.

Gene name	Uniprot ID	log <sub>2</sub> FC	p-value
Igf2bp1	Q88477	19.6065826	3.0626E-06
Tsc22d1	P62500	16.5822782	0.001799
Edc4	Q3UJB9	16.4387217	0.0040983
Clns1a	Q61189	16.3437557	0.00051536
Pdia6	Q922R8	16.2636856	0.01365758
Skic8	Q9ERF3	16.110227	0.00025735
Ubc	P0CG50	15.9232375	6.9973E-06
Rps6	P62754	15.8499128	9.0245E-05
Arf1	P84078	15.692765	3.2257E-05
Rpl6	P47911	15.530094	5.7734E-05
Pym1	Q8CHP5	15.2135119	0.00012622
Lsm14b	Q8CGC4	15.0571411	1.5143E-05
Gprasp1	Q5U4C1	14.9891396	0.00145592
Gna13	P27601	14.7375262	4.8403E-05
Cpeb3	Q7TN99	14.4234446	1.2565E-05
Habp4	Q9JKS5	14.3987514	0.00105969
Cirbp	P60824	14.3312588	0.00013284
Tnrc6b	Q8BK12	14.2964381	0.00012836
Hdgfl3	Q9JMG7	14.2654849	8.6404E-05
Rpl30	P62889	14.1949067	1.4176E-05
Hspbp1	Q99P31	14.1711456	0.00018031
Rln3	Q8CHK2	14.1114081	0.00018119
Ago2	Q8CJG0	14.1029956	0.00011959
Farsb	Q9WUA2	14.0440856	2.6275E-05
Ddx6	P54823	14.0384435	2.4316E-05
Iars1	Q8BU30	13.9914195	0.00012275
Lsm14a	Q8K2F8	13.9781675	0.0005675
Krt17	Q9QWL7	13.9566517	0.02564731
Atp6v1g1	Q9CR51	13.9383497	0.02884976
Larp4	Q8BWW4	13.923599	1.3275E-05
Fmr1	P35922	13.9136808	4.305E-05
Rps18	P62270	13.7634739	8.4265E-05
Eif3i	Q9QZD9	13.7302839	3.2365E-05
Aimp2	Q8R010	13.7054801	1.7576E-05
Rpl11	Q9CXW4	13.6908787	6.6281E-05
Qars1	Q8BML9	13.6653032	0.00049107
Prcc2a	Q7TSC1	13.6205346	0.00029907
Rps25	P62852	13.5575036	1.6831E-05
Ckmt1	P30275	13.5104401	0.03563842
Eif4e	P63073	13.406322	0.00020672
Brcc3	P46737	13.3950636	0.00037527
Sec16a	E9QAT4	13.3363754	0.00167366
Spats2	Q8K1N4	13.3264939	0.00063531
Tmx1	Q8VBT0	13.2792242	0.00019579
Slc17a8	Q8BFU8	13.2440208	0.04928857
Mcrip1	Q3UGS4	13.2006093	0.0007561
Otud4	B2RRE7	13.1838096	0.00020734
Ranbp2	Q9ERU9	13.1534302	0.0020674

Gene name	Uniprot ID	log <sub>2</sub> FC	p-value
Hdac11	Q91WA3	13.147718	0.00584106
Cpeb4	Q7TN98	13.1297179	1.3718E-05
Eri3	Q8C460	13.0964751	0.00101857
Keap1	Q9Z2X8	13.0380474	0.00035629
Gigyf2	Q6Y7W8	12.9983049	4.0938E-05
Nop14	Q8R3N1	12.9927754	9.9598E-05
Usp47	Q8BY87	12.9845227	0.00086378
Eif3b	Q8JZQ9	12.9839968	0.00973318
Ankrd17	Q99NH0	12.9448708	0.00134927
Cnot2	Q8C5L3	12.920895	6.5711E-05
Jazf1	Q80ZQ5	12.9072116	0.00749155
Rbmx11	Q91VM5	12.9002339	0.0008218
Mia3	Q8BI84	12.864351	0.02900959
Khdrbs1	Q60749	12.8446333	0.00056819
H2ac4	COHKE1	12.8295724	9.6388E-05
Slc25a31	Q3V132	12.820478	0.00010702
Tfcp2	Q9ERA0	12.7400222	0.00024816
Prcc2b	Q7TPM1	12.7378826	0.00408401
Rps11	P62281	12.6990302	0.00702722
Ola1	Q9CZ30	12.6789315	0.00597276
Sdcbp	O08992	12.6540776	0.00067872
Hnrnpa1	P49312	12.6439769	1.7027E-05
Rangap1	P46061	12.6437823	6.7476E-05
Rab18	P35293	12.5362163	0.00050842
Edc3	Q8K2D3	12.5084767	0.00680707
Eif3d	O70194	12.4660812	0.02343131
Fxr2	Q9WVR4	12.4345431	0.00010027
Bri3bp	Q8BXV2	12.4060812	0.00034195
Rpl18a	P62717	12.4023366	0.01955445
Plaa	P27612	12.3755885	0.00014701
Washc1	Q8VDD8	12.375543	0.00010497
Nacad	Q5SWP3	12.3531516	0.00294395
Cpeb2	Q812E0	12.347522	0.00240224
Txlna	Q6PAM1	12.2720454	0.00023534
Akap8l	Q9R0L7	12.2366055	1.8074E-05
Prkra Rax	Q9WTX2	12.219672	0.00011186
Spats2l	Q91WJ7	12.20358	0.00368746
Pcbp3	P57722	12.1740467	6.1575E-05
Rpl3	P27659	12.1641486	0.0001245
Trim28	Q62318	12.1276326	0.00092592
Pa2g4	P50580	12.0924734	0.02305199
Tsn	Q62348	12.0807407	0.00475877
Pip4p1	Q3TWL2	11.964392	0.00702941
Cars1	Q9ER72	11.8982145	0.01849655
Ints3	Q7TPD0	11.8738914	0.0012183
Tnpo1	Q8BFY9	11.8462	0.01055087
Tmem38a	Q3TMP8	11.8075188	0.00044567
Srpk1	O70551	11.7986183	0.00057261
Ddx5	Q61656	11.788414	0.0085479
Pgap1	Q3UUQ7	11.7848138	0.00589591

## ANNEX

Gene name	Uniprot ID	log <sub>2</sub> FC	p-value
Ipo7	Q9EPL8	11.7261918	0.01213646
Ilf3	Q9Z1X4	11.7209006	0.03674358
Eif4enif1	Q9EST3	11.7056903	0.00019814
Tkt	P40142	11.6995564	0.00040101
Cdkl5	Q3UTQ8	11.6861734	0.00087509
Nono	Q99K48	11.6614056	0.00017006
Dgke	Q9R1C6	11.6445184	0.00015958
Lrrc59	Q922Q8	11.6317338	0.02027861
Dync1i2	O88487	11.6214553	0.00017772
Exoc4	O35382	11.5991336	0.00421081
Clic4	Q9QYB1	11.5621279	0.00447269
Gripap1	Q8VD04	11.5546435	2.4077E-05
Anapc2	Q8BZQ7	11.552338	0.0008044
Pfdn1	Q9CWM4	11.5298862	0.01133165
Tars1	Q9D0R2	11.4989793	0.00013228
Psmb7	P70195	11.457599	0.00062837
Rbfox2	Q8BP71	11.4410237	0.00087677
Rbm4b	Q8VE92	11.4303435	0.01269933
prl	A0A1W2	11.3917049	0.00441511
Gpx4	O70325	11.3830527	0.00039362
Larp1	Q6ZQ58	11.3818828	3.7757E-05
Cluh	Q5SW19	11.3506836	0.00898416
Dync1i1	O88485	11.340382	0.00826616
Acbd3	Q8BMP6	11.3234216	0.00181343
Eif3f	Q9DCH4	11.282041	0.00051877
Madd 8	Q80U28	11.2631356	0.00870696
Dhx57	Q6P5D3	11.258283	2.511E-05
Rpl4	Q9D8E6	11.2323858	0.00333362
Farsa	Q8C0C7	11.2213207	0.00087184
Naa10	Q9QY36	11.2025292	0.02555258
Nrxn1	Q9CS84	11.1911363	0.00016038
Hck	P08103	11.1674363	0.02134966
Tnks1bp1	P58871	11.1444517	2.6864E-05
Trim32	Q8CH72	11.1007259	0.00017411
Osbpl8	B9EJ86	11.0801736	0.00123535
Ddx1	Q91VR5	11.030337	0.00325565
Mbnl2	Q8C181	10.9750901	0.00048804
Rtcb	Q99LF4	10.9632714	0.00015195
Safb	D3YXK2	10.9498666	0.00738786
Tp53bp1	P70399	10.937247	0.01194915
Begain	Q68EF6	10.9307102	0.00016258
Dhx9	O70133	10.9204623	0.00329071
Stard7	Q8R1R3	10.9122264	0.03151175
Maged1	Q9QYH6	10.8828372	0.00102277
Dvl3	Q61062	10.8475225	0.01896862
Arpp21	Q9DCB4	10.7985444	8.5181E-05
Ccsap	Q8QZT2	10.7486734	0.00284279
Bag6	Q9Z1R2	10.7067664	0.00377534
Magee1	Q6PCZ4	10.6690556	0.00028039
Hnrnpul2	Q00PI9	10.667731	0.01058207

Gene name	Uniprot ID	log <sub>2</sub> FC	p-value
Cmpk1	Q9DBP5	10.6401011	0.020578
Dcp2	Q9CYC6	10.6195541	0.00054152
Tnik	P83510	10.5348283	0.00016941
Shank1	D3YZU1	10.5225346	0.00059359
Cmas	Q99KK2	10.5171791	0.00026353
Ddx3y	Q62095	10.4168824	0.0148648
Clint1	Q99KN9	10.4138098	0.01864375
Slc4a8	Q8JZR6	10.3752788	0.04614603
Acbd6	Q9D061	10.3547414	0.00197378
Dzip3	Q7TPV2	10.3441212	0.01083241
Dock3	Q8CIQ7	10.3266202	0.03630225
Srp68	Q8BMA6	10.2962674	0.01940792
Dhx30	Q99PU8	10.2881746	3.5765E-05
Seh1l	Q8R2U0	10.2527218	0.00261976
Golga2	Q921M4	10.2396726	0.03998921
Rptor	Q8K4Q0	10.2372052	0.00722321
Cct3	P80318	10.2183132	0.00018761
Tdrd3	Q91W18	10.187295	0.01608414
Rpl9	P51410	10.17135	0.00540255
Eif2b5	Q8CHW4	10.1672984	0.02646272
Cnbp	P53996	10.1491604	0.01840798
Mrtfb	P59759	10.0149229	0.00036016
Pja1	O55176	10.0022315	0.00198202
Phf6	Q9D4J7	9.93550234	0.00138907
Larp6	Q8BN59	9.92689326	0.01627657
Dars1	Q922B2	9.908113	0.00100708
Cpne8	Q9DC53	9.85652979	0.00854404
Ppm1g	Q61074	9.82984943	0.04460206
Pitpnm2 r3	Q6ZPQ6	9.80556235	5.8694E-05
Vps11	Q91W86	9.79225069	0.00046415
Fan1	Q69ZT1	9.78899713	0.00032779
Naa15	Q80UM3	9.76700196	0.0093971
Ranbp3	Q9CT10	9.76311522	0.03207685
Arfgef1	G3X9K3	9.71084902	0.00124017
Ppip5k1	A2ARP1	9.69151025	0.03016825
Dcp1a	Q91YD3	9.62611668	0.04084787
Sphkap	Q6NSW3	9.59946233	0.03859296
Copb2	O55029	9.55796434	0.0003092
Dars2	Q8BIP0	9.53103208	0.00038702
Tnrc6c	Q3UHC0	9.51732302	0.00554918
Cct7	P80313	9.40936873	0.00028697
Golga3	P55937	9.37615034	0.00634733
Rrbp1	Q99PL5	9.32317325	0.00018409
Abcf1	Q6P542	9.30853575	0.00667278
Arfgap3	Q9D8S3	9.29620045	0.02306464
Nemf	Q8CCP0	9.23188592	0.00037004
Erbp4	Q61527	9.22894394	0.0403434
Ktn1	Q61595	9.06801645	0.02939733
Ago1	Q8CJG1	9.03042273	0.01376025
Armxc2	Q6A058	9.02177454	0.01921387

## ANNEX

Gene name	Uniprot ID	log <sub>2</sub> FC	p-value
Nup214	Q80U93	8.7665463	0.0003053
Rc3h2	P0C090	8.72674416	0.00518919
Usp4	P35123	8.70728044	0.00023881
Kcna10	B2RQA1	8.67955935	0.03097451
Frrmpd4	A2AFR3	8.60450093	0.00147504
Cep170b	Q80U49	8.34364586	0.00508781
Xpo1	Q6P5F9	8.29886404	0.00047788
Psmc5	P62196	8.21600153	0.00111048
Hnrnp11	Q921F4	8.12804187	0.02455779
Epn2	Q8CHU3	8.1103538	0.00036888
Mast1	Q9R1L5	8.02691507	0.00145403
Arhgef2	Q60875	7.96925363	0.0011993
Elavl3	Q60900	7.94584763	0.01582466
Dsc1	P55849	7.87750557	0.00043603
Usp8	Q80U87	7.86978204	0.00041689
Psmd2	Q8VDM4	7.65050337	0.00099588
Slain2	Q8CI08	7.57865842	0.01353822
Ogt	Q8CGY8	7.53566986	0.00176709
Hecw1	Q8K4P8	7.43802612	0.00236701
Pfkm	P47857	7.33784002	0.00047152
Nhs12	B1AXH1	7.25997715	0.03063609
Disp2	Q8CIP5	5.81196102	0.00145449
Eif4g2	Q62448	5.6955341	0.005025
Prrc2c	Q3TLH4	5.42577449	0.00335359
Hnrnp1	Q8R081	5.0606208	0.04345966
Elavl2	Q60899	4.90447298	0.01345715
R3hdm2	Q80TM6	4.89971631	0.03580422
Slk	O54988	4.87914889	0.04040193
Eif4a1	P60843	4.85360454	0.00358424
Hdlbp	Q8VDJ3	4.69106956	0.02438543
Fkbp3	Q62446	4.54694894	0.00743344
Rpl10l	P86048	4.39104757	0.02117993
Nufip2	Q5F2E7	4.35838999	0.01430446
Sec23ip	Q6NZC7	4.34452807	0.01465217
Dync1h1	Q9JHU4	4.30682583	0.02712158
Rps10	P63325	3.92242227	0.00979994
Pja2	Q80U04	3.68115868	0.02279375
Cbl	P22682	3.65523705	0.02733806
Ppp1r1b	Q60829	3.64428528	0.03693605
Rpl12	P35979	3.31072418	0.03042282
Grsf1	Q8C5Q4	2.95107722	0.03171562
Rps3	P62908	2.94641213	0.04186049
Larp4b	Q6A0A2	2.85526074	0.02645818
G3bp2	P97379	2.7204827	0.00985255
Rack1	P68040	2.69891842	0.0227237
Spata2	Q8K004	2.6759932	0.00453337
Eif4b	Q8BGD9	2.65571744	0.02943102
Atxn2	O70305	2.54131192	0.02162324
Atxn2l	Q7TQH0	2.52285142	0.0150644
G3bp1	P97855	2.47058154	0.00255011



Gene name	Uniprot ID	log <sub>2</sub> FC	p-value
Rps4x	P62702	2.4301027	0.03361259
Hnrnpk	P61979	2.38358225	0.02952358
Rps16	P14131	2.33397945	0.02102043
Khsrp	Q3U0V1	2.32699485	0.00191222
Eif3c	Q8R1B4	2.31484365	0.04206055
Pabpc1	P29341	2.30478189	0.02871469
Usp10	P52479	2.2575448	0.02551493
Purg	Q8R4E6	2.16081716	0.00654906
Ubap2l	Q80X50	2.15681244	0.02630227
Eprs1	Q8CGC7	1.96789124	0.01154557
Trap1	Q9CQN1	1.78838216	0.01088169
Caprin1	Q60865	1.75868145	0.02982112
Cnot3	Q8K0V4	1.75806745	0.04290199
Stau1	Q9Z108	1.73709667	0.02663978

**Supplementary Table 2. FLAG-APEX-DrebrinA significantly enriched interacting proteins.** FLAG-APEX-DrebrinA interacting proteins with log<sub>2</sub> fold change values > 1.5 and p-value < 0.05 are shown.

Gene	Uniprot ID	log <sub>2</sub> FC	p-value
Clns1a	Q61189	17.5572737	0.0001821
Pdia6	Q922R8	16.5488749	0.00011181
Ubc	POCG50	16.059832	9.1545E-05
Ttyh3	Q6P5F7	15.6430977	0.01551152
Skic8	Q9ERF3	15.6284906	0.00014667
Gnb2	P62880	15.4219941	1.2569E-05
Pak5	Q8C015	14.9452165	0.00040863
Hnrnpa1	P49312	14.9007455	8.3391E-05
Kcnab2	P62482	14.5520223	4.5157E-05
Rbfox2	Q8BP71	14.3593414	7.2913E-05
Ankrd40	Q5SUE8	14.3275561	9.0053E-05
Csrp1	P97315	14.3095416	0.00691883
Scamp4	Q9JKV5	14.2673885	0.00021481
Tsc22d1	P62500	14.228277	0.00032461
Mt-Cyb	P00158	14.07669	0.00985159
Polr2h	Q923G2	13.9872694	0.00013847
Dusp3	Q9D7X3	13.8806175	0.00027014
Ube2d2	P62838	13.8784627	7.4815E-05
Gabbr1	Q9WV18	13.8663249	0.00513716
Brcc3	P46737	13.8627652	1.7843E-05
Srsf1	Q6PDM2	13.7945757	1.2349E-05
Dvl3	Q61062	13.7579444	0.00018914
Rpl11	Q9CXW4	13.7322884	0.00013402
Tceal5	Q8CCT4	13.7306639	0.00032487
Tsn	Q62348	13.7166237	0.00030281
Anp32b	Q9EST5	13.7107989	0.00733674
Krt17	Q9QWL7	13.6963702	0.00408453
Homer1	Q9Z2Y3	13.68375	0.00354269
Sdcbp	O08992	13.6486108	0.00175997
Ddx5	Q61656	13.6228939	8.9602E-05
Cpne8	Q9DC53	13.5493758	1.447E-05
Tagln	P37804	13.4442735	0.00028444
Dcun1d3	Q8K0V2	13.4140013	0.0001854
Csrp2	P97314	13.3996871	8.4077E-05
Pea15	Q62048	13.3592257	0.00674076
Tkt	P40142	13.337306	9.1202E-05
Znf330	Q922H9	13.3371484	0.00046532
lqca1l	A6H690	13.2981129	0.00894708
Necab2	Q91ZP9	13.2175594	0.00073602
Sgtb	Q8VD33	13.2094479	0.00254747
Ckmt1	P30275	13.1232118	0.00994898
Khdrbs3	Q9R226	13.0989464	0.00211094
Ube2v2	Q9D2M8	13.093557	0.01475423
Phf21b	Q8C966	13.0874953	2.8673E-05
Pdlim3	O70209	13.0732118	0.00066621
Pdcd5	P56812	13.0205508	0.00014719
Coro2b	Q8BH44	12.9832544	0.00011447
Hnrnpu	Q8VEK3	12.9459414	0.04508842

Gene	Uniprot ID	log <sub>2</sub> FC	p-value
Akap2	O54931	12.8604158	0.00011386
Dync1i1	O88485	12.8299352	0.00011748
Pym1	Q8CHP5	12.7333097	0.00016192
Itpka	Q8R071	12.6255326	0.00795203
P33monox	Q9DBN4	12.4793	0.00019043
Fsd1	Q7TPM6	12.4319658	0.00015974
Rgs7bp	Q8BQP9	12.4234249	0.00013275
Gmfb	Q9CQI3	12.4117449	0.0008476
Nono	Q99K48	12.3930562	0.00048869
Gmds	Q8K0C9	12.2969159	0.01769456
Pcdh8	Q7TSK3	12.2632234	0.02321814
Stmn2	P55821	12.1960423	1.862E-05
Gabra1	P62812	12.1313621	0.02738515
Rbm14	Q8C2Q3	12.1280161	0.012233
Rab33b	O35963	12.1159408	0.00025308
Ubqln2	Q9QZM0	12.0805631	0.00402554
Afap1	Q8OYS6	12.0179335	0.02535042
Elmo2	Q8BHL5	11.9994591	0.00545466
Slc16a7	O70451	11.8795467	0.00854255
Tln2	Q71LX4	11.8795141	0.00012885
Nrxn1	Q9CS84	11.8756593	0.00026709
Gpx4	O70325	11.8233396	0.00023464
Dctn6	Q9WUB4	11.7788142	0.00590926
Zfr	O88532	11.7615293	0.01460632
Ddb1	Q3U1J4	11.7515413	0.00029758
Impact	O55091	11.7366421	0.00840643
Gabrb3 -3	P63080	11.7293951	6.2287E-05
Ctbp2	P56546	11.7229385	0.0004588
Cmtr2	Q8BWQ4	11.6978899	0.00411645
Rap1b	Q99JI6	11.6694056	0.00026109
Cnp	P16330	11.6320074	0.00637219
Cdk14	O35495	11.6024493	0.00880627
Pgm5	Q8BZF8	11.5627949	0.00022441
Pak1	O88643	11.5580662	0.0163195
Gprc5b	Q923Z0	11.5443557	0.00048712
Elfn2	Q68FM6	11.5285501	0.00041155
Cct3	P80318	11.4871442	0.00050392
Zyx	Q62523	11.4591866	0.01551996
Kif21b	Q9QXL1	11.4433478	0.00622868
Nherf1	P70441	11.4203497	0.00030164
Cplx1	P63040	11.3793774	0.00103073
Begain	Q68EF6	11.3337669	0.00012051
Plaa	P27612	11.3284593	0.00155253
Gabrb2 -2	P63137	11.321365	0.00256278
Acbd6	Q9D061	11.3102699	0.003708
Prickle2	Q80Y24	11.2992035	0.01841238
Cpsf6	Q6NVF9	11.2952454	0.03789945
Gab1	Q9QYY0	11.2555775	0.00711727
Vps28	Q9D1C8	11.2117704	0.00072744
Fth1	P09528	11.1446518	0.03088413

## ANNEX

Gene	Uniprot ID	log <sub>2</sub> FC	p-value
Ppp1cc	P63087	11.1242271	0.01957819
Ttyh1	Q9D3A9	11.108556	0.00043933
Irs2	P81122	11.0924881	0.00090186
Palld	Q9ET54	11.0924474	0.00667384
Aqp4	P55088	11.0839439	0.00021697
Plscr3	Q9JIZ9	11.0195544	3.388E-05
Stard7	Q8R1R3	11.0065783	0.00178753
Tnik	P83510	10.9989868	0.00034514
Slc12a9	Q99MR3	10.9384845	0.00114855
Ctif	Q6PEE2	10.9196413	0.00044936
Arhgap35	Q91YM2	10.8668595	0.0011309
Twf2	Q9Z0P5	10.8227117	0.00142118
Cttnbp2nl	Q99LJ0	10.7916625	0.00024533
Phrf1	A6H619	10.7589951	0.00088725
Rbmxl1	Q91VM5	10.7539154	0.00470327
Washc1	Q8VDD8	10.7422414	0.04302291
Wasl	Q91YD9	10.7398019	0.00094718
Dhx9	O70133	10.7383122	0.02265846
Diras1	Q91Z61	10.7228589	3.0418E-05
Ca198	Q8C3W1	10.71541	0.00023041
Ralb	Q9JIW9	10.7116833	0.00033562
Ca021	Q8K207	10.7113243	0.00048404
Supt5h	O55201	10.6379963	0.00016509
Gab2	Q9Z1S8	10.6311925	0.00031327
Trim28	Q62318	10.5394167	0.00745387
Zdhhc5	Q8VDZ4	10.5260281	0.02409258
Cacna1e	Q61290	10.5109215	0.01601505
Tnks1bp1	P58871	10.5093638	5.7638E-05
Ids	Q08890	10.5012152	0.00019379
Arvcf	P98203	10.4912257	0.00019203
Vasp	P70460	10.4754805	0.01054594
Cyria	Q8BHZ0	10.4543425	0.00125771
Ddhd1	Q80YA3	10.4062731	0.00015362
Pfdn1	Q9CWM4	10.4005972	0.00373054
Ap3s1	Q9DCR2	10.3700071	0.00017751
Gmps	Q3THK7	10.3163872	3.8538E-05
Slk	O54988	10.2643083	0.00653072
Gfod1	Q3UHD2	10.2477614	0.02164652
Rbbp8	Q80YR6	10.2361282	0.00036815
Lrrfip1	Q3UZ39	10.1859528	4.7926E-05
Flna	Q8BTM8	10.1058847	0.01237015
Arf1	P84078	10.0965811	9.6492E-05
Itpk1	Q8BYN3	10.0694136	0.00014917
Dync1i2	O88487	10.0484887	0.00022505
Fam98b	Q80VD1	10.0069013	4.7761E-05
Vps37a	Q8CHS8	9.98758855	0.00059338
Cadps	Q80TJ1	9.98702002	6.7551E-05
Itgb1	P09055	9.93434183	0.02651661
Ccny	Q8BGU5	9.91802709	0.00922053
Polr1a	O35134	9.90194006	0.00030878

Gene	Uniprot ID	log <sub>2</sub> FC	p-value
Pik3r3	Q64143	9.86020981	0.000207
Wwc1	Q5SXA9	9.84946021	0.01813021
Uqcrf51	Q9CR68	9.84081952	0.00101076
Ankrd28	Q505D1	9.78198816	0.00136344
Pfkm	P47857	9.7640659	0.01187026
Pex5l	Q8C437	9.72346816	0.04649234
Arhgap5	P97393	9.66508238	0.01156471
Slc25a22	Q9D6M3	9.62924221	7.1462E-05
Hcn1	O88704	9.61332614	0.00026543
Map3k3	Q61084	9.60901349	0.00022798
Psmc8	Q9CX56	9.58867854	4.7059E-05
Arhgef2	Q60875	9.39626219	0.04487609
Madd	Q80U28	9.36232137	0.00138539
Prkci	Q62074	9.34452843	0.00154559
Psmc5	Q9Z2U1	9.32337204	0.00291274
Rbmx	Q9WV02	9.30386275	0.01594965
Rab9a	Q9R0M6	9.28912488	0.00219492
Ahcyl2	Q68FL4	9.26302874	0.00020795
Adcy9	P51830	9.20517241	0.03216596
Ilf3	Q9Z1X4	9.20326335	7.8446E-05
Ptprd	Q64487	9.15894834	0.00727413
Flot1	O08917	9.15770575	0.00134601
Shank1	D3YZU1	9.14757081	0.00503041
Astn1	Q61137	9.11543153	9.6574E-05
Vps11	Q91W86	9.10476272	0.00152237
Relch	Q148V7	9.09157774	0.00292464
Abca1	P41233	8.98674936	0.00200417
Rpl6	P47911	8.94689946	0.00039569
Robo1	O89026	8.91397833	0.00857287
Slc4a7	Q8BTY2	8.91198169	0.00130045
Klhdc9	Q3USL1	8.86764992	0.00174335
Ylpm1	Q9R0I7	8.82326443	0.0357965
Tsply4	Q8VD63	8.82193158	0.00464873
Wdr45b	Q9CR39	8.74699983	0.00292016
Insr	P15208	8.6937091	0.01515715
ErbB4	Q61527	8.68979778	0.00204959
Fancg	Q9EQR6	8.68918853	0.00073822
Setx	A2AKX3	8.68057901	0.00069648
Mtmt1	Q9Z2C4	8.57209292	0.00424256
Hecw1	Q8K4P8	8.55314738	0.01578061
Grin2b	Q01097	8.52326518	0.00830006
Lrrc7	Q80TE7	8.48150893	0.00563389
Acot11	Q8VHQ9	8.34472601	0.00545601
Cdc42bpa	Q3UU96	8.31847076	0.00067865
Slain2	Q8CI08	8.13900305	0.00120247
Carmil2	Q3V3V9	8.02247399	0.01249998
Stat3	P42227	7.93348439	0.00143469
Stxbp2	Q64324	7.93310001	0.00322684
Usp4	P35123	7.88331914	0.00030104
Egfr	Q01279	7.88148024	0.01291655

## ANNEX

Gene	Uniprot ID	log <sub>2</sub> FC	p-value
Rilpl1	Q9JJC6	7.85467922	0.02394043
Arhgef4	Q7TNR9	7.84707568	0.0036844
Ajm1	A2AJA9	7.79283668	0.00045398
Habp4	Q9JKS5	7.69987871	0.00036374
Adgrl3	Q80TS3	7.63411119	0.00021911
Tmem63b	Q3TWI9	7.48951491	0.00134811
Dlgap3	Q6PFD5	7.28939279	0.00013883
Gigyf2	Q6Y7W8	7.2828539	0.01749585
Cep170b	Q80U49	6.89104439	0.00107354
Nhsl2	B1AXH1	6.87592796	0.00060619
K0930	Q3UE31	6.10059136	0.03961149
Trappc12	Q8K2L8	5.98850523	0.00692136
Pja1	O55176	5.02437197	0.01853403
Cpne2	P59108	4.88981987	0.02438439
Dbn1	Q9QXS6	3.39605151	0.01448905
Eps8	Q08509	3.34000263	0.01487498
Hnrnpd	Q60668	3.07496337	0.03775655
Hnrnpa2b1	O88569	2.75020694	0.03576726
Pdlim5	Q8CI51	2.58963159	0.01047982
Tagln3	Q9R1Q8	2.43656192	0.0333639
Ppp1r9b	Q6R891	2.41972272	0.00639851
Cadm3	Q99N28	2.1135331	0.01283064
Caskin1	Q6P9K8	2.06649962	0.02393501
Vdac1	Q60932	1.99237447	0.0005583
Atp2b1	G5E829	1.95786206	0.04209186
Nebi	Q9DC07	1.68692833	0.03467406
Kras	P32883	1.6742645	0.01933425
Spata2	Q8K004	1.59153315	0.04523612
Lasp1	Q61792	1.57734598	0.03369356

**Supplementary Table 3. FLAG-APEX-DrebrinA and FLAG-APEX-ZBP1 shared interacting proteins.** FLAG-APEX-ZBP1- and FLAG-APEX-DrebrinA-interacting proteins were compared and the shared interactors between them are shown. Gene name, Uniprot ID and protein names are detailed.

Gene name	UniprotID	Protein name
Acbd6	Q9D061	Acyl-CoA-binding domain-containing protein 6
Arf1	P84078	ADP-ribosylation factor 1
Arhgef2	Q60875	Rho guanine nucleotide exchange factor 2
Begain	Q68EF6	Brain-enriched guanylate kinase-associated protein
Brcc3	P46737	Lys-63-specific deubiquitinase BRCC36
Cct3	P80318	T-complex protein 1 subunit gamma
Cep170b	Q80U49	Centrosomal protein of 170 kDa protein B
Ckmt1	P30275	Creatine kinase U-type, mitochondrial
Clns1a	Q61189	Methylosome subunit pCln Chloride channel, nucleotide sensitive 1A
Cpne8	Q9DC53	Copine-8
Ddx5	Q61656	Probable ATP-dependent RNA helicase DDX5 RNA helicase p68
Dhx9	O70133	ATP-dependent RNA helicase A DEAH box protein 9
Dvl3	Q61062	Segment polarity protein dishevelled homolog 3
Dync1i1	O88485	Cytoplasmic dynein 1 intermediate chain 1
Dync1i2	O88487	Cytoplasmic dynein 1 intermediate chain 2
ErbB4	Q61527	Receptor tyrosine-protein kinase erbB-4
Gigyf2	Q6Y7W8	GRB10-interacting GYF protein 2
Gpx4	O70325	Phospholipid hydroperoxide glutathione peroxidase
Habp4	Q9JK55	Intracellular hyaluronan-binding protein 4
Hecw1	Q8K4P8	E3 ubiquitin-protein ligase HECW1
Hnrnpa1	P49312	Heterogeneous nuclear ribonucleoprotein A1
Ilf3	Q9Z1X4	Interleukin enhancer-binding factor 3
Krt17	Q9QWL7	Keratin, type I cytoskeletal 17
Madd	Q80U28	MAP kinase-activating death domain protein
Nhsl2	B1AXH1	NHS-like protein 2
Nono	Q99K48	Non-POU domain-containing octamer-binding protein
Nrxn1	Q9CS84	Neurexin-1
Pdia6	Q922R8	Protein disulfide-isomerase A6
Pfdn1	Q9CWM4	Prefoldin subunit 1
Pfkm	P47857	ATP-dependent 6-phosphofructokinase, muscle type
Pja1	O55176	E3 ubiquitin-protein ligase Praja-1
Plaa	P27612	Phospholipase A-2-activating protein
Pym1	Q8CHP5	Partner of Y14 and mago
Rbfox2	Q8BP71	RNA binding protein fox-1 homolog 2
Rbmxl1	Q91VM5	RNA binding motif protein, X-linked-like-1
Rpl11	Q9CXW4	Large ribosomal subunit protein uL5
Rpl6	P47911	Large ribosomal subunit protein eL6
Sdcbp	O08992	Syntenin-1
Shank1	D3YZU1	SH3 and multiple ankyrin repeat domains protein 1
Skic8	Q9ERF3	Superkiller complex protein 8
Slain2	Q8CI08	SLAIN motif-containing protein 2
Slk	O54988	STE20-like serine/threonine-protein kinase
Spata2	Q8K004	Spermatogenesis-associated protein 2
Stard7	Q8R1R3	StAR-related lipid transfer protein 7, mitochondrial

## ANNEX

<b>Gene name</b>	<b>UniprotID</b>	<b>Protein name</b>
Tkt	P40142	Transketolase
Tnik	P83510	Traf2 and NCK-interacting protein kinase
Tnks1bp1	P58871	182 kDa tankyrase-1-binding protein
Trim28	Q62318	Transcription intermediary factor 1-beta
Tsc22d1	P62500	TSC22 domain family protein 1
Tsn	Q62348	Translin
Ubc	P0CG50	Polyubiquitin-C
Usp4	P35123	Ubiquitin carboxyl-terminal hydrolase 4
Vps11	Q91W86	Vacuolar protein sorting-associated protein 11 homolog
Washc1	Q8VDD8	WASH complex subunit 1



## ARTICLE

# Stress granules display bistable dynamics modulated by Cdk

Galal Yahya<sup>1,2\*</sup>, Alexis P. Pérez<sup>1,3\*</sup>, Mònica B. Mendoza<sup>1</sup>, Eva Parisi<sup>1</sup>, David F. Moreno<sup>1</sup>, Marta H. Artés<sup>1</sup>, Carme Gallego<sup>1</sup>, and Martí Aldea<sup>1,3</sup>

**Stress granules (SGs) are conserved biomolecular condensates that originate in response to many stress conditions. These membraneless organelles contain nontranslating mRNAs and a diverse subproteome, but our knowledge of their regulation and functional relevance is still incipient. Here, we describe a mutual-inhibition interplay between SGs and Cdc28, the budding yeast Cdk. Among Cdc28 interactors acting as negative modulators of Start, we have identified *Whi8*, an RNA-binding protein that localizes to SGs and recruits the mRNA of *CLN3*, the most upstream G1 cyclin, for efficient translation inhibition and Cdk inactivation under stress. However, *Whi8* also contributes to recruiting Cdc28 to SGs, where it acts to promote their dissolution. As predicted by a mutual-inhibition framework, the SG constitutes a bistable system that is modulated by Cdk. Since mammalian cells display a homologous mechanism, we propose that the opposing functions of specific mRNA-binding proteins and Cdk's subjugate SG dynamics to a conserved hysteretic switch.**

## Introduction

Phase separation of proteins and nucleic acids into condensates is emerging as a general mechanism for cellular compartmentalization without the requirement of surrounding membranes (Banani et al., 2017; Alberti and Dormann, 2019; Shin and Brangwynne, 2017). These biomolecular condensates are based on weak multivalent interactions among component molecules that are mobile and exchange with the adjoining medium and play essential roles in cell physiology as reaction crucibles, sequestration centers, or organizational hubs. In a dynamic environment, cells need to control phase separation to form or dissolve condensates as a function of spatial and temporal cues. Thus, the molecular mechanisms that modulate phase separation will be critical to understanding how cells use biomolecular condensates to execute and control a growing list of cellular processes (Alberti et al., 2019; Snead and Gladfelter, 2019; Bratek-Sklicki et al., 2020).

Stress granules (SGs) are conserved cytoplasmic condensates that contain (1) pools of nontranslating mRNAs and (2) a variety of proteins, including translation initiation factors and RNA-binding proteins that form core stable substructures in SGs (Protter and Parker, 2016). Non-RNA-binding proteins such as posttranslational modification factors, and protein or RNA remodeling complexes, are recruited to SGs by protein-protein interactions often mediated by intrinsically disordered regions (IDRs) and modulate SG assembly and disassembly. However, a

predominant role has been recently attributed to intermolecular RNA-RNA interactions as upstream determinants of SG composition (Van Treec et al., 2018). Although SGs are thought to down-regulate translation and protect recruited mRNAs in many different stress conditions, we still do not have sufficient experimental evidence to comprehend the relevance of SGs in cell physiology.

Stress restricts cell cycle progression, and budding yeast cells display a diverse set of mechanisms as a function of the stress signal. The HOG pathway constitutes a prominent paradigm and operates on specific molecular targets to modulate different cell cycle phases and transitions in response to osmotic stress (Solé et al., 2015; de Nadal et al., 2011). Regarding entry into the cell cycle, osmotic shock causes a temporary repression of the G1/S regulon (Bellí et al., 2001), in which Hog1-mediated phosphorylation of *Whi5* and *Msa1* contributes to inhibiting transcription (González-Novo et al., 2015). Down-regulation of G1/S genes was also observed during heat and ER stress (Rowley et al., 1993; Vai et al., 1987), and because chaperones play important but limiting roles at Start (Vergés et al., 2007; Yahya et al., 2014; Parisi et al., 2018), we proposed that, by compromising chaperone availability, all stressful conditions would target the chaperone as a common means to hinder entry into the cell cycle (Moreno et al., 2019). However, the precise molecular environment in which diverse

<sup>1</sup>Molecular Biology Institute of Barcelona, Spanish National Research Council, Catalonia, Spain; <sup>2</sup>Department of Microbiology and Immunology, Zagazig University, Zagazig, Egypt; <sup>3</sup>Department of Basic Sciences, Universitat Internacional de Catalunya, Barcelona, Spain.

\*G. Yahya and A.P. Pérez contributed equally to this paper; Correspondence to Carme Gallego: carme.gallego@ibmb.csic.es; Martí Aldea: marti.aldea@ibmb.csic.es.

© 2021 Yahya et al. This article is distributed under the terms of an Attribution-Noncommercial-Share Alike-No Mirror Sites license for the first six months after the publication date (see <http://www.rupress.org/terms/>). After six months it is available under a Creative Commons License (Attribution-Noncommercial-Share Alike 4.0 International license, as described at <https://creativecommons.org/licenses/by-nc-sa/4.0/>).

## NEUROSCIENCE

# The elongation factor eEF1A2 controls translation and actin dynamics in dendritic spines

Mònica B. Mendoza<sup>1†</sup>, Sara Gutierrez<sup>1†</sup>, Raúl Ortiz<sup>1</sup>, David F. Moreno<sup>1</sup>, Maria Dermitt<sup>2</sup>, Martin Dodel<sup>2</sup>, Elena Rebollo<sup>1</sup>, Miquel Bosch<sup>3,4</sup>, Faraz K. Mardakheh<sup>2</sup>, Carme Gallego<sup>1\*</sup>

Copyright © 2021  
The Authors, some  
rights reserved;  
exclusive licensee  
American Association  
for the Advancement  
of Science. No claim  
to original U.S.  
Government Works

Synaptic plasticity involves structural modifications in dendritic spines that are modulated by local protein synthesis and actin remodeling. Here, we investigated the molecular mechanisms that connect synaptic stimulation to these processes. We found that the phosphorylation of isoform-specific sites in eEF1A2—an essential translation elongation factor in neurons—is a key modulator of structural plasticity in dendritic spines. Expression of a nonphosphorylatable eEF1A2 mutant stimulated mRNA translation but reduced actin dynamics and spine density. By contrast, a phosphomimetic eEF1A2 mutant exhibited decreased association with F-actin and was inactive as a translation elongation factor. Activation of metabotropic glutamate receptor signaling triggered transient dissociation of eEF1A2 from its regulatory guanine exchange factor (GEF) protein in dendritic spines in a phosphorylation-dependent manner. We propose that eEF1A2 establishes a cross-talk mechanism that coordinates translation and actin dynamics during spine remodeling.

## INTRODUCTION

Dendritic spines mediate the vast majority of excitatory synaptic transmission events in the mammalian brain. Structural changes in dendritic spines are essential for synaptic plasticity and brain development (1). The total excitatory input that a neuron can receive is dependent on the complexity of the dendritic network and the density and morphology of spines. Small alterations in average spine density and size may reveal a profound dysfunction at the cellular or circuit level (2). Inside dendritic spines, biochemical states and protein-protein interactions are dynamically modulated by synaptic activity, leading to the regulation of protein synthesis and reorganization of the actin cytoskeleton (3). An increasing number of studies support the idea that the actin cytoskeleton and the translation machinery are intrinsically connected and may show reciprocal regulation (4–6). Perturbation of the actin cytoskeleton is associated with a marked reduction in the rate of global protein synthesis in yeast and mammalian cells (7, 8).

Regulation of mRNA translation initiation and elongation is essential for synaptic plasticity and memory formation (9–11). Studies on the regulation of translation have traditionally focused on the initiation step. There is, however, growing evidence that the elongation step is also regulated to achieve a more robust transient control of the translational machinery in response to synaptic activity (12, 13). The eukaryotic elongation factor 1 alpha (eEF1A) is a classic G protein that delivers aminoacylated transfer RNAs (tRNAs) to the A site of the ribosome during translation elongation in a guanosine triphosphate (GTP)-dependent manner. Recycling of the inactive eEF1A–guanosine diphosphate (GDP) complex back to the active GTP-bound state is mediated by the eEF1B complex, which

acts as a guanine nucleotide exchange factor (GEF) (14). In addition to its well-established function in protein synthesis, a number of noncanonical functions have been reported for eEF1A (15). The most studied of these is the ability of eEF1A to interact with and modulate the actin cytoskeleton (16–18).

Vertebrates have two *eEF1A* genes that encode different isoforms: eEF1A1 and eEF1A2. Intriguingly, these isoforms are 92% identical at the amino acid level (19) but display very different expression patterns. Isoform eEF1A1 is expressed ubiquitously during development but is replaced by isoform eEF1A2 in neurons and muscle cells over the course of postnatal development (20). This expression switch is a vital process, and the complete loss of function of the isoform eEF1A2 in the mouse causes severe neurodegeneration, loss of muscle bulk, and death by 4 weeks (21). Despite the fact that numerous studies have been published on the two eEF1A variants, the reasons underlying the developmental switch between the two eEF1A isoforms in neurons and muscle cells remain poorly understood.

eEF1A displays a large repertoire of posttranslational modifications brought about by phosphorylation, most of them occurring within conserved regions of both isoforms (19, 22, 23). As an interesting exception, it has been reported that the kinase receptor for activated protein C kinase 1 (RACK1) recruits stress-activated c-Jun N-terminal kinase (JNK) to polysomes, where it phosphorylates eEF1A2 at Ser<sup>205</sup> and Ser<sup>358</sup> and promotes degradation of newly synthesized polypeptides by the proteasome. Because Ser<sup>358</sup> is evolutionarily conserved but not present in isoform eEF1A1, this post-transcriptional regulatory mechanism could constitute a relevant difference in the physiological roles of the two isoforms (24).

So far, although eEF1A2 is the most abundant isoform in mature neurons, most published work has been carried out in a nonneuronal context. It is worth noting that the developmental timeline of synaptic spines and neuronal circuit formation occurs when isoform eEF1A1 is totally replaced by isoform eEF1A2 in neurons. Another concern is that numerous data from experiments in mammalian cells have been analyzed with antibodies that do not distinguish between the two isoforms. Here, we demonstrate that the configuration of phosphorylation sites unique to the eEF1A2 isoform plays a

<sup>1</sup>Molecular Biology Institute of Barcelona (IBMB), CSIC, Catalonia 08028, Spain. <sup>2</sup>Centre for Cancer Cell and Molecular Biology, Barts Cancer Institute, Queen Mary University of London, Charterhouse square, London EC1M 6BQ, UK. <sup>3</sup>Department of Basic Sciences, Universitat Internacional de Catalunya (UIC-Barcelona), Sant Cugat del Vallès 08195, Spain. <sup>4</sup>Institute for Bioengineering of Catalonia (IBEC), The Barcelona Institute of Science and Technology (BIST), Barcelona 08028, Spain. \*Corresponding author. Email: cggibmc@ibmb.csic.es  
†These authors contributed equally to this work.

bioRxiv preprint doi: <https://doi.org/10.1101/2023.05.15.540804>; this version posted May 15, 2023. The copyright holder for this preprint (which was not certified by peer review) is the author/funder. All rights reserved. No reuse allowed without permission.

## **KIS counteracts PTBP2 and regulates alternative exon usage in neurons**

Marcos Moreno-Aguilera<sup>1</sup>, Mònica B. Mendoza<sup>1</sup>, Alba M. Neher<sup>1</sup>, Martin Dodel<sup>2</sup>, Faraz K.

Mardakheh<sup>2</sup>, Raúl Ortiz<sup>1</sup>, Carme Gallego<sup>1\*</sup>

<sup>1</sup>Molecular Biology Institute of Barcelona (IBMB), CSIC, Catalonia, 08028, Spain

<sup>2</sup>Centre for Cancer Cell and Molecular Biology, Barts Cancer Institute, Queen Mary University of London, London, UK.

\*Correspondence: [cggbmc@ibmb.csic.es](mailto:cggbmc@ibmb.csic.es)

### **Abstract**

Alternative RNA splicing is an essential and dynamic process to control neuronal differentiation and synapse maturation, and dysregulation of this process has been associated with neurodegenerative diseases. Recent studies have revealed the importance of RNA-binding proteins in the regulation of neuronal splicing programs. However, the molecular mechanisms involved in the control of these splicing regulators are still unclear. Here we show that KIS, a brain-enriched kinase with a domain shared by splicing factors, controls exon usage in differentiated neurons at a genome-wide level. KIS phosphorylates the splicing regulator PTBP2 complex and markedly counteracts its role in exon exclusion. At the molecular level, phosphorylation of unstructured domains within PTBP2 causes its dissociation from key co-regulators and hinders its RNA-binding capacity. Taken together, our data provide new insights into the post-translational control of splicing regulators and uncover an essential role of KIS in setting alternative exon usage in neurons.

**Keywords:** KIS kinase/ PTBP2/ alternative splicing/ exon usage/ neuronal differentiation





